Kindred Hydro

FINAL REPORT: NEAR-TERM ACTION (NTA) 2018-0827: FLEXIBLE INFILTRATION TEST METHODS FOR EVALUATING INFILTRATION FEASIBILITY
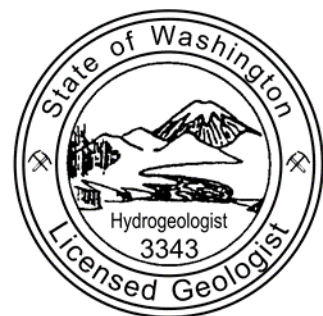
Prepared for: **City of Tacoma**

Project No. TAC-20-1 • October 10, 2022

Kindred Hydro, Inc.

_____

J. Scott Kindred, PE, LHG
scottk@kindredhydro.com

State of Washington
Licensed Geologist
Hydrogeologist
3343

J. SCOTT KINDRED

Final Report - Abstract

This is the final report for Puget Sound Partnership's Near-Term Action (NTA) 2018-082, titled: *Flexible Infiltration Test Methods for Evaluating Infiltration Feasibility*. The purpose of this grant is to evaluate different infiltration test methods and provide an expanded toolbox for evaluating stormwater infiltration feasibility and estimating infiltration capacity for different stormwater infiltration facilities. The final report includes the results of the technical work conducted for this study and is divided into six volumes:

1. **Volume I: Using the Uncased Steady-State Borehole Permeameter Method to Estimate Saturated Hydraulic Conductivity**. The purpose of this portion of the work was to calibrate the uncased steady-state borehole permeameter (USSBP) method for both glacially-overconsolidated and normally-consolidated soils that are often used for stormwater infiltration. It was conducted by comparing numerical results with analytical results calculated using the USSBP method.

2. **Volume II: Using the Cased Steady-State Borehole Permeameter Method to Estimate Saturated Hydraulic Conductivity**. The purpose of this portion of the work was to calibrate the cased steady-state borehole permeameter (CSSBP) method for both glacially-overconsolidated and normally-consolidated soils that are often used for stormwater infiltration. It was conducted by comparing numerical results with analytical results calculated using the CSSBP method.

3. **Volume III: Using the Falling-Head Borehole Permeameter Method to Estimate Saturated Hydraulic Conductivity**. The purpose of this portion of the work was to evaluate the falling-head borehole permeameter (FHBP) method for typical stormwater infiltration testing. It was conducted by comparing numerical results with analytical results calculated using the FHBP method.

4. **Volume IV: Shallow Infiltration Testing to Estimate Saturated Hydraulic Conductivity**. The purpose of this portion of the work was to conduct testing in pits and shallow (<10 ft deep) test wells to: 1) demonstrate the use of these three methods under field conditions and determine if they provide similar estimates of bulk hydraulic conductivity (K_b); 2) compare the results from pit test and shallow wells; 3) provide field evidence of K_b variability over a distance of 30 to 70 ft; and 4) provide data for evaluation of layering, perching, and groundwater mounding.

5. **Volume V: Deep Infiltration Testing to Estimate Saturated Hydraulic Conductivity.** The purpose of this portion of the study was to conduct testing in deep drilled wells to demonstrate the use of these three methods under field conditions and determine if they provide similar estimates of K_b. This testing will also provide data for evaluation of layering, perching, and groundwater mounding.

6. **Volume VI: Effects of Stratigraphic Layering and Groundwater Mounding on Infiltration Testing and Design.** The purpose of this portion of the study was to evaluate the effects of stratigraphic layering and groundwater mounding on infiltration testing and provide strategies and correction factors for addressing these effects in the design of infiltration facilities. The K_b provided by infiltration testing can be multiplied by appropriate correction factors to provide design hydraulic conductivity (K_d) used to size infiltration facilities.

The technical analysis in this report was used to develop infiltration testing and design procedures outlined in an infiltration guide. This guide may be incorporated into the Washington State stormwater manuals.

VOLUME I: USING THE UNCASED STEADY-STATE BOREHOLE PERMEAMETER METHOD TO ESTIMATE SATURATED HYDRAULIC CONDUCTIVITY

Near-Term Action (NTA) 2018-0827: Flexible Infiltration Test Methods for Evaluating Infiltration Feasibility

Project No. TAC-20-1 • October 10, 2022

Volume I - Contents

Volume I - List of Tables

Volume I - List of Figures

10 Simulated steady BP flow (Q) versus time in four advance outwash soils (Qva) and one glacial till soil (Qvt) (Table 4) for: (a) Testpit configuration with $H = 1$ m, $r = 1$ m; and (b) deep borehole configuration with $H = 20$ m, $r = 0.1$ m. The sudden change in slope of Q vs. t in the fine-medium Qva soil at approximately 12 hr (b) occurred because BP flow contacted the bottom flow domain boundary.

Volume I - Abstract

Volume I provides calibration and analysis of the uncased steady-state borehole permeameter (USSBP) method for estimating saturated hydraulic conductivity (K_s) to support design of stormwater infiltration facilities in the Puget Sound basin. The USSBP method was recently shown to be well suited for estimating the capacity of shallow and deep infiltration facilities in glacially over-consolidated soils (Kindred and Reynolds 2020.[1]).

The USSBP method was developed in the 1950's by the United States Bureau of Reclamation (Zanger 1953) to estimate K_s in shallow boreholes completed above the water table. The approach has been improved over the years, and now accounts for flow due to pressure, gravity, and soil capillarity. The USSBP method has not been widely used for stormwater infiltration testing and previous to Kindred and Reynolds (2020) was only calibrated for normally consolidated soils and infiltration test facilities with ponding depth (H) versus borehole radius (r) ratios (H/r) ≤ 22. Volume I includes calibration of the USSBP method for both glacially over-consolidated soils and normally consolidated soils with H/r ratios from 0.05 to 200.

Soil capillarity is accounted for in the USSBP method using the sorptive number (α^*), which can be estimated based on the unsaturated hydraulic conductivity curve. Volume I demonstrates how the unsaturated hydraulic conductivity curve can be estimated based on grainsize distribution (which is obtained using a simple laboratory procedure) and soil porosity (which can be estimated based on soil texture and density). Estimates of α^* are provided for the ten representative soils used for calibration.

Calibration was conducted using numerically simulated constant-head USSBP flow for ten representative soils to update the USSBP shape function fitting parameters (Z_1, Z_2, Z_3) for a broad range of test pit and borehole configurations. The representative soils included five glacially over-consolidated soils and five normally-consolidated soils and were designed to cover the range of soils typically considered for stormwater infiltration in the Puget Sound Basin.

After numerous trial calibration attempts, a good balance between accuracy and simplicity was achieved by calibrating separate fitting parameters for H/r ≤ 20 and H/r ≥ 20 and soils with < 12% silt content and soils with > 12% silt content. USSBP estimates of K_s provided a maximum error of 11.2% and an average error of 3.3% using these calibrated shape function parameters. In contrast, the original shape function parameters (developed by soil scientists for normally-consolidated soils and H/r ≤ 22) produced a maximum K_s error of 51% and an average error of 17% for the ten representative soils.

Additional finding from this task include:

- Reasonable variations in soil properties assumed in the numerical simulations had no significant effect on the results, except for glacial till results which varied by up to 4%.

- Approximate steady-state flow conditions (a key assumption of the USSBP method) were achieved within six hr for soils with less than 12% silt in all test configurations except for fine sands in deep boreholes with more than 4 m of ponding depth. In contrast, for soils with more than 12% silt, approximate steady state was achieved between 13 and 16 hr.

- Comparing the results of two six-hr infiltration tests spaced 24 hr apart demonstrated that infiltration tests in soils with less than 12% silt may over-estimate the performance of operational infiltration facilities by less than 2%, while infiltration tests in soils with more than 12% silt may over-estimate the performance of operational infiltration facilities by 5% to 19%, depending on the soil type and configuration of the infiltration facility. This is because fine-grained soils drain slowly, and the background moisture content was higher for the second test than the first test. The second test is likely

---

[1] https://kindredhydro.com/kindred-and-reynolds-2020

a good representation of conditions beneath an operational facility during a period of closely-spaced storm events.

- Based on the results summarized above, a correction factor of 5% to 30% is recommended for soils with more than 12% silt to account for different background moisture content beneath an operational infiltration facility compared with a test facility. Soils with less than 12% silt may not require any correction for background moisture content..

1 Introduction

Stormwater infiltration is now required where feasible for new development in Washington State and the 2019 Stormwater Management Manual for Western Washington (WSDOE 2019) provides a variety of methods for sizing infiltration facilities. The preferred method being either the small or large pilot infiltration test (PIT). The field portion of the PIT method is conducted by maintaining a steady-state ponding depth of 6-12 in. for 6-7 hrs in an excavated test pit with a bottom area of 12-100 ft^2. The analysis portion of the PIT method assumes only vertical water flow due to gravity and does not account for flow due to hydrostatic pressure, horizontal flow, or flow due to the capillary suction (capillarity) of the unsaturated soil surrounding the test facility. Since pressure flow, horizontal flow, and capillarity are often a large percentage of total flow, the PIT method does not accurately represent the soil's actual infiltration rate and capacity. In addition, the stormwater manual does not provide methods for testing deep infiltration capacity for dug or drilled drains.

A more accurate and reliable approach is to determine infiltration rate and capacity using measurements of soil saturated hydraulic conductivity (K_s) obtained from test methods that formally account for both flow directions (vertical, horizontal), and all three components of soil water flow (pressure, gravity, capillarity). The constant head well or borehole permeameter (USSBP) is one such test that is simple to use and well-suited for site investigations (Reynolds et al. 1983, 1985; Philip 1985; Stephens et al. 1987; Elrick et al. 1989; Reynolds 2008). Until recently, the USSBP method focused on ponded head (H) versus borehole radius (r) ratios (H/r) $\leq$ 22 and used a quasi-empirical shape function, C_u, which had been calibrated only for normally-consolidated soils (Zhang et al. 1998; Reynolds 2008).

In Puget Sound, stormwater infiltration is often practiced in very dense glacial soils that have been over-consolidated by hundreds of meters of glacial ice. These soils have smaller porosity and K_s values than normally-consolidated soils with similar grain-size distributions. Frequently, because of near surface soils that are not conducive to infiltration, drilled wells are used to infiltration into the deeper soils and can have H/r ratios as high as 200. We simulated USSBP tests numerically to determine if the original C_u functions developed by Zhang et al. (1998) were sufficiently accurate for a wide range of H/r ratios (0.05 – 200) and for the soils in the Puget Sound basin that are typically considered for stormwater infiltration. The original C_u functions produced a maximum K_s error of 51% and an average error of 17%, and K_s was over-estimated in 68% of the test simulations. Hence, the C_u functions presented by Zhang et al. (1998) were not deemed to be accurate enough for soils in the Puget Sound basin that are typically considered for stormwater infiltration.

1.1 Scope of Work and Purpose

The primary objective of this task was consequently to develop revised C_u shape function fitting parameters that would improve the accuracy of the USSBP method for a broad range of test configurations (i.e., H/r ratios between 0.05 and 200). Secondary objectives were to use numerical simulations of USSBP flow for a range of soil types and H/r ratios to: 1) demonstrate the relative importance of the three USSBP flow components (pressure, gravity, capillarity), 2) estimate the time required to approximate steady-state USSBP flow, and 3) determine the sensitivity of the USSBP analysis to background soil hydraulic properties (matric suction, unsaturated water content function, and unsaturated hydraulic conductivity function).

Previous work by Kindred and Reynolds (2020) focused on calibration of glacially over-consolidated soils. The work conducted for this grant was focused on calibration of the USSBP method for normally-consolidated soils typically considered for stormwater infiltration. In order to support the overall objectives of the grant, Volume I provides the calibration results for both glacially over-consolidated soils and normally consolidated soils. For consistency with previously published work, metric units are used throughout Volume I.

2   Materials and Methods

2.1   Uncased Steady-State Borehole Permeameter (USSBP) Equation

Considerable research has been conducted regarding analytical methods for estimating K_s from borehole infiltration tests in the unsaturated zone (see e.g., Reynolds 2010, 2011, 2013, 2015 and citations therein). These methods generally assume a flat-bottom cylindrical test facility (e.g., borehole or pit excavation), isotropic and homogeneous soil, and no water-table effects. Kindred and Reynolds (2020) provide a concise history of the evolution of this method since the 1950's. This work culminated in the mid-1980's when Reynolds et al. (1985), Reynolds and Elrick (1985), and Philip (1985) developed approximate analytical USSBP equations that formally account for pressure, gravity, and capillarity flow. The Reynolds analysis, which has been tested extensively over the years, has the form:

$$K_s = \frac{C_u Q}{2\pi H^2 + \ \pi r^2 C_u + \frac{2\pi H}{\alpha^*}} \quad (\text{Eq. 1.1})$$

where

$$C_u = \left[\frac{(H/r)}{Z_1 + Z_2 (H/r)} \right]^{Z_3} \quad (\text{Eq. 1.2})$$

α^* is the soil sorptive number (m^{-1}), C_u is the USSBP shape function (dimensionless), and Z_1, Z_2, and Z_3 are the shape function fitting parameters (dimensionless). Eq. 1.1 assumes that H is less than the uncased or screened portion of the test facility, while other constant-head and falling-head analyses assume that H is greater than the uncased or screened portion of the test facility (see e.g. Reynolds 2010, 2011). The three terms in the denominator of Eq. 1.1 account, respectively, for flow through the wall and base of the test facility due to the hydrostatic pressure of the ponded water, gravity flow through the base of the test facility, and capillarity flow through the wall and base of the test facility due to the surrounding unsaturated porous material. Flow due to hydrostatic pressure accounts for most of the flow out of the test facility when $H \gg r$, while gravity flow and capillarity flow often dominate when $H < r$ (Reynolds 2008; Elrick and Reynolds 1992). The relative importance of the three flow components is discussed in Section 3.3.

As described in Reynolds et al. (1985) and Elrick et al. (1989), soil capillarity can be parameterized using the "alpha" relationship, α (m^{-1}), which is defined by:

$$\alpha = \frac{K_s - K(\psi_i)}{\varnothing_m} \quad (\text{Eq. 2.1})$$

where the matric flux potential, $\varnothing_m$ (m^2/d), is given by:

$$\varnothing_m = \int_0^{\psi_i} K(\psi) \mathrm{d}\psi; \ 0 \ \leq \psi \ \leq \psi_i \quad (\text{Eq. 2.2})$$

$K(\psi)$ is soil hydraulic conductivity as a function of soil matric suction ψ (m), and ψ_i (m) is the antecedent matric suction in the background soil at the time of the test. (Note that matric suction is defined here as the negative of soil pore water pressure head, so ψ is positive when the soil is unsaturated). In effect, $\varnothing_m$ equals the area under the $K(\psi)$ curve between the matric suction in the background soil ($\psi = \psi_i$) and the matric suction at the leading edge of the saturated bulb surrounding the USSBP injection zone ($\psi = 0$) (Reynolds et al. 1985). This means that $\varnothing_m$ is a maximum when the background soil is dry (ψ_i large), small when the background soil is wet (ψ_i close to zero), and zero when the background soil is saturated ($\psi_i = 0$).

When the unsaturated soil is at field capacity or drier, $K(\psi_i) << K_s$; and hence, α in Eq. (2.1) can often be simplified to:

$$\alpha \approx \alpha^* = \frac{K_s}{\phi_m} \quad (\text{Eq. } 2.3)$$

and α^* is used in Eq. 1.1. Field studies have shown that α^* is relatively constant for a broad range of porous materials and can therefore be estimated using a lookup table based on soil texture and structure (Table 1; Elrick et al. 1989; Reynolds 2008, 2013). "Structured soil" (Table 1) refers to soil with cracks and/or biopores (e.g., root holes) that can increase bulk soil α^* and K_s. Generally speaking, target soils for stormwater infiltration are well below the plant root zone, and therefore have few cracks and biopores. Although not explicitly stated by Elrick et al. (1989) and Reynolds (2008, 2013), the α^* values and shape function parameters (Z_1, Z_2, Z_3) in Table 1 apply for near-surface, normally-consolidated soils and H/r ratios ≤ 22.

Table 1: *Sorptive Number* (α^*) and uncased shape function (C_u) parameters (Z_1, Z_2, Z_3) for a range of normally-consolidated soils where ratio of steady ponding depth (H) to borehole radius (r) ≤ 20 (adapted from Elrick et al. 1989; Zhang et al. 1998).

Soil Texture	α^* (m^{-1})	Z_1 (-)	Z_2 (-)	Z_3 (-)
Compacted clays and silts	1	2.081	0.121	0.672
Unstructured fine-grained soil	4	1.992	0.091	0.683
Structured fine-grained soil or unstructured fine-medium sandy soil	12	2.074	0.093	0.754
Structured fine-medium sandy soil or unstructured coarse-grained gravelly soil	36	2.074	0.093	0.754

2.2 USSBP Calibration

The calibration procedure involved calculating K_s via the USSBP equation (Eq. 1.1) using steady flow-rate values (Q) generated by numerical simulations of USSBP flow for 300 test scenarios. The test scenarios included all combinations of ten "representative" soils typically considered for stormwater infiltration in the Puget Sound Basin, two plausible K_s values for each soil type, and 15 USSBP test configurations where the H/r ratio varied from 0.05 to 200. Calibration was conducted using the Solver© optimization algorithm in Microsoft Excel©, which changes user-selected variables until a specified objective is minimized, maximized or becomes equal to a specified value. In this study, the C_u shape function fitting parameters (Z_1, Z_2, and Z_3 in Eq. 1.2) were varied by Solver© (using the generalized nonlinear reduced gradient method) until the maximum error between the USSBP-calculated K_s values and the specified K_s values was minimized for the 300 test scenarios.

The steady-state flow rates for the 300 scenarios were estimated using SEEP/W, a finite element numerical model that can simulate multidimensional and axisymmetric flow in saturated and unsaturated porous media (GEOSLOPE International Ltd., Calgary, Alberta, Canada). Unsaturated flow simulation requires specifying soil hydraulic properties in the form of the unsaturated volumetric soil water content function $\theta(\psi)$ (soil water content as a function of soil matric suction) and the unsaturated hydraulic conductivity function $K(\psi)$ (hydraulic conductivity as a function of soil matric suction). These hydraulic property functions are described in Section 2.2.3.

2.2.1 Model Domains and Test Configurations

The SEEP/W numerical flow domains for the three test configurations are shown in Fig. 1 and summarized in Table 2. The simulations assumed axisymmetric flow, with no-flow boundaries along the top and outside radius of the flow domain, and a unit hydraulic head gradient boundary at the bottom of the flow domain. The test facilities were cylindrical test pits or boreholes with constant hydraulic head boundaries defined along the base and submerged portion of the test facility wall. The facility radius (r), constant ponded head (H), and H/r ratios for each of the 15 test scenarios are provided in Table 3. The simulations used graded meshes of rectangular and triangular finite elements. As shown on Fig. 1, for pit simulations, element size increased in steps from 0.05 m by 0.05 m along the pit wall to 0.1 m by 0.1 m at distance. For shallow borehole simulations, element size increased in steps from 0.025 m by 0.025 m along the borehole wall to 0.1 m by 0.1 m at distance. For deep borehole simulations, element size increased in steps from 0.025 m by 0.025 m along the borehole wall to 0.5 m by 0.5 m at distance. Test simulations showed that larger flow domains and finer element sizes had minimal impact on Q and K_s (data not shown).

The numerical simulations calculated water flow rate or discharge, Q (m^3/d), versus time, t (d), out of the test facilities over either a 24-hr period or a 12-hr period (for a few scenarios that approached steady state quickly). As transient flow was simulated, true steady flow rate (constant Q) was usually closely approached but not truly achieved. True steady flow requires steady-state simulations that are often impractical because they require very large flow domains to avoid external boundary effects, as well as very large run times to achieve convergence. As a result, longer duration transient flow simulations generally result in slightly lower Q values, which in turn result in slightly lower K_s estimates by the USSBP approach. Section 3.5 illustrates the time required to obtain Q values that approximate steady state for the different soil types and test configurations.

Table 2: SEEP/W axisymmetric flow domain dimensions.

Model Domain	Domain Radius (m)	Domain Height (m)	Test Hole Radius (m)	Test Hole Depth (m)	Number of Elements
Test pit	4	8	1	4	4,047
Shallow borehole	3	12	0.25	6	10,609
Deep borehole	10	38	0.1	24	11,808

Table 3: Infiltration test configurations where *r* is radius of the test facility (pit or borehole) and *H* is steady ponding depth.

Test Hole Type	r (m)	H (m)	H/r Ratio (-)
Test pit	1.0	0.05	0.05
Test pit	1.0	0.1	0.1
Test pit	1.0	0.25	0.25
Test pit	1.0	0.5	0.5
Test pit	1.0	1.0	1
Shallow borehole	0.25	0.25	1
Shallow borehole	0.25	0.5	2
Shallow borehole	0.25	1.0	4
Shallow borehole	0.25	2.0	8
Shallow borehole	0.25	3	12
Deep borehole	0.1	1.2	12
Deep borehole	0.1	2	20
Deep borehole	0.1	4	40
Deep borehole	0.1	10	100
Deep borehole	0.1	20	200

2.2.2 *Representative Soil Types*

Ten "representative" soils (based on data from the Puget Sound region of Washington State) were defined for this analysis, including five glacially over-consolidated soils and five normally consolidated soils. The glacially over-consolidated soils included four advance outwash soils: silty Qva, fine Qva, fine-medium Qva, and fine-coarse Qva; and one glacial till: Qvt. The normally consolidated soils included well-sorted and poorly-sorted soils typical of recessional outwash or alluvium. These representative soils cover the range of soils usually considered for stormwater infiltration within the Puget Sound basin, although they likely cover most soil types considered for infiltration across the entire State of Washington. Fig. 2 shows grain-size distributions and Tables 4a and 4b summarize key properties assumed for the representative soils.

The four Qva soils represent materials that were deposited by streams in front of an advancing glacier, and then overrun and consolidated by the glacier. The silt content (particles passing through a 0.075-mm sieve) ranges from 3 to 17%. Using the Unified Soil Classification System (USCS, per ASTM D 2487), the four soils are classified as SP (poorly-graded sand with less than 5% silt), SW (well-graded sand with less than 5% silt), SP-SM (sand with 5 to 12% silt), or SM (sand with greater than 12% silt). The silty Qva, fine Qva and fine-medium Qva soils are relatively poorly graded, while the fine-coarse Qva soil is well graded (Fig. 2, Table 4). The Qvt represents glacial till soils which typically have minimal sorting and little or no layering. Qvt is well graded (Fig. 2) with 20% silt and a USCS classification of SM. Qvt often contains more than 20% fines but becomes unsuitable for infiltration at higher silt contents. Silt content, as used in this study, strictly includes clay content (i.e. soil particles smaller than 0.002 mm) and silt content. Together these are defined by others as "fines". For this study, "silt content" and "fines content" are synonymous.

Because of glacial over-consolidation, Qva soils range from medium dense to very dense, with standard penetration test (SPT, ASTM D1586 / D1586M-18) blow counts typically ranging from 20 to 80 blows per 30 cm. Qvt is usually very dense with SPT blow counts greater than 100 blows per 30 cm. The SPT is a standard geotechnical

method used to document relative soil density during drilling and soil sampling. The SPT is conducted by driving a 51-mm diameter sampler using a 63.5-kg slide-hammer dropped from a height of 76 cm.

The five normally-consolidated soils include two silty soils (silty fine sand with 25% silt and silty fine-coarse sand with 15% silt) classified as SM, and three relatively clean soils (fine sand with 9% silt, medium sand with 5% silt and sandy gravel with 3% silt) and USCS classifications of SM-SP, SP, and GW, respectively.

Two "typical" K_s values were assigned to each soil type (Tables 4a and 4b), based on the above soil properties and hundreds of K_s field measurements in the Puget Sound area. These K_s values do not cover the full range of values observed for soils with similar grainsize distributions. The validity of the calibration results to broader ranges of K_s was evaluated by running selected simulations using K_s values that were ten times greater than the baseline values and comparing the results with USSBP calculated values. Although not provided here, the USSBP results were within 10% of the simulated values, demonstrating that the calibration results were valid for a much broader range of K_s than evaluated in this study.

The remaining properties in Table 4 (porosity, liquid limit, residual soil water content, background soil matric suction, α', and n) are input parameters for either the Modified Kovacs $\theta(\psi)$ function (Aubertin et al. 2003) or the van Genuchten (1980) $\theta(\psi)$ function (Section 2.2.3). Most of the $\theta(\psi)$ input parameters are difficult to measure in-situ; hence, "representative" values are given in Tables 4a and 4b.

Assumed porosities θ_S of the five glacially over-consolidated soils were 17% for Qvt, 25% for silty Qva, and 30% for the fine, fine-medium, and fine-coarse Qva soils. These porosities are less than typically measured for normally-consolidated soils and are intended to reflect the effects of glacial compaction. Assumed porosities θ_S of the five normally-consolidated soils were 35% for the well-graded silty fine-coarse sand and 40% for the remaining normally-consolidated soils.

The Atterberg liquid limit (gravimetric water content at which soil behavior transitions from plastic to liquid, ASTM method D 4318) is controlled primarily by the soil clay/silt ratio on a weight-percent basis. Glacially derived and non-glacial coarse-grained soils (i.e., soils with a sand or gravel matrix) in the Puget Sound basin usually contain very little clay, hence Atterberg liquid limits were assumed to be low (between 0 and 10) for all the soils.

Residual soil water content θ_r, α', and n values were estimated during development of the $\theta(\psi)$ functions, as described in the following section. The background soil matric suction ψ_i was estimated from the $\theta(\psi)$ functions using an assumed background soil water content of 10% for the glacially over-consolidated soils and a background soil water content ranging from 6.3% to 10.4% for the normally-consolidated soils (5% higher than the residual moisture content θ_r).

Table 4a: Properties of representative glacially over-consolidated soil types and baseline SEEP/W soil parameters used in the soil water content and hydraulic conductivity models. *Qva* is advance outwash, *Qvt* is glacial till, D_{60} and D_{10} are grain diameters corresponding, respectively, to 60% passing and 10% passing on the grain-size distribution curve, and *USCS* is Unified Soil Classification System. *Background soil matric suction* is based on an assumed background volumetric soil water content of 10%. The van Genuchten fitting parameters apply for Eqs. 3 and 4.

Parameter	Soil Type				
	Qvt	Silty Qva	Fine Qva	Fine-Medium Qva	Fine-Coarse Qva
D_{60} (mm)	0.5	0.25	0.3	0.5	5
D_{10} (mm)	0.02	0.04	0.1	0.13	0.25
Silt Content (wt. %)	20	17	8	5	3
USCS Soil Type	SM	SM	SM-SP	SP	SW
Porosity, θ_S (vol. %)	17	25	30	30	30
Liquid Limit (%)	0	0	0	0	0
Saturated Hydraulic Conductivity, K_s (m/d)	0.1/0.2	0.5/1	2/4	10/20	5/10
Residual Soil Water Content, θ_r (vol. %)	5.5	4.8	3.0	2.6	1.5
Background Soil Water Content θ_b (%)	10	10	10	10	10
Background Soil Matric Suction, ψ_i (m)	3.1	1.8	0.8	0.5	0.09
van Genuchten Fitting Parameter α' (m⁻¹)	0.06	0.09	0.18	0.28	1.6
van Genuchten Fitting Parameter n (-)	2.40	3.64	4.10	4.18	3.68

Table 4b: Properties of representative normally-consolidated soil types and baseline SEEP/W soil parameters used in the soil water content and hydraulic conductivity models. *Qva* is advance outwash, *Qvt* is glacial till, D_{60} and D_{10} are grain diameters corresponding, respectively, to 60% passing and 10% passing on the grain-size distribution curve, and *USCS* is Unified Soil Classification System. *Background soil matric suction* is based on an assumed background volumetric soil water content ranging from 6.3% to 10.4%. The van Genuchten fitting parameters apply for Eqs. 3 and 4.

Parameter	Soil Type				
	Silty Fine Sand	Silty Fine-Coarse Sand	Fine Sand	Medium Sand	Sandy Gravel
D_{60} (mm)	0.15	1.4	0.28	1.0	8.0
D_{10} (mm)	0.04	0.02	0.079	0.18	0.4
Silt Content (wt. %)	25%	15%	9%	5%	3%
USCS Soil Type	SM	SM	SM-SP	SP	GW
Porosity, θ_S (vol. %)	40	35	40	40	40
Liquid Limit (%)	10	5	0	0	0
Saturated Hydraulic Conductivity, K_s (m/d)	0.25/0.5	0.5/1	3/6	10/20	30/60
Residual Soil Water Content, θ_r (vol. %)	4.8	5.4	2.9	2.2	1.3
Background Soil Water Content θ_b (%)	9.8	10.4	7.9	7.2	6.3
Background Soil Matric Suction, ψ_i (m)	1.39	0.64	0.75	0.24	0.05
van Genuchten Fitting Parameter α' (m⁻¹)	1.28	3.44	2.44	7.69	40
van Genuchten Fitting Parameter n (-)	4.3	3.2	4.2	4.3	3.9

2.2.3 Soil Hydraulic Property Functions

The unsaturated volumetric soil water content functions $\theta(\psi)$ for the ten soils were initially defined using the Modified Kovacs model (Aubertin et al. 2003). This $\theta(\psi)$ model uses soil porosity, grain diameters representing 10% passing and 60% passing on the grain-size distribution curve, and the Atterberg liquid limit. Tables 4a and 4b provides the soil properties used in the Modified Kovacs model and Fig. 3 shows soil water content versus matric suction (negative pore pressure) for each of the ten soil types using the Modified Kovacs model.

During sensitivity analyses, it was observed that the numerical model results were unrealistic for certain scenarios and it was determined that de-coupling of the soil water content function $\theta(\psi)$ (based on the Modified Kovac's model) and the unsaturated hydraulic conductivity function $K(\psi)$ (based on van Genuchten) was the likely cause. Therefore, van Genuchten $\theta(\psi)$ curves, which are coupled to the van Genuchten $K(\psi)$ curves, were fit to the Modified Kovacs $\theta(\psi)$ curves as shown on Fig. 3. The van Genuchten $\theta(\psi)$ equation is:

$$\theta(\psi) = \theta_r + \frac{\theta_s - \theta_r}{[1 + (\alpha'|\psi|)^n]^m} \quad \text{(Eq. 3)}$$

where θ_S is porosity, θ_r is residual soil water content, α' (m^{-1}), n (-) and m (-) are empirical fitting parameters, and the Mualem (1976) pore continuity model is assumed, i.e., $m = 1 - (1/n)$. Fitting of the van Genuchten $\theta(\psi)$ curves to the Modified Kovac's curves assumed that θ_S was fixed while θ_r, α', and n were allowed to vary. The fitted parameters are provided in Table 4 and the results of the curve fitting are shown in Fig. 3. Note that the van Genuchten $\theta(\psi)$ curves tend to systematically overestimate the Modified Kovacs curves in the dry soil end ($\psi > 10$ m, Fig. 3), however this is well beyond the maximum background matric suction (ψ_i) used for the simulations (Tables 4a and 4b). The SEEP/W simulations were performed using the van Genuchten $\theta(\psi)$ curves.

The unsaturated hydraulic conductivity function $K(\psi)$ was defined using the van Genuchten (1980) equation:

$$K(\psi) = K_s \frac{\{1 - (\alpha'\psi)^{n-1} [1 + (\alpha'\psi)^n]^{-m}\}^2}{[1 + (\alpha'\psi)^n]^{\frac{m}{2}}} \quad \text{(Eq. 4)}$$

where K_s (m/d) is saturated hydraulic conductivity, and α' (m^{-1}), n (-) and m (-) are the same fitting parameters used in Eq. 3. The SEEP/W model develops the van Genuchten $K(\psi)$ curves based on K_s and the van Genuchten $\theta(\psi)$ curves. The van Genuchten $K(\psi)$ curves are shown on Fig. 4.

2.2.4 Sorptive Number (α*) Calculations

The sorptive number (α^*) can be estimated for the ten soil types using Eq. 2.3 and the $K(\psi)$ functions generated by SEEP/W (Tables 4a and 4b, Fig. 4). The matric flux potential ($\emptyset_m$) was calculated by numerically integrating under the $K(\psi)$ curves, and α^* was calculated for background soil water content (θ_b) ranging from dry soil to virtual saturation. Numerical integration used the trapezoidal rule and the default matric suction/water content intervals generated by SEEP/W.

Plots of α^* versus background matric suction, ψ_i, shown in Fig. 5, reveal that α^* is relatively constant in dry and moist soil, but increases dramatically as the background soil approaches saturation (ψ_i approaches zero). The sudden and rapid increase occurs because the highly non-linear $\emptyset_m$ relationship suddenly decreases towards zero at near-saturation, signifying that capillarity is negligible in all near-saturated soils (and zero in all saturated soils). As shown in Table 5, the α^* values for glacially over-consolidated dry/moist soils range from 1.17 m^{-1} for Qvt to 25 m^{-1} for fine-coarse Qva, which reflects the fact that soil capillarity is often substantial in silty soils (e.g., Qvt, silty Qva), but can decrease significantly with decreasing silt content (e.g., fine-coarse Qva). Similarly, the α^* values for normally-consolidated dry/moist soils range from 1.8 m^{-1} for silty fine sand to 57 m^{-1} for sandy gravel.

Table 5: *Sorptive Number* (α^*) for dry/moist soil and C_u shape function (Eq. 1.2) parameters (Z_1, Z_2, Z_3) for the ten representative soils. Different shape function parameters are developed for test configurations where ponded head (H) to radius (r) ratio was $H/r \leq 20$ or $H/r \geq 20$, and for soils with > 12% silt (USCS soil type SM) or < 12% silt.

Soil Type	α^* (m^{-1})	Low Ponded Head ($H/r \leq 20$)			High Ponded Head ($H/r \geq 20$)		
		Z_1 (-)	Z_2 (-)	Z_3 (-)	Z_1 (-)	Z_2 (-)	Z_3 (-)
Silty fine sand (SM)	1.8	2.11	0.192	0.91	2.04	0.0224	0.547
Silty fine-coarse sand (SM)	5.5						
Qvt (SM)	1.17						
Silty Qva (SM)	1.33						
Fine sand (SP-SM)	3.5	2.03	0.207	0.98	2.11	0.0273	0.605
Medium sand (SP)	11						
Sandy gravel (GW)	57						
Fine Qva (SP-SM)	2.5						
Fine-Medium Qva (SP)	3.9						
Fine-Coarse Qva (SW)	25						

2.3 Sensitivity Analyses

Calibration of the uncased shape function C_u curves was conducted using deterministic values of the van Genuchten (1980) soil parameters (θ_S, θ_r, α', and n) used to develop the $\theta(\psi)$ and $K(\psi)$ curves. Sensitivity of the calibrated C_u fitting parameters to variations in the $\theta(\psi)$ and $K(\psi)$ curves was tested by modifying the underlying parameters used to develop the $\theta(\psi)$ and $K(\psi)$ curves (θ_S, θ_r, α', and n). Numerical sensitivity runs were performed for two different test configurations: the shallow borehole with $H = 2$ m and $r = 0.25$ m was used for the glacially over-consolidated soils and the test pit with $H = 0.1$ m and $r = 1.0$ m was used for the normally-consolidated soils. The sensitivity runs were conducted using the following changes to the $\theta(\psi)$ and $K(\psi)$ parameters: porosity θ_S was increased by 5%; θ_r and α' were increased by 50%, and n was decreased by 0.5.

Calibration of the shape function C_u curves assumes a constant value for α^* based on a background soil water content θ_b of 10% for the glacially over-consolidated soils and a background soil water content ranging from 6.3% to 10.4% for the normally consolidated soils. As shown in Fig. 5, α^* was constant for all soil types at this soil water content and did not change for dryer soil conditions. However, as discussed in Section 2.2.4, capillarity flow does decrease as soil water content approaches full saturation and USSBP flow is therefore expected to decrease as well. Sensitivity of the numerical flow results to θ_b is evaluated for the two test configurations described above using wetter θ_b values, as discussed in Section 3.4.

Only one parameter was changed for each sensitivity run and the percent difference between baseline Q and revised Q was calculated using:

$$Difference = (\frac{|Revised\ Q - Baseline\ Q|}{Baseline\ Q})100 \ \ (Eq. 5)$$

The results of the sensitivity analysis are provided in Section 3.4.

2.4 Evaluation of Steady-State Conditions

The borehole permeameter (USSBP) equation (Eq. 1.1) assumes steady-state flow rate (Q) within an infinite flow domain. This is difficult to simulate numerically, as it requires very long running times to achieve numerical

convergence of the steady-state flow equation, and very large numbers of elements to place the radial and bottom flow domain boundaries at "numerical infinity". It is possible, however, to conduct transient flow simulations in much smaller flow domains (e.g., Fig. 1) where the radial and bottom boundaries are just far enough away to allow near-steady USSBP flow before boundary effects occur (e.g., Fig. 6). We therefore simulated Q vs. t for test pit, shallow borehole, and deep borehole configurations, and compared Q determined after "t" hr (Q_t) and 24 hr (Q_{24}). We deemed $Q_t/Q_{24} \leq 1.05$ as indicative of effective steady flow after "t" hr of infiltration. Determining if and where $Q_6/Q_{24} \leq 1.05$ occurs was of particular interest because most field infiltration tests are terminated after about 6 hr (due to cost). Results are provided in Section 3.5.

2.5 Evaluation of Two Closely-Spaced Storm Events

As discussed later in Volume I, numerical simulations demonstrate that increasing the background moisture content can reduce the infiltration capacity of an infiltration facility. This is due to a decrease in the capillarity flux and is more significant for fine-grained soils than coarse-grained soils. The sensitivity analysis assumes a significant increase in background moisture content (θ_b) but does not evaluate how quickly the soil will dry following a precipitation event. Therefore, additional numerical simulations were conducted to demonstrate how the infiltration capacity of the test facility is affected when two six-hr infiltration tests are spaced 24 hr apart. The simulations were conducted for all ten soils and for the following test configurations: testpit with $H = 1$ m and deep borehole with $H = 10$ m. Results are provided in Section 3.6.

3   Results

3.1   Numerical Simulations

SEEP/W simulations of USSBP flow were conducted for ten soil types, two K_s values for each soil type, and 15 test configurations, for a total of 300 simulations (Tables 3, 4a, and 4b). The simulations were run for 24 hr, except for the fine-medium Qva, the fine-coarse Qva, and the sandy gravel, which were terminated after 6 hr because the wetted zone started to impinge on flow domain boundaries. As demonstrated later in Volume I, six hr was still sufficient to achieve approximate steady-state flow in these coarse-textured soils.

Zero matric suction and water content contours are provided in Fig. 6 for each soil type and one test configuration ($H = 2$ m, $r = 0.25$ m, $H/r = 8$) after 6 hr of flow. As shown in the figure, zero matric suction (dashed blue contour line) extends deeper below the borehole as K_s and α^* increase. Borehole flux reached the bottom of the simulated domain for the coarser-grained soils (fine-medium Qva, fine-coarse Qva, medium sand, and sandy gravel) which are the soil types with the largest K_s and α^* values. Because unit hydraulic gradient was specified on this boundary, borehole flux reaching the bottom of the domain does not affect simulated flow appreciably as long as the boundary is not contacted by the zero matric suction contour.

3.2   Calibrations

As discussed in Section 2.2, a spreadsheet was set up to estimate the K_s specified in the SEEP/W simulations using the USSBP equation (Eq. 1.1) and recalibrated C_u shape function fitting parameters (Z_1, Z_2, Z_3 in Eq. 1.2). The calibration process was designed to minimize the maximum individual error in the USSBP estimate of K_s across the 300 test scenarios. The maximum individual K_s error was minimized (instead of minimizing the average K_s error) to ensure that the USSBP analysis always met or exceeded a known degree of accuracy.

Initial recalibration tests indicated that a single set of C_u shape function fitting parameters would not provide sufficiently accurate K_s determinations across the full range of soil types and test configurations. The next phase of calibration therefore extended the approach of Reynolds et al. (1983, 1985), and assumed that the shape function parameters (Z_1, Z_2, Z_3) depended on both soil type (i.e., α^* value) and H/r ratio. This resulted in four sets of C_u shape function parameters that applied separately for fine-grained soil (> 12% silt), coarse-grained soil (< 12% silt), small H/r ratio (≤ 20), and large H/r ratio (≥ 20). These parameters provided USSBP estimates of K_s with a maximum error of 11.2% and an average error of 3.3%, relative to the K_s specified in the numerical simulations. Maximum error for each soil type and H/r range are summarized in Table 6.

Plots of the calibrated C_u shape functions are given in Fig. 7 and the corresponding Z_1, Z_2 and Z_3 fitting parameters are given in Table 5. The two shape functions for silty soils and the two shape functions for sandy soils are joined together at $H/r = 20$ and a slight jog is apparent in the plots, as shown on Figure 7b. Figs. 7a and 7b also show the Zhang et al. (1998) C_u shape function for $\alpha^* = 4$ m^{-1}, which is seen to overestimate the re-calibrated shape functions when H/r is less than 30 to 40 and underestimate the shape functions when H/r is greater than 30 to 40.

Table 6: Maximum percent difference between specified K_s in the numerical model and USSBP K_s for the ten representative soils. H (m) is steady ponded head, and r (m) is test facility radius.

Soil Type	Sorptive Number α^* (m^{-1})	Maximum Error, Low Ponded Head ($H/r < 20$)	Maximum Error, High Ponded Head ($H/r \geq 20$)
Silty Soils (>12% Silt)			
Silty fine sand	1.8	11.2%	8.8%
Silty fine-coarse sand	5.5	11.1%	7.8%
Qvt	1.17	11.3%	4.4%
Silty Qva	1.33	8.0%	8.4%
Sandy Soils (<12% Silt)			
Fine sand	3.5	7.2%	2.6%
Medium sand	11	8.0%	2.9%
Sandy gravel	57	9.5%	3.7%
Fine Qva	2.5	9.5%	3.7%
Fine-Medium Qva	3.9	5.2%	3.0%
Fine-Coarse Qva	25	8.8%	3.1%

3.3 Relative Importance of Pressure Flow, Gravity Flow and Capillarity Flow

The USSBP flow equation can be re-arranged to:

$$Q_T = K_s \left[\frac{2\pi H^2}{C_u} + \pi r^2 + \frac{2\pi H}{C_u \alpha^*} \right] = Q_P + Q_G + Q_C \quad (\text{Eq. 6})$$

where Q_T is total flow from the test facility (borehole or pit), Q_P refers to the first term on the left and represents 3-D pressure flow through the sides and base of the test facility due to the hydrostatic pressure of the ponded water; Q_G refers to the second term on the left and represents vertical gravity flow through the test facility base; and the third term on the left, Q_C, represents 3-D capillarity flow through the facility walls and base due to the capillary suction of the background unsaturated soil. The relative importance of Q_P, Q_G and Q_C varies with soil type and H/r ratio and is illustrated in Fig. 8 using the ten representative soils (Tables 4a and 4b) and calibrated shape function fitting parameters (Table 5).

For all soils, the relative contribution of pressure flow (Q_P) increases as H/r ratio increases, accounting for less than 25% of total flow (Q_T) when H/r is less than 0.1, but at least 90% of Q_T when H/r exceeds 10 (Fig. 8). For H/r less than 1.0, capillarity flow (Q_C) is relatively important for fine-grained soils (Qvt, silty Qva, and silty fine sand) and less important for coarse-grained soils (fine-coarse Qva and sandy gravel). When H/r is less than 0.1, gravity flow (Q_G) dominates in coarse-grained soils such as fine-coarse Qva, silty fine-coarse sand, medium sand, and sandy gravel. In general, the glacially over-consolidated soils have a greater degree of capillarity than the normally-consolidated soils with similar grainsize distributions. This is due to the lower porosity of the glacially over-consolidated soils.

3.4 Numerical Model Sensitivity Analysis

The ten "representative" soil types were defined using soil properties that exhibit significant variability and uncertainty in the field. This section examines how modifying some soil properties impacts the numerically simulated Q values. The sensitivity analyses were conducted using the shallow borehole configuration ($H = 2$ m, $r = 0.25$ m, $H/r = 8$) for the five glacially over-consolidated soils and the testpit configuration ($H = 0.25$ m, $r = 1.0$ m, $H/r = 0.25$) for the five normally-consolidated soils. Baseline and revised Q values were obtained using the baseline and revised soil properties provided in Tables 7a and 8a for the glacially over-consolidated soils and in Tables 7b and 8b for the normally-consolidated soils. As evident in Eqs. 1.1 and 7, K_s is linearly related to Q so variation in Q produces the same variation in K_s.

As discussed in Section 2.2.3, the van Genuchten (1980) equations were used to define the K(ψ) and $\theta(\psi)$ functions. Sensitivity to changes in these functions was tested by changing the van Genuchten (1980) parameters (θ_S, θ_r, α', and n) as shown on Tables 7a and 7b. Comparison of the revised Q values with the baseline Q values indicate that the results were virtually unchanged for all the soil types except Qvt, which changed by $\pm 4\%$ or less (Table 7a).

SEEP/W simulation of USSBP flow requires an activation pressure, which is the specified background matric suction ψ_i, and corresponding background soil water content θ_b of the soil surrounding the test facility. As shown on Tables 8a and 8b, sensitivity to θ_b was determined by specifying a lower ψ_i (and thereby wetter θ_b). Increasing background soil water content resulted in less than 2% reduction in steady Q for the sandy soils with less than 12% silt and between 2% and 11% for the silty soils with more than 12% silt. The greater impact for silty soils occurred because: 1) the capillarity of the background soil (as represented by $\emptyset_m$, Eq. 2.2) decreases as ψ_i decreases and θ_b increases; and 2) sensitivity to capillarity increases with increasing silt content (Fig. 8). In theory, this sensitivity could be mitigated by measuring θ_b in the field and recalculating α^*. However, accurate field measurements of θ_b can be difficult due to drilling and sampling effects and recalculation of α^* may be too complex for some practitioners.

Table 7a: Comparison of SEEP/W-simulated *steady flow rates Q* for glacially over-consolidated soils using different values of van Genuchten (1980) parameters, including *porosity* θ_S, *residual soil water content* θ_r, and the fitting parameters *α' and n.* Baseline and revised *steady flow rates* are shown for four types of advance outwash soil (*Qva*) and one glacial till soil (*Qvt*).

Soil Property	Qvt	Silty Qva	Fine Qva	Fine-Medium Qva	Fine-Coarse Qva
Effect of Increasing θ_S by 5%					
Baseline θ_S (%)	17%	25%	30%	30%	30%
Revised θ_S (%)	22%	30%	35%	35%	35%
Baseline Q (m³/d)	1.85	8.57	28.9	134	59.1
Revised Q (m³/d)	1.91	8.64	28.9	134	59.1
Difference (%)	3%	1%	0%	0%	0%
Effect of Increasing θ_r by 50%					
Baseline θ_r (%)	5.5%	4.8%	3.0%	2.6%	1.5%
Revised θ_r (%)	8.3%	7.2%	4.5%	3.9%	2.3%
Baseline Q (m³/d)	1.85	8.57	28.9	134	59.1
Revised Q (m³/d)	1.81	8.54	28.9	134	59.1
Difference (%)	-2%	0%	0%	0%	0%
Effect of Increasing α* by 50%					
Baseline α' (kPa)	0.06	0.09	0.18	0.28	1.6
Revised α' (kPa)	0.09	0.14	0.27	0.42	2.4
Baseline Q (m³/d)	1.85	8.57	28.9	134	59.1
Revised Q (m³/d)	1.82	8.51	28.9	134	59.1
Difference	-2%	-1%	0%	0%	0%
Effect of Decreasing n by 0.5					
Baseline n	2.40	3.64	4.10	4.18	3.68
Revised n	1.90	3.14	3.60	3.68	3.18
Baseline Q (m³/d)	1.85	8.57	28.9	134	59.1
Revised Q (m³/d)	1.78	8.52	28.9	134	59.1
Difference	-4%	-1%	0%	0%	0%

Table 7b: Comparison of SEEP/W-simulated *steady flow rates Q* for normally-consolidated soils using different values of van Genuchten (1980) parameters, including *porosity* θ_S, *residual soil water content* θ_r, and the fitting parameters *α' and n.* Baseline and revised *steady flow rates* are shown for five types of normally consolidated soils.

Soil Property	Silty Fine Sand	Silty Fine-Coarse Sand	Fine Sand	Medium Sand	Sandy Gravel
Effect of Increasing θ_S by 5%					
Baseline θ_S (%)	40%	35%	40%	40%	40%
Revised θ_S (%)	45%	40%	45%	45%	45%
Baseline Q (m³/d)	3.27	4.30	29.2	78	209
Revised Q (m³/d)	3.31	4.31	29.2	77.8	209
Difference (%)	1%	0%	0%	0%	0%
Effect of Increasing θ_r by 50%					
Baseline θ_r (%)	4.8%	5.4%	2.9%	2.2%	1.3%
Revised θ_r (%)	7.2%	8.1%	4.4%	3.3%	2.0%
Baseline Q (m³/d)	3.27	4.30	29.2	77.8	209
Revised Q (m³/d)	3.25	4.29	29.2	77.8	209
Difference (%)	-1%	0%	0%	0%	0%
Effect of Increasing α* by 50%					
Baseline α' (kPa)	7.7	2.9	4.0	1.3	0.25
Revised α' (kPa)	11.5	4.3	6.0	1.9	0.37
Baseline Q (m³/d)	3.27	4.30	29.2	77.8	209
Revised Q (m³/d)	3.20	4.30	29.2	77.8	209
Difference	-2%	0%	0%	0%	0%
Effect of Decreasing *n* by 0.5					
Baseline *n*	4.30	3.20	4.20	4.30	3.90
Revised *n*	3.80	2.70	3.70	3.80	3.40
Baseline Q (m³/d)	3.27	4.30	29.2	77.8	209.0
Revised Q (m³/d)	3.25	4.29	29.2	77.8	209.0
Difference	-1%	0%	0%	0%	0%

Table 8a: Comparison of SEEP/W-simulated *steady flow rates Q* for glacially over-consolidated soils using different values of *background soil matric suction ψ_i* and *background soil water content θ_b* for four types of advance outwash soil *(Qva)* and one glacial till soil *(Qvt)*.

Background Soil Matric Suction and Water Content					
Soil Property	**Qvt**	**Silty Qva**	**Fine Qva**	**Fine-Medium Qva**	**Fine-Coarse Qva**
Baseline ψ_i (m)	3.1	1.8	0.8	0.5	0.09
Revised ψ_i (m)	1.4	0.9	0.5	0.3	0.05
Baseline θ_b (%)	10	10	10	10	10
Revised θ_b (%)	14	20	21	23	22
Baseline α^* (m^{-1})	1.17	1.33	2.5	3.9	25
Revised α^* (m^{-1})	1.17	1.33	2.6	4.1	27
Baseline Q (m^3/d)	1.85	8.57	28.9	134	59.1
Revised Q (m^3/d)	1.64	7.87	28.3	134	58.3
Difference (%)	-11%	-8%	-2%	0%	-1%

Table 8b: Comparison of SEEP/W-simulated *steady flow rates Q* for normally-consolidated soils using different values of *background soil matric suction ψ_i* and *background soil water content θ_b* for five types of normally-consolidated soil.

Background Soil Matric Suction and Water Content					
Soil Property	**Silty Fine Sand**	**Silty Fine-Coarse Sand**	**Fine Sand**	**Medium Sand**	**Sandy Gravel**
Baseline ψ_i (m)	13.6	6.3	7.4	2.4	0.5
Revised ψ_i (m)	8.7	3.3	5.2	1.7	0.36
Baseline θ_b (%)	9.8	10.4	7.9	7.2	6.3
Revised θ_b (%)	20	21	16	14	13
Baseline α^* (m^{-1})	1.8	5.5	3.5	11	57
Revised α^* (m^{-1})	1.8	5.6	3.5	11	58
Baseline Q (m^3/d)	3.27	4.30	29.2	77.8	209.0
Revised Q (m^3/d)	3.11	4.21	29	77.6	208
Difference (%)	-5%	-2%	-1%	0%	0%

3.5 Time to Achieve Steady-State Conditions

As discussed in Section 2.4, simulations were conducted to estimate when approximate steady-state conditions were achieved. For practical reasons, we deemed $Q_t/Q_{24} \leq 1.05$ as indicative of effective steady flow after "t" hr of infiltration. In addition, the ratio of Q_6/Q_{24} was evaluated because most field infiltration tests are terminated after about 6 hr (due to cost and feasibility).

As in actual field tests, simulated USSBP flow rate (Q) decreased with time to become effectively constant (Figs. 10a and 10b). The four coarse-grained soils (fine-medium Qva, fine-coarse Qva, medium sand, and sandy gravel) exhibited boundary interference effects for the deep borehole with $H = 20$ m. This is evidenced on Fig. 10b by an abrupt change in slope of Q vs. t at about 12 hr for fine-medium Qva and fine-coarse Qva.

Q_6/Q_{24} ratios are provided in Table 9a for glacially over-consolidated soils and in Table 9b for normally consolidated soils. Approximate steady-state flow conditions were achieved within six hr for soils with less than 12% silt in all test configurations except for fine Qva and fine sand in deep boreholes with 10 m and 20 m of ponding depth, with Q_6/Q_{24} ratios of 1.06 and 1.09, respectively. For soils with more than 12% silt the Q_6/Q_{24} ratios ranged from 1.04 to 1.27, indicating that steady-state conditions were not achieved within 6 hr for most of the test configurations.

Tables 10a and 10b summarize the time to achieve near-steady BP flow rate (i.e., $Q_t/Q_{24} \leq 1.05$) for the different representative soils and test configurations. This time varied substantially among test configurations and soil types, ranging from <0.2 hr for sandy gravel in the test pit configuration to <15.9 hr for silty fine sand in the test pit configuration.

Table 9a: SEEP/W simulated steady USSBP flow rate after 6-hr (Q_6) divided by steady USSBP flow rate after 24-hr (Q_{24}) for the glacially over-consolidated soils and the 15 test configurations. Soil conditions specified in Table 4 using the low estimate of K_s.

Test Configuration	Ratio of 6-hr Flow Rate (Q_6) to 24-hr Flow Rate (Q_{24})				
	Qvt	Silty Qva	Fine Qva	Fine-Medium Qva	Fine-Coarse Qva
Testpit (H = 0.05 m)	1.16	1.07	1.00	1.00	1.00
Testpit (H = 0.1 m)	1.16	1.07	1.01	1.00	1.00
Testpit (H = 0.25 m)	1.18	1.08	1.01	1.00	1.00
Testpit (H = 0.5 m)	1.19	1.09	1.01	1.00	1.00
Testpit (H = 1 m)	1.21	1.11	1.02	1.00	1.00
Shallow Borehole (H = 0.25 m)	1.10	1.05	1.00	1.00	1.00
Shallow Borehole (H = 0.5 m)	1.12	1.06	1.00	1.00	1.00
Shallow Borehole (H = 1 m)	1.15	1.07	1.01	1.00	1.00
Shallow Borehole (H = 2 m)	1.17	1.09	1.01	1.00	1.00
Shallow Borehole (H = 3 m)	1.18	1.11	1.02	1.00	1.00
Deep Borehole (H = 1.2 m)	1.12	1.06	1.01	1.00	1.00
Deep Borehole (H = 2 m)	1.14	1.07	1.01	1.00	1.00
Deep Borehole (H = 4 m)	1.15	1.09	1.02	1.00	1.00
Deep Borehole (H = 10 m)	1.17	1.13	1.06	1.00	1.01
Deep Borehole (H = 20 m)	1.17	1.14	1.09	-[a]	-[a]
Range	**1.10-1.21**	**1.05-1.14**	**1.00-1.09**	**1.00**	**1.00-1.01**

[a] Not valid since 24 hr results are impacted by boundary condition effects.

Table 9b: SEEP/W simulated steady USSBP flow rate after 6-hr (Q_6) divided by steady USSBP flow rate after 24-hr (Q_{24}) for the normally-consolidated soils and the 15 test configurations. Soil conditions specified in Table 4 using the low estimate of K_s.

Test Configuration	Ratio of 6-hr Flow Rate (Q_6) to 24-hr Flow Rate (Q_{24})				
	Silty Fine Sand	Silty Fine-Coarse Sand	Fine Sand	Medium Sand	Sandy Gravel
Testpit (H = 0.05 m)	1.19	1.05	1.00	1.00	1.00
Testpit (H = 0.1 m)	1.19	1.05	1.00	1.00	1.00
Testpit (H = 0.25 m)	1.21	1.07	1.00	1.00	1.00
Testpit (H = 0.5 m)	1.23	1.09	1.01	1.00	1.00
Testpit (H = 1 m)	1.27	1.13	1.01	1.00	1.00
Shallow Borehole (H = 0.25 m)	1.12	1.04	1.00	1.00	1.00
Shallow Borehole (H = 0.5 m)	1.15	1.06	1.01	1.00	1.00
Shallow Borehole (H = 1 m)	1.18	1.08	1.01	1.00	1.00
Shallow Borehole (H = 2 m)	1.21	1.12	1.02	1.00	1.00
Shallow Borehole (H = 3 m)	1.23	1.14	1.02	1.00	1.00
Deep Borehole (H = 1.2 m)	1.15	1.07	1.01	1.00	1.00
Deep Borehole (H = 2 m)	1.16	1.09	1.01	1.00	1.00
Deep Borehole (H = 4 m)	1.19	1.13	1.02	1.00	1.00
Deep Borehole (H = 10 m)	1.20	1.15	1.06	1.01	1.01
Deep Borehole (H = 20 m)	1.20	1.16	1.09	-[a]	-[a]
Range	**1.12-1.27**	**1.04-1.16**	**1.00-1.09**	**1.00-1.01**	**1.00-1.01**

[a] Not valid since 24 hr results are impacted by boundary condition effects.

Table 10a: SEEP/W-estimated time to achieve steady USSBP flow (Q_t) defined as Q within 5% of USSBP flow after 24-hr (Q_{24}) for glacially over-consolidated soils. Results are summarized for different H values and based on soil conditions specified in Table 4 using the low estimate of K_s.

Test Configuration	Time to Achieve Approximate Steady-State USSBP Flow				
	Qvt	Silty Qva	Fine Qva	Fine-Medium Qva	Fine-Coarse Qva
Testpit (r = 1 m)	<15.5 hrs	<10.1 hrs	<3.1 hrs	<0.5 hrs	<0.8 hrs
Shallow Borehole (r = 0.25 m)	<14.8 hrs	<10.3 hrs	<3.7 hrs	<0.7 hrs	<1.2 hrs
Deep Borehole (r = 0.1 m)	<14.8 hrs	<13 hrs	<9.2 hrs	<2.3 hrs	<4.2 hrs

Table 10b: SEEP/W-estimated time to achieve steady USSBP flow (Q_t) defined as Q within 5% of USSBP flow after 24-hr (Q_{24}) for normally-consolidated soils. Results are summarized for different H values and based on soil conditions specified in Table 4 using the low estimate of K_s.

Test Configuration	Time to Achieve Approximate Steady-State USSBP Flow				
	Silty Fine Sand	Silty Fine-Coarse Sand	Fine Sand	Medium Sand	Sandy Gravel
Testpit (r = 1 m)	<16.5 hrs	<10.6 hrs	<3.0 hrs	<0.8 hrs	<0.2 hrs
Shallow Borehole (r = 0.25 m)	<16.0 hrs	<12.4 hrs	<3.7 hrs	<1.0 hrs	<0.4 hrs
Deep Borehole (r = 0.1 m)	<15.9 hrs	<14.1 hrs	<9.8 hrs	<3.9 hrs	<1.2 hrs

3.6 Simulation Results for Two Closely-Spaced Storm Events

As demonstrated in Section 3.4, increasing the background moisture content can reduce the infiltration capacity of an infiltration facility for fine-grained soils. It is likely that during the wet season an infiltration facility will experience closely spaced rain events and the background moisture content may be significantly higher than during the infiltration testing conducted to support design of the infiltration facility. Therefore, the maximum infiltration capacity of an operational infiltration facility during wet periods may be less than predicted based on infiltration testing. As discussed in Section 2.5, this hypothesis was evaluated by comparing the results of two six-hr infiltration tests spaced 24 hr apart.

The results for all 10 soils are provided in Table 11a for a testpit with 1 m of ponding ($H/r = 1.0$) and in Table 11b for a deep well with 10 m of ponding ($H/r = 100$). As shown in these Tables, the flow rate during the second test decreased by 5% to 19% for fine-grained soils in the test pit configuration and by 5% to 9% for fine-grained soils in the deep borehole configuration. For the soils with less than 12% silt the flow reduction was 2% or less in both configurations. These results are consistent with the results of Section 3.5, which showed that USSBP test in fine-grained soils did not achieve steady-state conditions by the end of a six-hr test. In addition, the second test is likely a good representation of conditions beneath an operational facility during a period with closely-spaced storm events.

Comparison of the Qvt and silty fine sand results for the testpit (Table 11a) and the deep well (Table 11b) demonstrates that higher background moisture has a more significant impact when H/r_e is smaller. Simulations were not conducted for $H/r < 1.0$ and it is likely that the flow reduction for Qvt and silty fine sand will be greater for smaller values of H/r.

Based on the results summarized above, a correction factor of 5% to 30% is recommended for soils with more than 12% silt to account for different background moisture content beneath an operational infiltration facility compared with a test facility. Soils with less than 12% silt may not require any correction for background moisture content.

Table 11a: Comparison of SEEP/W-simulated *steady flow rates Q* for two six-hr infiltration test conducted in a testpit with 1 m of ponding ($H/r = 1.0$). There is a 24-hr recovery period between the tests and the time to completely drain the facility after the first test is also provided. Results provided for 10 representative soils, including four types of advance outwash soil (*Qva*) and one glacial till soil *(Qvt)*.

Soil	Test 1 Flow (m³/d)	Drain Time (hr)	Test 2 Flow (m³/d)	Flow Reduction
Silty Fine Sand	9	18.1	7.41	18%
Silty Fine-Coarse Sand	11.1	13.6	10.4	6%
Fine Sand	63.5	2.3	63.2	0%
Medium Sand	182	0.9	182	0%
Sandy Gravel	507	0.3	507	0%
Qvt	4.02	>24	3.25	19%
Silty Qva	15.7	8.7	14.9	5%
Fine Qva	45.3	2.6	45.3	0%
Fine-Medium Qva	203	0.7	204	0%
Fine-Coarse Qva	87.5	2.1	87.5	0%

Table 11b: Comparison of SEEP/W-simulated *steady flow rates Q* for two six-hr infiltration test conducted in a deep borehole with 10 m of ponding ($H/r_e = 100$). There is a 24-hr recovery period between the tests and the time to completely drain the facility after the first test is also provided. Results provided for 10 representative soils, including four types of advance outwash soil (*Qva*) and one glacial till soil *(Qvt)*.

Soil	Test 1 Flow (m³/d)	Drain Time (hr)	Test 2 Flow (m³/d)	Flow Reduction
Silty Fine Sand	38.6	21.1	35	9%
Silty Fine-Coarse Sand	64.2	24	59.5	7%
Fine Sand	336	6.1	328	2%
Medium Sand	1025	1.1	1023	0%
Sandy Gravel	3010	0.2	3010	0%
Qvt	15	>24	14	7%
Silty Qva	66.6	14.5	63.1	5%
Fine Qva	227	7.1	223	2%
Fine-Medium Qva	1045	1.5	1045	0%
Fine-Coarse Qva	509	1.0	509	0%

4 Discussion

4.1 Uncertainty in the USSBP Analysis

As discussed in Section 3.2, the calibration conducted in this study provides K_s estimates with maximum error of 11.2% and average error of 3.3% for a selected range of representative soils (Tables 4a and 4b) and H/r ratios (Table 3). Fig. 9 shows the 95% confidence limits for K_s for each shape function. As shown on the figure, the 95% confidence bands are less than 8.0% for all H/r ratios and all soil types. Although these errors might be reduced by defining more than four shape functions (Table 5), this is likely not warranted as actual field soils have unknown and uncontrollable degrees of heterogeneity and anisotropy.

The figure also illustrates that the shape functions for $H/r \geq 20$ (Figures 9c and 9d) are more accurate than the shape functions for $H/r \leq 20$ (Figures 9a and 9b) when $H/r = 20$. Therefore, the high ponding depth shape functions should be used when $H/r = 20$.

The sorptive number, α^* (m^{-1}), represents the capillarity of the soil, and can be determined for each soil using Eq. 2.3. and the method illustrated in Sections 2.2.3 and 2.2.4.   However, given natural variability and other uncertainties, most practitioners will likely be satisfied selecting the most appropriate α^* in Table 5 based on soil texture and density information. The relative proportion of capillarity flow usually increases with increasing fines (i.e., increasing silt content), and this is represented in the USSBP analysis (Eq. 8) by smaller α^* values (i.e. capillarity flow increases as α^* decreases). Hence, uncertainty in α^* has proportionately greater impact on K_s accuracy in fine soils than in coarse soils. This can always be mitigated, however, by increasing the H/r ratio, which decreases the proportion of capillarity flow relative to pressure flow (Fig. 8, see also Reynolds 2008).

4.2 Limitations of the USSBP Method

As discussed in Reynolds (2008), Archer et al. (2014) and others, the USSBP approach does not account for the following factors:

- Entrapped or encapsulated air. Rapidly infiltrating water from the USSBP test facility can entrap/encapsulate air in soil pores, which may decrease flow and reduce the effective K_s value. This air often dissolves gradually, resulting in an increase in effective K_s over time.
- Siltation and/or drill-induced smearing and compaction along the test facility wall and base. Infiltration surfaces that are substantially silted, smeared or compacted have lower K_s values than the background soil.
- Proximity of a water table. A regional or perched water table that intersects or occurs just below a test facility can reduce hydraulic gradients, producing flow and K_s estimates that are artificially low.
- Heterogeneity and/or anisotropy. In heterogeneous soils, the USSBP method provides a bulk average K_s of the soil volume wetted by the test facility (Fig. 6). In materials with vertical-horizontal anisotropy, the USSBP tends to yield a K_s value that falls between the vertical K_s and the horizontal K_s (e.g. Reynolds and Elrick 1985).

As one or more of these factors are likely present in all borehole infiltration tests, K_s estimates from field testing will inevitably reflect the aggregate effects of manmade and natural porous medium conditions within the wetted soil surrounding the pit/borehole injection zone. One might argue, however, that the same porous medium conditions will also exist in production-scale stormwater infiltration facilities; and hence K_s estimates perturbed by the above factors are appropriate, and perhaps even preferred, for feasibility assessments and facility design.

The results provided in Section 3.5 (steady-state analysis) and Section 3.6 (two six-hr tests conducting within 24 hr) demonstrate that six-hr USSBP tests in fine-grained soils do not achieve steady state and may overestimate the maximum performance of operational infiltration facilities by 5% to 19% during periods of high precipitation. Based on these results, a correction factor of 10% to 30% is recommended for soils with more than 12% silt if

infiltration test durations are limited to six hr. A correction factor of 5% to 10% is recommended for 6-hr deep borehole tests in fine sands with more than 4 m of ponding depth. Medium- and coarse-grained sandy soils may not require any correction for test methodology.

4.3 Applicability of these USSBP Fitting Parameters

The C_u shape function parameters in Table 5 were developed based on soils in the Puget Sound region that are typically considered for stormwater infiltration. These shape function parameters are likely valid in other parts of the world with glacially over-consolidated soils and normally consolidated soils with similar grain-size distributions. Glacially over-consolidated soils are also found across most of Canada, southern Alaska, the mid-western and northeast portions of the United States, Scandinavia, the northern portions of the British Isles, the northern portions of eastern Europe, portions of Russia, and within the world's major mountain ranges (ArcGIS 2017).

The shape function parameters in Table 5 require further validation, however, before use in in soils with different structure or grainsize distributions. In particular, shape function parameters were not developed for soils with more than 30% silt content, as these soils are typically considered unsuitable for infiltration in the Puget Sound region. Additional calibration and field validation is warranted to develop shape function parameters for very silty soils.

5 Conclusions

Numerical simulations of USSBP tests were used to develop four sets of recalibrated C_u uncased shape function fitting parameters (Z_1, Z_2, Z_3, Eq. 1.2, Table 5) for use in glacially over-consolidated soils (advance outwash and glacial till) and normally-consolidated soils. The parameters were developed for H/r ratios between 0.05 and 200 and apply to both excavated pits and boreholes completed above the water table. The parameters provided USSBP estimates of soil K_s with a maximum error of 11.2% and an average error of 3.3%, which is more than accurate enough for feasibility assessment and design of stormwater infiltration facilities. The original C_u fitting parameters published by Zhang et al. (1998) caused unacceptably large K_s errors up to 51%. The numerical simulations were also used to develop criteria for estimating time required to achieve steady USSBP flow, and for correcting K_s estimates when steady USSBP flow was not achieved.

It was concluded that the USSBP method using recalibrated C_u shape functions is suitable for estimating K_s in glacially over-consolidated and normally-consolidated soils generally considered for stormwater infiltration within the Puget Sound region of western Washington State (United States), and in other parts of the world with similar soils. The calibration approach developed here could be used to develop USSBP shape functions for other soil types and specialized testing configurations.

References

ArcGIS (2017) Ice extent and coastline at the last glacial maximum, https://www.arcgis.com/home/item.html?id =f1e7378b962d42168fdefec3b6eb8b5f.

Archer NA, Bonell M, MacDonald AM, Coles N (2014) A constant head well permeameter formula comparison: its significance in the estimation of field-saturated hydraulic conductivity in heterogeneous shallow soils, Hydrology Research 45(6):788-805, DOI:10.2166/nh.2014.159

Aubertin M, Mbonimpa M, Bussière B, Chapuis RP (2003) A model to predict the water retention curve from basic geotechnical properties, Canadian Geotechnical Journal 40(6):1104-1122, DOI:10.1139/t03-054

Elrick DE, Reynolds WD, Tan KA (1989) Hydraulic conductivity measurements in the unsaturated zone using improved well analyses, Ground Water Monitoring Review IX(3):184-193, DOI:10.1111/j.1745-6592.1989.tb01162.x

Elrick DE, Reynolds WD (1992) Methods for analyzing constant head well permeameter data, Soil Science Society of America Journal 56(1):320-323, DOI:10.2136/sssaj1992.03615995005600010052x

Kindred JS, Reynolds WD (2020) Using the borehole permeameter to estimate saturated hydraulic conductivity for glacially over-consolidated soils, Hydrogeology Journal 28:1909–1924, DOI:10.1007/s10040-020-02149-3

Mualem Y (1976) A new model predicting the hydraulic conductivity of unsaturated porous media, Water Resources Research. 12(3):513–522, DOI:10.1029/WR012i003p00513

Philip JR (1985) Approximate analysis of the borehole permeameter in unsaturated soil, Water Resources Research v. 21(7):1025-1033, DOI:10.1029/WR021i007p01025

Reynolds WD, Elrick DE, Topp CG (1983) A reexamination of the constant head well permeameter method for measuring saturated hydraulic conductivity above the water table. Soil Science 136(4): 250-268, DOI:10.1016/0016-7061(93)9

Reynolds WD, Elrick DE, Clothier BE (1985) The constant head well permeameter: effect of unsaturated flow. Soil Science 139(2): 172-180, DOI: 10.1097/00010694-198502000-00011

Reynolds WD, Elrick DE (1985) In situ measurement of field-saturated hydraulic conductivity, sorptivity, and the α-parameter using the Guelph permeameter. Soil Science 140(4):292-302, DOI: 10.1097/00010694-198510000-00008

Reynolds WD (2008) Saturated hydraulic properties: well permeameter. In M.R. Carter and E.G. Gregorich (ed.) Soil sampling and methods of analysis. 2nd ed. CRC Press, Boca Raton, FL. p. 1025–1042

Reynolds WD (2010) Measuring soil hydraulic properties using a cased borehole permeameter: steady flow analyses, Vadose Zone Journal, Volume 9(3):637-652, DOI:10.2136/vzj2009.0136

Reynolds WD (2011) Measuring soil hydraulic properties using a cased borehole permeameter: falling-head analysis, Vadose Zone Journal, Volume 10(3):999–1015, DOI: 10.2136/vzj2010.0145

Reynolds WD (2013) An assessment of borehole infiltration analyses for measuring field-saturated hydraulic conductivity in the vadose zone, Engineering Geology 159:119-130, DOI: 10.1016/j.enggeo.2013.02.006

Reynolds WD (2015) A generalized variable-head borehole permeameter analysis for saturated, unsaturated, rigid or deformable porous media, Engineering Geology 185:10-19, DOI: 10.1016/j.enggeo.2014.11.019

Stephens DB, Neuman SP (1982) Vadose zone permeability tests: summary. American Society Civil Engineering, Proc. Journal of the Hydraulics Division, Volume 108(5):623-639

Stephens DB, Lambert K, Watson D (1987) Regression models for hydraulic conductivity and field test of the borehole permeameter, Water Resources Research, v. 23(12):2207-2214, DOI:10.1029/WR023i012p02207

van Genuchten (1980) A closed-form equation for predicting the hydraulic conductivity of unsaturated soils, Soil Science Society of America Journal 44(5):892-898, DOI: 10.2136/sssaj1980.03615995004400050002x

WSDOE (Washington State Department of Ecology) (2019) Stormwater Management Manual for Western Washington, July 2019, Publication Number 19-10-021

Zangar CN (1953) Theory and problems of water percolation, U.S. Department of the Interior, Bureau of Reclamation, Denver, CO, Engineering Monogram No. 8

Zhang ZF, Groenevelt PH, Parkin GW (1998) The well-shape factor for the measurement of soil hydraulic properties using the Guelph permeameter, Soil and Tillage Research, 49(3):219-221, DOI:10.1016/S0167-1987(98)00174-3

Figures

Figure 1: SEEP/W axisymmetric model domains and boundary conditions for the three test facility configurations (test pit, shallow borehole, deep borehole) used for calibration of the BP shape function fitting parameters. The "fixed head" boundary condition applies to the base and submerged portion of the test facility wall, and it refers to specified hydraulic head that is constant in space and time.
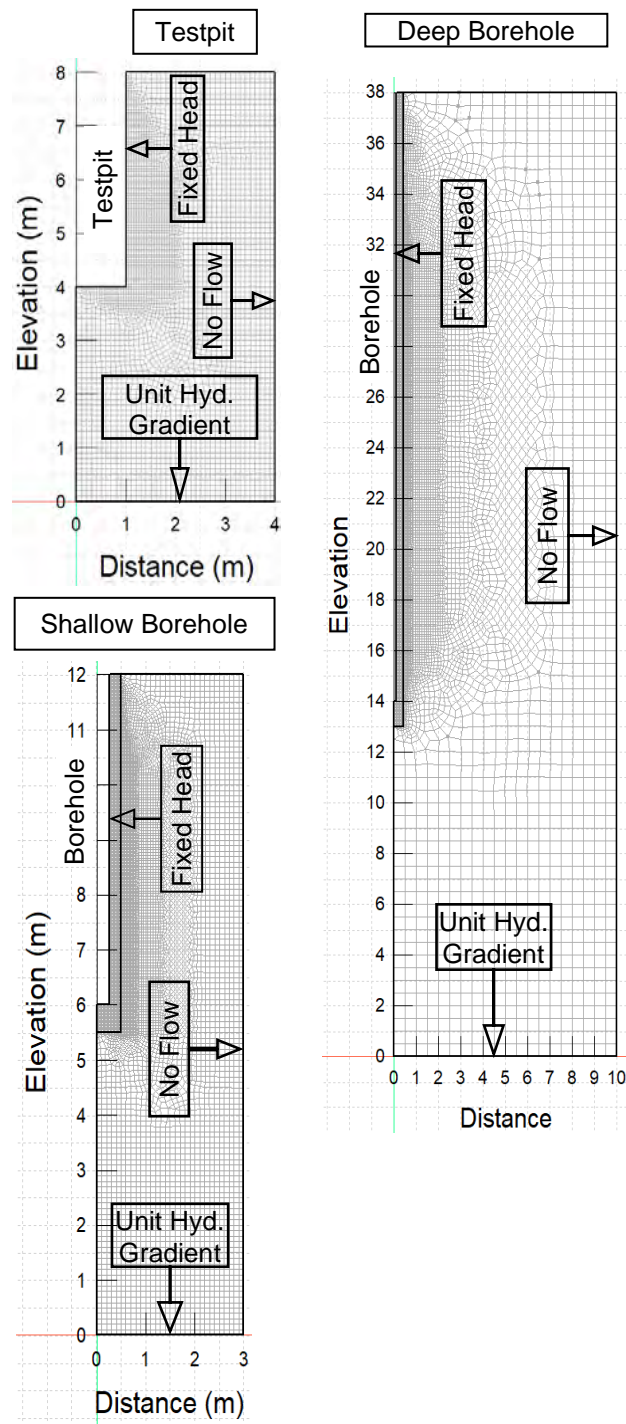
Figure 2: Grainsize distribution curves (percent passing) for representative soils that were used for calibration. The grain size percent-passing values, D_{60} and D_{10}, for each soil were used in SEEP/W for creating the Modified Kovacs soil water content curves shown in Fig. 3.
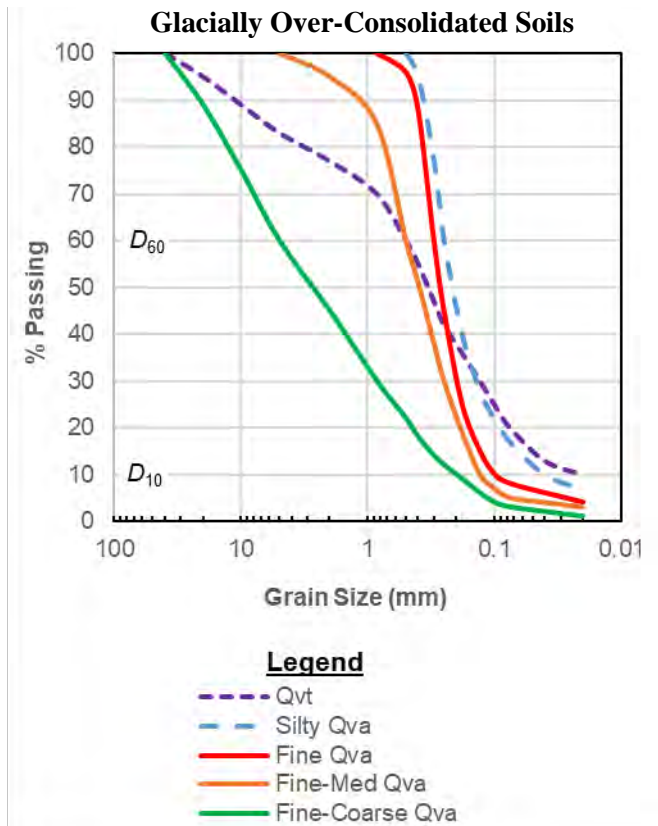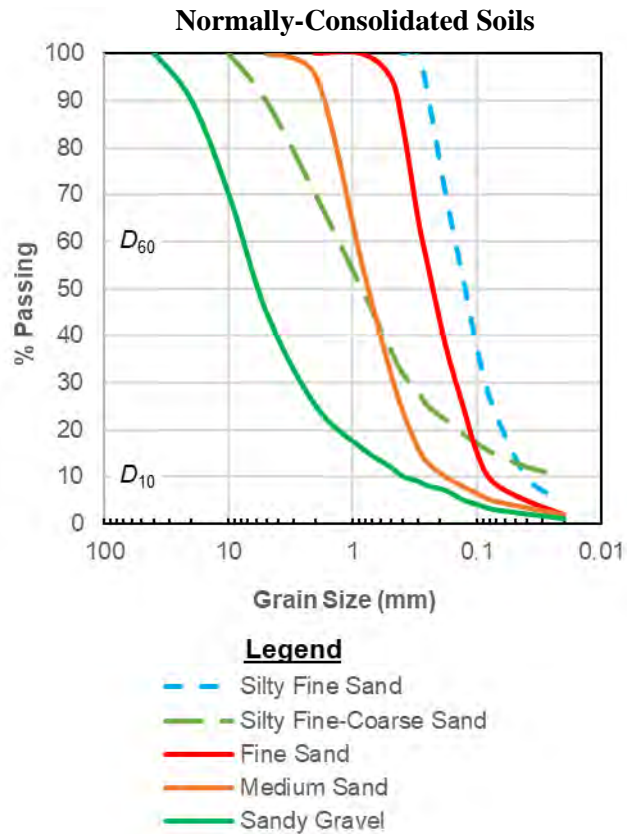
Figure 3: Volumetric soil water content curves used for SEEP/W simulation of USSBP flow (see Table 4 for soil properties). This figure illustrates the match between the Modified Kovacs model (solid blue line) and the van Genuchten model (dashed orange line).
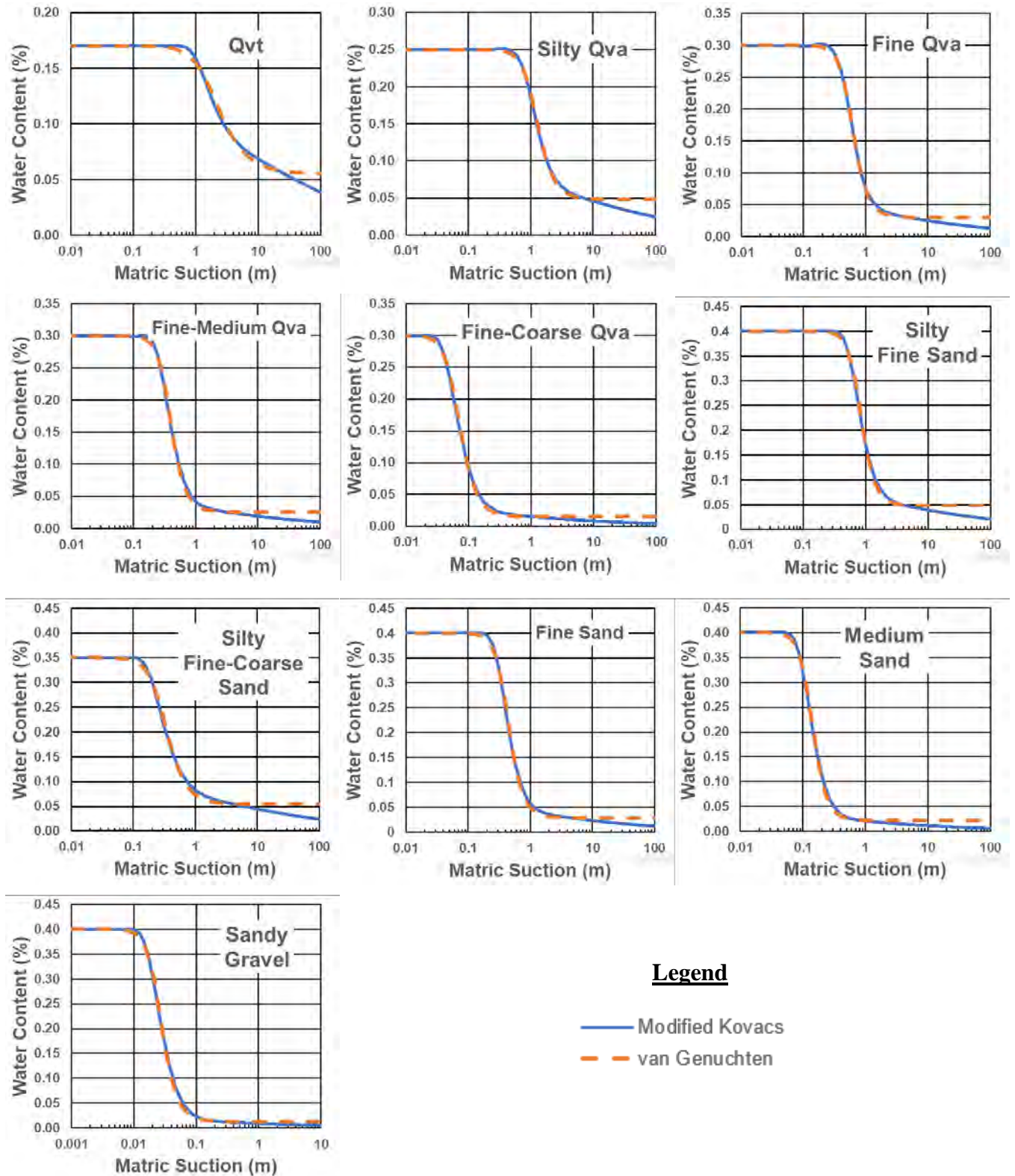
Figure 4: Example unsaturated hydraulic conductivity curves $K(\psi)$ used for SEEP/W simulation of BP flow. Soil properties provided in Table 4.
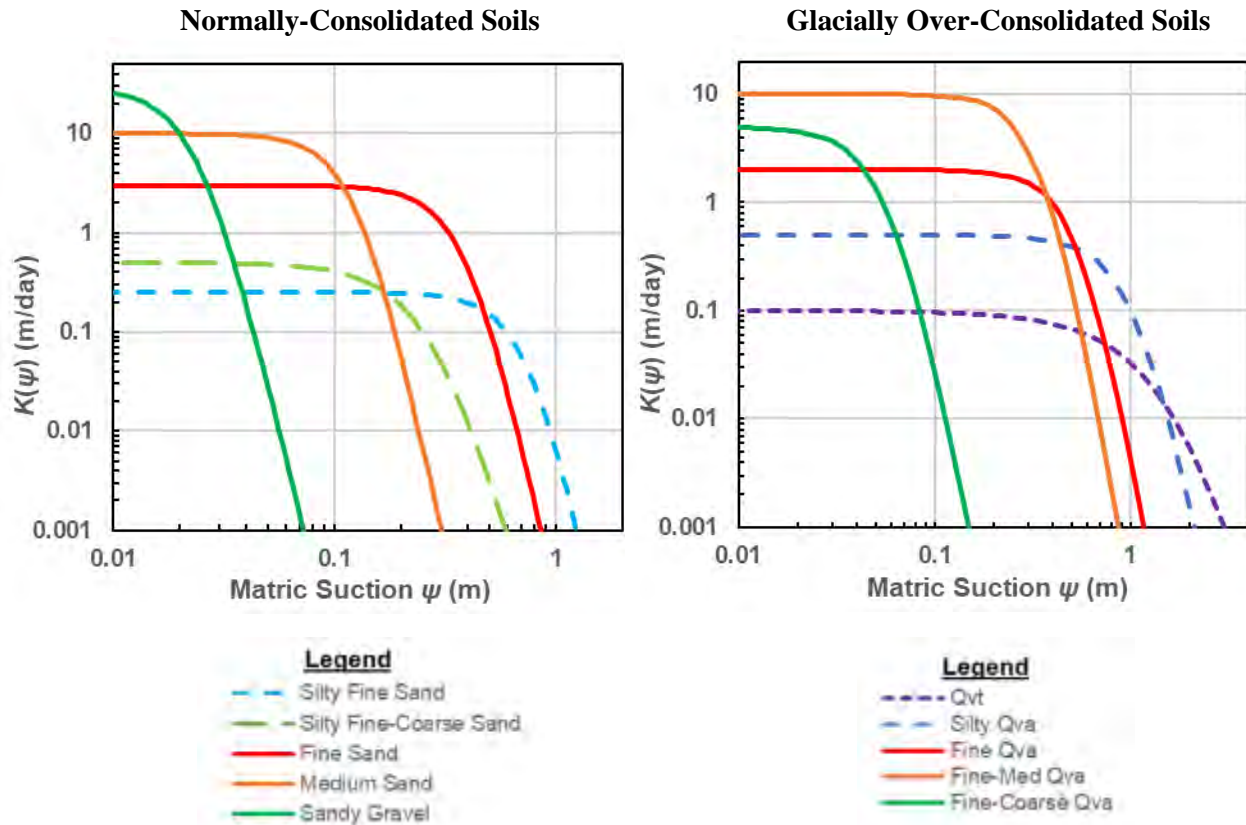
Figure 5: Calculated values of α^* as a function of background soil water content, θ_b. Soil properties provided in Table 4. Note that α^* is relatively constant until the soil approaches full saturation. The black dots indicate the matric suction used for background conditions in the simulations.
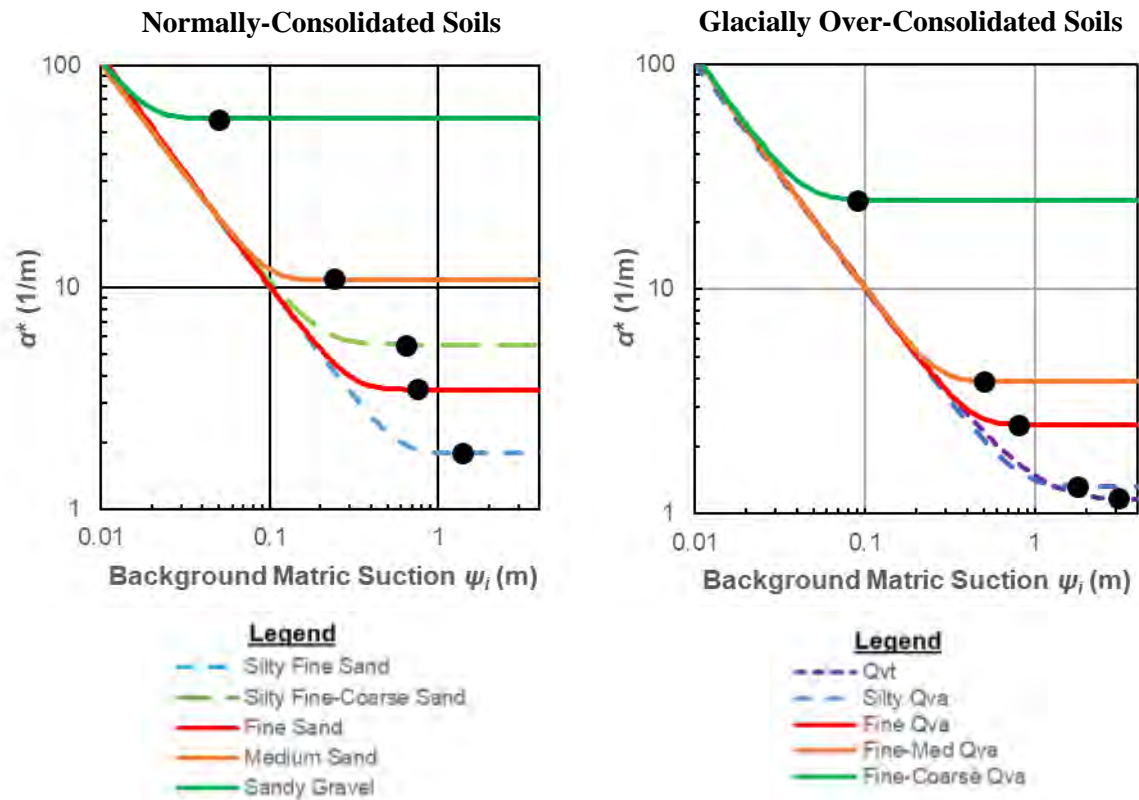
Figure 6: Zero matric suction and water content contours after 6 hr of SEEP/W simulated flow. Borehole configuration was $H = 2$ m and $r = 0.25$ m, $H/r = 8$.
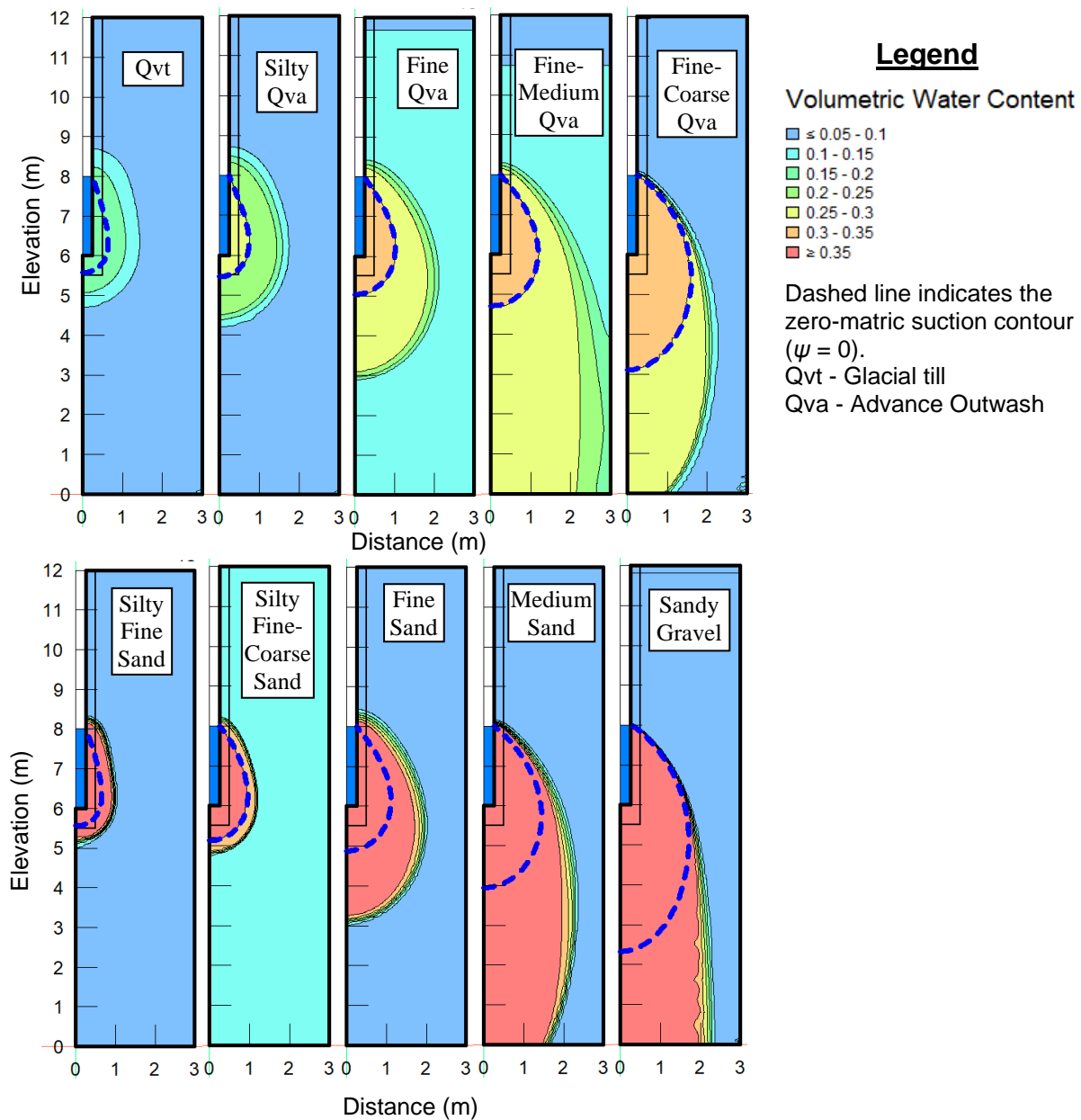
Figure 7: Calibrated uncased shape functions (C_u) for soils with < 12% silt (green lines) and soils with > 12% silt (red lines), Panel (a) shows shape functions for H/r between 0 and 200; panel (b) shows a close up for H/r less than 22. Zhang et al. (1998) shape function for $\alpha^* = 4.1$ m^{-1} is provided for comparison. H is borehole ponding depth, r is test facility (pit or borehole) radius.
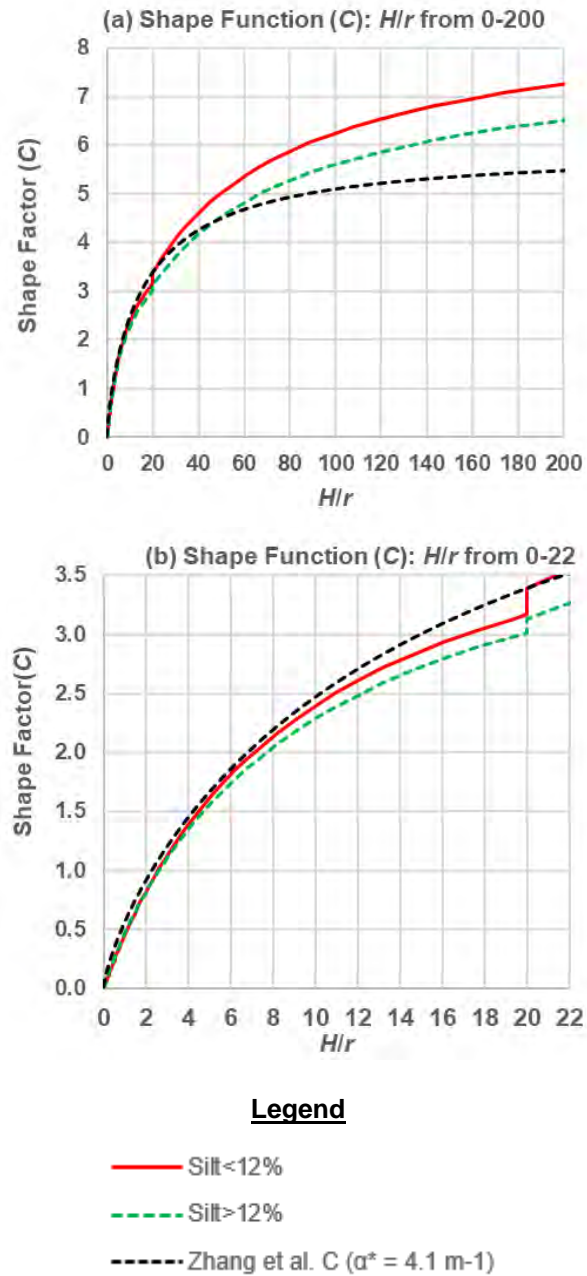
Figure 8: Relative importance of steady BP pressure flow (blue solid line), gravity flow (orange dashed line), and capillarity flow (green dotted line) versus H/r ratio for the ten representative soils. Soil properties are provided in Table 4. Percentages are calculated using Eq. 6 with borehole radius, r, fixed at 1 m; and borehole ponding depth, H, varied from 0.01 m to 100 m.
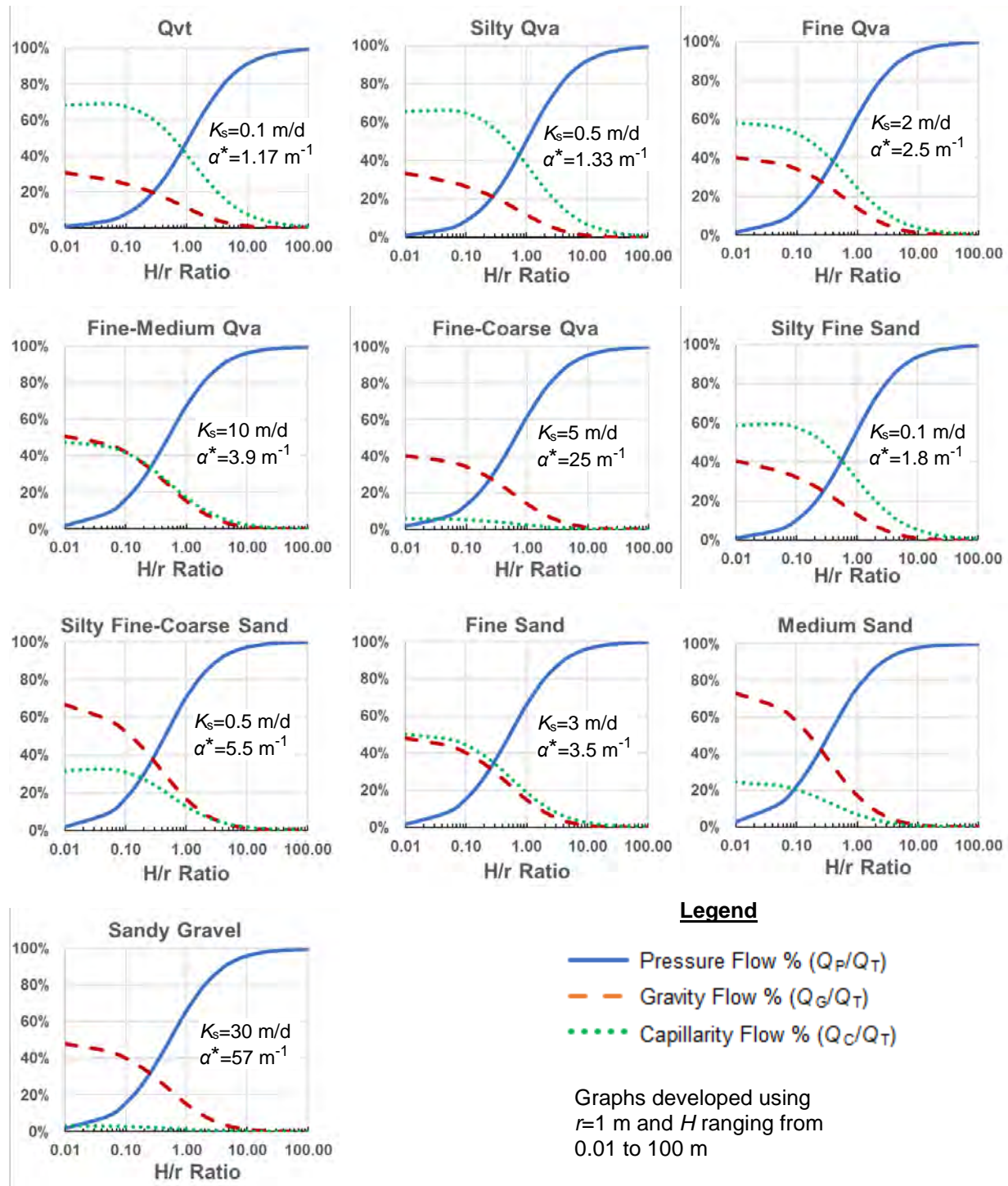
Figure 9: Mean and 95th percentile confidence limits (CL) for USSBP estimates of saturated hydraulic conductivity (K_s). Each graph represents one of the four uncased shape functions (C_u) developed for different silt content and H/r ratios.
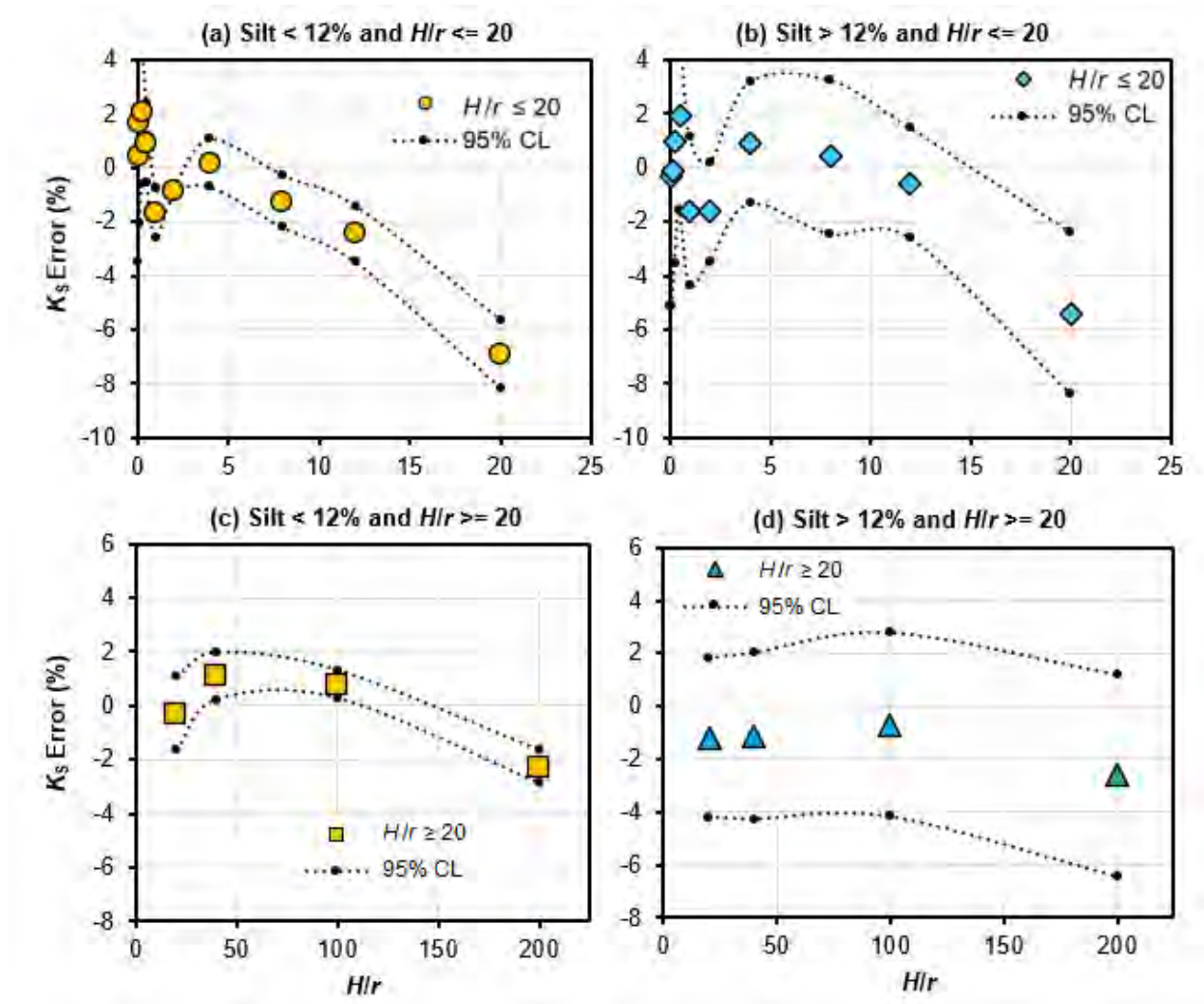
Figure 10: Simulated steady BP flow (*Q*) versus time in four advance outwash soils (Qva) and one glacial till soil (Qvt) (Table 4) for: (a) Testpit configuration with *H* = 1 m, *r* = 1 m; and (b) deep borehole configuration with *H* = 20 m, *r* = 0.1 m. The sudden change in slope of *Q* vs. *t* in the fine-medium Qva soil at approximately 12 hr (b) occurred because BP flow contacted the bottom flow domain boundary.
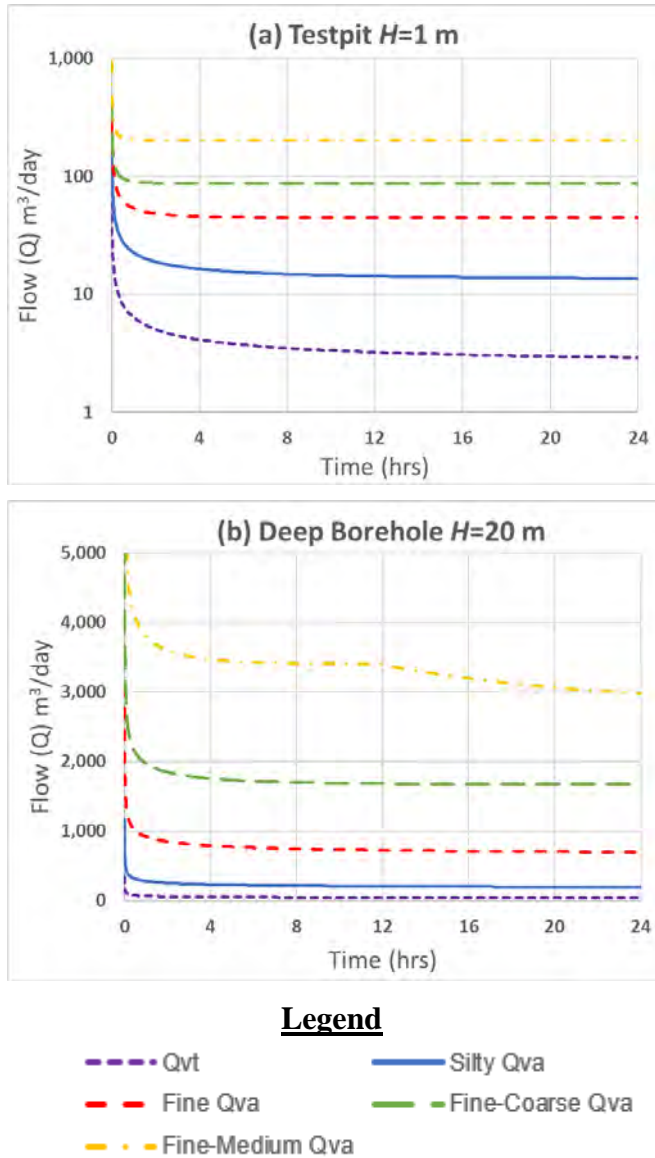
VOLUME II: USING THE CASED STEADY-STATE BOREHOLE PERMEAMETER METHOD TO ESTIMATE SATURATED HYDRAULIC CONDUCTIVITY

Near-Term Action (NTA) 2018-0827: Flexible Infiltration Test Methods for Evaluating Infiltration Feasibility

Project No. TAC-20-1 • October 10, 2022

Volume II - Contents

Volume II - List of Tables

Volume II - List of Figures

Volume II - Abstract

As described in Volume I, the uncased steady-state borehole permeameter (USSBP) method was developed in the 1950's by the United States Bureau of Reclamation to estimate saturated soil hydraulic conductivity (K_s) in shallow boreholes and excavated pits completed above the water table when the ponding depth does not exceed the gravel or sandpack interval of the facility in direct connection with native soils. Reynolds (2010) extended this method for cased boreholes (i.e., wells) where the ponding depth is greater than the sandpack interval of the well and rises up into a solid casing. This approach is referred to as the cased steady-state borehole permeameter (CSSBP) method.

Volume II provides calibration of the CSSBP method for both glacially over-consolidated soils and normally consolidated soils with ponding depth (H) ranging from 1 m to 40 m, sandpack interval (L) ranging from 0 m to 20 m, and borehole radius (r_b) ranging from 5 cm to 75 cm. Calibration was conducted using numerically simulated pseudo steady-state flow simulations for ten representative soils to calibrate CSSBP shape function fitting parameters (Z_1, Z_2, Z_3) for a broad range of well configurations, including hand-augered wells with r_b of 5 cm, drilled test wells with r_b of 10 cm and 25 cm, and large-diameter drywells with r_b of 75 cm. The representative soils included five glacially over-consolidated soils and five normally-consolidated soils and were designed to cover the range of soils typically considered for stormwater infiltration in the Puget Sound Basin.

After numerous trial calibration attempts, a good balance between accuracy and simplicity was achieved by calibrating separate fitting parameters for $L/r_b < 20$ and $L/r_b \geq 20$ and soils with < 12% silt content and soils with > 12% silt content. CSSBP estimates of K_s provided a maximum error of 13.3% and an average error of 5.1% using these calibrated shape function parameters.

Additional findings from this task include:

- Approximate steady-state flow conditions (a key assumption of the CSSBP method) were generally achieved for soils with $K_s > 5$ m/d within 6 hr. In contrast, 6-hr infiltration tests in fine-grained soils with lower K_s may need correction factors to better estimate steady-state flow rates and more accurately predict K_s. These correction factors, expressed as the ratio of steady-state flow divided by the 6-hr flow, can range from 0.88 to 1.0 for soils with K_s between 1 and 5 m/d (with the lowest values for the drywell scenarios and the test well scenarios with $L \geq 10$ m) and from 0.77 to 0.94 for soils with K_s less than 1 m/d. In general, lower correction factors were observed as r_b increased.

- Low permeability sandpack material ($K_s < 1,000$ m/d) and/or well losses due to turbulent flow through the screen and within the sandpack can significantly impact the infiltration capacity of test wells in permeable native soils. Future field testing will evaluate the potential impact of low sandpack permeability and well losses.

- The USSBP method is calibrated for uncased scenarios where $H = L$ and the CSSBP method is calibrated for cased scenarios where $H > L$. However, there is a transition interval as the water level begins to rise above the sandpack into the solid casing extending above the sandpack. Based on comparison of both methods with numerical simulation results, the CSSBP method should be used rather than the USSBP method when H/L is > 1.2.

- Results from small-diameter test wells were compared with results from large-diameter wells for a broad range of soils and test configurations. Most of the results were within 10%, although the results were up to 19% different in a few scenarios.

National Estuary Program (NEP) Stormwater Strategic Initiative in support of Puget Sound Partnership's Near-Term Action (NTA) 2018-0827. The Washington State Department of Ecology is administrating this study under agreement with the City of Tacoma. The City of Tacoma has contracted with a consultant team led by Kindred Hydro, Inc. to complete the work.

1 Introduction

Stormwater infiltration is now required where feasible for new development in Washington State and the 2019 Stormwater Management Manual for Western Washington (WSDOE 2019) provides a variety of methods for sizing infiltration facilities. The preferred method is either the small or large pilot infiltration test (PIT). Volume I provides a brief summary of the PIT method.

A more accurate and reliable approach is to determine infiltration rate and capacity using measurements of soil saturated hydraulic conductivity (K_s) obtained from the borehole permeameter (BP) methods that formally account for both flow directions (vertical, horizontal), and all three components of soil water flow (pressure, gravity, capillarity). A summary of the BP methods was provided by Kindred and Reynolds (2020). Volume I provided calibration parameters for the uncased steady-state well or borehole permeameter (USSBP) method for soils that are typically considered for stormwater infiltration in the Puget Sound basin and H/r_b ratios ranging from 0.05 to 200.

The previous work in Kindred and Reynolds (2020) and Volume I did not address the steady-state BP methods for cased wells, that is, wells where H is greater than the sandpack interval (L), referred to here as the cased steady-state borehole permeameter (CSSBP) method. Reynolds (2010) developed equations for cased wells with vertical flow only (flow out of the bottom of the well casing, $L = 0$) and a combination of vertical and horizontal flow (wells with $L > 0$). Reynolds (2010) limited his analysis to the following dimensions: r between 3 and 7.5 cm, L between 0 and 0.45 m, and H between 0.03 and 2 m. Typical stormwater infiltration wells, including test wells, have much larger dimensions. Volume II evaluates r between 5 and 75 cm, L between 0.5 and 20 m, and H between 1 and 30 m for the CSSBP method.

1.1 Scope of Work and Purpose

The primary objective of this task was to evaluate the cased steady-state borehole permeameter (CSSBP) equations provided by Reynolds (2010) for typical well configurations and soils that are usually considered for stormwater infiltration in the Puget Sound Basin and develop calibration parameters for the CSSBP equations. Secondary objectives were to: 1) develop criteria for correcting K_s estimates when steady CSSBP flow was not achieved; 2) evaluate the potential impacts of screen and sandpack head losses, 3) evaluate when to transition from the USSBP method to the CSSBP method as H gradually rises above the well sandpack, and 4) the ability of infiltration tests in small-diameter wells to predict the capacity of larger-diameter wells. For consistency with previously published work, metric units are used throughout Volume II.

2 Materials and Methods

2.1 Cased Steady-State Borehole Permeameter (CSSBP) Equation

As summarized in Volume I, considerable research has been conducted regarding analytical methods for estimating K_s from borehole infiltration tests in the unsaturated zone. Kindred and Reynolds (2020) provide a concise history of the evolution of this method for uncased boreholes and pit excavations. Reynolds (2010) provides the following equation for cased boreholes and wells:

$$Q = \frac{2\pi LHK_s}{C_c} + \pi r^2 K_s + \frac{2\pi L\emptyset_m}{C_c} \quad \text{(Eq. 1.1)}$$

where

$$C_c = \left[\frac{(L/r_b)}{Z_1 + Z_2(L/r_b)}\right]^{Z_3} \quad \text{(Eq. 1.2)}$$

Q (m³/d) is the flow rate at steady state, L (m) is the sandpack interval, $\emptyset_m$ (m²/d) is the matric flux potential, C_c is the CSSBP shape function (dimensionless), and Z_1, Z_2, and Z_3 are the shape function fitting parameters (dimensionless). Reynolds (2010) uses a different form of C_c that is physically based but the empirical fitting relationship provided in Eq. 1.2 is consistent with the approach used by Kindred and Reynolds (2010) and others.

Although Reynolds (2010) provides methods for estimating both K_s and $\emptyset_m$, stormwater design professionals are typically only interested in K_s. Using the precedent utilized by Kindred and Reynolds (2020), $\emptyset_m$ can be replaced with the following relationship:

$$\emptyset_m = \frac{K_S}{\alpha^*} \quad \text{(Eq. 2)}$$

where α^* is the soil sorptive number (m⁻¹). Using Eq. 2 and rearranging Eq. 1.1 to solve for K_s provides:

$$K_S = \frac{C_c Q}{2\pi LH + \pi r_b^2 C_c + \frac{2\pi L}{\alpha^*}} \quad \text{(Eq. 3)}$$

Eq. 3 assumes that L is less than H and is the same form as the USSBP equation (Equation 1.1 in Volume I). The three terms in the denominator of Eq. 3 account, respectively, for flow through the wall and base of the well due to the hydrostatic pressure of the ponded water, gravity flow through the base of the well, and capillarity flow through the wall and base of the well due to the surrounding unsaturated porous material. Flow due to hydrostatic pressure accounts for most of the flow out of the test facility when L and $H \gg r$, while gravity flow and capillarity flow often dominate when L and/or $H < r$ (Reynolds 2008; Elrick and Reynolds 1992). The relative importance of the three flow components is evaluated in Volume I for USSBP tests.

2.2 CSSBP Calibration

The calibration procedure involved calculating K_s via the CSSBP equations (Eqs. 3 and 5) using steady flow-rate values (Q) generated by numerical simulations of CSSBP flow for 180 test scenarios. The test scenarios included all combinations of ten "representative" soils typically considered for stormwater infiltration in the Puget Sound Basin and 18 CSSBP test configurations where r varied from 5 cm to 75 cm, L varied from 0.5 m to 20 m, H varied from 1.0 m to 30 m, and the L/r ratio varied from 4 to 100. Calibration was conducted using the Solver© optimization

algorithm in Microsoft Excel©, which changes user-selected variables until a specified objective is minimized, maximized or becomes equal to a specified value. In this study, the C_c shape function fitting parameters (Z_1, Z_2, and Z_3 in Eq. 1.2) were varied by Solver© (using the generalized nonlinear reduced gradient method) until the maximum error between the CSSBP-calculated K_s values and the specified K_s values was minimized for the 180 test scenarios.

The pseudo steady-state flow rates for the 180 scenarios were estimated using SEEP/W, a finite element numerical model that can simulate multidimensional and axisymmetric flow in saturated and unsaturated porous media (GEOSLOPE International Ltd., Calgary, Alberta, Canada). Unsaturated flow simulation requires specifying soil hydraulic properties in the form of the unsaturated volumetric soil water content function $\theta(\psi)$ (soil water content as a function of soil matric suction) and the unsaturated hydraulic conductivity function $K(\psi)$ (hydraulic conductivity as a function of soil matric suction). These hydraulic property functions are described in Volume I.

2.2.1 *Model Domains and Test Configurations*

The SEEP/W numerical flow domains for the 18 test configurations are summarized in Table 1. As an example, Fig. 1 shows the large test well domain with $L = 1$ m. The simulations assumed axisymmetric flow, with no-flow boundaries along the top and outside radius of the flow domain, and a unit hydraulic head gradient boundary at the bottom of the flow domain. The simulations were designed to simulate test wells with a sandpack around the screen in the lower portion of the well and an impervious seal around the solid casing in the upper portion of the well. A fixed-head boundary conditions was applied to the center of the screened portion of the well.

The space inside the screen and casing was simulated as a SEEP/W material with 100% porosity and K_s of 10,000 m/d. The sandpack was simulated as a SEEP/W material with 40% porosity and K_s of 10,000 m/d. Simulating these regions in this manner resulted in no significant head losses during the simulations and provided results that matched the USSBP results for identical scenarios. In reality, sandpack K_s may be significantly less than 10,000 m/d and for native soils with high K_s, there may be significant head losses through the well screen and within the sandpack material. This dynamic is evaluated separately from the calibration process later in the Volume II.

Table 1 provides the screen and casing radius (r_s), boring radius (r_b), the screen and sandpack height (L), ponding depth (H), L/r ratio, and the width and height of the simulation domain for each of the 18 test scenarios. The simulations used graded meshes of rectangular and triangular finite elements. As illustrated in Fig. 1, element size increased in steps from the well casing to the outer regions of the simulation domain with a minimum size of approximately 0.8 cm and a maximum size of 50 cm.

The numerical simulations calculated water flow rate or discharge, Q (m³/d), versus time, t (d), out of the test facilities over a 24-hr period or a 12-hr period (for highly permeable soils that reached steady state quickly). As transient flow was simulated, true steady flow rate (constant Q) was usually closely approached but not truly achieved. True steady flow requires steady-state simulations that are often impractical because they require very large model domains to avoid external boundary effects, as well as very large run times to achieve convergence. As a result, longer duration transient flow simulations generally result in slightly lower Q values, which in turn result in slightly lower K_s estimates by the CSSBP approach. Section 3.5 summarizes the difference between Q after 6 hr compared to Q after 24 hr for the different soil types and test configurations.

Table 1: Infiltration test configurations used for calibration, with screen casing radius (r_s), boring radius (r_b), screen and sandpack height (L), ponding depth (H), L/r ratio, and the width and height of the simulation domain.

Well Type	Screen r_s (m)	Boring r_b (m)	Screen L (m)	Ponding H (m)	L/r_b Ratio	Domain Width (m)	Domain Height (m)
Hand Auger	0.025	0.05	0.5	1	10	2	4
			0.5	2	10		
			1	2	20		
Small Test Well	0.025	0.1	1	2	10	4	8
			4	10	40	9	22
			4	20			
			10	20	100	24	28
			10	30			
Large Test Well	0.05	0.25	1	2	4	4	8
			1	3			
			2	10	8	8	12
			2	20			
			4	10	16	12	24
			10	30	40	15	32
Dry well	0.1	0.75	4	10	5.3	12	24
			10	15	13.3	15	32
			10	30			
			20	30	26.7	18	42

2.2.2 *Representative Soil Types*

The soil types used in the CSSBP calibration were the same ten "representative" soils defined in Volume I for the USSBP calibration, including five glacially over-consolidated soils and five normally consolidated soils. The glacially over-consolidated soils included four advance outwash soils: silty Qva, fine Qva, fine-medium Qva, and fine-coarse Qva; and one glacial till: Qvt. The normally consolidated soils included well-sorted and poorly-sorted soils typical of recessional outwash or alluvium. These representative soils cover the range of soils usually considered for stormwater infiltration within the Puget Sound basin. Tables 2a and 2b summarize key properties assumed for the representative soils. A full discussion of the soil parameters is provided in Volume I. Volume I also provides a description of the unsaturated volumetric soil water content functions $\theta(\psi)$, the unsaturated hydraulic conductivity function $K(\psi)$, and the sorptive number (α^*) for each of the 10 soils.

While two K_s values were assigned to each soil type for the USSBP calibration (Volume I) only a single K_s value for each soil type was used for the CSSBP calibration. The USSBP experience indicated that including a second K_s value in the calibration process did not materially affect the results.

Table 2a: Properties of representative glacially over-consolidated soil types and baseline SEEP/W soil parameters used in the soil water content and hydraulic conductivity functions. *Qva* is advance outwash, *Qvt* is glacial till, D_{60} and D_{10} are grain diameters corresponding, respectively, to 60% passing and 10% passing on the grain-size distribution curve, and *USCS* is Unified Soil Classification System. *Background soil matric suction* is based on an assumed background volumetric soil water content of 10%.

Parameter	Soil Type				
	Qvt	Silty Qva	Fine Qva	Fine-Medium Qva	Fine-Coarse Qva
D_{60} (mm)	0.5	0.25	0.3	0.5	5
D_{10} (mm)	0.02	0.04	0.1	0.13	0.25
Silt Content (wt. %)	20	17	8	5	3
USCS Soil Type	SM	SM	SM-SP	SP	SW
Porosity, θ_S (vol. %)	17	25	30	30	30
Liquid Limit (%)	0	0	0	0	0
Saturated Hydraulic Conductivity, K_s (m/d)	0.1	0.5	2	10	5
Residual Soil Water Content, θ_r (vol. %)	5.5	4.8	3.0	2.6	1.5
Background Soil Water Content θ_b (%)	10	10	10	10	10
Background Soil Matric Suction, ψ_i (m)	3.1	1.8	0.8	0.5	0.09
van Genuchten Fitting Parameter α' (m^{-1})	0.06	0.09	0.18	0.28	1.6
van Genuchten Fitting Parameter n (-)	2.40	3.64	4.10	4.18	3.68
Sorptive Number α^* (m^{-1})	1.17	1.33	2.5	3.9	25

Table 2b: Properties of representative normally-consolidated soil types and baseline SEEP/W soil parameters used in the soil water content and hydraulic conductivity functions. D_{60} and D_{10} are grain diameters corresponding, respectively, to 60% passing and 10% passing on the grain-size distribution curve, and *USCS* is Unified Soil Classification System. *Background soil matric suction* is based on an assumed background volumetric soil water content ranging from 6.3% to 10.4%.

Parameter	Soil Type				
	Silty Fine Sand	Silty Fine-Coarse Sand	Fine Sand	Medium Sand	Sandy Gravel
D_{60} (mm)	0.15	1.4	0.28	1.0	8.0
D_{10} (mm)	0.04	0.02	0.079	0.18	0.4
Silt Content (wt. %)	25%	15%	9%	5%	3%
USCS Soil Type	SM	SM	SM-SP	SP	GW
Porosity, θ_S (vol. %)	40	35	40	40	40
Liquid Limit (%)	10	5	0	0	0
Saturated Hydraulic Conductivity, K_s (m/d)	0.25	0.5	3	10	30
Residual Soil Water Content, θ_r (vol. %)	4.8	5.4	2.9	2.2	1.3
Background Soil Water Content θ_b (%)	9.8	10.4	7.9	7.2	6.3
Background Soil Matric Suction, ψ_i (m)	1.39	0.64	0.75	0.24	0.05
van Genuchten Fitting Parameter α' (m^{-1})	1.28	3.44	2.44	7.69	40
van Genuchten Fitting Parameter n (-)	4.3	3.2	4.2	4.3	3.9
Sorptive Number α^* (m^{-1})	1.8	5.5	3.5	11	57

2.3 Evaluation of Steady-State Conditions

The CSSBP equation (Eq. 3) assumes steady-state flow rate (Q) within an infinite flow domain. This is difficult to simulate numerically, as it requires very long running times to achieve numerical convergence of the steady-state flow equation, and very large numbers of elements to place the radial and bottom flow domain boundaries at "numerical infinity". It is possible, however, to conduct transient flow simulations in much smaller flow domains where the radial and bottom boundaries are just far enough away to allow near-steady CSSBP flow before boundary effects occur.

The simulations were run for either 12 hr or 24 hr, depending on when the simulation reached steady state and when the wetted zone started to impinge on flow domain boundaries. All the scenarios with $K_s < 5$ were run for 24 hr. Many of the simulations for fine-medium Qva, fine-coarse Qva, medium sand and sandy gravel were terminated after 12 hr because steady state had been achieved (generally defined as less than 1% change in flow rate over several hr) and the wetted zone started to impinge on flow domain boundaries. As demonstrated later in Volume II, 6 hr was still sufficient to achieve approximate steady-state flow in these coarse-textured soils.

Because it can be logistically challenging and expensive to conduct testing longer than 6 hr, the flow results after 6 hr (Q_6) were compared with flow after either 12 hr (Q_{12}) or 24 hr (Q_{24}) for all the soils and test well configurations. Results are provided in Section 3.5.

2.4 Flow Limitations due to Screen and Sandpack Head Losses

The numerical simulations were conducted using a "sandpack" material in the annular space between the casing and the borehole wall with a K_s of 10,000 m/d. This K_s was determined to provide no reduction in flow rate compared with an open borehole for the native soils evaluated in this assessment. This was based on comparison of several cased scenarios with uncased scenarios (open hole) using the same soil types, ponding depth, and borehole radius.

It is likely, however, that infiltration test wells may be constructed using sandpack materials with $K_s < 10,000$ m/d. In addition, well losses due to high groundwater velocities near the well casing and within the sandpack are well documented for groundwater pumping wells (Houben 2015). The same phenomenon may limit the capacity of infiltration test wells when the native soils are very permeable and the ponding depth in the well is high.

Potential flow limitations due to well losses were evaluated by comparing results for sandpack K_s of 10,000 m/d, 1,000 m/d, and 100 m/d with different soil types and well configurations. It is important to realize that these lower K_s values may not correlate with the actual K_s of the sandpack because velocities near the well screen may cause non-linear and turbulent flow and Darcy's law is based on linear laminar flow. (Darcy flow is assumed by SEEPW, the numerical modeling software used for this work.) Therefore, even if the sandpack has a $K_s > 10,000$ m/d, the "effective" K_s may be significantly lower due to turbulent flow through the screen and/or within the sandpack. The simulation results with lower sandpack K_s are provided in Section 3.4.

2.5 Transition Between USSBP and CSSBP Methods

The USSBP method is calibrated for uncased scenarios where $H = L$ and the CSSBP method is calibrated for cased scenarios when $H > L$. However, there is a transition interval as the water level begins to rise above the sandpack into the solid casing extending above the sandpack. This transition was evaluated for three soils (Qvt, fine sand, and sandy gravel) and two well scenarios (a hand auger with $L = 0.5$ m and a drywell with $L = 10$ m) to determine when the practitioner should switch from the USSBP method to the CSSBP method. The results are provided in Section 3.5.

2.6 Using Small-Diameter Tests to Predict Performance of Drywells

The design of deep infiltration systems using cased drywells is typically based on drilled soil borings to characterize subsurface soil and groundwater conditions and infiltration testing in small-diameter test wells. One purpose of this

work is to determine the potential to use infiltration test results from small-diameter test wells to estimate the capacity of large-diameter drywells. This was evaluated by using the CSSBP K_s estimates from small-diameter wells to estimate the capacity of large-diameter drywells using the CSSBP approach. The results are provided in Section 3.6.

3   Results

3.1   Numerical Simulations

SEEP/W simulations of CSSBP flow were conducted for ten soil types and 18 test configurations, for a total of 180 simulations (Tables 1, 2a, and 2b). Zero matric suction and water content contours are provided in Fig. 2 for each soil type and one test configuration (large test well with $L = 4$ m, $H = 10$ m, and $r_s = 0.25$ m) after 6 hr of flow. As shown in the figure, zero matric suction (dashed blue contour line) extends deeper below the borehole as K_s and α^* increase. Borehole flux reached the bottom of the simulated domain for the sandy gravel, which is the soil type with the largest K_s and α^* values. Because a unit hydraulic gradient was specified on this boundary, borehole flux reaching the bottom of the domain does not affect simulated flow appreciably as long as the boundary is not contacted by the zero matric suction contour.

3.2   Calibrations

As discussed in Section 2.2, a spreadsheet was set up to estimate K_s for each simulated scenario using the flow rates generated by the SEEP/W simulations, the CSSBP equation (Eq. 3), and calibrated C_c shape function fitting parameters (Z_1, Z_2, Z_3 in Eq. 1.2). The calibration process was designed to minimize the maximum individual error in the CSSBP estimate of K_s across the 180 test scenarios. The maximum individual K_s error was minimized (instead of minimizing the average K_s error) to ensure that the CSSBP analysis always met or exceeded a known degree of accuracy.

Initial calibration attempts evaluated the potential for using the USSBP shape functions (Volume I) for the CSSBP scenarios. This resulted in a maximum error of 47% and an average error of 24%. The USSBP shape functions significantly overpredicted K_s in all cased scenarios with $H > L$. This was not considered acceptable and is due to the difference in flow dynamics around the well. Comparison of an uncased scenario with a cased scenario is provided in Fig. 3. As shown in the figure, the zone of saturated flow is significantly higher above the sandpack in the cased scenario than the uncased scenario, resulting in a different flow dynamic around the borehole. There is no upward flow near the top of the sandpack in the uncased scenarios: flow is horizontal out of the borehole. In contrast, there is upward flow near the top of the sandpack in the cased scenarios. The calibration process demonstrates that the CSSBP scenarios need different shape factors than the USSBP scenarios.

In order to maintain consistency with the USSBP approach, four sets of C_c shape function parameters were calibrated for the CSSBP approach to address fine-grained soil (> 12% silt), coarse-grained soil (< 12% silt), small L/r_b ratio (<20), and large L/r_b ratio ($\geq$ 20). These parameters provided CSSBP estimates of K_s with a maximum error of 13.3% and an average error of 5.1%, relative to the K_s specified in the numerical simulations. Maximum error for each soil type and L/r_b range are summarized in Table 3.

Fig. 4 shows the 95% confidence limits for K_s for each shape function. As shown on the figure, the 95% confidence bands are less than 10% for all L/r_b ratios greater than 20 and less than 15% for all L/r_b ratios less than 20. Although these errors might be reduced by defining more than four shape functions, this is likely not warranted as actual field soils have unknown and uncontrollable degrees of heterogeneity and anisotropy.

Plots of the calibrated C_c shape functions are given in Fig. 5 (a and b) and the corresponding Z_1, Z_2 and Z_3 fitting parameters are given in Table 4. The two shape functions for silty soils and the two shape functions for sandy soils are joined together at $L/r_b = 20$ and a slight jog is apparent in the plots, as shown on Fig. 5b. Figs. 5c and 5d show the USSBP shape functions (C_u) calibrated in Volume I, which are significantly different than the CSSBP shape functions C_c.

Table 3: Maximum percent difference between specified K_s in the numerical model and CSSBP calculated K_s for the ten representative soils. L (m) is the screen/sandpack length, and r_b (m) is borehole radius.

Soil Type	Sorptive Number α^* (m^{-1})	Maximum Error ($L/r_b < 20$)	Maximum Error ($L/r_b \geq 20$)
Silty Soils (>12% Silt)			
Qvt	1.17	12.6%	9.8%
Silty Qva	1.33	13.2%	11.8%
Silty fine sand	1.8	13.3%	11.9%
Silty fine-coarse sand	5.5	13.3%	11.5%
Sandy Soils (<12% Silt)			
Fine Qva	2.5	6.3%	8.5%
Fine sand	3.5	7.1%	8.9%
Fine-medium Qva	3.9	6.2%	8.4%
Medium sand	11	6.6%	8.4%
Fine-coarse Qva	25	6.7%	8.5%
Sandy gravel	57	7.0%	8.7%

Table 4: *Sorptive Number* (α^*) for dry/moist soil and C_c shape function (Eq. 1.2) parameters (Z_1, Z_2, Z_3) for the ten representative soils. Different shape function parameters are developed for test configurations where screen/sandpack length (L) to borehole radius (r_b) ratio was $L/r_b < 20$ or $L/r_b \geq 20$, and for soils with > 12% silt (USCS soil type SM) or < 12% silt.

Soil Type	α^* (m^{-1})	Short Sandpack ($L/r_b < 20$)			Long Sandpack ($L/r_b \geq 20$)		
		Z_1 (-)	Z_2 (-)	Z_3 (-)	Z_1 (-)	Z_2 (-)	Z_3 (-)
Qvt (SM)	1.17	3.06	0.12	0.674	2.32	0.0286	0.463
Silty Qva (SM)	1.33						
Silty fine sand (SM)	1.8						
Silty fine-coarse sand (SM)	5.5						
Fine Qva (SP-SM)	2.5	2.45	0.214	0.93	1.87	0.0354	0.501
Fine sand (SP-SM)	3.5						
Fine-medium Qva (SP)	3.9						
Medium sand (SP)	11						
Fine-coarse Qva (SW)	25						
Sandy gravel (GW)	57						

3.3 Comparison of 6-hr Flow Results with Steady-State Flow

As discussed in Section 2.4, steady-state results were achieved in either 12 hr or 24 hr, depending on the soil type and test configuration. The flow results after 6 hr (Q_6) were compared with steady-state flow results Q_{ss} to illustrate the proximity to steady state after a 6-hr test. The Q_{ss}/Q_6 ratios are provided in Table 5a for glacially over-consolidated soils and in Table 5b for normally-consolidated soils. For soils with $K_s > 5$ m/d, approximate steady-state flow conditions ($Q_{ss}/Q_6 > 0.95$) were achieved within 6 hr in all well configurations. For soils with K_s between 1 and 5 m/d, Q_{ss}/Q_6 ranged from 0.88 to 1.00 with the lowest values for the drywell scenarios and the test well scenarios with $L \geq 10$ m. For soils with K_s less than 1 m/d, Q_{ss}/Q_6 ranged from 0.77 to 0.94, with the lowest values for the drywell scenarios and some of the test well scenarios.

The important conclusion from this analysis is that the 6-hr results for fine-grained soils may need correction factors to better estimate steady-state flow rates and more accurately predict K_s.

Table 5a: SEEP/W simulated steady-state CSSBP flow rate (Q_{ss}) divided by flow rate after 6-hr (Q_6) for the glacially over-consolidated soils and the 18 test configurations. Red text indicates $Q_{ss}/Q_6 < 0.85$; blue text indicates Q_{ss}/Q_6 between 0.85 and 0.95.

Well Type	Screen L (m)	Ponding H (m)	Ratio of Steady State Flow Rate (Q_{ss}) to 6-hr Flow Rate (Q_6)				
			Qvt	Silty Qva	Fine Qva	Fine-Medium Qva	Fine-Coarse Qva
Hand Auger	0.5	1	0.94	0.96	1.00	1.00	1.00
		2	0.94	0.97	1.00	1.00	1.00
	1	2	0.93	0.96	0.99	1.00	1.00
Small Test Well	1	2	0.91	0.95	0.99	1.00	1.00
	4	10	0.89	0.92	0.97	1.00	1.00
		20	0.91	0.93	0.97	1.00	1.00
	10	20	0.87	0.90	0.94	1.00	0.98
		30	0.88	0.91	0.95	1.00	0.98
Large Test Well	1	2	0.89	0.94	0.99	1.00	1.00
		3	0.90	0.94	0.99	1.01	1.00
	2	10	0.90	0.93	0.97	1.00	1.00
		20	0.92	0.94	0.97	1.00	1.00
	4	10	0.87	0.91	0.96	1.00	1.00
	10	30	0.86	0.89	0.94	0.99	0.98
Dry well	4	10	0.83	0.88	0.94	1.00	0.99
	10	15	0.79	0.83	0.91	0.99	0.98
		30	0.83	0.87	0.92	0.99	0.98
	20	30	0.79	0.83	0.89	0.98	0.96

Table 5b: SEEP/W simulated steady-state CSSBP flow rate (Q_{ss}) divided by flow rate after 6-hr (Q_6) for the normally-consolidated soils and the 18 test configurations. Red text indicates $Q_{ss}/Q_6 < 0.85$; blue text indicates Q_{ss}/Q_6 between 0.85 and 0.95.

Well Type	Screen L (m)	Ponding H (m)	Ratio of Steady State Flow Rate (Q_{ss}) to 6-hr Flow Rate (Q_6)				
			Silty Fine Sand	Silty Fine-Coarse Sand	Fine Sand	Medium Sand	Sandy Gravel
Hand Auger	0.5	1	0.93	0.97	1.00	1.00	1.00
		2	0.93	0.97	1.00	1.00	1.00
	1	2	0.91	0.95	0.99	1.00	1.00
Small Test Well	1	2	0.89	0.94	1.00	1.00	1.00
	4	10	0.87	0.90	0.97	1.00	1.00
		20	0.90	0.93	0.97	1.00	1.00
	10	20	0.86	0.88	0.94	0.99	1.00
		30	0.87	0.90	0.94	0.98	1.00
Large Test Well	1	2	0.86	0.92	0.99	1.00	1.00
		3	0.87	0.92	0.99	1.00	0.98
	2	10	0.88	0.91	0.97	1.00	1.00
		20	0.90	0.93	0.97	1.00	1.00
	4	10	0.84	0.88	0.96	1.00	1.00
	10	30	0.85	0.88	0.93	0.98	1.00
Dry well	4	10	0.80	0.85	0.94	0.99	1.00
	10	15	0.77	0.82	0.90	0.98	1.00
		30	0.81	0.85	0.91	0.98	1.00
	20	30	0.78	0.82	0.88	0.97	1.00

3.4 Potential Impacts of Screen and Sandpack Head Losses

As discussed in Section 2.4, flow limitations through the screen and sandpack can have a significant impact on the flow rate for tests in permeable soils. The potential impacts were evaluated by comparing numerical simulations with sandpack K_s = 10,000 m/d (no head losses) with numerical simulations using sandpack K_s = 1,000 m/d and K_s = 100 m/d. Future field testing will attempt to identify the range of "effective" K_s values that are suitable for different sandpack materials and well configurations.

Sandpack effects were initially evaluated for all the soils types and a large test well configurations with L = 4 m and H = 10 m. The results, provided in Table 6, indicate that reducing the sandpack K_s to 1,000 m/d results in less than 1% flow reduction for all the soils except sandy gravel (with 2.2% flow reduction). Reducing the sandpack K_s to 100 m/d results in less than 1% of flow reduction in all the soils with K_s < 1 m/d and between 1.8% and 18.7% flow reduction for soils with K_s > 1 m/d. The remaining comparisons were limited to four soils: fine Qva, fine-coarse Qva, medium sand and sandy gravel, all having K_s > 1 m/d.

Tables 7a and 7b provide the flow reduction for different well configurations when L = 1 m and H = 2 m, and sandpack K_s = 1,000 m/d and K_s = 100 m/d. At K_s = 1,000 m/d (Table 7a) the flow reduction is less than 2% for all the soils and well configurations except for sandy gravel in the small and large test wells, when the flow reduction is as high as 3.9%. As shown in Table 7b, the flow reductions are much larger when K_s = 100 m/d, ranging from 0.9% for the hand auger in fine Qva to 30% for the large test well in sandy gravel. In both cases, the flow reduction increases as r_b increases from 5 cm for the hand auger to 25 cm for the large test well.

Tables 8a and 8b provide the flow reduction for different well configurations when L = 4 m and H = 10 m, and sandpack K_s = 1,000 m/d and K_s = 100 m/d. Again, at K_s = 1,000 m/d (Table 8a) the flow reduction is less than 2% for all the soils and well configurations except for sandy gravel in the large test well and drywell, when the flow reduction is as high as 5.4%. When sandpack K_s = 100 m/d (Table 8b), the flow reductions are much larger, ranging from 0.6% for the hand auger in fine Qva to 38% for the large test well in sandy gravel. Again, the flow reduction increases as r_b increases from 10 cm for the small test well to 75 cm for the drywell.

Simulations were also conducted to evaluate flow reduction when L remains constant and H increases. These simulations indicated no significant increase in flow reduction as H increases, assuming sandpack K_s remains constant. However, these simulations are for linear laminar flow and may not mimic actual well performance since higher H results in higher flow velocities which would increase well losses and reduce the effective K_s of the screen and sandpack. Therefore, one would expect greater well losses as H increases and L remains constant.

Table 6: Flow reduction due to reduced sandpack K_s for different soil types using the large test well configuration with $L = 4$ m and $H = 10$ m. Results provided for $K_s = 1,000$ m/d and $K_s = 100$ m/d (compared to $K_s = 10,000$ m/d). Soils included glacial till (Qvt), four types of glacially consolidated advance outwash (Qva) and five normally-consolidated soils.

Soil	Native Soil K_s (m/d)	Flow Reduction Compared to Sandpack $K_s = 10,000$ m/d	
		Sandpack $K_s = 1,000$ m/d	Sandpack $K_s = 100$ m/d
Qvt	0.1	0.0%	0.7%
Silty fine sand	0.25	0.0%	0.3%
Silty Qva	0.5	0.0%	0.5%
Silty fine-coarse sand	0.5	0.0%	0.5%
Fine Qva	2	0.0%	1.8%
Fine sand	3	0.3%	2.4%
Fine-coarse Qva	5	0.4%	3.9%
Fine-medium Qva	10	0.8%	7.4%
Medium sand	10	0.8%	7.5%
Sandy gravel	30	2.2%	18.7%

Table 7a: Flow reduction for different well configurations when $L = 1$ m, $H = 2$ m, and sandpack $K_s = 1,000$ m/d. Soils included two types of glacially-consolidated advance outwash (Qva) and two normally-consolidated soils.

Soil	Native Soil K_s (m/d)	Flow Reduction Compared to Sandpack $K_s = 10,000$ m/d		
		Hand Auger	Small Test Well	Large Test Well
Fine Qva	2	0.0%	0.0%	0.0%
Fine-coarse Qva	5	0.2%	0.3%	0.6%
Medium sand	10	0.4%	0.9%	1.9%
Sandy gravel	30	0.7%	3.7%	3.9%

Table 7b: Flow reduction for different well configurations when $L = 1$ m and $H = 2$ m, and sandpack $K_s = 100$ m/d. Soils included two types of glacially-consolidated advance outwash (Qva) and two normally-consolidated soils.

Soil	Native Soil K_s (m/d)	Flow Reduction Compared to Sandpack $K_s = 10,000$ m/d		
		Hand Auger	Small Test Well	Large Test Well
Fine Qva	2	0.9%	2.0%	2.8%
Fine-coarse Qva	5	1.7%	4.4%	7.1%
Medium sand	10	3.4%	8.4%	13.0%
Sandy gravel	30	8.8%	20.7%	29.7%

Table 8a: Flow reduction for different well configurations when L = 4 m and H = 10 m, and sandpack K_s = 1,000 m/d. Soils included two types of glacially-consolidated advance outwash (Qva) and two normally-consolidated soils.

Soil	Native Soil K_s (m/d)	Flow Reduction Compared to Sandpack K_s = 10,000 m/d		
		Small Test Well	**Large Test Well**	**Drywell**
Fine Qva	2	0.0%	0.0%	0.5%
Fine-coarse Qva	5	0.3%	0.4%	0.9%
Medium sand	10	0.5%	0.8%	1.9%
Sandy gravel	30	1.5%	2.2%	5.4%

Table 8b: Flow reduction for different well configurations when L = 4 m and H = 10 m, and sandpack K_s = 100 m/d. Soils included two types of glacially-consolidated advance outwash (Qva) and two normally-consolidated soils.

Soil	Native Soil K_s (m/d)	Flow Reduction Compared to Sandpack K_s = 10,000 m/d		
		Small Test Well	**Large Test Well**	**Drywell**
Fine Qva	2	0.6%	1.8%	4.4%
Fine-coarse Qva	5	2.7%	3.9%	9.6%
Medium sand	10	5.0%	7.5%	17.5%
Sandy gravel	30	12.9%	18.7%	37.9%

3.5 Transition Between USSBP and CSSBP Methods

The USSBP method is calibrated for uncased scenarios where $H = L$ and the CSSBP method is calibrated for cased scenarios when $H > L$. However, as the water level begins to rise above the sandpack into the solid casing above the sandpack it is unclear when to transition from the USSBP method to the CSSBP method. Fig. 6 illustrates the absolute error for both the USSBP method and the CSSBP method for three soils (Qvt, fine sand, and sandy gravel) and two well scenarios (a hand auger with $L = 0.5$ m and a drywell with $L = 10$ m). The CSSBP method is more accurate than the USSBP method when the solid line drops below the dashed line of the same color. For example, as shown in Fig. 6(a) for the hand-auger well, the CSSBP method is more accurate for sandy gravel when H/L exceeds 1.35. The H/L ratio where the CSSBP method becomes more accurate ranges from 1.05 for fine sand and the hand auger well to 2.0 for Qvt and the hand auger well. The variability in the transition point between the USSBP method and the CSSBP method makes it difficult to provide precise guidelines regarding which method to use when H/L is less than 2. In general, it is reasonable to use the USSBP method when H/L is less than 1.2 and use the CSSBP method when H/L is greater than 1.2.

3.6 Using Small-Diameter Tests to Predict Performance of Drywells

As discussed in Section 2.6, an important outcome of this study is to determine if infiltration testing in small-diameter test wells can effectively predict the performance of larger-diameter wells. Tables 9a through 9f compare K_s values calculated from small-diameter infiltration tests using either the USSBP method (when $H = L$) or the CSSBP method with K_s values calculate from larger-diameter tests using the CSSBP method. All ten soils are evaluated in each table. The comparisons within each table are based on the same L value, since test wells should be screened across the same interval as the proposed production wells whenever possible. Results using different H values were compared since it is likely that ponding depths during testing may not be as high as maximum ponding depths for proposed production wells. This is due to the challenge of obtaining high enough flow rates to maximize the ponding depths during testing, at least for more permeable soils.

Table 9a compares the results from a hand auger test ($L = H = 1$ m) with the results from two tests in a large test well with $H = 2$ m and $H = 3$ m. As shown in the table, the hand auger test is within 10% of the K_s estimates for more permeable soils and within 19% for less permeable soils.

Table 9b compares the results from a hand auger test ($L = 1$ m and $H = 2$ m) with two infiltration tests in a large test well with $H = 2$ m and $H = 3$ m. All the results are within 6%.

Table 9c compares the results from a small test well ($L = 4$ m and $H = 4$ m) with an infiltration test in a large test well ($H = 10$ m) and a drywell ($H = 10$ m). All the results are within 7%.

Table 9d compares the results from a small test well ($L = 4$ m and $H = 10$ m) with an infiltration test in a large test well ($H = 10$ m) and a drywell ($H = 10$ m). All the results are within 5%.

Table 9e compares the results from a small test well ($L = 10$ m and $H = 20$ m) with an infiltration test in a large test well ($H = 30$ m) and a drywell ($H = 30$ m). All the results are within 16%.

Table 9f compares the results from a small test well ($L = 10$ m and $H = 30$ m) with an infiltration test in a large test well ($H = 30$ m) and a drywell ($H = 30$ m). All the results are within 10%.

In summary, for the scenarios evaluated, the results from the small-diameter test wells provided K_s values that were within 19% of the K_s values for tests in larger-diameter wells. These results are consistent with the maximum error estimates provided in Section 3.2 of $\pm 13.3\%$ since one test scenario may error to the negative while the other test scenario errors to the positive.

Table 9a: Difference between K_s predicted by a simulated infiltration test in a hand auger well ($H = 1$ m) and K_s predicted by two simulated infiltration tests in a large test well ($H = 2$ m and $H = 3$ m). $L = 1$ m for all three tests. The hand auger results were analyzed using the USSBP method since $L = H$.

Soil	Actual K_s (m/d)	Hand Auger ($L = 1$ m, $H = 1$ m) Predicted K_s (m/d)	Large Test Well ($L = 1$ m, $H = 2$ m)		Large Test Well ($L = 1$ m, $H = 3$ m)	
			Predicted K_s (m/d)	Difference	Predicted K_s (m/d)	Difference
Qvt	0.1	0.11	0.089	-19%	0.091	-18%
Silty fine sand	0.25	0.26	0.23	-11%	0.24	-9%
Silty Qva	0.5	0.52	0.43	-17%	0.44	-15%
Silty fine-coarse sand	0.5	0.47	0.44	-6%	0.45	-4%
Fine Qva	2	2.15	1.90	-11%	1.94	-10%
Fine sand	3	3.16	2.86	-9%	2.93	-7%
Fine-coarse Qva	5	4.89	4.78	-2%	4.89	0%
Fine-medium Qva	10	10.4	9.53	-8%	9.75	-6%
Medium sand	10	10.0	9.56	-4%	9.78	-2%
Sandy gravel	30	29	28.3	-2%	29.1	0%

Table 9b: Difference between K_s predicted by a simulated infiltration test in a hand auger well ($H = 2$ m) and K_s predicted by two simulated infiltration tests in a large test well ($H = 2$ m and $H = 3$ m). $L = 1$ m for all three tests.

Soil	Actual K_s (m/d)	Hand Auger ($L = 1$ m, $H = 2$ m) Predicted K_s (m/d)	Large Test Well ($L = 1$ m, $H = 2$ m)		Large Test Well ($L = 1$ m, $H = 3$ m)	
			Predicted K_s (m/d)	Difference	Predicted K_s (m/d)	Difference
Qvt	0.1	0.090	0.089	-2%	0.091	1%
Silty fine sand	0.25	0.23	0.23	0%	0.24	2%
Silty Qva	0.5	0.45	0.43	-3%	0.44	-1%
Silty fine-coarse sand	0.5	0.44	0.44	-1%	0.45	2%
Fine Qva	2	2.02	1.90	-6%	1.94	-4%
Fine sand	3	3.03	2.86	-5%	2.93	-3%
Fine-coarse Qva	5	5.02	4.78	-5%	4.89	-3%
Fine-medium Qva	10	10.09	9.53	-6%	9.75	-3%
Medium sand	10	10.06	9.56	-5%	9.78	-3%
Sandy gravel	30	29.9	28.3	-5%	29.1	-3%

Table 9c: Difference between K_s predicted by a simulated infiltration test in a small test well ($H = 4$ m) and K_s predicted by a simulated infiltration test in a large test well ($H = 10$ m) and a drywell ($H = 10$ m). $L = 4$ m for all three tests. The small test well results were analyzed using the USSBP method since $L = H$.

Soil	Actual K_s (m/d)	Small Test Well ($L = 4$ m, $H = 4$ m) Predicted K_s (m/d)	Large Test Well ($L = 4$ m, $H = 10$ m)		Drywell ($L = 4$ m, $H = 10$ m)	
			Predicted K_s (m/d)	Difference	Predicted K_s (m/d)	Difference
Qvt	0.1	0.104	0.096	-7%	0.099	-4%
Silty fine sand	0.25	0.27	0.25	-5%	0.26	-1%
Silty Qva	0.5	0.49	0.46	-7%	0.46	-7%
Silty fine-coarse sand	0.5	0.47	0.47	-1%	0.48	1%
Fine Qva	2	2.08	2.06	-1%	1.99	-4%
Fine sand	3	3.09	3.09	0%	2.99	-3%
Fine-coarse Qva	5	4.99	5.12	3%	4.96	-1%
Fine-medium Qva	10	10.20	10.23	0%	9.90	-3%
Medium sand	10	10.03	10.24	2%	9.91	-1%
Sandy gravel	30	29.6	30.5	3%	29.4	-1%

Table 9d: Difference between K_s predicted by a simulated infiltration test in a small test well ($H = 10$ m) and K_s predicted by a simulated infiltration test in a large test well ($H = 10$ m) and a drywell ($H = 10$ m). $L = 4$ m for all three tests.

Soil	Actual K_s (m/d)	Small Test Well ($L = 4$ m, $H = 10$ m) Predicted K_s (m/d)	Large Test Well ($L = 4$ m, $H = 10$ m)		Drywell ($L = 4$ m, $H = 10$ m)	
			Predicted K_s (m/d)	Difference	Predicted K_s (m/d)	Difference
Qvt	0.1	0.097	0.096	0%	0.099	2%
Silty fine sand	0.25	0.25	0.25	0%	0.26	5%
Silty Qva	0.5	0.46	0.46	-2%	0.46	-1%
Silty fine-coarse sand	0.5	0.47	0.47	-1%	0.48	1%
Fine Qva	2	2.05	2.06	0%	1.99	-3%
Fine sand	3	3.07	3.09	1%	2.99	-2%
Fine-coarse Qva	5	5.10	5.12	0%	4.96	-3%
Fine-medium Qva	10	10.22	10.23	0%	9.90	-3%
Medium sand	10	10.21	10.24	0%	9.91	-3%
Sandy gravel	30	30.5	30.5	0%	29.4	-4%

Table 9e: Difference between K_s predicted by a simulated infiltration test in a small test well ($H = 20$ m) and K_s predicted by a simulated infiltration test in a large test well ($H = 30$ m) and a drywell ($H = 30$ m). $L = 10$ m for all three tests.

Soil	Actual K_s (m/d)	Small Test Well ($L = 10$ m, $H = 20$ m) Predicted K_s (m/d)	Large Test Well ($L = 10$ m, $H = 30$ m)		Drywell ($L = 10$ m, $H = 30$ m)	
			Predicted K_s (m/d)	Difference	Predicted K_s (m/d)	Difference
Qvt	0.1	0.094	0.104	11%	0.107	14%
Silty fine sand	0.25	0.25	0.27	11%	0.28	15%
Silty Qva	0.5	0.44	0.49	11%	0.49	11%
Silty fine-coarse sand	0.5	0.45	0.51	12%	0.51	13%
Fine Qva	2	1.85	2.10	14%	2.13	15%
Fine sand	3	2.78	3.16	14%	3.21	16%
Fine-coarse Qva	5	4.58	5.21	14%	5.26	15%
Fine-medium Qva	10	9.16	10.35	13%	10.44	14%
Medium sand	10	9.16	10.40	14%	10.52	15%
Sandy gravel	30	27.4	30.9	13%	31.1	14%

Table 9f: Difference between K_s predicted by a simulated infiltration test in a small test well ($H = 30$ m) and K_s predicted by a simulated infiltration test in a large test well ($H = 30$ m) and a drywell ($H = 30$ m). $L = 10$ m for all three tests.

Soil	Actual K_s (m/d)	Small Test Well ($L = 10$ m, $H = 30$ m) Predicted K_s (m/d)	Large Test Well ($L = 10$ m, $H = 30$ m)		Drywell ($L = 10$ m, $H = 30$ m)	
			Predicted K_s (m/d)	Difference	Predicted K_s (m/d)	Difference
Qvt	0.1	0.099	0.104	5%	0.107	8%
Silty fine sand	0.25	0.26	0.27	6%	0.28	10%
Silty Qva	0.5	0.47	0.49	4%	0.49	4%
Silty fine-coarse sand	0.5	0.48	0.51	5%	0.51	6%
Fine Qva	2	1.98	2.10	6%	2.13	7%
Fine sand	3	2.97	3.16	6%	3.21	8%
Fine-coarse Qva	5	4.90	5.21	6%	5.26	7%
Fine-medium Qva	10	9.79	10.35	6%	10.44	7%
Medium sand	10	9.79	10.40	6%	10.52	7%
Sandy gravel	30	29.3	30.9	6%	31.1	6%

4 Conclusions

Numerical simulations of CSSBP tests were used to develop four sets of calibrated C_c shape function fitting parameters (Z_1, Z_2, Z_3, Eq. 1.2, Table 4) for use in glacially over-consolidated soils (advance outwash and glacial till) and normally-consolidated soils. The parameters were developed for r_b between 5 and 75 cm, L between 0.5 and 20 m, and H between 1 and 30 m and apply to cased wells completed above the water table with $H > L$. The parameters provided CSSBP estimates of soil K_s with a maximum error of 13.3% and an average error of 5.1%, which is accurate enough for feasibility assessment and design of stormwater infiltration facilities. The numerical simulations were also used to: 1) develop criteria for correcting K_S estimates when steady CSSBP flow was not achieved; 2) evaluate the potential impacts of screen and sandpack head losses, 3) evaluate when to transition from the USSBP method to the CSSBP method as H gradually rises above the well sandpack, and 4) assess the ability of infiltration tests in small-diameter wells to predict the capacity of larger-diameter wells.

It was concluded that the CSSBP method using calibrated C_c shape functions is suitable for estimating K_s in glacially over-consolidated and normally-consolidated soils generally considered for stormwater infiltration within the Puget Sound region of western Washington State (United States), and in other parts of the world with similar soils.

References

Elrick DE, Reynolds WD (1992) Methods for analyzing constant head well permeameter data, Soil Science Society of America Journal 56(1):320-323, DOI:10.2136/sssaj1992.03615995005600010052x

Houben GJ (2015) Review: Hydraulics of water wells - flow laws and influence of geometry. Hydrogeology Journel 23:1633–1657, DOI:10.1007/s10040-015-1312-8

Kindred JS, Reynolds WD (2020) Using the borehole permeameter to estimate saturated hydraulic conductivity for glacially over-consolidated soils, Hydrogeology Journal 28:1909–1924, DOI:10.1007/s10040-020-02149-3

Reynolds WD (2008) Saturated hydraulic properties: well permeameter. In M.R. Carter and E.G. Gregorich (ed.) Soil sampling and methods of analysis. 2nd ed. CRC Press, Boca Raton, FL. p. 1025–1042

Reynolds WD (2010) Measuring soil hydraulic properties using a cased borehole permeameter: steady flow analyses, Vadose Zone Journal, Volume 9(3):637-652, DOI:10.2136/vzj2009.0136

WSDOE (Washington State Department of Ecology) (2019) Stormwater Management Manual for Western Washington, July 2019, Publication Number 19-10-021

Figures

Figure 1: SEEP/W axisymmetric model domain and boundary conditions for the large test well with $L = 1$. This figures illustrates the model arrangements for the four test configurations (hand auger, small test well, large test well, and drywell) used for calibration of the CSSBP shape function fitting parameters. The "fixed head" boundary condition applies to the center of the well screen ($r = 0$) and refers to specified hydraulic head that is constant in space and time.
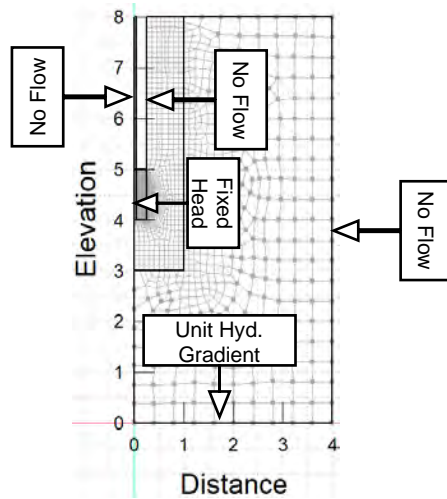
Figure 2: Zero matric suction and water content contours after 6 hr of SEEP/W simulated flow. Results for the large test well with $L = 4$ m, $H = 10$ m, and $r_b = 0.25$ m.
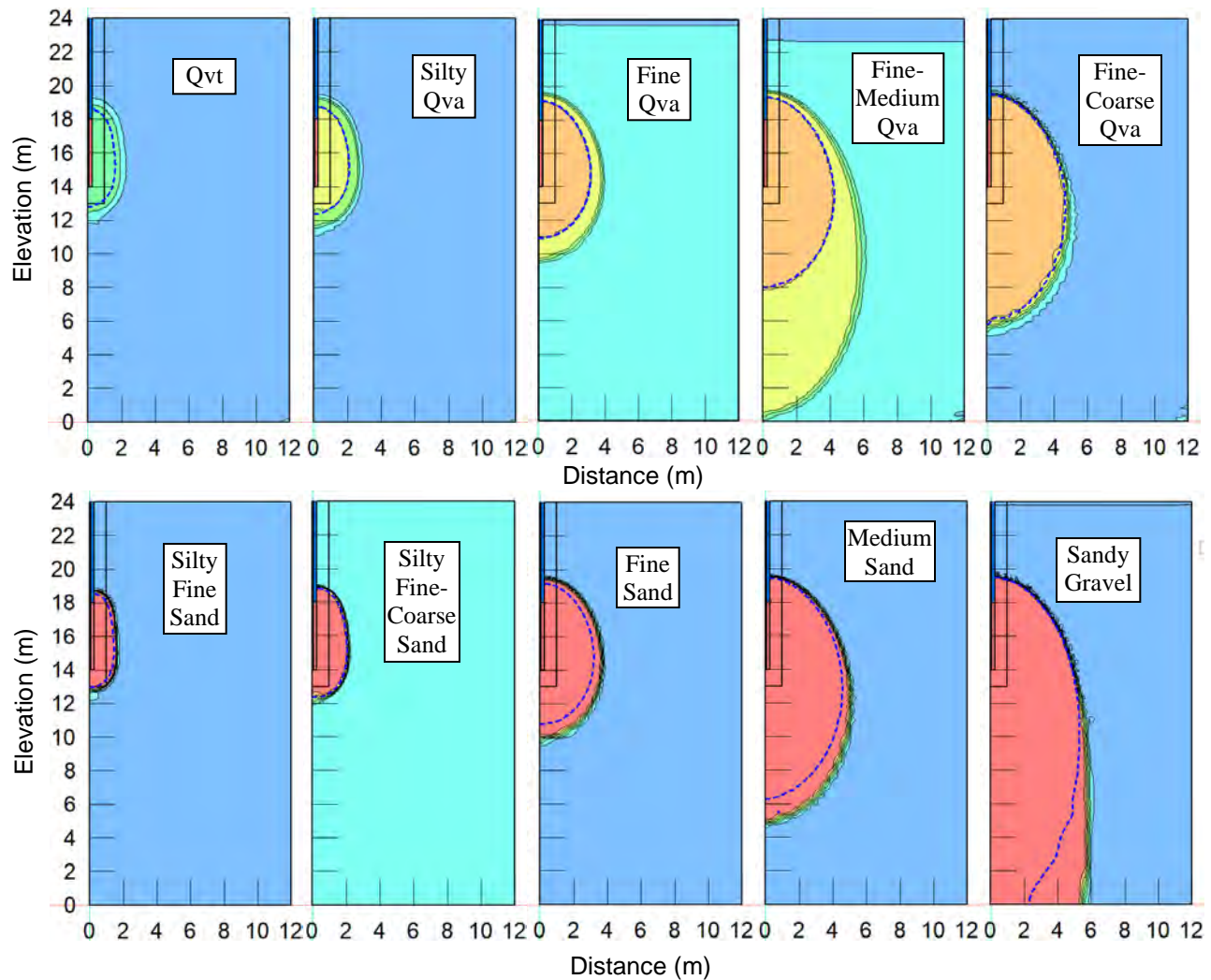
Figure 3: Comparison of uncased scenario ($H = 2$ m) with cased scenario ($H = 10$ m) for fine sand with $L = 2$ m and $r_b = 0.25$ m. Figures show zero matric suction and water content contours after 6 hr of SEEP/W simulated flow. The zone of saturated flow (illustrated by the zero-matric suction contour) has risen approximately 1.5 m above the sandpack in the cased scenario, resulting in different flow dynamics around the borehole compared with the uncased scenario.
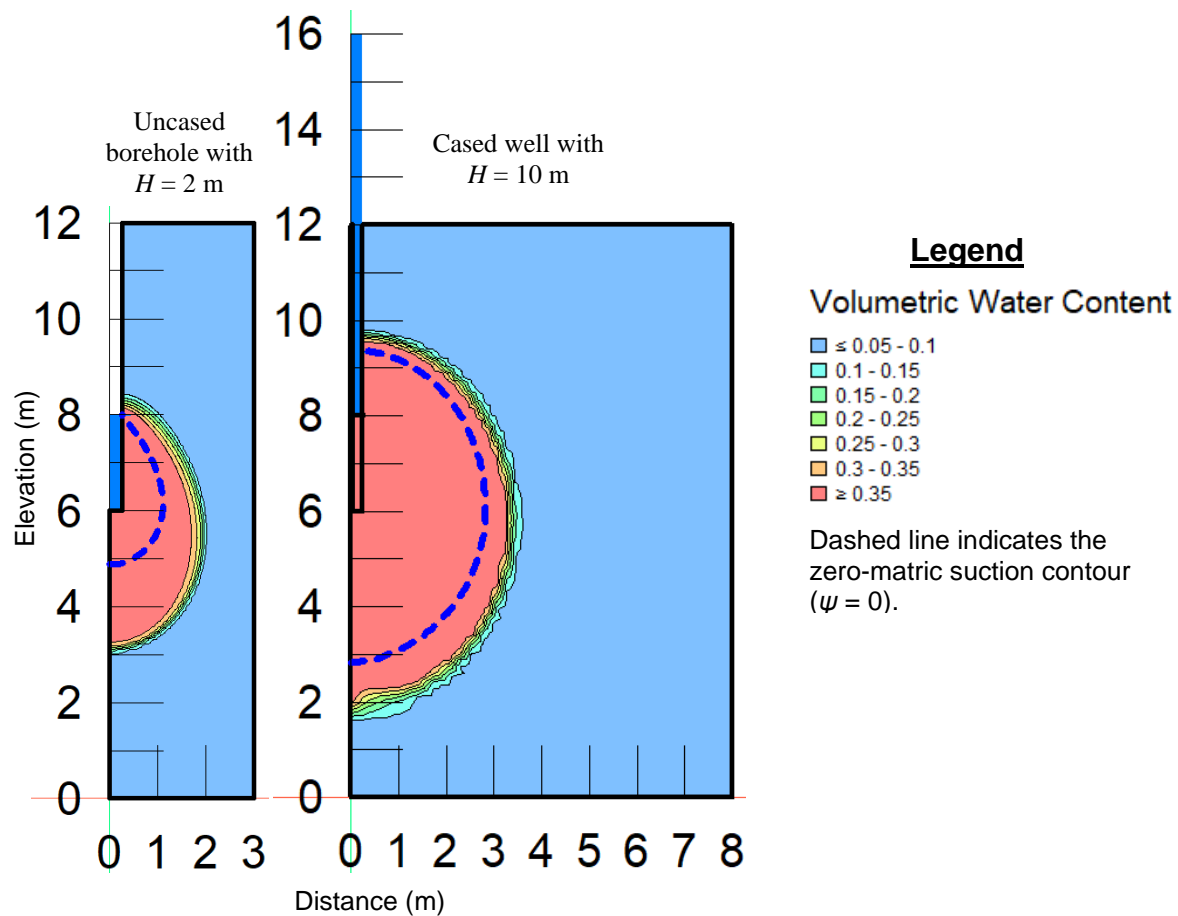
Figure 4: Mean and 95th percentile confidence limits (CL) for CSSBP estimates of saturated hydraulic conductivity (K_s). Each graph represents one of the four shape functions C_c developed for different silt content and L/r_b ratios.
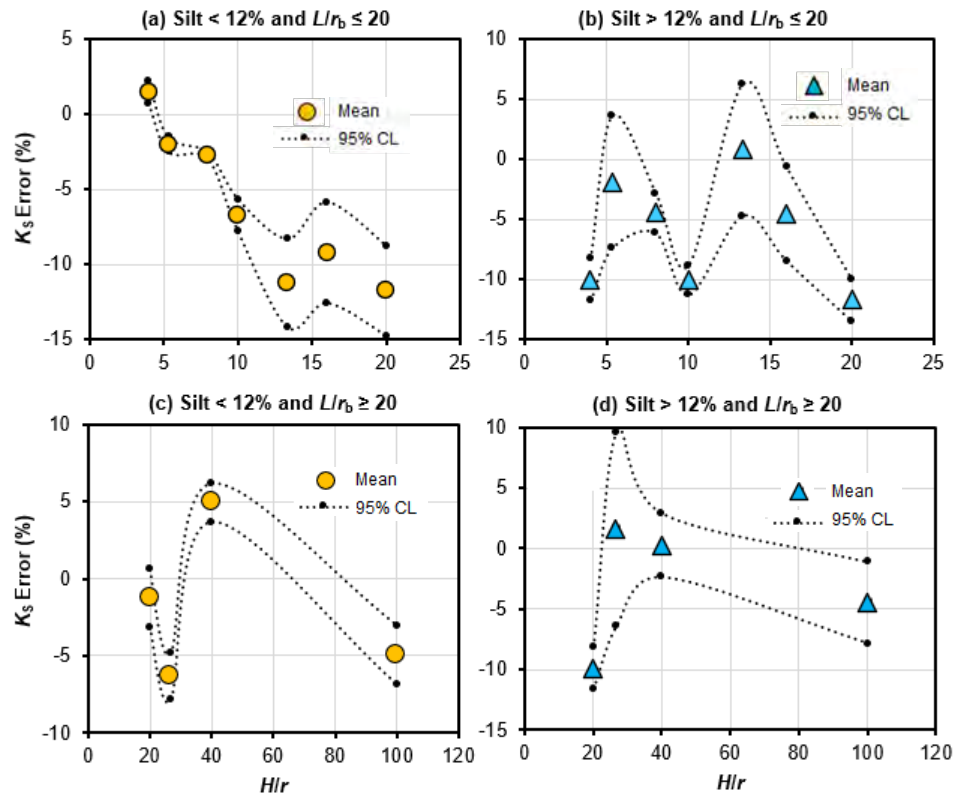
Figure 5: Calibrated cased shape functions (C_c) and uncased shape functions (C_u) for soils with < 12% silt (green lines) and soils with > 12% silt (red lines), Panels (a) and (c) shows shape functions for H/r between 0 and 200; panels (b) and (d) show a close up for H/r less than 22. L is the screen/sandpack length, H is borehole ponding depth, r_b is the borehole radius.
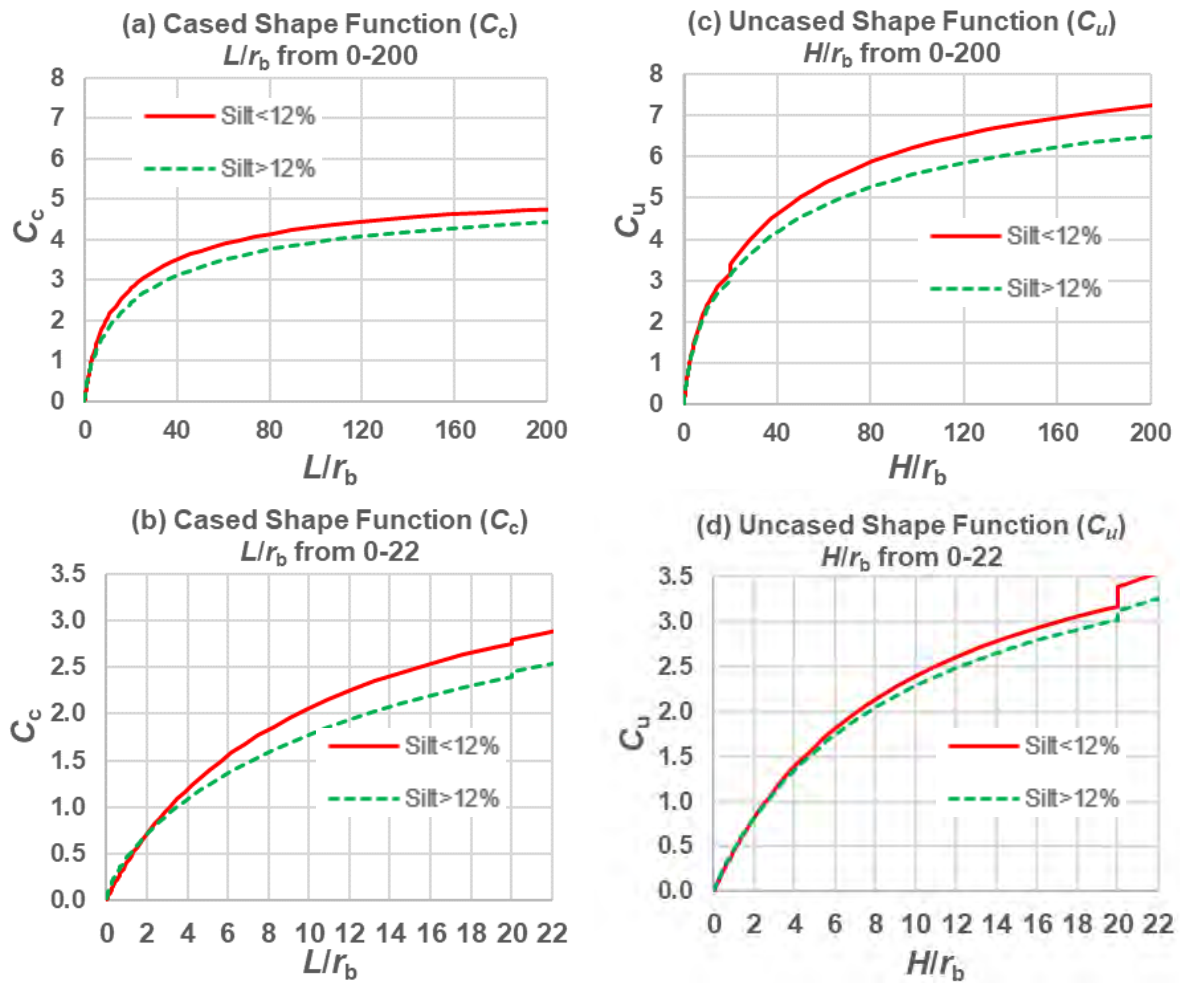
Figure 6: Comparison of USSBP and CSSBP methods in the transition from uncased to cased scenarios as the ponding head begins to exceed the screen/sandpack length (i.e., $H/L > 1$). Results provided for glacial till (Qvt), fine sand, and sandy gravel for a hand auger well with $L = 0.5$ m (a) and a drywell with $L = 10$ m (b).
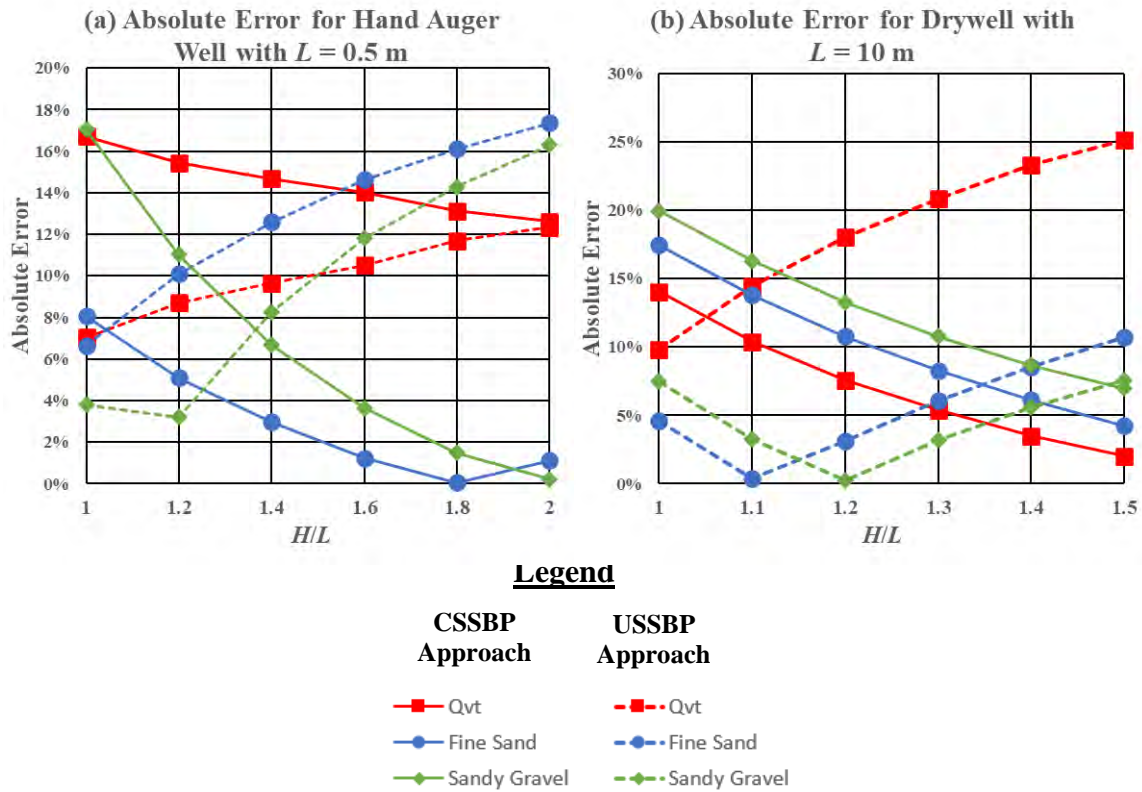
VOLUME III: USING THE FALLING-HEAD BOREHOLE PERMEAMETER METHOD TO ESTIMATE SATURATED HYDRAULIC CONDUCTIVITY

Near-Term Action (NTA) 2018-0827: Flexible Infiltration Test Methods for Evaluating Infiltration Feasibility

Project No. TAC-20-1 • October 10, 2022

Volume III - Contents

Volume III - List of Tables

Volume III - List of Figures

4   Comparison of numerical falling-head results with the predicted falling-head curves using the FHBP single-point solution and the FHBP curve-fitting solution for fine sand using the hand-auger test well with $L = 0.5$ m and $D_0 = 2$.

5   Falling-head curves for flow rates of 0.4, 5, and 8 L/s compared with instantaneous fill for Qvt and the small test well with $L = 1$ m and $D_0 = 2$ m.

Volume III - Abstract

The purpose of Volume III is to evaluate the cased falling-head borehole permeameter (FHBP) and develop FHBP methods suitable for typical stormwater infiltration testing based on numerical analysis.

Numerical simulations were conducted to evaluate the FHBP equations provided by Reynolds (2011) for typical well configurations and soils that are usually considered for stormwater infiltration in the Puget Sound Basin. Assuming instantaneous filling of the test well, these simulations demonstrated that the FHBP estimates of K_s were more accurate for soils with $K_s \le 0.5$ m/d (Qvt, silty Qva, silty fine sand, and silty fine-coarse sand) with errors less than 18%. K_s errors for soils with $K_s \ge 2$ m/d were as high as 47%. In general, the FHBP method tended to underestimate K_s for the soils considered suitable for stormwater infiltration and the systematic negative bias was greater for coarse-grained soils. The negative bias increased significantly for non-instantaneous simulations that were conducted using typical flow rates for a residential hose connection (0.4 L/s), a water truck (5 L/s) and a fire hydrant (8 L/s).

Sensitivity analyses were conducted to evaluate the potential effects of uncertainty in the borehole radius (r_b), volumetric soil-air content ($\Delta\theta$), and the soil sorptive number (α^*). Generally, changing these parameters by $\pm$ 20% resulted in significant changes to the K_s estimates, ranging from +6% to -26%. Although these uncertainties are modest compared with the inaccuracies associated with more permeable soils and non-instantaneous fill rates, they should be considered when evaluating the usefulness of the FHBP method.

Although the FHBP method has significant limitations, falling-head tests can be conducted much quicker and with less water than steady-state methods. In addition, falling-head tests do not require measuring the flow rate during the test. Furthermore, steady-state tests can be difficult to conduct in low permeability soils due to the very low flow rates that must be maintained during the test and the need to precisely control the water level by adjusting the flow rate. Therefore, the FHBP method may be useful for testing soils with $K_s \le 0.5$ m/d using relatively small test wells (e.g., $L \le 1$ m, $D_0 \le 2$ m, $r_b \le 10$ cm).

One disadvantage of the FHBP method is that water only penetrates a few centimeters into the native soil during the test and the volume of tested soil is much smaller than with a steady-state test. As a result, the FHBP test results may overestimate K_s due to loosening of the native soil around the borehole during drilling and well construction. This is a significant concern in gravelly soil. In addition, the larger volume of water used in a steady-state test provides greater opportunity for the test results to reflect macro effects such as layering and groundwater mounding. These macro effects tend to reduce the bulk hydraulic conductivity and more accurately represent the performance of an operational infiltration facility during extended runoff events that infiltrate large volumes of water. Therefore, the FHBP method should not be used for predicting the long-term infiltration capacity of an infiltration facility without applying a significant factor of safety.

Important practices to improve the accuracy of the FHBP method include: 1) Measuring r_b as carefully as possible, 2) utilizing laboratory testing or field measurements to accurately estimate porosity (θ_s) and background soil-water content (θ_i), 3) conducting sufficient grainsize analyses to determine the soil texture within the tested zone, 4) accurately assessing if the soil is glacially consolidated or not, and 5) filling the well as quickly as possible during the test to approximate instantaneous fill.

1 Introduction

Stormwater infiltration is now required where feasible for new development in Washington State and the 2019 Stormwater Management Manual for Western Washington (WSDOE 2019) provides a variety of methods for sizing infiltration facilities. The preferred method is either the small or large pilot infiltration test (PIT). Volume I provides a brief summary of the PIT method.

A more accurate and reliable approach is to determine infiltration rate and capacity using measurements of soil saturated hydraulic conductivity (K_s) obtained from test methods that formally account for both flow directions (vertical, horizontal), and all three components of soil water flow (pressure, gravity, capillarity). The cased falling-head well or borehole permeameter (FHBP) is one such test that has been shown to provide accurate estimates of K_s in carefully controlled numerical simulations (Reynolds 2011). The falling-head method is conducted by filling a cased borehole with water to the target fill depth (D_0) and measuring the falling-head as a function of time. In the right soil conditions, it can be conducted quickly with a relatively small amount of water (Muñoz-Carpena et al., 2001, 2002) compared with constant-head methods.

The first FHBP method was developed by Philip (1993) and is referred to as the Philip-Dunne (PD) permeameter. It uses a fully cased or lined borehole with vertical flow out of the bottom of the borehole. Reynolds (2011) expanded this method to include boreholes/wells with a screen that allowed horizontal flow out of the borehole. Ahmed et al. (2014) provided the Modified Philip-Dunne (MPD) method that accounts for interactions with the ground surface and facilitates falling head tests near the ground surface.

One challenge with the PD and MPD methods is that they require a tight seal between the casing and the ground so there is not a preferential pathway for water to flow up along the outside of the casing. Field testing of these methods has been conducted in fine-gained soils by driving a casing into the ground and removing the soil inside the casing (Ahmed et al., 2014) or by drilling a hole slightly less in diameter than the casing and then inserting the casing into the hole (Muñoz-Carpena et al., 2002). These methods of placing the casing would not be effective in soils with gravel due to disturbance of the soil structure during the driving and or drilling process. In theory, a tight seal could be created by drilling a borehole that is larger than the casing and placing a bentonite seal in the annular space after inserting the casing. This method has not been demonstrated and requires no leakage of the bentonite inside the casing at the bottom of the hole.

The other disadvantage of the PD and MPD methods is that flow is limited to the bottom of the borehole and they test a relatively small volume of soil using a relatively small volume of water. Many tests would need to be conducted to obtain an accurate representation of the average K_s at a site and these small-scale tests may not reflect the flow dynamics of layered soils, typically found in glacial and alluvial environments. This is particularly true for a project that is evaluating the feasibility and capacity of drywells, where both the horizontal variability and the vertical variability would need to be characterized and simulated to predict the performance of a drywell.

Given the preponderance of gravelly, layered soils in Puget Sound and many other areas with similar depositional environments, methods that rely solely on flow out of the bottom of the casing, such as the PD and MPD methods, are not considered well-suited for characterizing the feasibility and capacity of stormwater infiltration facilities.

The FHBP method developed by Reynolds (2011) is suitable for a broad range of test facility geometries, including test wells with a screen to facilitate horizontal flow from the borehole. The FHBP geometry evaluated in this work is referred to "VR2" by Reynolds (2011) and is shown in Fig. 1. The VR2 geometry isolates an open borehole interval with both vertical and horizontal flow with solid casing above the open interval that is smaller than the borehole diameter. Test wells featuring this geometry can be installed using standard methods commonly used by geotechnical and hydrogeologic professionals. The borehole can be drilled using a hand auger, a vacuum extraction (vactor) truck, or a variety of drilling methods (hollow-stem auger, solid-stem auger, air-rotary, Sonic, etc.) The wells are constructed by installing a screen and sandpack over the target test interval and the rest of the annular space is sealed off with bentonite well-sealing products. Another advantage of this test configuration is that steady state infiltration tests (either cased on uncased) can be conducted in the same facilities. Although Reynolds (2011)

VR2 scenario did not include a screen and sandpack, this region is fully saturated during the duration of the test and the addition of the screen and sandpack will not change the results as long as the permeability of the sand pack is high enough to prevent any significant head loss.

1.1 Scope of Work and Purpose

The primary objective of this task was to evaluate the FHBP equations provided by Reynolds (2011) for typical well configurations and soils that are usually considered for stormwater infiltration in the Puget Sound Basin. Reynolds (2011) limited his validation analysis to fine-grained soils with K_s values between 8.6×10^{-3} and 4.3×10^{-2} m/d and test wells with the following dimensions: casing radius r_c between 2 and 5 cm, borehole radius (r_b) between 2 to 8 cm, sandpack length (L) between 0 and 0.35 m, and initial water depth (D_0) between 0.09 and 1 m. Given these soil types and well dimensions, Reynolds (2011) demonstrated that the FHBP method provided relatively accurate measurements of K_s ($\pm 20\%$).

In Washington State, stormwater infiltration is generally considered feasible in soils with much higher K_s values than those assumed by Reynolds (2011) and this analysis evaluates K_s values between 0.1 and 30 m/d. In addition, typical stormwater infiltration wells, including test wells, have much larger dimensions than those assumed by Reynolds (2011). The work presented here evaluates test wells with r_c between 2.5 and 5 cm, r_b between 5 and 25 cm, L between 0.5 and 4 m, and D_0 between 1 and 10 m.

Secondary objectives of this study were to: 1) Compare results using a single-point solution with the iterative, non-linear, curve-fitting solution used by Reynolds (2011), 2) evaluate the effects of non-instantaneous fill rates on the K_s estimates, and 3) determine the sensitivity of the K_s estimates to variations in parameters with a significant degree of uncertainty. For consistency with previously published work, metric units are used throughout Volume III.

2 Materials and Methods

2.1 Cased Falling-Head Borehole Permeameter (FHBP) Equation

Considerable research has been conducted regarding analytical methods for estimating K_s from cased falling-head borehole infiltration tests in the unsaturated zone (see e.g., Philip, 1993, Muñoz-Carpena et al., 2001, 2002, Reynolds 2011, Ahmed et al., 2014, and citations therein). These methods generally assume a flat-bottom cylindrical test facility (e.g., borehole or pit excavation), isotropic and homogeneous soil, and no water-table effects. The methods are only valid while the water level is above the screen or sandpack interval. Following the approach by Philip (1993), all of the methods assume an equivalent sphere discharge surface and a three-dimensional Green-Ampt infiltration model (Green and Ampt, 1911). The Green-Ampt infiltration model assumes a sharp wetting front such that:

$$\theta(\psi) = \theta_s \quad \text{and} \quad K(\psi) = K_s \quad Eq.\,1.1$$

inside the wetted zone around the borehole, and

$$\theta(\psi) = \theta_i \quad \text{and} \quad K(\psi) = K_i \ll K_s \quad Eq.\,1.2$$

outside the wetted zone; where ψ is pore-water pressure head, $\theta(\psi)$ is the soil-water content relationship, $K(\psi)$ is the hydraulic conductivity relationship, θ_s is the porosity (aka field-saturated volumetric soil-water content), θ_i is the background volumetric soil-water content, and K_i is the hydraulic conductivity at the background soil-water content.

As discussed in Section 1.0, the Reynolds (2011) VR2 formulation for a screened well is best-suited for infiltration testing in gravelly, layered soils typical of Puget Sound and many other glacial and alluvial environments. Based on the derivative procedures of Philip (1993), Reynolds (2011) provides the following equation:

$$t = \frac{C_E\, r_c^2}{4\, r_0\, K_s}\, \tau_E \quad \text{(Eq. 2)}$$

where r_c is the radius of the casing, r_0 is the radius of the equivalent sphere discharge surface (elaborated below), and t is the time when K_s is estimated. C_E is the flow efficiency parameter to account for the fact that the actual flow out of the borehole may be less efficient than flow out of the assumed equivalent sphere surface. C_E is relevant for test wells with no screened interval (i.e., only vertical flow out of the casing) but flow through a screened well is about as efficient as flow through the equivalent sphere surface and $C_E = 1$ (Reynolds 2011). Therefore, Eq. 2 can be simplified to:

$$t = \frac{r_c^2}{4\, r_0\, K_s}\, \tau_E \quad \text{(Eq. 3.1)}$$

where τ_E is dimensionless time, based on the following equation:

$$\tau_E = \left(1 + \frac{1}{2A_E}\right) ln\left(\frac{A_E^3 - 1}{A_E^3 - \rho_E^3}\right) - \frac{3}{2A_E} \ln\left(\frac{A_E - 1}{A_E - \rho_E}\right) + \frac{\sqrt{3}}{A_E}\left[\tan^{-1}\left(\frac{A_E + 2\rho_E}{\sqrt{3}\,A_E}\right) - \tan^{-1}\left(\frac{A_E + 2}{\sqrt{3}\,A_E}\right)\right] \quad \text{(Eq. 3.2)}$$

where:

$$A_E^3 = \frac{3r_c^2\left(H_0 + \alpha^{*-1} + G_E\right)}{4r_0^3\,\Delta\theta} + 1 \quad \text{(Eq. 3.3)}$$

$$\rho_E^3 = \frac{3r_c^2(H_0 - H_t)}{4r_0^3\,\Delta\theta} + 1 \quad \text{(Eq. 3.4)}$$

$$\Delta\theta = \theta_{fs} - \theta_i \quad \text{(Eq. 3.5)}$$

H_0 is the effective pressure head in the borehole screen at $t = 0$, H_t is the effective pressure head in the borehole screen at time t (elaborated below), α^* is the soil sorptive number, G_E is the gravity factor (elaborated below), and $\Delta\theta$ is the initial or background volumetric soil-air content. As described in Kindred and Reynolds (2020) α^* represents the capillarity of the soil.

As discussed in Reynolds (2011), the Philip (1993) solution demonstrated that the gravity parameter (G_E) varied as a function of time. However, the integral in the Philip (1993) derivation required G_E to be a constant. Reynolds evaluated a range of options for estimating G_E and determined that $G_E = 0$ provided the most accurate estimates for K_s and α^*. Therefore, equation 3.3 can be simplified to:

$$A_E^3 = \frac{3r_c^2\left(H_0 + \alpha^{*-1}\right)}{4r_0^3\,\Delta\theta} + 1 \quad \text{(Eq. 4)}$$

The equivalent sphere radius (r_0) is obtained by equating the area of a sphere (A_s) to the surface area of the exposed portion of the borehole (A_b), such that:

$$A_s = 4\pi r_0^2 = A_b = \pi r_b^2 + 2\pi r_b L \quad \text{(Eq. 5)}$$

which provides the following expression:

$$r_0 = \left(\frac{r_b^2}{4} + \frac{r_b L}{2}\right)^{1/2} \quad \text{(Eq 5.2)}$$

where r_b = radius of the borehole and L is the length of the sandpack interval.

As discussed in Reynolds (2011), the effective pressure head H_t is calculated using:

$$H_t = D_t - E \quad \text{(Eq. 6.1)}$$

where E is the screen factor:

$$E = \frac{L^2}{r_b + 2L} \quad \text{(Eq. 6.2)}$$

for combined vertical and radial discharge. D_t is actual water depth at time t. H_0, the initial effective pressure head, is calculated using Eq. 6.1 by replacing H_t with H_0 and D_t with D_0, the initial or target fill depth.

2.2 Iterative Curve Fitting and Single-Point Solutions

Using the iterative, nonlinear curve-fitting approach as demonstrated by Reynolds (2011), Eq. 3.1 was solved using a spreadsheet with calculations for the equations provided in Section 2.1. Values for both K_s and α^* were estimated by solving the equations for multiple points in time. This approach was implemented using Excel Solver to adjust the values of K_s and α^* to minimize the difference between the falling-head curve predicted by the FHBP and the falling-head curve generated by the numerical simulation. The objective function for this approach is:

$$\min\left[\sum_{i=1}^{n}\left(t_i^{\text{Data}} - t_i^{\text{Analy}}\right)^2\right] \quad \text{(Eq. 7)}$$

where n is the number of (H_t,t) values ($n \geq 2$), t_i^{Data} are the simulated times when certain H_t values are reached and t_i^{Analy} are the corresponding times predicted by the fitted analytical solution (Eq. 3.1) for the same H_t values.

The single-point solution used for this study assumed a value for α^* based on soil characteristics and calculated K_s for a single pair of (H_t, t) values. This approach uses a re-arranged version of Eq. 3.1 that solve for K_s:

$$K_s = \frac{r_c^2}{4\, r_0\, t}\, \tau_E \quad \text{(Eq. 8)}$$

The disadvantage of this approach is that it does not provide an estimate for α^*. The advantage is that it is easier to calculate than the iterative, nonlinear, curve-fitting approach.

2.3 FHBP Numerical Validation

Validation of the FHBP method provided in Section 2.1 involved calculating K_s via the FHBP equations (Eqs. 2.1 or 8) using falling-head results (D_t, t) generated by numerical simulations of falling-head tests for 90 test scenarios. The test scenarios included all combinations of ten "representative" soils typically considered for stormwater infiltration in the Puget Sound Basin (Section 2.3.2) and nine FHBP test configurations (Section 2.3.1).

The numerical falling-head results for the 90 scenarios were estimated using SEEP/W, a finite element numerical model that can simulate multidimensional and axisymmetric flow in saturated and unsaturated porous media (GEOSLOPE International Ltd., Calgary, Alberta, Canada). Unsaturated flow simulation requires specifying soil hydraulic properties in the form of the unsaturated volumetric soil water content function $\theta(\psi)$ (soil water content as a function of soil matric suction) and the unsaturated hydraulic conductivity function $K(\psi)$ (hydraulic conductivity as a function of soil matric suction). These hydraulic property functions are described in Volume I.

The analytical FHBP methods all assume instantaneous filling of the test well. Numerically, this can be accomplished in SEEP/W by first conducting a very short (1.0×10^{-3} or 1.0×10^{-4} s) transient simulation with an initial fill depth of D_0 within the casing and the sandpack and a second transient simulation that uses the results of the first simulation as the initial conditions. "Instantaneous" simulations were conducted for all 90 test scenarios to demonstrate the theoretical accuracy of the analytical FHBP method. The shorter initial simulation duration of 1.0×10^{-4} s was used to simulate "instantaneous" filling for some of the sandy gravel tests that recovered in less than 0.5 s. The shorter filling duration provided more accurate results due to the very quick recovery time in more permeable soils.

In field testing, instantaneous filling of the test well is not feasible. Depending on the equipment and the water source, maximum flow rates can range from 0.4 L/s (6.34 gpm) for a household hose bib, to 5 L/s (79 gpm) for a water truck, to 8 L/s (127 gpm) for a fire hydrant. In addition, in moderately to highly permeable soils, significant water will flow into the native soils outside the well before the water depth has achieved the target fill depth. This can significantly extend the time to fill the well to the target depth and significantly degrade the accuracy of the analytical FHBP method.

Because the purpose of this work is to provide infiltration testing methods that are practical and cost-effective, validation of the FHBP method included comparisons with "non-instantaneous" simulations that relied on typical maximum flow rates available to the design professional. This approach was useful to define when the FHBP method was feasible and provided a reasonable level of accuracy, given a range of test facility dimensions and soil types.

The iterative, non-linear, curve-fitting approach utilized by Reynolds (2011) has the advantage of fitting the entire falling-head curve and providing estimates for both K_s and α^*. This approach is recommended for low-permeability soils and small test facilities where the target fill depth can be achieved quickly enough to be considered "instantaneous". However, for scenarios when the test facility cannot be filled quickly, the early part of the falling-head curve deviates significantly from the FHBP model and fitting the entire curve is not useful. This is the case for most of the soils and test facilities considered suitable for stormwater infiltration. Therefore, the single-point approach, with assumed value for α^* (based on soil type), was utilized for the bulk of the validation analysis.

2.3.1 Model Domains and Test Configurations

The SEEP/W numerical flow domains for the nine test configurations are summarized in Table 1. The test configurations covered the following dimensions: r_c varied from 2.5 cm to 5 cm, r_b varied from 5 cm to 25 cm, L varied from 0.5 m to 4 m, D_0 varied from 1.0 m to 10 m, and the L/r_b ratio varied from 4 to 20. As an example, Fig. 2 shows the large test well domain with $L = 1$ m and $D_0 = 2$ m. The simulations assumed axisymmetric flow, with no-flow boundaries along the top and outside radius of the flow domain, and a unit hydraulic head gradient boundary at the bottom of the flow domain. The simulations were designed to simulate test wells with a sandpack around the screen in the lower portion of the well and an impervious seal around the solid casing in the upper portion of the well. The impervious seal was simulated as a no-flow boundary.

The space inside the well screen and casing was simulated as a SEEP/W material with 100% porosity and K_s of 1×10^8 m/d (essentially infinite). The sandpack was simulated as a SEEP/W material with 40% porosity and K_s of 10,000 m/d. Simulating these regions in this manner resulted in no significant head losses during the simulations. As discussed in Volume II, sandpack K_s may be significantly less than 10,000 m/d and for native soils with high K_s, there may be significant head losses through the well screen and within the sandpack material.

Table 1 provides the screen and casing radius (r_c), boring radius (r_b), the screen and sandpack height (L), initial fill depth (D_0), L/r_b ratio, and the width and height of the simulation domain for each of the 9 test scenarios. The simulations used graded meshes of rectangular and triangular finite elements. Element size ranged from 0.2 cm to 5 cm. The smallest elements were used in the area of the wetting front (native soils just outside the sandpack) and the drying front (inside the casing above the sandpack) to accurately represent the abrupt changes in moisture content and hydraulic properties. Trial simulations with different element sizes determined that 0.2 cm was sufficiently small to minimize numerical error. Using such small element sizes resulted in models that contained between 25,000 and 150,000 elements and were computationally intensive.

Table 1: Infiltration test configurations used for validation, with screen and casing radius (r_c), boring radius (r_b), screen and sandpack height (L), fill depth (D_0), L/r_b ratio, and the width and height of the simulation domain.

Well Type	Casing r_c (m)	Boring r_b (m)	Screen L (m)	Fill Depth D_0 (m)	L/r_b Ratio	Domain Width (m)	Domain Height (m)
Hand-Auger Well	0.025	0.05	0.5	1	10	0.5	1.6
			0.5	2	10	0.5	1.6
			1	2	20	0.5	1.6
Small Test Well	0.025	0.1	1	2	10	0.5	1.6
			4	10	40	0.5	4.7
Large Test Well	0.05	0.25	1	2	4	0.5	1.6
			1	3	4	0.5	1.6
			2	10	8	0.5	2.7
			4	10	16	0.5	4.7

2.3.2 Representative Soil Types

The soil types used in the FHBP validation were the same ten "representative" soils defined in Volume I for the USSBP calibration, including five glacially over-consolidated soils and five normally consolidated soils. The glacially over-consolidated soils included four advance outwash soils: silty Qva, fine Qva, fine-medium Qva, and fine-coarse Qva; and one glacial till: Qvt. The normally consolidated soils included well-sorted and poorly-sorted soils typical of recessional outwash or alluvium. These representative soils cover the range of soils usually considered for stormwater infiltration within the Puget Sound basin. Tables 2 and 3 summarize key properties assumed for the representative soils. A full discussion of the soil parameters is provided in Volume I. Volume I also

provides a description of the unsaturated volumetric soil water content functions $\theta(\psi)$, the unsaturated hydraulic conductivity function $K(\psi)$, and the soil sorptive number (α^*) for each of the 10 soils.

While two K_s values were assigned to each soil type for the USSBP calibration (Volume I) only a single K_s value for each soil type was used for the FHBP validation. The USSBP experience indicated that including a second K_s value in the calibration process did not materially affect the results.

Table 2: Properties of representative glacially over-consolidated soil types and baseline SEEP/W soil parameters used in the soil water content and hydraulic conductivity functions.

Parameter	Soil Type				
	Qvt	Silty Qva	Fine Qva	Fine-Medium Qva	Fine-Coarse Qva
D_{60} (mm)	0.5	0.25	0.3	0.5	5
D_{10} (mm)	0.02	0.04	0.1	0.13	0.25
Silt Content (wt. %)	20	17	8	5	3
USCS Soil Type	SM	SM	SM-SP	SP	SW
Porosity, θ_s (vol. %)	17	25	30	30	30
Liquid Limit (%)	0	0	0	0	0
Saturated Hydraulic Conductivity, K_s (m/d)	0.1	0.5	2	10	5
Residual Soil Water Content, θ_r (vol. %)	5.5	4.8	3.0	2.6	1.5
Background Soil Water Content θ_b (%)	10	10	10	10	10
Background Soil Matric Suction, ψ_i (m)	3.1	1.8	0.8	0.5	0.09
van Genuchten Fitting Parameter α' (m^{-1})	0.06	0.09	0.18	0.28	1.6
van Genuchten Fitting Parameter n (-)	2.40	3.64	4.10	4.18	3.68
Soil Sorptive Number α^* (m^{-1})	1.17	1.33	2.5	3.9	25

Notes:
Qva is advance outwash and *Qvt* is glacial till.
D_{60} and D_{10} are grain diameters corresponding, respectively, to 60% passing and 10% passing on the grain-size distribution curve
USCS is Unified Soil Classification System
Background soil matric suction is based on an assumed background volumetric soil water content of 10%.

Table 3: Properties of representative normally-consolidated soil types and baseline SEEP/W soil parameters used in the soil water content and hydraulic conductivity functions.

Parameter	Soil Type				
	Silty Fine Sand	Silty Fine-Coarse Sand	Fine Sand	Medium Sand	Sandy Gravel
D_{60} (mm)	0.15	1.4	0.28	1.0	8.0
D_{10} (mm)	0.04	0.02	0.079	0.18	0.4
Silt Content (wt. %)	25%	15%	9%	5%	3%
USCS Soil Type	SM	SM	SM-SP	SP	GW
Porosity, θ_s (vol. %)	40	35	40	40	40
Liquid Limit (%)	10	5	0	0	0
Saturated Hydraulic Conductivity, K_s (m/d)	0.25	0.5	3	10	30
Residual Soil Water Content, θ_r (vol. %)	4.8	5.4	2.9	2.2	1.3
Background Soil Water Content θ_b (%)	9.8	10.4	7.9	7.2	6.3
Background Soil Matric Suction, ψ_i (m)	1.39	0.64	0.75	0.24	0.05
van Genuchten Fitting Parameter α' (m^{-1})	1.28	3.44	2.44	7.69	40
van Genuchten Fitting Parameter n (-)	4.3	3.2	4.2	4.3	3.9
Soil Sorptive Number α^* (m^{-1})	1.8	5.5	3.5	11	57

Notes:
D_{60} and D_{10} are grain diameters corresponding, respectively, to 60% passing and 10% passing on the grain-size distribution curve
USCS is Unified Soil Classification System
Background soil matric suction is based on an assumed background volumetric soil water content ranging from 6.3% to 10.4%.

2.4 Sensitivity Analysis

The FHBP method equations provided in Section 2.1 utilize parameters with a significant amount of uncertainty, including the borehole radius (r_b), the volumetric soil-air content ($\Delta\theta$, see Eq. 3.5), and the soil sorptive number α^*. Uncertainties in r_b are generally due to an irregular borehole wall and/or caving of the borehole wall during drilling. Uncertainties in $\Delta\theta$ are due to both uncertainty in total porosity and the degree of soil saturation, which can change significantly over time. Because α^* cannot be directly measured and is estimated based on grainsize and compaction level, it is considered an approximation of soil capillarity.

Parameters such as the length of sandpack (L) and the casing radius (r_c) are generally known well enough that a sensitivity analysis is not warranted. Uncertainties in the van Genuchten parameters are addressed using α^* and are evaluated in Volume I for the USSBP method.

Sensitivity of the FHBP method to these parameters was evaluated using the single-point solution with an instantaneous fill time and varying a single parameter at a time to determine the changes in the predicted K_s. Two soils types (Qvt and fine sand) and a single test configuration (hand-auger test well with $L = 0.5$ m and $D_0 = 2$ m) were used for the sensitivity analyses.

3 Results

3.1 Instantaneous Fill Simulations using the Single-Point Solution

SEEP/W simulations of FHBP flow were conducted for ten soil types (Tables 2 and 3) and nine test configurations (Table 1) using the "instantaneous" fill approach. As an example, Fig. 3 shows the volumetric water content for one of the large test well configurations in silty fine sand just as the water level in the well casing approaches the top of the sandpack (the end of the test). As indicated on the figure, the wetting front (illustrated by the dark blue dashed line) has barely penetrated the native soil at the end of the test. This result illustrates the small amount of soil tested during a falling-head test.

The results for all the scenarios were analyzed using the single-point approach described in Section 2.2. The falling-head recovery times (the time for the water level to fall from D_0 to just above the sandpack) are summarized in Tables 4 and 5. As indicated in the tables, recovery times ranged from less than 0.1 s (sandy gravel with a small test well configuration) to 300 s (Qvt with a hand-auger configuration). Although short recovery times can be simulated using numerical simulations with very short timesteps, field tests with very quick recovery times are unlikely to provide accurate results due to a variety of reasons (e.g., well losses and non-laminar flow).

The percent difference between the FHBP K_s estimates using the single-point solution and the K_s values used in the numerical simulations are provided in Tables 6 and 7 for all 90 test scenarios. As indicated in the tables, the FHBP results were more accurate for the soils with $K_s \leq 0.5$ m/d (Qvt, silty Qva, silty fine sand, and silty fine-coarse sand) with errors ranging from -18% to +14%. FHBP errors for soils with $K_s \geq 2$ m/d were greater, ranging from -47% to +3%. As shown in Tables 6 and 7, the average errors for each soil type ranged from +4% for Qvt to -35% for fine-coarse Qva. Other than Qvt and silty Qva, the FSBP results tended to underestimate K_s and the systematic negative bias was greater for coarse-grained soils.

3.2 Comparison of Single-point Solution and Curve-Fitting Solution

A limited number of simulations were analyzed using the iterative, non-linear, curve-fitting approach for comparison with the single-point results. The purpose of this comparison was to determine if the curve-fitting solution provided more accurate estimates of K_s than the single-point solution.

Fig. 4 compares the numerical results with the predicted falling-head curves using the FHBP single-point solution and the FHBP curve-fitting solution for fine sand using the hand-auger test well with $L = 0.5$ m and $D_0 = 2$ m. As shown on the figure, the FHBP results align closely with the numerical results with very slight deviations. In theory, any point on the single-point curve (i.e., any pair of H_t, t values) could be used to calculate K_s. However, head elevations are changing slower at later time and may be more accurate than head values at early time. Therefore, it is best to use a point at later time when the ponding depth approaches the top of the sandpack.

The results for all nine soils are summarized in Table 8 for the hand-auger test well with $L = 0.5$ m and $D_0 = 2$ m. With one exception, both the single-point solution and the curve-fitting solution provide estimates of K_s that are within 10% of the value used in the numerical simulations for the hand-auger scenario. The one exception is the single-point estimate for fine-coarse Qva, which underestimates K_s by 33% for fine-coarse Qva. The curve-fitting solution provides a much more accurate estimate of K_s for fine-coarse Qva (within 3%). With one exception, the curve-fitting solution also provides relatively accurate estimates of α^* for the hand-auger test well, with estimates that are generally within 23% of the α^* value used in the numerical simulations. The exception is sandy gravel with an error of 61%.

The results for all nine soils are summarized in Table 9 for the large well configuration with $L = 1.0$ m and $D_0 = 3$. The FHBP results for this large test well scenario are less accurate that the hand-auger scenario, with K_s estimates that average 15% less for the single-point solution and 17% less for the curve-fitting solution (compared with K_s values used in the numerical simulations). Again, the curve-fitting solution provided better estimates of K_s for fine-

coarse Qva than the single-point solution (-15% error versus -34% error). However, the single-point solution provided a better estimate of K_s for sandy gravel than the curve-fitting solution (-28% error versus -37% error).

The curve-fitting solution for the large test well scenario also provides less accurate estimates of α^* than the hand-auger scenario, with errors ranging from -21% to -87% for five of the ten soils. In general, α^* estimates were progressively less accurate for coarser-grained soils.

In summary, the curve-fitting solution doesn't appear to provide significantly more accurate estimates of K_s than the single-point solution, except for the fine-coarse Qva. Estimates of α^* provided by the curve-fitting solution were more accurate for fine-grained soils than coarse-grained soils. To some extent, this may be due to the relatively low capillarity flux for coarse-grained soils, resulting in low sensitively to changes in α^*.

Table 4: Falling-head test duration for glacially over-consolidated soils for the nine test configurations and instantaneous fill. Test duration is the length of time for the water level to fall from the initial fill depth (D_0) to the top of the sandpack.

Well Type	Sandpack L (m)	Fill Depth D_0 (m)	Falling Head Recovery Time - Instantaneous Fill (s)				
			Qvt	Silty Qva	F Qva	F-C Qva	F-M Qva
Hand-Auger Well	0.5	1	86	12	3.6	2.5	0.85
		2	350	52	15	9.7	3.7
	1	2	68	9.0	2.5	1.4	0.58
Small Test Well	1	2	25	3.0	0.85	0.50	0.20
	4	10	21	2.5	0.60	0.30	0.14
Large Test Well	1	2	58	6.5	1.8	1.1	0.42
		3	172	21	5.2	2.9	1.2
	2	10	322	40	9.5	4.4	2.1
	4	10	57	6.4	1.5	0.70	0.34

Table 5: Falling-head test duration for normally-consolidated soils for the nine test configurations and instantaneous fill. Test duration is the length of time for the water level to fall from the initial fill depth (D_0) to the top of the sandpack.

Well Type	Sandpack L (m)	Fill Depth D_0 (m)	Falling Head Recovery Time - Instantaneous Fill (s)				
			St F Sand	St F-C Sand	F Sand	M Sand	Sandy Gravel
Hand-Auger Well	0.5	1	17	16	1.8	0.83	0.35
		2	86	72	9.0	3.4	1.3
	1	2	13	10	1.3	0.49	0.19
Small Test Well	1	2	4.0	3.4	0.45	0.18	0.071
	4	10	3.2	2.1	0.29	0.11	0.036
Large Test Well	1	2	8.3	6.8	0.88	0.34	0.14
		3	26	21	2.5	0.93	0.39
	2	10	51	34	4.5	1.5	0.56
	4	10	7.6	5.1	0.68	0.24	0.096

Table 6: FHBP error in K_s for glacially over-consolidated soils for the nine test configurations using the single-point method and instantaneous fill.

Well Type	Sandpack L (m)	Fill Depth D_0 (m)	K_s Error (Instantaneous Fill)				
			Qvt	Silty Qva	F Qva	F-C Qva	F-M Qva
Hand-Auger Well	0.5	1	5%	3%	-4%	-47%	-6%
		2	7%	7%	3%	-33%	3%
	1	2	14%	7%	-1%	-31%	-3%
Small Test Well	1	2	-2%	-10%	-19%	-47%	-26%
	4	10	11%	-2%	-14%	-29%	-24%
Large Test Well	1	2	-5%	-8%	-17%	-44%	-21%
		3	-4%	-5%	-11%	-34%	-15%
	2	10	3%	0%	-5%	-18%	-9%
	4	10	3%	-4%	-13%	-27%	-21%
Average Bias			*4%*	*-1%*	*-9%*	*-35%*	*-14%*

Table 7: FHBP error in K_s for normally-consolidated soils for the nine test configurations using the single-point method and instantaneous fill.

Well Type	Sandpack L (m)	Fill Depth D_0 (m)	K_s Error (Instantaneous Fill)				
			St F Sand	St F-C Sand	F Sand	M Sand	Sandy Gravel
Hand-Auger Well	0.5	1	-3%	-2%	-5%	-10%	-16%
		2	4%	4%	3%	3%	-2%
	1	2	-2%	-3%	-6%	-9%	-17%
Small Test Well	1	2	-18%	-18%	-28%	-34%	-43%
	4	10	-15%	-13%	-22%	-32%	-33%
Large Test Well	1	2	-14%	-16%	-19%	-27%	-38%
		3	-11%	-10%	-13%	-15%	-28%
	2	10	-5%	-3%	-6%	-10%	-19%
	4	10	-12%	-11%	-17%	-26%	-41%
Average Bias			*-9%*	*-8%*	*-13%*	*-18%*	*-26%*

Table 8: Comparison of numerical results with FSBP results using either the single-point solution or the iterative, non-linear, curve-fitting solution for the hand-auger test well with $L = 0.5$ m and $D_0 = 2$ m.

Soil Type	K_s (m/d)			α^* (m^{-1})	
	Numerical	Single-Point FHBP	Curve-Fitting FHBP	Numerical	Curve-Fitting FSBP
Silty Fine Sand	0.25	0.26	0.25	1.8	1.6
Silty Fine-Coarse Sand	0.5	0.52	0.51	5.5	5.2
Fine Sand	3	3.09	2.96	3.5	3.1
Medium Sand	10	10.27	9.85	11	8.6
Sandy Gravel	30	29.43	27.95	57	22
Qvt	0.1	0.11	0.11	1.17	1.2
Silty Qva	0.5	0.54	0.54	1.33	1.3
Fine Qva	2	2.06	2.02	2.5	2.4
Fine-Coarse Qva	5	3.34	5.16	25	19
Fine-Medium Qva	10	10.26	9.95	3.9	3.5
Average bias:		*0%*	*1%*		*-14%*

Table 9: Comparison of numerical results with FSBP results using either the single-point solution or the iterative, non-linear, curve-fitting solution for the large test well with $L = 1.0$ m and $D_0 = 3$ m.

Soil Type	K_s (m/d)			α^* (m^{-1})	
	Numerical	Single-Point FHBP	Curve-Fitting FHBP	Numerical	Curve Fitting FSBP
Silty Fine Sand	0.25	0.22	0.21	1.8	1.4
Silty Fine-Coarse Sand	0.5	0.45	0.44	5.5	4.6
Fine Sand	3	2.62	2.39	3.5	2.4
Medium Sand	10	8.45	7.74	11	5.4
Sandy Gravel	30	21.50	19.01	57	7
Qvt	0.1	0.10	0.10	1.17	1.3
Silty Qva	0.5	0.47	0.46	1.33	1.3
Fine Qva	2	1.78	1.71	2.5	2.2
Fine-Coarse Qva	5	3.28	4.24	25	13
Fine-Medium Qva	10	8.53	8.07	3.9	3.1
Average bias:		*-15%*	*-17%*		*-28%*

3.3 Effects of Non-Instantaneous Fill

As discussed in Section 2.3, instantaneous filling of the test well is not feasible. Typical flows can range from less than 1.0 L/s to as high as 10 L/s depending on the water source. Times to fill the casing and sandpack voids for three flow rates and the nine test scenarios are provided in Table 10. In theory, fill times can range from 0.4 seconds for a hand-auger test well with $L = 0.5$ m and $D_0 = 1.0$ m with a flow rate of 8 L/s, to 950s for a large well with $L = 4$ m and $D_0 = 10$ m with a flow rate of 0.4 L/s. These fill times do not account for water that flows into the native soils outside the well before the water depth has achieved the target fill depth, which would increase the fill times. In practice, fill times less than about 2 seconds are not feasible due to turbulence, air entrapment, and limitation of sandpack permeability.

The long fill times are problematic because water is flowing into native soils as the water level rises. In permeable soils, it may not be possible to fill the test well to the target depth at all or within a reasonable period of time. In

addition, when the water is turned off, the falling-head rates are significantly different than predicted by the FHBP method because water has already begun flowing into the native soils. Fig. 5 shows the falling-head curves for flow rates of 0.4, 5, and 8 L/s compared with instantaneous fill for Qvt and the small test well with $L = 1$ m and $D_0 = 2$ m. As shown on the figure, the recovery time increases from 26 s for instantaneous fill to 55 s for the slowest fill (0.4 L/s). Note that the fill times shown in Table 11 for 5 L/s and 0.4 L/s are longer than the times shown in Table 10 because the fill times shown in Table 10 do not account for flow into the native soils during filling.

Moreover, as shown in Table 11, the K_s estimate for Qvt (using the single-point solution) decreases from 0.098 m/d for instantaneous fill (-2% error) to 0.046 m/d (-54% error) for the 0.4 L/s fill rate. Even for very quick fill times (2 s), the error in K_s increases from -2% to -21%. This table illustrates that the filling rates should be as high as possible to minimize the error in K_s.

The effects of non-instantaneous fill were evaluated for all the soil types and two test well scenarios: 1) hand-auger test well with $L = 0.5$ and $D_0 = 2$ (Table 12), and 2) large test well with $L = 1$ m and $D_0 = 3$ m (Table 13). Only the 0.4 L/s and 5 L/s fill rates were used for the hand-auger test well because it may not be feasible to deliver 8 L/s from a fire hydrant into a well casing with $r_c = 5$ cm due to flow restrictions associated with a smaller drop pipe. Only the 5 L/s and the 8 L/s fill rates were used for the large test well because the large test well could not be filled to the target fill depth using 0.4 L/s for most of the soil types. As indicated on Tables 12 and 13, the target fill depths could not be achieved given certain combinations of soils, test well, and fill rates.

In general, the FHBP method significantly under-estimates K_s using non-instantaneous fill rates. The degree of under-estimation is greater for more permeable soils and lower fill rates and was significantly greater for the large test well compared with the hand-auger test well. For tests performed in the hand-auger test well with a flow rate of 5 L/s, the error is less than 20% for soils with K_s less than 2 m/d and as high as 38% for medium sand with $K_s = 10$ m/d. For tests performed in the hand-auger test well with a flow rate of 0.4 L/s, only Qvt had an error < 20% and the error is as high as 68% for fine-coarse Qva. For tests performed in the large test well, none of the soils had an error < 20% and the average error was -61% for a fill rate of 8 L/s and -65% for a fill rate of 5 L/s.

Table 10: The time to fill the casing and sandpack voids with water for nine different test well configurations and three different flow rates. These fill times assume a sandpack porosity of 0.4 and no flow into native soils.

Well Type	Casing r_c (cm)	Boring r_b (cm)	Sandpack L (m)	Fill Depth D_0 (m)	Time to Fill Screen and Sandpack (s)		
					Flow = 0.4 L/s	Flow = 5 L/s	Flow = 8 L/s
Hand-Auger Well	2.5	5	0.5	1	7.9	0.6	0.4*
				2	13	1.0	0.6*
			1	2	16	1.3	0.8*
Small Test Well	2.5	10	1	2	39	3.1	2.0*
			4	10	167	13	8.3*
Large Test Well	5	25	1	2	228	18	11
				3	247	20	12
			2	10	573	46	29
			4	10	950	76	47

* - Field experience has shown that it may not be feasible to get 8 L/s into a well casing with $r_c = 2.5$ cm due to flow restrictions associated with a smaller drop pipe.

Table 11: Summary of FHBP results for different fill rates assuming Qvt soils (K_s = 0.1 m/d) and the small test well with L = 1 m and D_0 = 2 m.

Description	Fill Rate (L/s)			
	Instant	**8**	**5**	**0.4**
Screen/Casing Fill Time (s)	0.001	2	4	44
Recovery Time (s)	26	32	35	51
FHBP K_s (m/d)	0.098	0.079	0.069	0.047
FHBP K_s Accuracy (%)	-2%	-21%	-31%	-55%

Table 12: Effects of different fill times on estimated values of Ks for all ten soil types using the hand-auger test well with L = 0.5 m and D_0 = 2 m and the single-point solution.

Soil Type	K_s (m/d)			
	Numerical	**Instant Fill**	**5 L/s Fill Rate**	**0.4 L/s Fill Rate**
Silty Fine Sand	0.25	0.26	0.23	0.19
Silty Fine-Coarse Sand	0.5	0.52	0.47	0.38
Fine Sand	3	3.1	2.1	1.4
Medium Sand	10	10.3	6.2	Did not fill
Sandy Gravel	30	29	16	Did not fill
Qvt	0.1	0.11	0.10	0.097
Silty Qva	0.5	0.54	0.46	0.38
Fine Qva	2	2.1	1.6	1.3
Fine-Coarse Qva	5	3.3	2.5	1.6
Fine-Medium Qva	10	10.3	6.7	Did not fill
Average bias:	*0%*	*-24%*	*-33%*	

Table 13: Effects of different fill times on estimated values of K_s for all ten soil types using the large test well with L = 1 m and D_0 = 3 m and the single-point solution.

Soil Type	K_s (m/d)			
	Numerical	**Instant Fill**	**8 L/s Fill Rate**	**5 L/s Fill Rate**
Silty Fine Sand	0.25	0.22	0.13	0.12
Silty Fine-Coarse Sand	0.5	0.45	0.26	0.23
Fine Sand	3	2.7	0.73	0.61
Medium Sand	10	8.5	1.5	1.11
Sandy Gravel	30	21.5	Did not fill	Did not fill
Qvt	0.1	0.10	0.078	0.074
Silty Qva	0.5	0.47	0.26	0.24
Fine Qva	2	1.8	0.72	0.60
Fine-Coarse Qva	5	3.3	0.99	1.14
Fine-Medium Qva	10	8.5	2.0	1.45
Average bias:	*-15%*	*-61%*	*-65%*	

3.4 Sensitivity Analysis Results

The sensitivity analyses were conducted as described in Section 2.4 and the results are summarized in Table 14. As shown in the Table, changing borehole radius (r_b), volumetric soil-air content ($\Delta\theta$), and the soil sorptive number (α^*) by $\pm$ 20% resulted in significant changes to the K_s estimates, ranging from +6% to -26%. Although these uncertainties are modest compared with the inaccuracies associated with more permeable soils and non-instantaneous fill rates, they should be considered when evaluating the usefulness of the FHBP method.

Table 14: Summary of sensitivity analyses for fine sand and Qvt using the hand-auger test well with $L = 0.5$ m and $D_0 = 2$ m and the single-point solution. Table shows K_s estimates using the FHBP method when the input parameters are changed by $\pm$20%. Percent difference from the baseline FHBP result is shown in parentheses.

Sensitivity Analysis	K_s (m/d)	
	Fine Sand	**Qvt**
Numerical Value	3.0	0.1
Baseline FHBP Result	3.09 (0%)	0.107 (0%)
Increase r_b 20%	2.31 (-26%)	0.086 (-21%)
Decrease $\Delta\theta$ 20%	3.55 (+15%)	0.116 (+9%)
Increase α^* 20%	3.26 (+6%)	0.118 (+11%)

4 Discussion

4.1 Accuracy of the FHBP Method

Reynolds (2011) demonstrated that the FHBP method was relatively accurate (<20% error) for fine-grained soils with K_s values between 8.6×10^{-3} and 4.3×10^{-2} m/d and test wells with the following dimensions: borehole radius (r_b) between 2 and 8 cm, sandpack length (L) between 0 and 0.35 m, and initial fill depth (D_0) between 0.09 and 1 m. In addition, Reynolds assumed instantaneous fill of the test well, a reasonable assumption for these low-permeability soils and small test wells.

The theoretical accuracy of the FHBP method for more permeable soils and larger test wells was evaluated in this study using numerical simulations that assumed instantaneous filling of the test wells. This evaluation demonstrated that the FHBP method is relatively accurate (<20% error) for soils with $K_s \leq 0.5$ m/d. FHBP errors were as high as 47% for soils with $K_s \geq 2$ m/d. Other than Qvt and silty Qva, the FHBP results tended to underestimate K_s and the systematic negative bias was greater for coarse-grained soils.

Instantaneous filling of larger test wells with more permeable soils ($K_s > 0.5$ m/d) is not feasible. The negative bias increased significantly for simulations that were based on non-instantaneous filling rates, increasing from 0% for instantaneous fill to -33% for a fill rate of 0.4 L/s in a hand-auger test well with $L = 0.5$ m and $D_0 = 2$ m and from -15% for instantaneous fill to -65% for a fill rate of 5 L/s in a large test well with $L = 1$ m and $D_0 = 3$ m.

Sensitivity analyses demonstrated that the K_s estimates provided by the FHBP method are relatively sensitive to uncertainties in borehole radius (r_b), volumetric soil-air content ($\Delta\theta$), and the soil sorptive number (α^*). Generally, these parameters can be difficult to accurately estimate due to caving during drilling, uncertainty in the degree of saturation, and variability in soil texture.

In summary, the FHBP method is relatively accurate for soils with $K_s \leq 0.5$ m/d and small test wells that can be filled to the target fill depth quickly. The FHBP method is not well suited for large test wells or soils with $K_s > 2$ m/s.

4.2 Utility of the FHBP Method

One advantage of the FHBP method is that falling-head tests can be conducted much quicker and with less water than steady-state methods. In addition, falling-head test do not require measuring the flow rate during the test, eliminating the need for a flow meter. Furthermore, steady-state tests can be difficult to conduct in low permeability soils due to the challenge of measuring very low flow rates and ensuring that the water level is steady at the end of the test. Therefore, the FHBP method may be useful for testing soils with $K_s \leq 0.5$ m/d using relatively small test wells (e.g., $L \leq 1$ m, $D_0 \leq 2$ m, $r_b \leq 10$ cm).

One disadvantage of the FHBP method is that water only penetrates a few centimeters into the native soil during the test and the volume of tested soil is much smaller than with a steady-state test. As a result, the FHBP test results may overestimate K_s due to loosening of the native soil around the borehole during drilling and well construction. This is a significant concern in gravelly soils. In addition, the larger volume of water used in a steady-state test provides greater opportunity for the test results to reflect macro effects such as layering and groundwater mounding. These macro effects tend to reduce the bulk hydraulic conductivity and steady-state tests more accurately represent the performance of an operational infiltration facility during extended runoff events that infiltrate large volumes of water. Therefore, the FHBP method should not be used for predicting the long-term infiltration capacity of an infiltration facility without including a significant factor of safety.

Important practices to improve the accuracy of the FHBP method include: 1) Measuring r_b as carefully as possible, 2) utilizing laboratory testing or field measurements to accurately estimate porosity (θ_s) and background volumetric soil-water content (θ_i), 3) conducting sufficient grainsize analyses to determine the soil texture within the tested

zone, 4) accurately assessing if the soil is glacially consolidated or not, and 5) filling the well as quickly as possible during the test to approximate instantaneous fill.

5 Conclusions

Numerical simulations were conducted to evaluate the FHBP equations provided by Reynolds (2011) for typical well configurations and soils that are usually considered for stormwater infiltration in the Puget Sound Basin. Some of the simulations were conducted using a method that approximated instantaneous fill (a key assumption of the FHBP method). These simulations demonstrated that the FHBP estimates of K_s were more accurate for soils with $K_s \leq 0.5$ m/d (Qvt, silty Qva, silty fine sand, and silty fine-coarse sand) with errors less than $\pm 18\%$. K_s errors for soils with $K_s \geq 2$ m/d were as high as -47%. In general, the FHBP method tended to underestimate K_s for the soils considered suitable for stormwater infiltration and the systematic negative bias was greater for coarse-grained soils.

FHBP solutions were conducted using both a single-point solution and an iterative, nonlinear curve-fitting approach similar to the approach demonstrated by Reynolds (2011). The curve-fitting approach provides an estimate for both K_s and α^* but requires a more complex methodology. The single-point solution only provides a value for K_s after assuming a value for α^* (e.g., using the values provided in Tables 2 and 3 for different soil textures and compaction levels). The advantage of the single-point solution is that it is easier to calculate than the curve-fitting approach and is more likely to be used by practitioners.

Comparison of K_s estimates provided by the two solution methods indicates that the curve-fitting solution does not appear to provide significantly more accurate estimates of K_s than the single-point solution, except for the fine-coarse Qva. Estimates of α^* provided by the curve-fitting solution were relatively accurate (i.e., generally within $\pm 20\%$) for fine-grained soils with $K_s \leq 0.5$ m/d. For coarse-grained soils with $K_s \geq 0.5$ m/d, the α^* estimates were significantly less accurate, with errors as high as -87%. In general, the curve-fitting estimates of α^* tended to under-estimate the values used in the numerical simulations.

The FHBP method is based on falling-head data once the water level reaches the target fill depth and the water is turned off. Furthermore, the method assumes instantaneous filling of the test well. Although instantaneous filling can be simulated numerically, instantaneous filling is generally not feasible in the field. Simulations were conducted using typical flow rates for a residential hose connection (0.4 L/s), a water truck (5 L/s) and a fire hydrant (8 L/s). The time to fill the test facilities considered in this study (assuming no flow into native soils) ranged from 0.4 s to 950 s depending on the flow rate and well configuration. Flow into the native soils as the well is filling can significantly increase the fill times. For some well configurations with permeable soils, it was not possible to achieve the target fill depth at these flow rates by the time the flow rate out of the well matched the flow entering the well. Even when the target fill depths were achieved, estimates of K_s were significantly impacted by non-instantaneous fill rates.

The simulations conducted for this study demonstrate that the FHBP method significantly under-estimates K_s using non-instantaneous fill rates. The degree of under-estimation is greater for more permeable soils and lower fill rates and was significantly greater for the large test well compared with the hand-auger test well. For tests performed in the hand-auger test well with a flow rate of 5 L/s, the error is less than 20% for soils with K_s less than 2 m/d and as high as -38% for medium sand with $K_s = 10$ m/d. For tests performed in the hand-auger test well with a flow rate of 0.4 L/s, only Qvt had an error < 20% and the error is as high as -68% for fine-coarse Qva. For test performed in the large test well, none of the soils had an error < 20% and the average error was -61% for a fill rate of 8 L/s and -65% for a fill rate of 5 L/s. Bottom-line, given the well configurations considered in this study, the FHBP method is not well suited for large test wells or soils with $K_s > 2$ m/d.

Sensitivity analyses were conducted to evaluate the potential effects of uncertainty in the borehole radius (r_b), volumetric soil-air content ($\Delta\theta$), and the soil sorptive number (α^*). Generally, changing these parameters by $\pm 20\%$ resulted in significant changes to the K_s estimates, ranging from +6% to -26%. Although these uncertainties are modest compared with the inaccuracies associated with more permeable soils and non-instantaneous fill rates, they should be considered when evaluating the usefulness of the FHBP method.

References

Green WH, and Ampt GA, 1911. Studies in soil physics: I. The flow of air and water through soils, Journal of Agricultural Science, 4:1–24. doi:10.1017/S0021859600001441

Kindred JS, Reynolds WD (2020) Using the borehole permeameter to estimate saturated hydraulic conductivity for glacially over-consolidated soils, Hydrogeology Journal 28:1909–1924, DOI:10.1007/s10040-020-02149-3

Muñoz-Carpena, R., Regalado CM, and Álvarez-Benedí J (2001) The Philip–Dunne permeameter: A low-tech/low-cost field saturated hydraulic conductivity device. ASAE Paper 01-2146. American Society Agricultural Engineering, St. Joseph, MI.

Muñoz-Carpena, R., Regalado CM, Álvarez-Benedí J, and Bartoli F (2002) Field evaluation of the new Philip–Dunne permeameter for measuring saturated hydraulic conductivity, Soil Science 167:9–24, doi:10.1097/00010694-200201000-00002

Philip, JR (1993) Approximate analysis of falling-head lined borehole permeameter, Water Resources. Research 29:3763–3768, DOI:10.1029/93WR01688

Reynolds WD (2011) Measuring soil hydraulic properties using a cased borehole permeameter: falling-head analysis, Vadose Zone Journal, Volume 10(3):999–1015, DOI: 10.2136/vzj2010.0145

WSDOE (Washington State Department of Ecology) (2019) Stormwater Management Manual for Western Washington, July 2019, Publication Number 19-10-021

Volume 3 - Figures

Figure 1: VR2 test well geometry. r_c is the casing radius, r_b is the borehole radius, L is the sandpack length and D_0 is the initial fill depth.
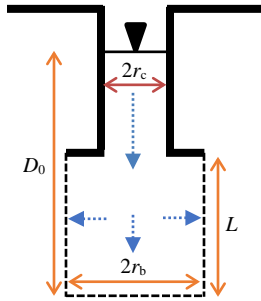
Figure 2: Large test well domain with r_c = 5 cm, r_b = 25 cm, L = 1 m and D_0 = 2 m.
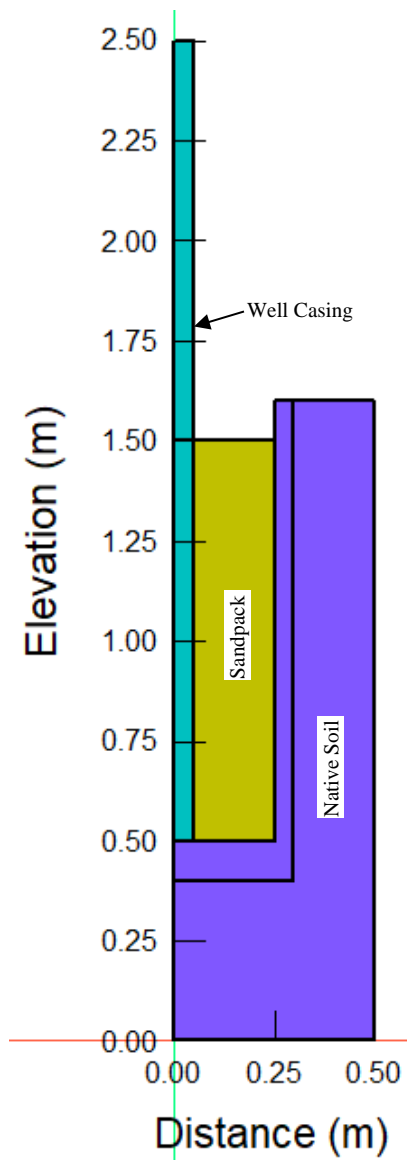
Figure 3: Volumetric water content results for a falling-head test in silty fine sand with the large test well configuration. Results shown as the water level in the well casing approaches the top of the sandpack (the end of the test). The dashed blue line delineates the location of the wetting front (pore-water pressure = 0) at the end of the test.
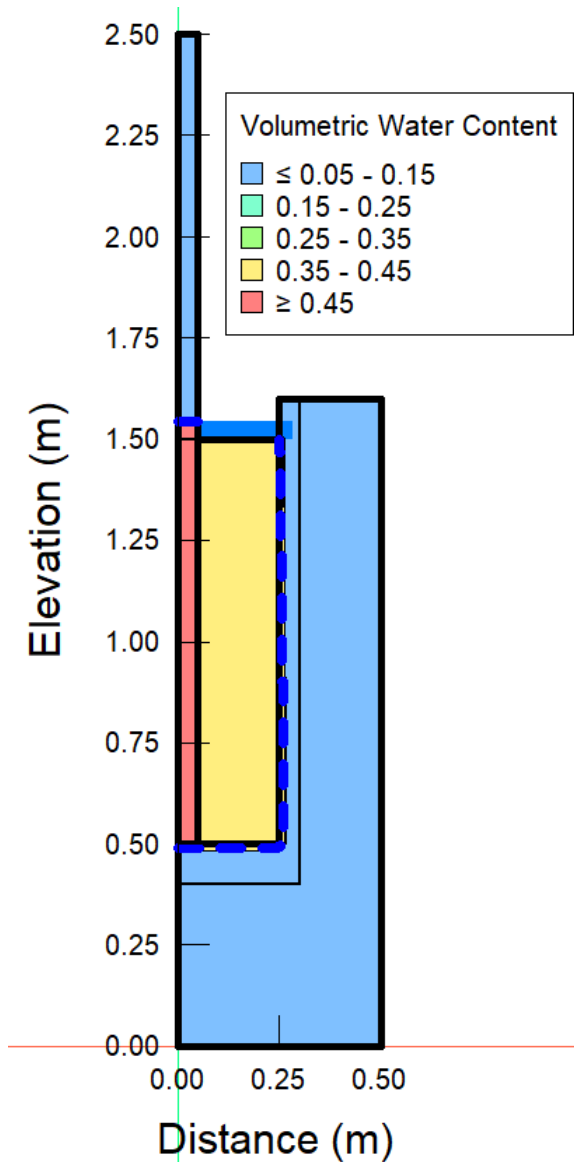
Figure 4: Comparison of numerical falling-head results with the predicted falling-head curves using the FHBP single-point solution and the FHBP curve-fitting solution for fine sand using the hand-auger test well with $L = 0.5$ m and $D_0 = 2$.
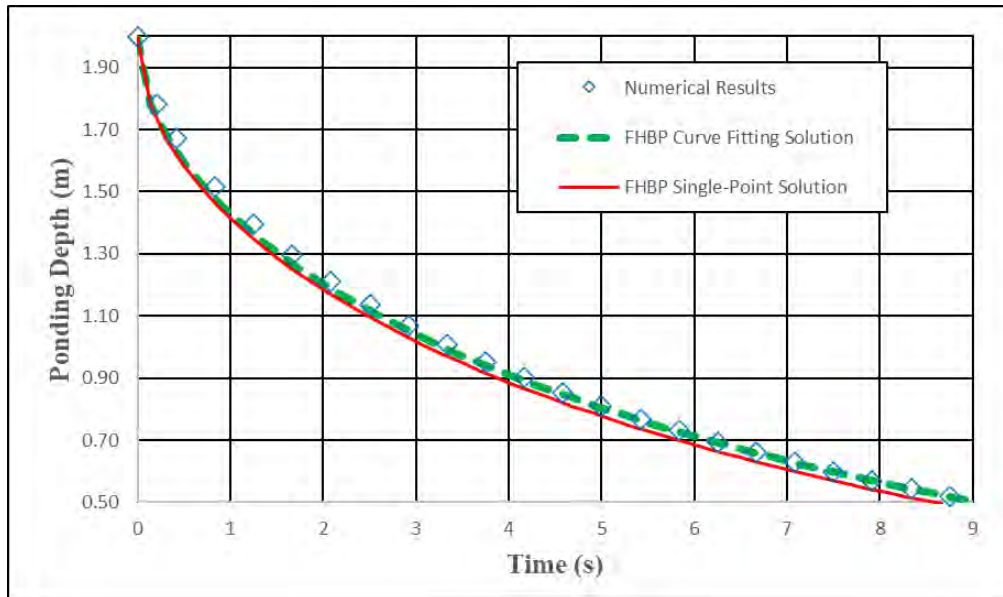
Figure 5: Numerical simulations of falling-head curves for flow rates of 0.4, 5, and 8 L/s compared with instantaneous fill for Qvt and the small test well with $L = 1$ m and $D_0 = 2$ m.
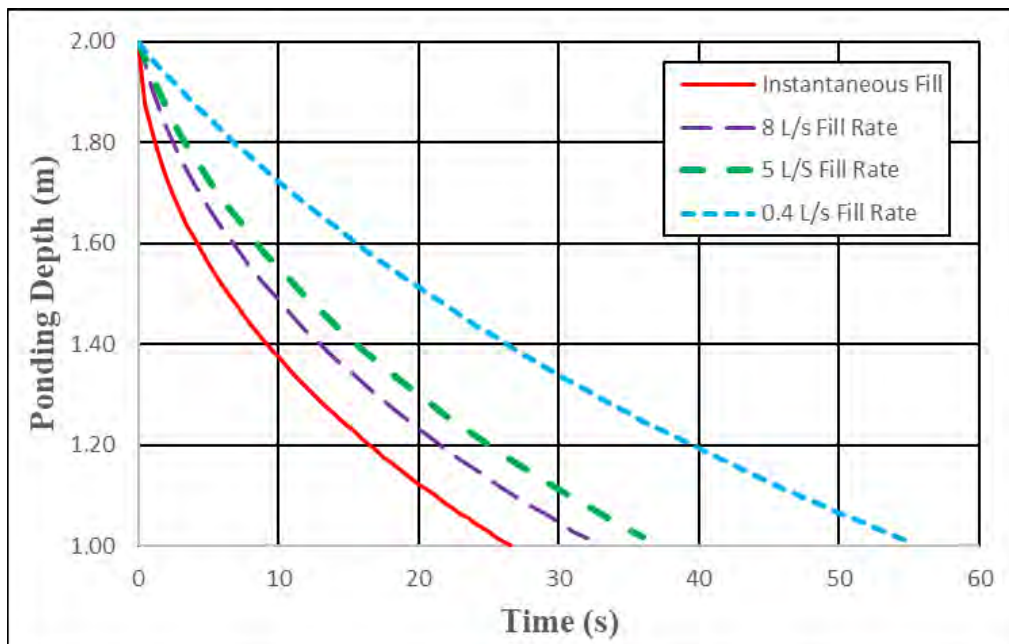
VOLUME IV: SHALLOW INFILTRATION TESTING TO ESTIMATE SATURATED HYDRAULIC CONDUCTIVITY

Near-Term Action (NTA) 2018-0827: Flexible Infiltration Test Methods for Evaluating Infiltration Feasibility

Project No. TAC-20-1 • **October 10, 2022**

Volume IV - Contents

Volume IV - List of Tables

Volume IV - List of Figures

Volume IV - Abstract

Volume IV provides the results of infiltration testing in pits and shallow test wells to: 1) demonstrate the use of these three methods under field conditions and determine if they provide similar estimates of bulk hydraulic conductivity (K_b); 2) compare the results from pit test and shallow wells; 3) provide field evidence of K_b variability over a distance of 30 to 70 ft; and 4) provide data for evaluation of layering, perching, and groundwater mounding. Future numerical modeling will evaluate the effects of layering, perching, and groundwater mounding.

Infiltration testing was conducted at four sites within the City of Tacoma. Two pits and three shallow test wells were tested at each site. The pits ranged from 4 to 8.5 ft deep and were typically 4 ft wide and 6-7 ft long. The wells were drilled using either a solid-stem auger mounted on a backhoe or a vactor truck typically used to clean sewers or excavate borings to clear for utilities. The test wells ranged in depth from 6.25 ft to 10.5 ft and were completed with 2.5 ft of screen with a sandpack interval that covered a slightly longer interval. The test facilities were conducted in a range of soil types, including glacial till, fill, advance outwash, and recessional outwash.

Drilling boreholes with the solid-stem auger was difficult given the gravelly soils encountered at all four test sites. Cobbles were sometimes difficult to remove from the bottom of the hole and caving was a challenge in looser soils. Drilling shallow boreholes with the vactor truck was much faster and provided a clean and well-defined borehole.

The FHBP method provided reasonable estimates of K_b in the glacial till soils. However, the FHBP tests in more permeable soils significantly underestimated K_b, consistent with numerical simulations that demonstrated the difficulty of conducting FHBP tests in soils with $K_b > 1.6$ ft/d (0.5 m/d).

USSBP and CSSBP tests were conducted in each of the test wells. K_b values from the four sites ranged from 0.08 in the fill soils to 61 ft/d in the recessional outwash. In most of the wells the CSSBP method provides higher estimates of K_b than the USSBP method, ranging from a difference factor of 1.07 to a difference factor of 4. (The difference factor is the larger K_b divided by the smaller K_b.) The reason for this difference will be evaluated later in the study using numerical simulations.

Comparison of test well result with test pit results at each site indicates that the well tests provide higher K_b estimates that the pit tests, generally by a difference factor of 1.1 to 3.4. This is likely because well tests are dominated by horizontal flow and test pit tests are dominated by vertical flow. Layered soils usually include lower-permeability layers that restrict vertical flow, resulting in a higher apparent K_b in well tests than pit tests. This will be evaluated later in the study using numerical simulations.

 Although the test facilities at each site are within 70 ft of each other, the K_b estimates for comparable facilities (wells compared with wells and pits compared with pits) demonstrate significant variability over relatively short distances. For the glacial till soils at Point Defiance Elementary and the recessional outwash soils at Roosevelt Park the spatial variability difference factors ranged from 1.25 to 1.8. The advance outwash soils at Verlo Playfield included one test well with significantly different soils than the other test facilities and the spatial variability difference factors ranged from 1.2 for the test pits to 6.5 for the test wells. The fill soils at Tacoma Power were highly variable, although there was a trend from lower K_b at one end of the site to higher K_b at the other end of the site. The spatial variability difference factors for Tacoma Power ranged from 6.6 for the test pits to 7.2 for the test wells.

Most of the infiltration tests conducted in test wells appeared to be at or very close to steady state at the end of the 6-hr test, although there are some exceptions. Steady state conditions were not achieved in most of the pit tests, even those tests conducted in permeable sandy gravel. Although it's expected that tests in lower permeable soils such as TP-TP-1 would not achieve steady state in 6 hr, the non-steady test results in relatively

permeable soils at Roosevelt Park and Verlo Playfield are not consistent with numerical simulations. One potential explanation for this difference between field results and numerical results is that the test facility may be underlain by a less permeable layer that is causing groundwater mounding. This potential explanation will be evaluated later in the study using numerical simulations.

1 Introduction

Stormwater infiltration is now required where feasible for new development in Washington State and the 2019 Stormwater Management Manual for Western Washington (WSDOE 2019) provides a variety of methods for sizing infiltration facilities. The preferred method is either the small or large pilot infiltration test (PIT). Volume I provides a brief summary of the PIT method.

A more accurate and reliable approach is to determine infiltration rate and capacity using measurements of soil saturated hydraulic conductivity (K_b) obtained from test methods that formally account for both flow directions (vertical, horizontal), and all three components of soil water flow (pressure, gravity, capillary). This study evaluates three different infiltration methods that do account for these flow dynamics, including the uncased steady-state borehole permeameter (USSBP), the cased steady-state borehole permeameter (CSSBP) and the cased falling-head borehole permeameter (FHBP). As reported in Volumes I, II, and III, numerical simulations were conducted to calibrate and evaluate these methods for relatively permeable soils typically considered for stormwater infiltration.

Numerical simulations facilitate calibration and validation for a broad range of soil types using prescribed soil parameters intended to generally represent the range of soils suitable for infiltration. The numerical validation efforts conducted for this study simulated homogenous and isotropic conditions, in accordance with the assumptions of the borehole permeameter methodology. In the real world, soils are generally layered (anisotropic) and can be highly variable over short distances. In order to illustrate that the isotropic and homogeneous assumptions are violated in the real world, the term "bulk hydraulic conductivity" (K_b) is used rather than K_b for reporting field test results.

The purpose of this field study is to conduct testing in actual test facilities using readily available equipment and water sources to: 1) demonstrate the use of these three methods under field conditions and determine if they provide similar estimates of K_b; 2) compare the results from pit test and shallow wells; 3) provide field evidence of K_b variability over a distance of 30 to 70 ft; and 4) provide data for evaluation of layering, perching, and groundwater mounding.

As reported in Volume V, deep infiltration testing was conducted to validate these methods in test wells with 15 to 20 ft of screen. Volume VI includes numerical analysis to evaluate the effects of layering, perching, and groundwater mounding.

1.1 Scope of Work

The scope of work for this task included field infiltration testing at four sites in the City of Tacoma, including both pit tests and machine-dug borehole tests at each site. The original scope included hand-auger boreholes, but all four test sites were gravelly and hand-augering was not feasible. The sites were selected to include a range of permeabilities, and this objective was generally achieved (K_b ranged from 0.17 ft/d at the glacial till site to 61 ft/d at the recessional outwash site). The original plan was to implement the USSBP method in the pits and all three test methods in the boreholes. However, two sites (Verlo Playfield and Roosevelt Park) were not suitable for FHBP testing since the K_b values were higher than 1.6 ft/d, which is considered too high for the FHBP method (Volume III).

The test results were analyzed using previously developed analytical methods, as described in Volumes I, II, and III. The results using different testing methods within the same facility were compared to determine the degree of agreement or divergence between the methods and the range of K_b values at each site. A summary of the results, lessons learned, and recommendations are provided in this volume.

2   Materials and Methods

2.1   Test Site Selection

The shallow infiltration test sites were all located within the City of Tacoma and were selected based on the following criteria:

- Sites were located on public property with permission from the controlling agency. One site was on school property, one site was on Tacoma Power property, and two sites were on Tacoma Metro Parks property.
- Test sites should include soil types that are typically used for stormwater infiltration, such as advance outwash (Qva), recessional outwash, sandy glacial till, or other sandy soils with K_b above 0.25 in./hr (0.5 ft/d).
- A fire hydrant within 600 ft of the test wells that did not require running hose across a busy street.
- No shallow groundwater within 10 ft of the base of the test well sand pack (to avoid groundwater mounding effects).

Twenty-five potential test sites were evaluated based on geologic maps, aerial photographs, and site visits. Initially, four sites were identified as potentially suitable sites and permission was obtained to investigate these sites. Explorations and testing were conducted at two of the sites (Point Defiance Elementary and the Tacoma Power site). Explorations were conducted at the other two sites and they were eliminated due to unsuitable soils or shallow groundwater. Another four potential sites were identified for the second round of testing and the first two sites were suitable for testing (Roosevelt Park and Verlo Playfield). The locations of the four test sites are shown on Fig. 1.

2.2 Test Pit Excavation and Test Well Construction

The test pits were excavated using a 4-ft wide bucket and were between 4.0 to 8.5 ft deep. The test pits were tested the same day they were excavated. The wetted area during the tests were 4 ft wide and between 6 and 7.5 ft long. Soil samples were collected from the bottom of the pits and delivered to a soil testing laboratory for moisture content and grainsize analyses. Following testing, the pits were backfilled and the surface restored with topsoil and either sod or grass seed.

Test wells at Point Defiance Elementary and the Tacoma Power site were excavated using a solid-stem auger mounted on a backhoe. The test wells at Roosevelt Park and Verlo playfield were excavated using a vactor truck. Vactor boreholes are excavated using a water jet on a long rod to loosen the soils and removing the soils and water using the vactor truck. Soil samples were collected approximately every foot using a hand auger. The samples that best represented the soils observed in the sandpack interval were submitted to a soil testing laboratory for moisture and grainsize analyses.

Based on experience on previous projects and this project, we have demonstrated that the vactor truck method is suitable for installing test wells in a broad range of soils. Although it can be slow, we have successfully drilled through very dense glacial till with the vactor truck method and a large vactor truck is capable of removing boulders up to 12 inches in diameter. The other advantage of the vactor truck method is that any caved soils and standing water can be removed from the bottom of the borehole before the soil samples are collected. Since water is used to loosen the soils, it is possible that the moisture content in soil samples collected from vactor boreholes may be higher than the surrounding soil.

This was the first project that we attempted installing test wells with a solid-stem auger. The auger struggled with the gravelly soils founds at Point Defiance Elementary and the loose sandy soils at the Tacoma Power site. It was not possible to remove all the cobbles encountered during drilling and caving was a constant struggle. Because of the caving, it was also difficult to confirm that soil samples were representative of the soils at the sampled interval and not contaminated by caved material. We do not recommend using a solid-stem auger for installing test wells unless the soils are free of cobbles and the sidewalls remain standing when the auger is removed from the hole.

The borehole diameters ranged from 10 in. to 16 in. and the wells were constructed similar to groundwater monitoring wells, although they were screened above the water table. In general, the wells were constructed with 2.5 ft of 2-in. diameter slotted polyvinyl chloride (PVC) well screen and solid casing extending above the ground surface. The annular space within the screened interval was filled with clean sand to provide a filter pack between the screen and the native soils and the sandpack intervals ranged from 2.5 to 4.5 ft. The annular space above the sandpack was sealed with bentonite chips.

The typical cross section at each site is shown in Fig. 2. In general, the test wells were screened between approximately 1 ft above the bottom of the test pits to 2-3 ft below the bottom of the test pits. This test interval was intended to provide the best representation of soils near the bottom of the test pits. Fig. 3 provides the plan view for each of the test sites, showing the locations of the test wells and pits.

Fig. 1: Locations of test sites.
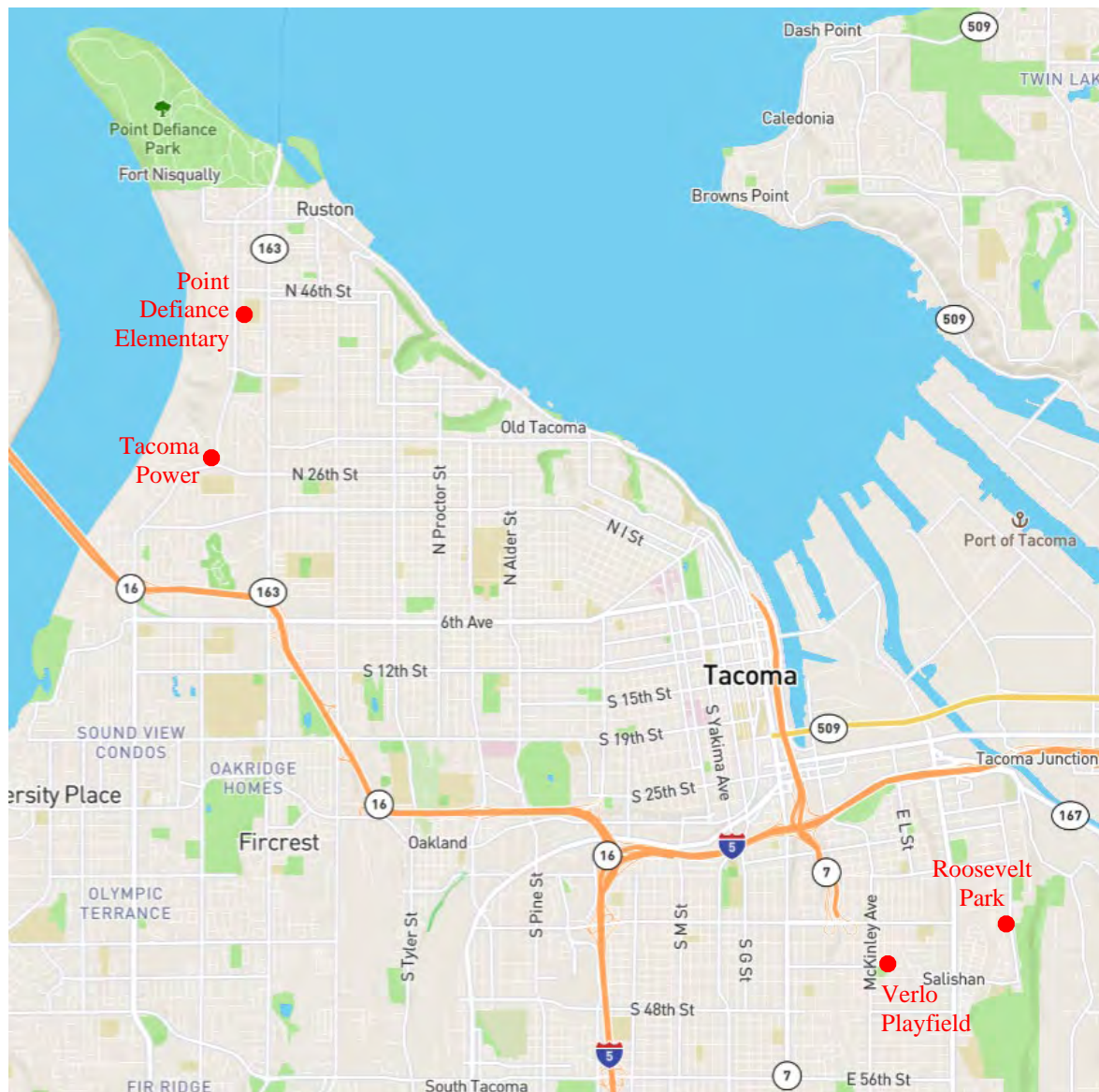
Fig. 2: Cross section showing typical arrangement of test pits and wells and approximate water levels during tests.
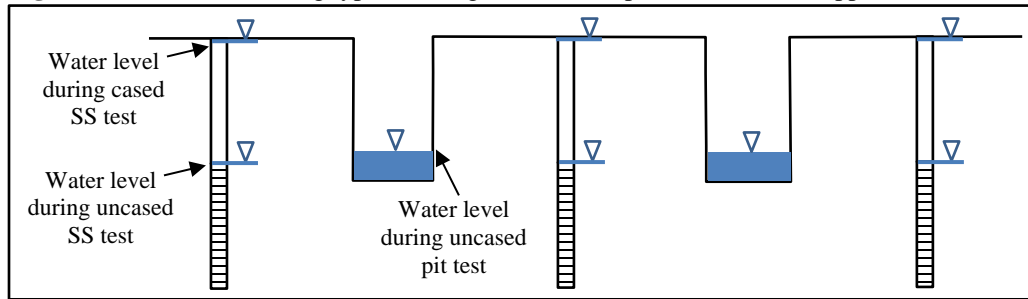
Fig. 3: Test Site Layouts (not to scale).

Point Defiance Elementary

Tacoma Power

Roosevelt Park

Verlo Playfield
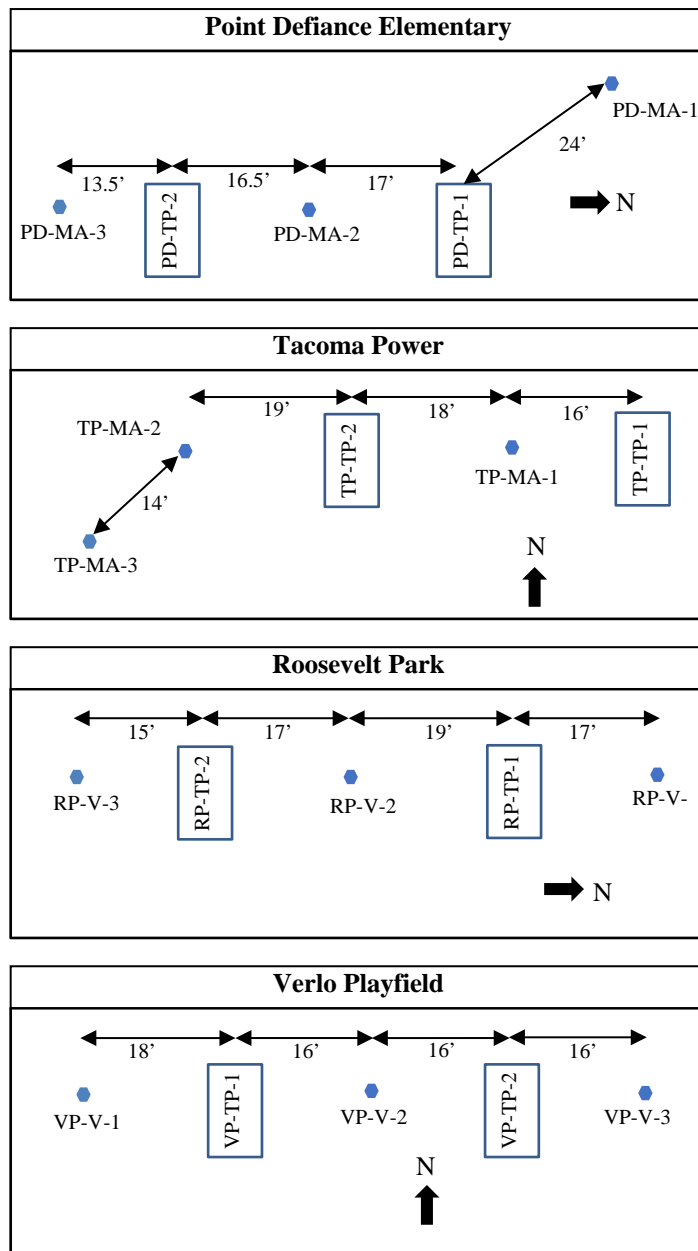
2.3 Test Procedures

All the infiltration tests for this study were conducted in June and November of 2021. A variety of infiltration tests were conducted in each of the test wells. FHBP tests were attempted in all the Point Defiance test wells, Tacoma Power wells TP-MA-2 and TP-MA-3, and the Verlo Playfield test wells. As discussed in Section 3.3, only some of the FHBP tests were considered valid. As shown in Fig. 2, USSBP tests were conducted in all the wells by maintaining the water level near the top of the sandpack interval and CSSBP tests were conducted in all the wells by maintaining the water level near the ground surface. Details of the test methodology are provided below.

2.3.1 Falling-Head Borehole Permeameter Tests

The FHBP tests were conducted using the following procedures:

1) A pressure transducer was placed in the bottom of the well and was set to record the water depth every second. The pressure transducer was connected to a data cable that allowed real-time monitoring of the depth of water during the test.

2) All head elevations used in the analysis are referenced from the bottom of sandpack, based on the assumption that water flows freely through the sandpack with minimal head loss. Therefore, the depth of sandpack beneath the screen was added to the transducer reading for graphing and analysis.

3) Water from a fire hydrant was discharged into the well as quickly as possible with the intention of filling the well to the top of casing. If the water level did not reach the top of the casing within one-two minutes the water was turned off.

4) The amount of water discharged into the test well was recorded.

5) The water level in the well was allowed to fall until it reached the top of the screened interval.

6) The results were evaluated using the FHBP method provided in Volume III.

2.3.2 Uncased Steady-State Borehole Permeameter Tests in Pits

The USSBP tests were conducted in pits using the following procedures:

1) After excavation of the test pit, a pressure transducer was placed in the bottom of the pit and was set to record the water depth once per minute. The pressure transducer was connected to a data cable that allowed real-time monitoring of the depth of water during the test.

2) Water from a fire hydrant was discharged into the test pit at a rate that maintained the water level (based on the pressure transducer in the bottom of the pit) approximately 12 inches above the bottom of the pit.

3) The USSBP tests were conducted for approximately 5.25 to 6.4 hr.

4) Flow rates were measured using flowmeters and recorded at regular intervals during the tests.

5) The flow rate in PD-TP-1 and PD-TP-2, and TP-TP-1 was less than 0.2 gpm, significantly less than the calibration range of the smallest flowmeter. For these tests, water was added at the beginning of the test and in the middle of the test to maintain the water depth within a range of approximately 0.1 ft. The flow rate was calculated by multiplying the rate of fall by the wetted area of the pit.

6) The transducer was left in the pit after the water was turned off to record the water levels during the falling head portion of the test. This information is useful for identifying perching layers or groundwater mounding using numerical simulations.

7) The results were evaluated using the USSBP method provided in Volume I.

2.3.3 Uncased Steady-State Borehole Permeameter Tests in Wells

The USSBP tests were conducted in wells using the following procedures:

1) A pressure transducer was placed in the bottom of the well and was set to record the water depth once per minute. The pressure transducer was connected to a data cable that allowed real-time monitoring of the depth of water during the test.

2) All head elevations used in the analysis are referenced from the bottom of sandpack, based on the assumption that water flows freely through the sandpack with minimal head loss. Therefore, the depth of sandpack beneath the screen was added to the transducer reading in the bottom of the well for graphing and analysis.

3) Water from a fire hydrant was discharged into the well at a rate that maintained the water level (based on the pressure transducer in the bottom of the well) near the top of the sandpack.

4) A drop pipe was attached to the flowmeter assembly to convey the water into the well casing.

5) USSBP tests of approximately 6 - 8 hr were conducted in all the wells.

6) Flow rates were measured using flowmeters and recorded at regular intervals during the tests.

7) The flow rate in PD-MA-2 and PD-MA-3 was less than 0.2 gpm, significantly less than the calibration range of the smallest flowmeter. For this test, short bursts of water were added at regular intervals to maintain the water depth within a 1 ft interval. The flow rate was calculated by dividing the volume of water added by the duration between bursts of water.

8) Water levels were recorded at regular intervals during the tests to determine when it was necessary to change the flow rate to maintain the water level near the top of the sandpack.

9) The transducer was left in the well after the water was turned off to record the water levels during the falling head portion of the test. This information is useful for identifying perching layers or groundwater mounding using numerical simulations.

10) The results were evaluated using the USSBP method provided in Volume I.

2.3.4 Cased Steady-State Borehole Permeameter Tests

The CSSBP tests were conducted using the following procedures:

1) A pressure transducer was placed in the bottom of the well and was set to record the water depth once per minute. The pressure transducer was connected to a data cable that allowed real-time monitoring of the depth of water during the test.

2) All head elevations used in the analysis are referenced from the bottom of sandpack, based on the

assumption that water flows freely through the sandpack with minimal head loss. Therefore, the depth of sandpack beneath the screen was added to the transducer reading in the bottom of the well for graphing and analysis.

3) Water from a fire hydrant was discharged into the well at a rate that maintained the water level (based on the pressure transducer in the bottom of the well) near the top of the well, or as high as possible given the maximum capacity of the fire hydrant and hose assembly. The flow rates were significantly limited by the 1-inch hose used to convey the water to the test wells and ranged from 10 to 28 gpm depending on the pressure in the hydrant, the number of simultaneous tests, the length of fire hose, and the diameter and length of the drop pipe.

4) A drop pipe was attached to the flowmeter assembly to convey the water into the well casing.

5) When feasible given the hydrant capacity, the flow rate was adjusted to maintain the water level near the top of the well. If the water level was significantly below the top of the well at the maximum hydrant capacity, the flow rate was set at the maximum rate and the water level was allowed to rise during the duration of the tests.

6) The CSSBP tests were all between 4 and 8 hr long.

7) Flow rates were measured using flowmeters and recorded at regular intervals during the tests.

8) Water levels were recorded at regular intervals during the tests to determine when it was necessary to change the flow rate to maintain the water level near constant in the well.

9) The transducer was left in the well after the water was turned off to record the water levels during the falling head portion of the test. This information is useful for identifying perching layers or groundwater mounding using numerical simulations.

10) The results were evaluated using the CSSBP method provided in Volume II.

2.4 Analysis of Test Results

The test results were analyzed to determine K_b using the methods for FHBP tests (Volume III), USSBP tests (Volume I), and CSSBP tests (Volume II). All three methodologies assume a flat-bottom cylindrical test facility, isotropic and homogeneous soil, and no water-table effects.

2.4.1 FHBP Test Analysis Method

The FHBP test analysis method is only valid while the water level is above the screen or sandpack interval. As described in Volume III, the single-point FHBP method used for this study is based on the following equation:

$$K_b = \frac{r_c^2}{4\, r_0\, t}\, \tau_E \text{ (Eq. 1)}$$

where r_c is the radius of the casing, r_0 is the radius of the equivalent sphere discharge surface (elaborated below), and t is the time when K_b is estimated. τ_E is dimensionless time, based on the following equation:

$$\tau_E = \left(1 + \frac{1}{2A_E}\right) ln\left(\frac{A_E^3 - 1}{A_E^3 - \rho_E^3}\right) - \frac{3}{2A_E} ln\left(\frac{A_E - 1}{A_E - \rho_E}\right) + \frac{\sqrt{3}}{A_E}\left[\tan^{-1}\left(\frac{A_E + 2\rho_E}{\sqrt{3}\, A_E}\right) - \tan^{-1}\left(\frac{A_E + 2}{\sqrt{3}\, A_E}\right)\right] \text{ (Eq. 2)}$$

where:

$$A_E^3 = \frac{3r_c^2\left(H_0 + \alpha^{*-1}\right)}{4r_0^3\, \Delta\theta} + 1 \text{ (Eq. 3)}$$

$$\rho_{\text{E}}^3 = \frac{3r_c^2(H_0 - H_t)}{4r_0^3\,\Delta\theta} + 1 \text{ (Eq. 4)}$$

$$\Delta\theta = \theta_{\text{fs}} - \theta_{\text{i}} \text{ (Eq. 5)}$$

H_0 is the effective pressure head in the borehole screen at $t = 0$, H_t is the effective pressure head in the borehole screen at time t (elaborated below), α^* is the soil sorptive number, θ_{s} is the porosity (aka field-saturated volumetric soil-water content), and θ_{i} is the background volumetric soil-water content. The θ_{s} used in the FHBP analyses is based on the soil texture and density.

As described in Kindred and Reynolds (2020) α^* represents the capillarity of the soil. The single-point FHBP method used for this study assumed a value for α^* based on soil characteristics, as calculated in Volume I and summarized in Table 1.

The equivalent sphere radius (r_0) is calculated the following expression:

$$r_0 = \left(\frac{r_b^2}{4} + \frac{r_b L}{2}\right)^{1/2} \text{ (Eq. 6)}$$

where r_b = radius of the borehole and L is the length of the sandpack interval. As discussed in Reynolds (2011), the effective pressure head H_t is calculated using:

$$H_t = D_t - E \text{ (Eq. 7)}$$

where E is the screen factor:

$$E = \frac{L^2}{r_b + 2L} \text{ (Eq. 8)}$$

for combined vertical and radial discharge. D_t is actual water depth at time t. H_0, the initial effective pressure head, is calculated using Eq. 7 by replacing H_t with H_0 and D_t with D_0, the initial or target fill depth.

Table 1: *Sorptive Number (α^*)* and volumetric saturated water content (porosity, θ_{s}) for the 10 representative soils types used to calibrate the steady-state BP methods.

Soil Type	*Sorptive Number α^* (ft^{-1})*	**Porosity θ_{s}**
Silty fine sand (SM)	0.5	0.4
Silty fine-coarse sand (SM)	1.7	0.35
Qvt (SM)	0.36	0.17
Silty Qva (SM)	0.41	0.25
Fine sand (SP-SM)	1.1	0.4
Medium sand (SP)	3.4	0.4
Sandy gravel (GW)	17.4	0.4
Fine Qva (SP-SM)	0.76	0.3
Fine-Medium Qva (SP)	1.2	0.3
Fine-Coarse Qva (SW)	7.6	0.3

2.4.2 USSBP Test Analysis Method

As discussed in Volume I and Kindred and Reynolds (2020), the USSBP method is based on the following equation:

$$K_S = \frac{C_u Q}{2\pi H^2 + \pi r_b^2 C_u + \frac{2\pi H}{\alpha^*}} \quad \text{(Eq. 9)}$$

where

$$C_u = \left[\frac{(H/r_b)}{Z_1 + Z_2(H/r_b)} \right]^{Z_3} \quad \text{(Eq. 10)}$$

H is the ponding head at the end of the steady state test and Q is the flow rate at the end of the steady state test. Eq. 9 assumes that H is less than the uncased or screened portion of the test facility. α^* is the soil sorptive number (ft^{-1}), C_u is the uncased shape function (dimensionless), and Z_1, Z_2, and Z_3 are the shape function fitting parameters (dimensionless). Values for Z_1, Z_2, Z_3 for the USSBP method are provided in Table 2.

USSBP tests were conducted in both test wells and pit. The test pits were not circular in shape and the equivalent borehole radius was calculated using the following equation:

$$r_b = \sqrt{pit\ width * pit\ length/\pi} \quad \text{(Eq. 11)}$$

Table 2: Uncased *shape function* (C_u) parameters for USSBP tests based on different soil classifications using the Unified Soil Classification System.

Soil Type	Low Ponded Head ($H/r \leq 20$)			High Ponded Head ($H/r \geq 20$)		
	Z_1 (-)	Z_2 (-)	Z_3 (-)	Z_1 (-)	Z_2 (-)	Z_3 (-)
Sand and gravel with > 12% Silt (SM, GM)	2.11	0.192	0.91	2.04	0.0224	0.547
Sand and gravel with < 12% Silt (SP-SM, SP, SW, GW, GP)	2.03	0.207	0.98	2.11	0.0273	0.605

2.4.3 CSSBP Test Analysis Method

As discussed in Volume II, the CSSBP method uses the same form of the equation used in the USSBP method with minor adjustments:

$$K_S = \frac{C_c Q}{2\pi LH + \pi r_b^2 C_c + \frac{2\pi L}{\alpha^*}} \quad \text{(Eq. 12)}$$

and

$$C_c = \left[\frac{(L/r_b)}{Z_1 + Z_2(L/r_b)} \right]^{Z_3} \quad \text{(Eq. 13)}$$

where L, the length of the sandpack or screen, replaces one of the H values in the first term of the denominator and the H in the third term of the denominator. C_c is the cased shape function and used different Z_1, Z_2, and Z_3 fitting parameters than the C_u shape function, as provided in Table 3.

The USSBP method is calibrated for uncased scenarios where $H = L$ and the CSSBP method is calibrated for cased scenarios when $H > L$. However, there is a transition interval as the water level begins to rise above the sandpack into the solid casing extending above the sandpack. Based on simulations reported in Volume II, the USSBP method is recommended when H/L is less than 1.2 and the CSSBP method is recommended when H/L is greater than 1.2

Table 3: Uncased *shape function* (C_c) parameters for CSSBP tests based on different soil classifications using the Unified Soil Classification System.

Soil Type	Short Sandpack ($L/r_b < 20$)			Long Sandpack ($L/r_b \geq 20$)		
	Z_1 (-)	Z_2 (-)	Z_3 (-)	Z_1 (-)	Z_2 (-)	Z_3 (-)
Sand and gravel with > 12% Silt (SM, GM)	3.06	0.12	0.674	2.32	0.0286	0.463
Sand and gravel with < 12% Silt (SP-SM, SP, SW, GW, GP)	2.45	0.214	0.93	1.87	0.0354	0.501

3 Results

This section presents the test results for the eight test pits and 12 test wells included in this study. Testing at Point Defiance Elementary and Tacoma Power was conducted in June 2021 and testing at Roosevelt Park and Verlo Playfield was conducted in November 2021.

3.1 Grainsize Analyses

The primary soil samples were submitted to Hayre McElroy & Associates, LLC in Redmond, Washington for moisture content testing in accordance with ASTM D2216 and grainsize analyses according to ASTM D6913. Additional samples were submitted to Eurofins TestAmerica Laboratories in Seattle, Washington for quality control and quality assurance. The results are provided in Appendix A and summarized in Table A-1 of Appendix A.

Most of the soil horizons targeted for infiltration testing contained significant large gravels and cobbles. Gravels larger than 2-inches in diameter were not included in the samples sent to laboratories for grainsize analysis since the soils hydraulic conductivity is primarily a function of the ratio of silt to sand. Therefore, the grainsize results may underestimate the percentage of gravel and cobbles in the soil.

3.2 Subsurface Characteristics

Eight test pits and 12 test wells were constructed and tested at the four sites. Soil logs and well completion details are provided in Appendix B. A range of soils were encountered at the four sites, including Qvt at Point Defiance Elementary, fill at Tacoma Power, recessional outwash at Roosevelt Park, and advance outwash at Verlo Playfield.

As summarized in Table 4, the test pits ranged in depth from 4.0 to 8.5 ft deep with bottom dimensions of 4 ft wide and 6.0-7.5 ft long. The silt content in the bottom of the test pits ranged from less than 1% in RP-TP-1 to 25% in TP-MA-1. Moisture content in the bottom of the test pits ranged from 4% in RP-TP-1 and RP-TP-2 to 12% in TP-TP-1.

As summarized in Table 5, the test wells ranged in depth from 6.25 to 10.5 ft deep with diameters ranging from 10 to 16 in. The silt content in the test wells ranged from 1.4% in RP-V-1 and RP-V-2 to 25% in TP-MA-1. Moisture content in the test wells ranged from 4% in several wells to 16% in TP-MA-1.

Table 4: Shallow infiltration test pits.

Pit Name	Install Date	Depth (ft)	Bottom Dimensions	UCSC Class	Best-Fit Soil Type	% Silt	Moisture Content
PD-TP-1	6/7/21	4.0	4.0 by 7.5	SM	Qvt	18	0.09
PD-TP-2	6/7/21	4.0	4.0 by 7.0	SM	Qvt	22	0.07
TP-TP-1	6/8/21	7.5	4.0 by 6.0	SM	St F-C sand	19	0.12
TP-TP-2	6/8/21	7.5	4.0 by 6.5	SP-SM	St F-C sand	8.2	0.09
RP-TP-1	11/4/21	4.25	4.0 by 7.0	GP	Sd gravel	0.8	0.04
RP-TP-2	11/4/21	4.5	4.0 by 6.0	GP	Sd gravel	1.6	0.04
VP-TP-1	11/2/21	8.5	4.0 by 6.0	GP-GM	F-C Qva	10	0.10
VP-TP-2	11/2/21	8.5	4.0 by 6.0	GP-GM	F-C Qva	9-11	0.09

Notes: Qva - Vashon advance outwash; Qvr – Vashon recessional outwash; Qvt – Vashon glacial till; Sd – Sandy; St – silty; F-C – fine-coarse

The BP method requires identifying which representative soil type used to calibrate the constant-head BP fitting parameters best represents the soil encountered in the tested interval. Table 1 identifies the 10 representative soils

types used for calibration. The representative soil types that provide the best fit for each test facility are provided in Tables 4 and 5.

Table 5: Shallow infiltration test wells.

Well Name	Depth (ft)	Install Date	Drilling Method	Sandpack Interval (ft)	Diameter (in.)	UCSC Class	Best-Fit Soil Type	% Silt	Moisture Content
PD-MA-1	6.25	6/7/21	Auger	3.75-6.25	12	SM	Qvt	4.4[1]	0.04[1]
PD-MA-2	7.0	6/7/21	Auger	3.6-7.0	12	SP-SM	Qvt	10	0.08
PD-MA-3	6.5	6/7/21	Auger	3.3-6.5	10	SM	Qvt	16	0.15
TP-MA-1	10	6/8/21	Auger	7-10	11	SP/SM	St F-C Sand	25/5[2]	0.13-0.16[2]
TP-MA-2	10	6/8/21	Auger	7-10	11	SP-SM	St F-C Sand	6.5	0.04
TP-MA-3	10	6/8/21	Auger	6-10	11	SP	Sd gravel	1.1-2.9	0.04-0.05
RP-V-1	7.5	11/1/21	Vactor	4.5-7.5	11	GP	Sd gravel	1.4	0.04
RP-V-2	7.5	11/1/21	Vactor	4.5-7.5	11	GP	Sd gravel	1.4	0.04-0.05
RP-V-3	7.5	11/1/21	Vactor	3.5-7.5	11	GP-GM	Sd gravel	5.9	0.07
VP-V-1	10	11/1/21	Vactor	6-10	14	GW	F-C Qva	4.0	0.10
VP-V-2	10.5	11/1/21	Vactor	6-10.5	16	GP-GM	F-C Qva	8.7	0.09
VP-V-3	10	11/1/21	Vactor	6-10	15	GP-GM	F-C Qva	7.2	0.08

Notes: Qva - Vashon advance outwash; Qvr – Vashon recessional outwash; Qvt – Vashon glacial till; Sd – sandy; St – silty; F-C – fine-coarse
[1] Grainsize analysis not representative of soil in sandpack interval.
[2] Two distinct soil types within sandpack interval

3.3 FHBP Results

As discussed in Volume III, the FHBP method assumes instantaneous filling of the well casing to a depth that is higher than the top of the sandpack. Numerical simulations have demonstrated that slight deviations from the instantaneous filling assumption can adversely impact the results when $K_b \geq 1.6$ ft/d and for larger test wells (e.g., $L \geq 3.3$ ft, $D_0 \geq 6.6$ ft, $r_b \geq 4$ in.). None of the test facilities included in this scope of work were within these dimensions and only the wells at the Point Defiance Elementary site had $K_b < 1.6$ ft/d.

Despite these limitations, FHBP tests were attempted in all the wells at Point Defiance Elementary and Verlo Playfield and two of the wells at the Tacoma Power site. Initially, the intention was to shut the water off when the water rose to the top of casing. However, in the case of the Tacoma Power and Verlo Playfield wells, the water did not reach the top of the casing during a reasonable period of time and the water was turned off after 60-160 s. Results for tests with fill times greater than 30 s are not considered valid.

3.3.1 FHBP Results for Point Defiance Elementary

FHBP tests were conducted on three different days in all three Point Defiance Elementary wells. Fig. 4 illustrates the FHBP test results for these nine tests and Tables 6-8 summarize the results. In Fig. 4, the solid black line represents the ground surface and the dashed line represents the top of sandpack. The head elevations are based on data from a transducer in the bottom of the well.

All three wells were completed with 2.5 ft of screen and 5 ft of solid casing so the water level at the top of the well could not rise higher than 7.5 ft. However, in several cases (e.g., the PD-MA-1 June 10th test) the pressure head in the bottom of the well rose to a height of 8 – 8.5 ft, significantly higher than the water level at the top of the well. As discussed in Volume V, this additional head below the drop pipe was likely due to velocity head (the force of the

water exiting the drop pipe). Since velocity head disappears as soon as the water is turned off, the initial water level was limited to 7.5 ft for the FHBP test analysis (as shown in Tables 6-8).

Since it took several seconds to turn the flow rates up and down, the flow rates shown on the figures were generally estimated by dividing the total volume of water used to fill the well by the time to fill the well. The flow rate during the fill period varied significantly for each of tests, ranging from 10 gpm in the PD-MA-3 June 11 test to 56 gpm in the PD-MA-3 June 10 test.

FHBP analysis requires the soil porosity and the background water content at the time of the test. The soil porosity assumed for each test was based on moisture contents for representative soils used to calibrate the steady-state BP fitting parameters (provided in Table 1). The background water content for the first FHBP test at each test well was based on the water content in soil samples from the tested soil horizon (provided in Table 5). The second and third FHBP tests were conducted after steady-state tests had been conducted in the wells and it is likely that the soils contained higher moisture content from this testing. Therefore, the background moisture content for the June 11 and June 16 tests were assumed to be 5% higher than in the soil samples collected during well construction.

The sorptive number (α^*) value for all three wells was assumed to be 0.36 ft^{-1}, assuming that the most representative soil was Qva (Table 1). The calculation times provided in Tables 6-8 were selected to be when the water level was near the top of the sandpack and are calculated by subtracting the fill time. For example, the calculation time for PD-MA-1 June 10 test is 65 s (77 s minus the fill time of 12 s). As shown in Table 6, the water depth at this time was 2.6 ft.

Table 6 summarizes the results for PD-MA-1. The tests on June 10 and June 11 provides similar K_b values of 0.09 and 0.1 ft/d. The June 16th test provides a K_b values of 0.24 ft/d. It is not known why the later FHBP tests provided a higher K_b, although this trend was observed in the other two test wells. It's possible that infiltration testing can improve infiltration capacity by flushing silt from the sandpack into the lower portion of the well or into the formation. We did not observe any significant accumulation of silt in the bottom of the well screen after testing.

Table 7 summarizes the results for PD-MA-2. The test on June 10 provided a K_b values of 0.13 ft/d and the two later tests provided K_b values of 0.38 and 0.57 ft/d, again demonstrating higher K_b values in later tests. The June 16 test in this well had the shortest fill time and is probably the most reliable results.

Table 8 summarizes the results for PD-MA-3. The test on June 10 provided a K_b value of 0.046 ft/d. As illustrated by the irregular head curve during the fill period, the flow rate during the June 11 test was variable and this test is considered unreliable. The K_b value of 1.6 ft/d for the June 16 test was more than an order of magnitude higher than the June 10 test. As discussed later in the Volume IV, the capacity in this well increased substantially during the CSSBP test performed on June 11 (after the FHBP test). It is not known why the capacity of this well dramatically increased during the second day of testing although potential reasons are discussed later in Volume IV.

Fig. 4: FHBP test results for Point Defiance Elementary site.
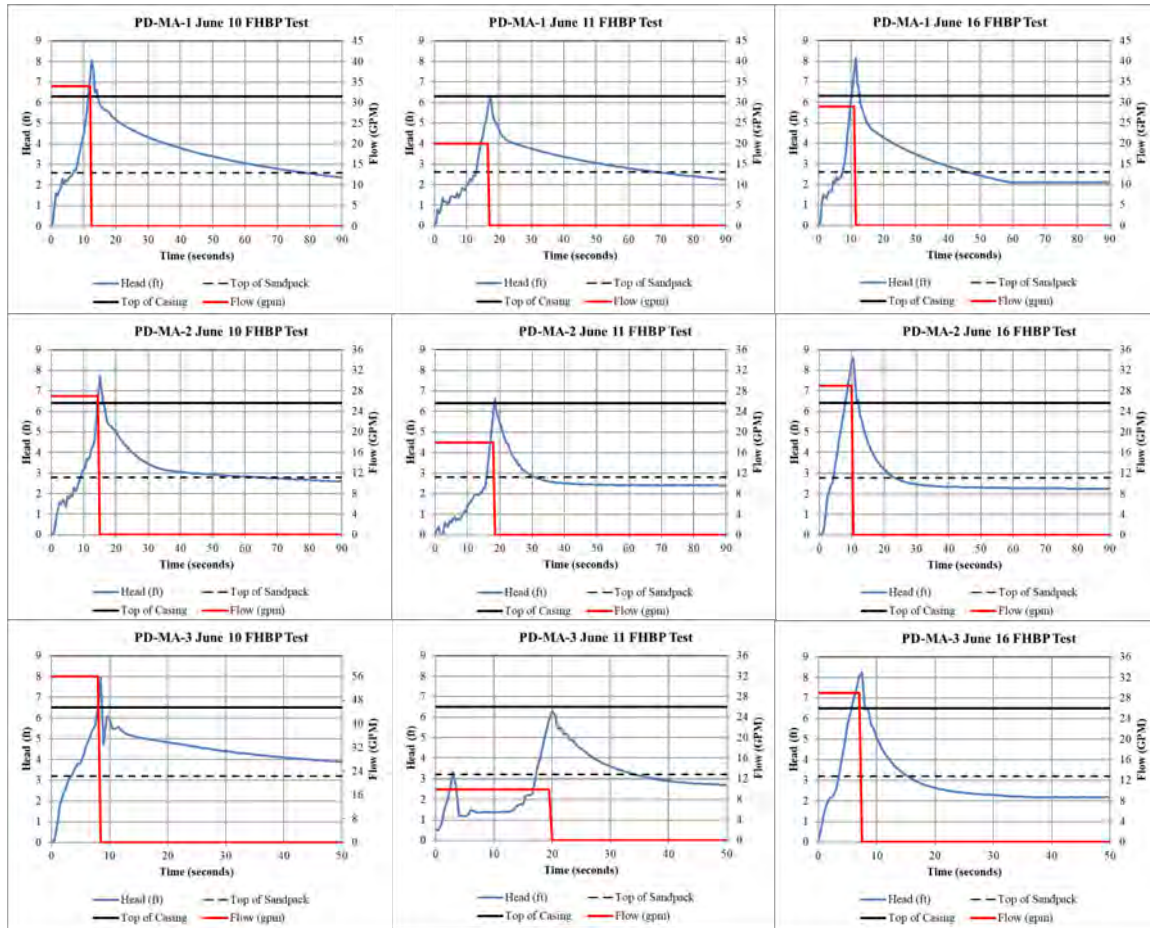
Table 6: Results of FHBP method for PD-MA-1 at Point Defiance Elementary site.

Parameter	Units	PD-MA-1 6/10/21	PD-MA-1 6/11/21	PD-MA-1 6/16/21
Initial water depth (D_0)	ft	7.5	6.21	7.5
Water depth at time t (D_t)	ft	2.6	2.6	2.6
Calculation time (t)	s	65	52	35
Casing radius (r_c)	in.	0.083		
Borehole radius (r_b)	in.	0.51		
Sandpack length (L)	ft	2.6		
Assumed Saturated volumetric soil-water content (θ_s)	-	0.25		
Background volumetric soil-water content (θ_i)	-	0.09	0.14	0.14
Assumed Sorptive Number (α^*)	1/ft	0.36	0.36	0.36
Calculated K_b	**ft/d**	**0.09**	**0.10**	**0.24**

Table 7: Results of FHBP method for PD-MA-2 at Point Defiance Elementary site.

Parameter	Units	PD-MA-2 6/10/21	PD-MA-2 6/11/21	PD-MA-2 6/16/21
Initial water depth (D_0)	ft	7.5	6.6	7.5
Water depth at time t (D_t)	ft	2.9	2.8	3.2
Calculation time (t)	s	33	12	9
Casing radius (r_c)	in.	0.083		
Borehole radius (r_b)	in.	0.49		
Sandpack length (L)	ft	2.8		
Assumed Saturated volumetric soil-water content (θ_s)	-	0.25		
Background volumetric soil-water content (θ_i)	-	0.08	0.13	0.13
Assumed Sorptive Number ($\alpha*$)	1/ft	0.36	0.36	0.36
Calculated K_b	**ft/d**	**0.13**	**0.38**	**0.57**

Table 8: Results of FHBP method for PD-MA-3 at Point Defiance Elementary site.

Parameter	Units	PD-MA-3 6/10/21	PD-MA-3 6/11/21	PD-MA-3 6/16/21
Initial water depth (D_0)	ft	7.5	6.3	7.5
Water depth at time t (D_t)	ft	3.3	3.3	3.3
Calculation time (t)	s	141	26	7
Casing radius (r_c)	in.	0.083		
Borehole radius (r_b)	in.	0.42		
Sandpack length (L)	ft	3.2		
Assumed Saturated volumetric soil-water content (θ_s)	-	0.25		
Background volumetric soil-water content (θ_i)	-	0.15	0.2	0.2
Assumed Sorptive Number ($\alpha*$)	1/ft	0.36	0.36	0.36
Calculated K_b	**ft/d**	**0.046**	**0.52**	**1.6**

3.3.2 FHBP Results for the Tacoma Power Site

FHBP tests were conducted in TP-MA-2 and TP-MA-3. A FHBP test was not conducted in TP-MA-1 because we were not able to seal off the well above the sandpack on the day of the test. Fig. 5 illustrates the FHBP test results for these two tests and Table 9 summarize the results. In Fig. 5, the solid black line represents the ground surface and the dashed line represents the top of sandpack. The head elevations are based on data from a transducer in the bottom of the well.

Both wells were completed with 2.5 ft of screen and 10 ft of solid casing so the water level at the top of the well could not rise higher than 12.5 ft. The water level did not rise above the top of casing in either test. Since it took several seconds to turn the flow rates up and down, the flow rates shown on the figures were generally estimated by dividing the total volume of water used to fill the well by the time to fill the well. The flow rate during the fill period ranged from 20 gpm in the TP-MA-3 test to 25 gpm in the TP-MA-2 test.

Based on the grainsize analyses, the soil observed in TP-MA-2 was assumed to be silty fine-coarse sand with a $\alpha*$ value of 17.4 ft^{-1} and a soil porosity of 0.4 (Table 1). Based on the moisture content results (Table 5), the background moisture content was assumed to be 4%. The soil observed in TP-MA-3 was assumed to be sandy

gravel with a α^* value of 1.68 ft^{-1} and a soil porosity of 0.35 (Table 1). Based on the moisture content results for the sample from this well (Table 5), the background moisture content was assumed to be 5%.

Table 9 summarizes the results for both wells. TP-MA-2 provided an estimated K_b value of 0.47 ft/d and TP-MA-3 provided a K_b value of 0.74 ft/d. Neither of these values are considered valid given the long fill times and high K_b values provided by the USSBP and CSSBP tests reported below. The higher value in TP-MA-3 can be explained by the lower silt content in this well (1.1-2.9% compared with 6.5% in TP-MA-2).

Fig. 5: FHBP test results for Tacoma Power Site.
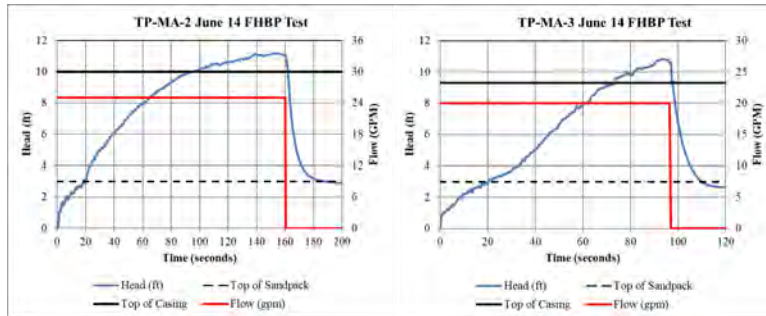
Table 9: Results of FHBP method for TP-MA-2 and TP-MA-3 at Tacoma Power site.

Parameter	Units	TP-MA-2 6/14/21	TP-MA-3 6/15/21
Initial water depth (D_0)	ft	11.1	10.6
Water depth at time t (D_t)	ft	3.2	3.5
Calculation time (t)	s	20	20
Casing radius (r_c)	in.	0.083	
Borehole radius (r_b)	in.	0.47	0.45
Sandpack length (L)	ft	3.0	3.3
Assumed Saturated volumetric soil-water content (θ_s)	-	0.35	0.4
Background volumetric soil-water content (θ_i)	-	0.04	0.05
Assumed Sorptive Number (α^*)	1/ft	1.68	17.4
Calculated K_b	**ft/d**	**0.47**	**0.74**

3.3.3 FHBP Results for Verlo Playfield

FHBP tests were conducted in all three test wells at Verlo Playfield. Fig. 6 illustrates the FHBP test results and Table 10 summarize the results. In Fig. 6, the solid black line represents the ground surface and the dashed line represents the top of sandpack. The head elevations are based on data from a transducer in the bottom of the well.

All three wells were completed with 2.5 ft of screen and 10 ft of solid casing so the water level at the top of the well could not rise higher than 12.5 ft. The water level did not rise above the top of casing in any of the tests. Since it took several seconds to turn the flow rates up and down, the flow rates shown on the figures were generally estimated by dividing the total volume of water used to fill the well by the time to fill the well. The flow rate during the fill period ranged from 18 gpm in the VP-V-2 test to 83 gpm in the VP-V-3 test.

Based on the grainsize analyses, the soil in all three wells was assumed to be fine-coarse Qva with a α* value of 7.63 ft^{-1} and a soil porosity of 0.3 (Table 1). Based on the moisture content results (Table 5), the background moisture content was assumed to range from 0.08 in VP-V-3 to 0.1 in VP-V-1.

Table 10 summarizes the results for all three wells. The estimated K_b values ranged from 0.07 ft/d in VP-V-2 to 0.24 ft/d in VP-V-1. None of the values are considered valid given the long fill times and high K_b values provided by the USSBP and CSSBP tests reported in the next section.

Fig. 6: FHBP test results for Verlo Playfield Site.
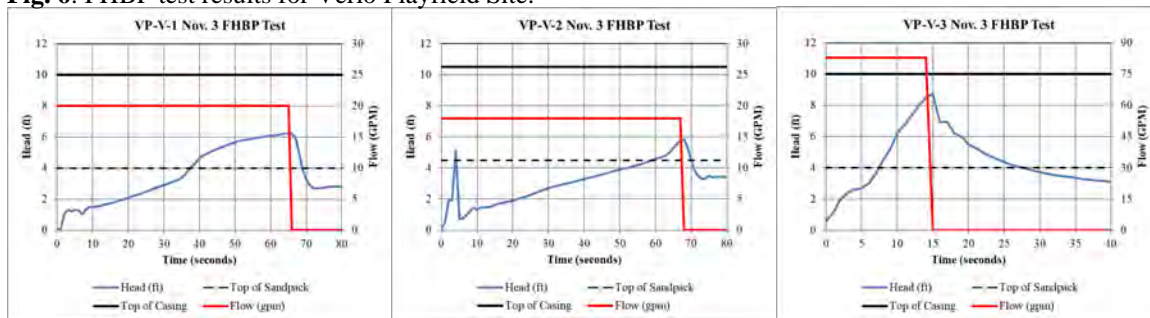
Table 10: Results of FHBP method for VP-V-1, VP-V-2, and VP-V-3 at Verlo Playfield site.

Parameter	Units	VP-V-1 11/3/21	VP-V-2 11/3/21	VP-V-3 11/3/21
Initial water depth (D_0)	ft	6.2	5.8	8.7
Water depth at time t (D_t)	ft	3.9	4.5	4.1
Calculation time (t)	s	3	3	12
Casing radius (r_c)	in.	0.083		
Borehole radius (r_b)	in.	0.6	0.68	0.63
Sandpack length (L)	ft	4	4.5	4
Assumed Saturated volumetric soil-water content (θ_s)	-	0.3		
Background volumetric soil-water content (θ_i)	-	0.1	0.09	0.08
Assumed Sorptive Number (α*)	1/ft	7.6		
Calculated K_b	**ft/d**	**0.24**	**0.07**	**0.15**

3.4 USSBP Test Pit Results

This section provides the USSBP results for the eight test pits. The test pits were not circular in shape and the equivalent borehole radius was calculated using Eq. 11. As provided in Table 4, the pit width was 4 ft for all the test pits and the pit length ranged from 6.0 to 7.5 ft. The difference factors referenced below are calculated by dividing the highest K_b by the lowest K_b.

3.4.1 *Steady-State Test Pit Results for Point Defiance Elementary*

Fig. 7 illustrates the USSBP test results for PD-TP-1 and PD-TP-2. The flow rate to maintain a constant head was below the range of the smallest meter available so water was only added once during the test after the ponding depth reached the target depth of approximately 1 ft. The tests lasted for at least 360 minutes after the target ponding depth was reached. The flow rates at the end of the tests were estimated by multiplying the rate of falling head during the last hour of the tests by the ponding area.

Based on the grainsize analyses, the soil in both test pits was assumed to be Qvt with a α^* value of 0.36 ft^{-1}. Table 11 summarizes the results for both test pits. The estimated K_b value was 0.17 ft/d in PD-TP-1 and 0.23 ft/d in PD-TP-2, a difference factor of 1.35.

Fig. 7: USSBP tests in Point Defiance Elementary test pits.
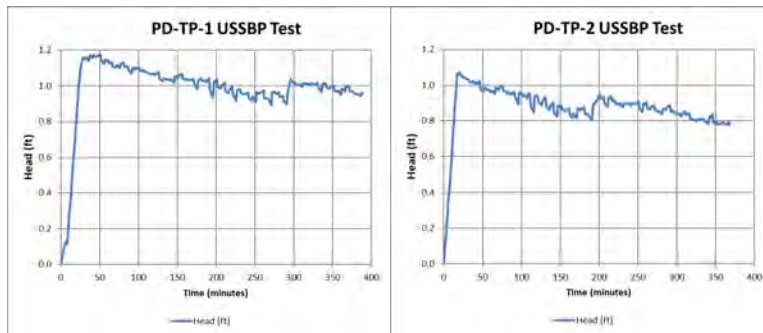
Table 11: Results of USSBP tests in Point Defiance Elementary test pits.

Parameter	Units	PD-TP-1	PD-TP-2
Depth Interval Tested	ft	3-4	3-4
Equivalent radius (r_b)	ft	3.1	3.0
Soil USCS Class		SM	SM
Soil Type		Qvt	Qvt
Sorptive Number (α^*)	ft^{-1}	0.36	0.36
Ponding Head at end of test(H)	ft	0.96	0.78
Falling Head at end of test	ft/hr	0.047	0.06
Flow Rate at end of test (Q)	gpm	0.18[1]	0.21[1]
Calculated K_b	**ft/d**	**0.17**	**0.23**

Qvt – glacial till

[1] Flow was too low to control with available valves. Estimated by multiplying ponded area by rate of falling head.

3.4.2 *Steady-State Test Pit Results for Tacoma Power*

Fig. 8 illustrates the USSBP test results for TP-TP-1 and TP-TP-2. The flow rate to maintain a constant head for TP-TP-1 was below the range of the smallest meter available so water was not added after the ponding depth reached the target depth of approximately 1 ft. The flow rate at the end of the TP-TP-1 test was estimated by multiplying the rate of falling head during the last hour of the test by the ponding area. The flow rate for TP-TP-2 (0.24 gpm) was within the range of the available flow meters. The tests lasted for at least 360 minutes after the target ponding depth was reached.

Based on the grainsize analyses, the soil in both test pits was assumed to be silty fine-coarse sand with a α^* value of 1.68 ft^{-1}. Table 12 summarizes the results for both test pits. The estimated K_b value was 0.08 ft/d for TP-TP-1 and 0.53 ft/d for TP-TP-2. As shown in Table A-1, the significant different can be attributed to the much higher silt content in TP-TP-1 (19%) compared with TP-TP-2 (8.2%). The fill soils tested at this site were significantly different over a distance of 34 ft.

Fig. 8: USSBP tests in Tacoma Power test pits.
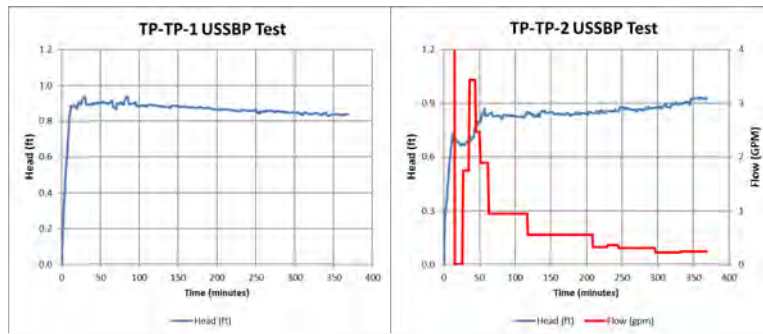
Table 12: Results of USSBP tests in Tacoma Power test pits.

Parameter	Units	TP-TP-1	TP-TP-2
Depth Interval Tested	ft	6.5-7.5	6.5-7.5
Equivalent radius (r_b)	ft	2.8	2.9
Soil USCS Class		SM	SP-SM
Soil Type		St F-C Sand	St F-C Sand
Assumed Sorptive Number ($\alpha*$)	ft^{-1}	1.68	1.68
Ponding Head at end of test(H)	ft	0.84	0.93
Falling Head at end of test	ft/hr	0.011	
Flow Rate at end of test (Q)	gpm	0.03[1]	0.24
Calculated K_b	**ft/d**	**0.08**	**0.53**

St F-C – silty fine-coarse

[1] Flow was too low to control with available valves. Estimated by multiplying ponded area by rate of falling head.

3.4.3 *Steady-State Test Pit Results for Roosevelt Park*

Fig. 9 illustrates the USSBP test results for RP-TP-1 and RP-TP-2. The flow rate for both tests were well within the range of the available flow meters. The tests were conducted simultaneously and the maximum flow rates during the filling portion of the test were 23 and 28 gpm. Given these limited flow rates, it took several hours to reach the target ponding depth of approximately 1 ft. The tests lasted for at least 360 minutes from the beginning of the test. As evidenced by the falling flow rates during the tests, neither test was at steady state by the end of the test.

Based on the grainsize analyses, the soil in both test pits was assumed to be sandy gravel with a $\alpha*$ value of 17.4 ft^{-1}. Table 13 summarizes the results for both test pits. The estimated K_b value was 24 ft/d for RP-TP-1 and 30 ft/d for RP-TP-2, a difference factor of 1.25.

Fig. 9: USSBP tests in Roosevelt Park test pits.
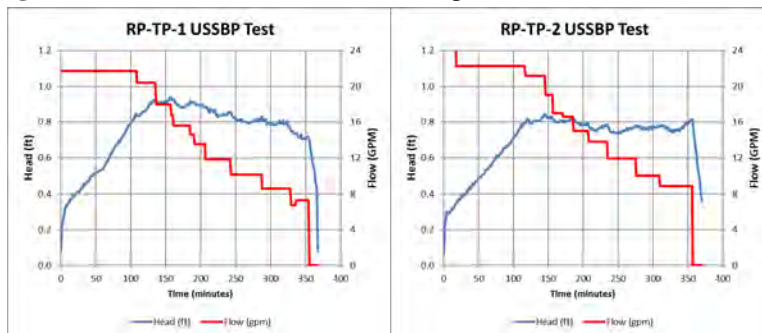
Table 13: Results of USSBP tests in Roosevelt Park test pits.

Parameter	Units	RP-TP-1	RP-TP-2
Depth Interval Tested	ft	3.5-4.25	3.75-4.5
Equivalent radius (r_b)	ft	3.0	2.8
Soil USCS Class		GP	GP
Soil Type		Sandy Gravel	Sandy Gravel
Assumed Sorptive Number (α^*)	ft^{-1}	17.4	17.4
Ponding Head at end of test(H)	ft	0.71	0.80
Flow Rate at end of test (Q)	gpm	7.3	8.9
Calculated K_b	**ft/d**	**24**	**30**

3.4.4 Steady-State Test Pit Results for Verlo Playfield

Fig. 10 illustrates the USSBP test results for VP-TP-1 and VP-TP-2. The flow rate for both tests were well within the range of the available flow meters. The VP-TP-1 test lasted for 353 minutes and the VP-TP-2 test lasted for 316 minutes. The tests were less than 360 minutes long because they appeared to be at steady state and to facilitate closing the pits before the end of the day.

Based on the grainsize analyses, the soil in both test pits was assumed to be fine-coarse Qva with a α^* value of 7.63 ft^{-1}. Table 14 summarizes the results for both test pits. The estimated K_b value was 1.6 ft/d for VP-TP-1 and 1.9 ft/d for VP-TP-2, a difference factor of 1.19.

Fig. 10: USSBP tests in Verlo Playfield test pits.
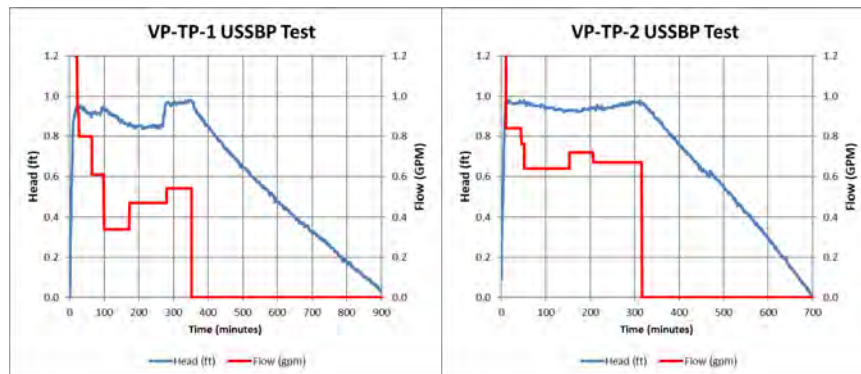
Table 14: Results of USSBP tests in Verlo Playfield test pits.

Parameter	Units	VP-TP-1	VP-TP-2
Depth Interval Tested	ft	7-8	7-8
Equivalent radius (r_b)	ft	2.8	2.8
Soil USCS Class		GP-GM	GP-GM
Soil Type		F-C Qva	F-C Qva
Assumed Sorptive Number (α^*)	ft^{-1}	7.63	7.63
Ponding Head at end of test(H)	ft	0.98	0.97
Flow Rate at end of test (Q)	gpm	0.54	0.67
Calculated K_b	**ft/d**	**1.6**	**1.9**

3.5 USSBP and CSSBP Test Well Results

This section provides the USSBP and CSSBP results for the 12 test wells. The difference factors referenced below are calculated by dividing the highest K_b by the lowest K_b.

3.5.1 *Steady State Test Well Results for Point Defiance Elementary*

Fig. 11 illustrates the USSBP and CSSBP test results for the three test wells PD-MA-1, PD-MA-2, and PD-MA-3. USSBP tests were run in all three wells on June 10 and CSSBP tests were run in all three wells on June 11. Another round of testing was conducted on June 16, including a USSBP test in PD-MA-1, a CSSBP test in PD-MA-2, and a combined USSBP and CSSBP test in PD-MA-3.

Initially, the flow rate for the three USSBP tests run on June 10 were below the range that could be effectively controlled with a valve. Eventually, the flow rates in PD-MA-1 and PD-MA-2 rose high enough that they could be controlled with the valve. This was not possible for PD-MA-3 and the flow rate was estimated by adding water periodically and dividing the added water by the time between water additions.

Based on the grainsize analyses, the soil in all three test wells was assumed to be Qvt with a α* value of 0.36 ft^{-1}. Table 15 summarizes the results for all three test wells. A slash "/" separates the results for the same test in the same test well on different days.

The USSBP tests in PD-MA-1 provided estimated K_b values of 0.41 and 0.56 ft/d. The CSSBP test in PD-MA-1 provided a significantly higher K_b value of 1.9 ft/d. The USSBP test in PD-MA-2 provided an estimated K_b value of 0.36 ft/d. The CSSBP tests in PD-MA-2 provided K_b values of 0.47 and 0.4 ft/d.

The first USSBP test in PD-MA-3 provided an estimated K_b value of 0.03 ft/d, an order of magnitude less than the other two test wells. Similar results were observed during the first 360 minutes of the CSSBP test in PD-MA-3 the following day. However, at 360 minutes there was a dramatic drop in the head elevation, and it was necessary to increase the flow rate by more than an order of magnitude to restore the head elevation to the top of casing. This higher flow rate provided a CSSBP K_b value of 2.7 ft/d. The USSBP and CSSBP tests conducted 5 days later, on June 16 provided K_b values of 2.9 and 2.6 ft/d, a relatively tight range. The reason for this dramatic change in flow capacity in PD-MA-3 is not known, but it suggests either a problem with well construction or a nearby high permeability channel, such as a utility trench. In either case, the test results in this well are suspect and of limited use.

Fig. 11: USSBP and CSSBP tests in Point Defiance Elementary test wells.
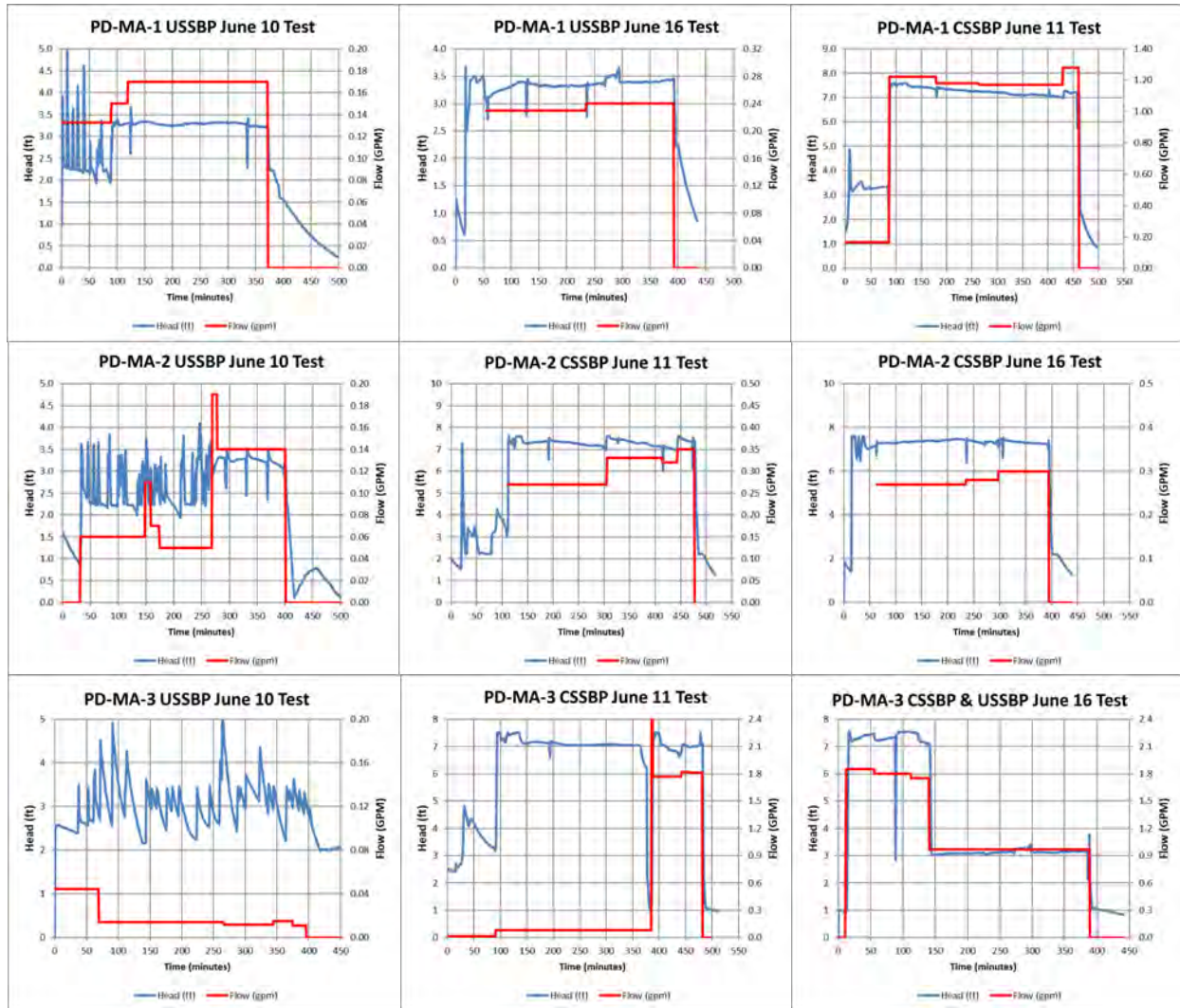
Table 15: Results of USSBP and CSSBP tests in Point Defiance Elementary test wells.

Parameter	Units	PD-MP-1		PD-MP-2		PD-MP-3	
		USSBP	CSSBP	USSBP	CSSBP	USSBP	CSSBP
Depth Interval Tested	ft	3.7-6.3		3.6-6.4		3.3-6.5	
Borehole radius (r_b)	ft	0.51		0.55		0.42	
Soil USCS Class		SM		SM		SM	
Soil Type		Qvt		Qvt		Qvt	
Assumed Sorptive Number (α^*)	ft^{-1}	0.36		0.36		0.36	
Head at end of test (H)	ft	3.2/3.4	7.2	3.1	7.4/7.2	3.2/3.2	7.1/7.1
Flow Rate at end of test (Q)	gpm	0.17/0.24	1.3	0.14	0.35/0.30	0.011[1]/0.97	1.8/1.7
Calculated K_b	**ft/d**	**0.41/0.56**	**1.9**	**0.36**	**0.47/0.40**	**0.03/2.9**	**2.7/2.6**

Qvt – glacial till

[1] Flow was too low to control with available valves. Estimated by adding water periodically and dividing added water by time between water additions.

3.5.2 *Steady State Test Well Results for Tacoma Power*

Fig. 12 illustrates the USSBP and CSSBP test results for the three test wells TP-MA-1, TP-MA-2, and TP-MA-3. USSBP tests were run in all three wells on June 14 and CSSBP tests were run in all three wells on June 15.

Based on the grainsize analyses, the soil in TP-MA-1 and TP-MA-2 was assumed to be silty fine-coarse sand with a $\alpha*$ value of 1.68 ft^{-1}. The soil in TP-MA-3 was assumed to be sandy gravel with a $\alpha*$ value of 17.4 ft^{-1}. Table 16 summarizes the results for all three test wells.

The USSBP test in TP-MA-1 provided an estimated K_b value of 0.39 ft/d while the CSSBP test in the same well provided a K_b value of 7.2 ft/d, a dramatic difference. This difference may be due to the two different soil layers within the test interval, one with a much higher silt content that the other layer. The USSBP tests in TP-MA-2 and TP-MA-3 provided relatively similar K_b values of 2.8 ft/d and 3.3 ft/d. In comparison, the CSSBP tests in both wells provided K_b values of 7.6 and 6.2 ft/d.

Fig. 12: USSBP and CSSBP tests in Tacoma Power test wells.
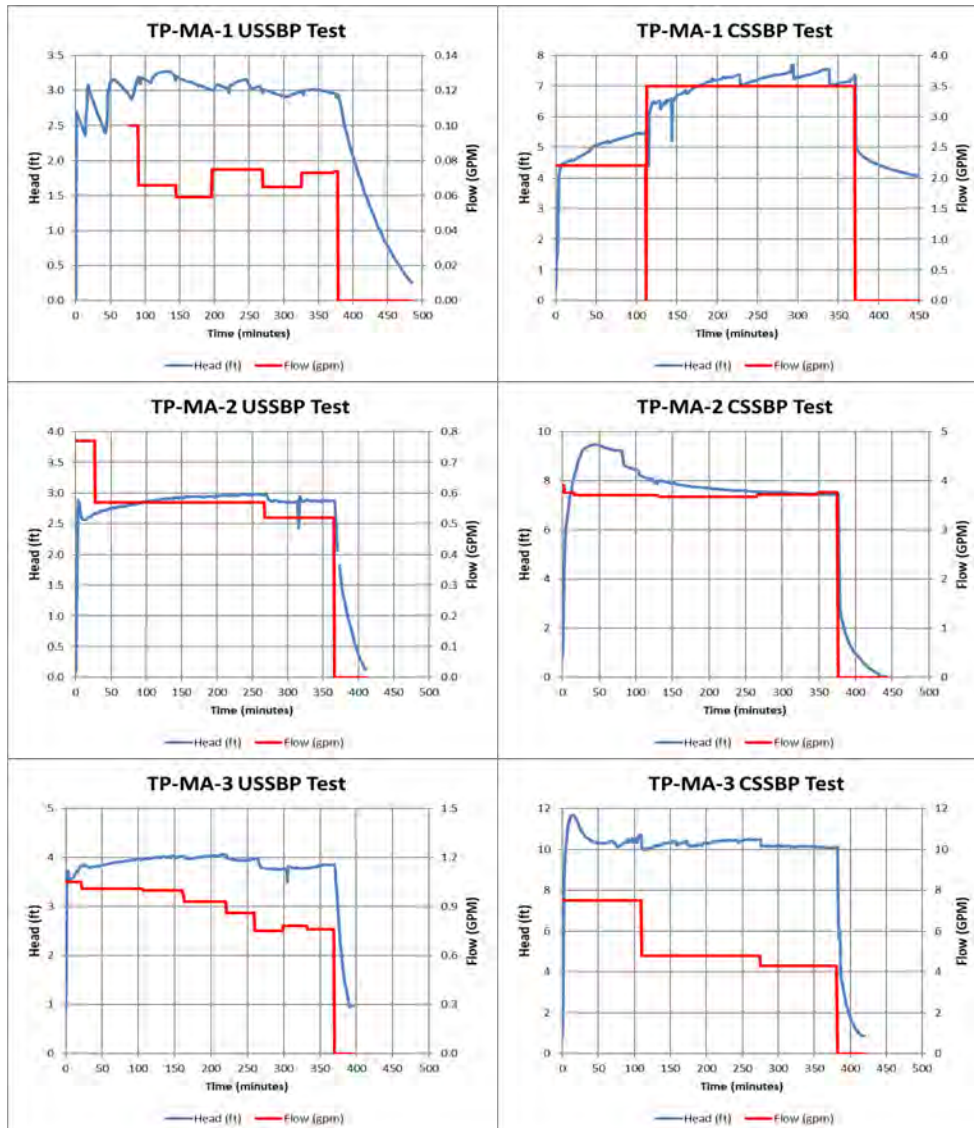
Table 16: Results of USSBP and CSSBP tests in Tacoma Power test wells.

Parameter	Units	TP-MP-1		TP-MP-2		TP-MP-3	
		USSBP	CSSBP	USSBP	CSSBP	USSBP	CSSBP
Depth Interval Tested	ft	7-10		7-10		7-10	
Borehole radius (r_b)	ft	0.47		0.47		0.45	
Soil USCS Class		SP-SM		SP-SM		SP	
Soil Type		St F-C Sand		St F-C Sand		Sd Gravel	
Assumed Sorptive Number (α^*)	ft^{-1}	1.68		1.68		17.4	
Head at end of test (H)	ft	2.9	7.4	2.9	7.4	3.9	10.1
Flow Rate at end of test (Q)	gpm	0.07	3.5	0.52	3.8	0.76	4.3
Calculated K_b	**ft/d**	**0.39**	**7.2**	**2.8**	**7.6**	**3.3**	**6.2**

St F-C – silty fine-coarse; Sd - sandy

3.5.3 *Steady State Test Well Results for Roosevelt Park*

Fig. 13 illustrates the USSBP and CSSBP test results for the three test wells RP-V-1, RP-V-2, and RP-V-3. USSBP tests were run in all three wells on November 6 and CSSBP tests were run in all three wells on November 7.

Based on the grainsize analyses, the soil in all three test wells was assumed to be sandy gravel with a α^* value of 17.4 ft^{-1}. Table 17 summarizes the results for all three test wells. The USSBP test in RP-V-1 provided an estimated K_b value of 61 ft/d while the CSSBP test in the same well provided a K_b value of 67 ft/d, a difference factor of 1.1. The USSBP test in RP-V-2 provided an estimated K_b value of 34 ft/d while the CSSBP test in the same well provided a K_b value of 53 ft/d, a difference factor of 1.56. The USSBP test in RP-V-3 provided an estimated K_b value of 47 ft/d while the CSSBP test in the same well provided a K_b value of 54 ft/d, a difference factor of 1.15. In general, the CSSBP tests provided a higher value of K_b than the USSBP tests in the same well.

3.5.4 *Steady State Test Well Results for Verlo Playfield*

Fig. 14 illustrates the USSBP and CSSBP test results for the three test wells VP-V-1, VP-V-2, and VP-V-3. USSBP tests were run in all three wells on November 3 and CSSBP tests were run in all three wells on November 5.

Based on the grainsize analyses, the soil in all three test wells was assumed to be fine-coarse Qva with a α^* value of 7.63 ft^{-1}. Table 18 summarizes the results for all three test wells. The USSBP test in VP-V-1 provided an estimated K_b value of 15 ft/d while the CSSBP test in the same well provided a K_b value of 16 ft/d, a difference factor of 1.07. The USSBP test in VP-V-2 provided an estimated K_b value of 5.5 ft/d while the CSSBP test in the same well provided a K_b value of 10 ft/d, a difference factor of 1.8. The USSBP test in VP-V-3 provided an estimated K_b value of 2.3 ft/d while the CSSBP test in the same well provided a K_b value of 5.2 ft/d, a difference factor of 2.2. VP-V-3 did not have the cleaner gravel zone observed in the first two wells, which likely explains the lower value of K_b in VP-V-3.

Fig. 13: USSBP and CSSBP tests in Roosevelt Park test wells.
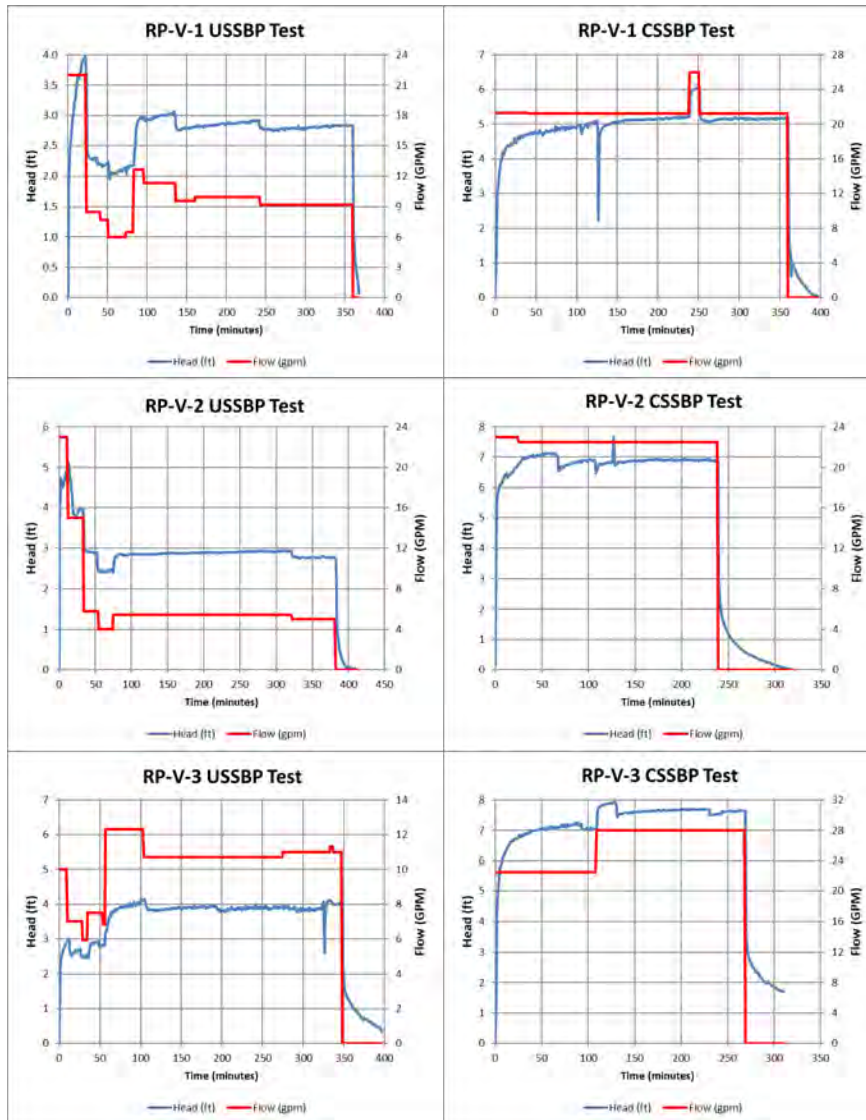
Table 17: Results of USSBP and CSSBP tests in Roosevelt Park test wells.

Parameter	Units	RP-V-1		RP-V-2		RP-V-3	
		USSBP	CSSBP	USSBP	CSSBP	USSBP	CSSBP
Depth Interval Tested	ft	4.5-7.5		4.5-7.5		3.5-7.5	
Borehole radius (r_b)	ft	0.46		0.46		0.45	
Soil USCS Class		SP		SP		SP	
Soil Type		Sd Gravel		Sd Gravel		Sd Gravel	
Assumed Sorptive Number (α^*)	ft^{-1}	17.4		17.4		17.4	
Head at end of test (H)	ft	2.8	5.2	2.7	6.9	4.0	7.6
Flow Rate at end of test (Q)	gpm	9.2	21	5.0	22	11	28
Calculated K_b	**ft/d**	**61**	**67**	**34**	**53**	**47**	**54**

Sd – sandy

Fig. 14: USSBP and CSSBP tests in Verlo Playfield test wells.
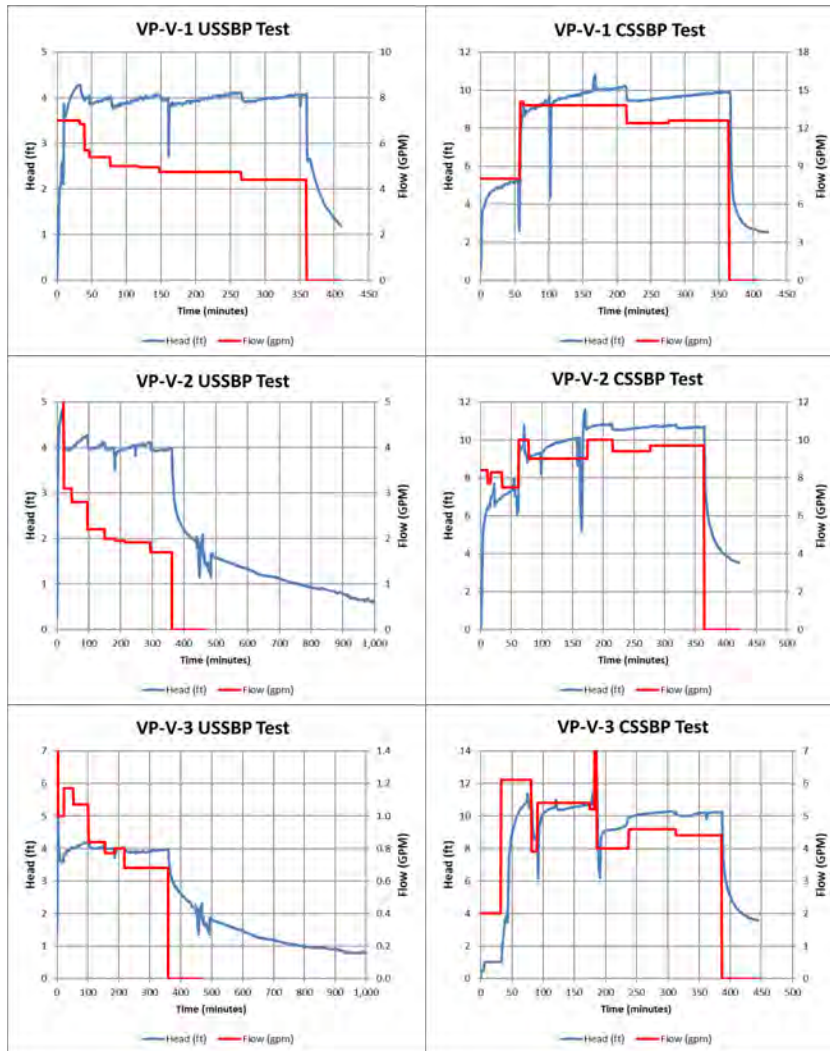
Table 18: Results of USSBP and CSSBP tests in Verlo Playfield test wells.

Parameter	Units	VP-V-1		VP-V-2		VP-V-3	
		USSBP	CSSBP	USSBP	CSSBP	USSBP	CSSBP
Depth Interval Tested	ft	6-10		6-10.5		6-10	
Borehole radius (r_b)	ft	0.60		0.68		0.63	
Soil US USCS Class		GW		GW		GW	
Soil Type		F-C Qva		F-C Qva		F-C Qva	
Assumed Sorptive Number (α^*)	ft^{-1}	7.63		7.63		7.63	
Head at end of test (H)	ft	4.0	9.9	4.0	10.7	4.0	10.2
Flow Rate at end of test (Q)	gpm	4.4	13	1.7	9.7	0.68	4.4
Calculated K_b	**ft/d**	**15**	**16**	**5.5**	**10**	**2.3**	**5.2**

F-C – fine-coarse

4   Discussion

4.1   Comparison of Different Methods in Same Test Well

Table 19 summarizes the K_b estimates from all the infiltration tests for each of the 12 test wells. This section compared the three test methods, FHBP, USSBP, and CSSBP, for each test well. The difference factors referenced below are calculated by dividing the highest K_b by the lowest K_b.

As discussed in Section 3.3, the FSBP method results are unreliable when $K_b \geq 1.6$ ft/d and for larger test wells (e.g., $L \geq 3.3$ ft, $D_0 \geq 6.6$ ft, $r_b \geq 4$ in.). None of the test facilities included in this scope of work were within these dimensions and only PD-MA-2 had USSBP and CSSBP results with $K_b < 1.6$ ft/d. As shown in Table 19, the FHBP results for PD-MA-2 were similar to the USSBP and CSSBP results. The FHBP results for PD-MA-1 and PD-MA-3 provided K_b estimates that are significantly less than the USSBP and CSSBP results. These limited results confirm the numerical simulations provided in Volume III, indicating that the FSBP method underpredicts K_b when $K_b \geq 1.6$ ft/d. A more extensive field analysis of the FHBP method in lower permeability soils is warranted to confirm the numerical analysis provided in Volume III.

Table 19 provides a comparison of USSBP and CSSBP results in each of the test wells. With one exception (PD-MA-3, where the USSBP and CSSBP results are within 10%)) the CSSBP method provides higher estimates of K_b than the USSBP method, ranging from a difference factor of 1.07 in VP-V-1 to a difference factor of 4 in most of the wells. The difference factor was 8 times larger in TP-MA-1, but this difference likely reflects the variability of the fill soils and is not considered representative of native soils.

Numerical simulations provided in Volume II demonstrate that CSSBP tests create a saturated zone that can extend 3-6 ft above the sandpack interval. In comparison, the saturated zone for USSBP tests does not extend higher than the ponding depth in the test facility. It is possible that the CSSBP method provides higher estimates of K_b than the USSBP method because the soils are layered and the CSSBP method is more likely to be dominated by flow into a permeable layer in the upper part of the test zone or above the test zone. This could be the reason why the CSSBP method tends to provide higher K_b estimates than the USSBP method. This hypothesis will be evaluated later in the study using numerical simulations.

Table 19: Summary of test well results considered valid for each test facility.

Test Well	Soil USCS Class	Soil Type	K_b Estimates (ft/d)			Comparison
			FHBP	**USSBP**	**CSSBP**	
PD-MA-1	SM	Qvt	0.09-0.24	0.41/0.56	1.9	FHBP << USSBP CSSBP 4 times > USSBP
PD-MA-2	SM	Qvt	0.13-0.57	0.36	0.47/0.40	FHBP similar to USSBP CSSBP 1.1-1.3x > USSBP
PD-MA-3	SM	Qvt	1.6	2.9	2.7/2.6	FHBP << USSBP CSSBP similar to USSBP
TP-MA-1	SP-SM	St F-C Sand (fill)	NT	0.39	7.2	CSSBP 8x > USSBP
TP-MA-2	SP-SM	St F-C Sand (fill)	IT	2.8	7.6	CSSBP 2.7x > USSBP
TP-MA-3	SP	Sd Gravel (fill)	IT	3.3	6.2	CSSBP 1.9x > USSBP
RP-V-1	SP	Sd Gravel	NT	61	67	CSSBP 1.1x > USSBP
RP-V-2	SP	Sd Gravel	NT	34	53	CSSBP 1.6x > USSBP
RP-V-3	SP	Sd Gravel	NT	47	54	CSSBP 1.15x > USSBP
VP-V-1	GW	F-C Qva	IT	15	16	CSSBP 1.07x > USSBP
VP-V-2	GW	F-C Qva	IT	5.5	10	CSSBP 1.8x > USSBP
VP-V-3	GW	F-C Qva	IT	2.3	5.2	CSSBP 2.3x > USSBP

NT – not tested; IT – invalid test; Qvt – glacial till; Qva – advance outwash; Sd – sandy; St – silty; f-c – fine-coarse

4.2 Comparison of Results at each Test Site

Table 20 summarizes the K_b estimates from both the test pits and the test wells at each of the four sites. The purpose of this section is to compare the range of K_b estimates at each site; in particular the USSBP test pit results with the USSBP test well results. The USSBP well tests were designed to test a similar soil interval as the USSBP pit tests and are suitable for comparison. As discussed in the previous section, the CSSBP method creates a saturated zone that extends above the sandpack, and the results are poorly suited for comparison with USSBP pit tests.

As discussed in Section 3.5.1, test well PD-MA-3 initially provided a significantly lower K_b estimate that the other test facilities but that dramatically changed on the second day of testing when PD-MA-3 provided a significantly higher K_b estimate than the other test facilities. Test results in this well are not considered valid for comparison with other test facilities.

Table 20 provides difference factors (Well K_b /Pit K_b) for comparing results from test wells with results from test pits. Comparison of test well results with test pit results at each site indicates that the well tests provide higher K_b estimates than the pit tests, generally by a difference factor of 1.1 to 3.4. This is likely because well tests are dominated by horizontal flow and test pit tests are dominated by vertical flow. Layered soils usually include lower-permeability layers that restrict vertical flow, resulting in a higher apparent K_b in well tests than pit tests. Test well VP-V-1 contains significantly less silt than the Verlo Playfield test pits and was not used for calculating the well/pit difference factor.

Table 20: Comparison of tests performed at each test site.

Test Well	Soil USCS Class	Silt Content (%)	USSBP K_b Estimates (ft/d)	Comparisons
Point Defiance Elementary				
PD-MA-1	SM	NA[1]	0.41/0.56	PD-MA-3 test results not representative of observed soil and excluded from comparison. Well/Pit difference factor = 1.6-3.3. Spatial variability difference factor = 1.35 (pits) to 1.55 (wells).
PD-TP-1	SM	18	0.17	
PD-MA-2	SM	10	0.36	
PD-TP-2	SM	22	0.23	
PD-MA-3	SM	16	IT	
Tacoma Power				
TP-TP-1	SM	19	0.08	Soil varies from SM to SP across site and not valid to compare well results with pit results. Spatial variability difference factor = 6.6 (pits) to 7.2 (wells).
TP-MA-1	SP-SM	25/5[2]	0.39	
TP-TP-2	SP-SM	8.2	0.53	
TP-MA-2	SP-SM	6.5	2.8	
TP-MA-3	SP	1.1-2.9	3.3	
Roosevelt Park				
RP-V-1	SP	1.4	61	Well/Pit difference factor = 1.1-2.5. Spatial variability difference factor = 1.25 (pits) to 1.8 (wells).
RP-TP-1	GP	0.8	24	
RP-V-2	SP	1.4	34	
RP-TP-2	GP	1.6	30	
RP-V-3	SP	5.9	47	
Verlo Playfield				
VP-V-1	GW	4.0	15	VP-V-1 represents significantly different soil. Excluding VP-V-1, Well/Pit difference factor = 1.2-3.4. Spatial variability difference factor = 1.2-6.5
VP-TP-1	GP-GM	10	1.6	
VP-V-2	GW	8.7	5.5	
VP-TP-2	GP-GM	9-11	1.9	
VP-V-3	GW	7.2	2.3	

NA – Not available; IT – invalid test
[1] Grainsize analysis not representative of soil in sandpack interval.
[2] Two distinct soil types within sandpack interval

Although the test facilities at each site are within 70 ft of each other, the K_b estimates for comparable facilities (wells compared with wells and pits compared with pits) demonstrate significant variability over relatively short distances. For the glacial till soils at Point Defiance Elementary (excluding PD-MA-3) and the recessional outwash soils at Roosevelt Park, the spatial variability difference factors ranged from 1.25 to 1.8. The advance outwash soils at Verlo Playfield included one test well with significantly different soils and the spatial variability difference factors ranged from 1.2 for the test pits to 6.5 for the test wells. The fill soils at Tacoma Power were highly variable, although there was a trend from lower K_b at one end of the site (TP-TP-1) to higher K_b at the other end (TP-MA-3). The spatial variability difference factors for Tacoma Power ranged from 6.6 for the test pits to 7.2 for the test wells.

4.3 Challenges with FHBP Tests in Shallow Test Wells

The FHBP method assumes instantaneous filling of the well casing before the falling head test begins and slight deviations from this assumption can significantly impact the results. As determined using numerical simulations (Volume III, Table 6), FHBP tests using realistic flow rates to fill the well casing and sandpack tend to underpredict K_b. These simulations suggest that FHBP test results are not valid when $K_b \geq 1.6$ ft/d and for larger test wells (e.g., $L \geq 3.3$ ft, $D_0 \geq 6.6$ ft, $r_b \geq 4$ in.). None of the test facilities included in this scope of work were within these dimensions and only three test wells (PD-MA-1, PD-MA-2, and TP-MA-1) had $K_b \leq 1.6$ ft/d. As discussed in Section 3.3.2, a FHBP test was not conducted in TP-MA-1.

The field FHBP tests in this study generally confirm the conclusions of the numerical study. The FHBP K_b estimates for the two tested wells with $K_b \leq 1.6$ ft/d were similar to or less than the USSBP K_b estimates. The FHBP K_b estimates for the wells with $K_b > 1.6$ ft/d were significantly less than the USSBP K_b estimates.

4.4 Time to Achieve Steady-State Conditions

Volume I includes numerical simulations to compare results after 6 hr with results after 24 hr to determine if steady state conditions had been achieved at the end of a 6-hr test. The ratio of flow capacity after 6-hr (Q_6) divided by flow capacity after 24-hr (Q_{24}) in test pits with a head of 0.8 ft and shallow test wells with a head of 3.3 ft ranged from 1.0 for sandy gravel and fine-coarse Qva to 1.2 for Qvt.

Most of the infiltration tests conducted in test wells appeared to be at or very close to steady state at the end of the 6-hr test, although there are some exceptions. In particular, the head was still rising at the end of the tests in most of the Verlo Playfield test wells (Fig. 14). Steady state conditions were not achieved in most of the pit tests. For example, the head was still rising at the end of the pit test in TP-TP-1 (Fig. 8) and the flow rate was decreasing at the end of the pit tests at Roosevelt Park and Verlo Playfield (Figs. 9 and 10).

Although it's expected that tests in lower permeable soils such as TP-TP-1 would not achieve steady state in 6 hr, the non-steady test results in relatively permeable soils at Roosevelt Park and Verlo Playfield are not consistent with numerical simulations. One potential explanation for this difference between field results and numerical results is that the test facility may be underlain by a less permeable layer that is causing groundwater mounding. This potential explanation will be evaluated later in the study using numerical simulations.

5   Conclusions

The purpose of this portion of the study (Task 4.1) was to conduct testing in pits and shallow (<10 ft deep) test wells to: 1) demonstrate the use of these three methods under field conditions and determine if they provide similar estimates of K_b; 2) compare the results from pit tests and shallow wells; 3) provide field evidence of K_b variability over a distance of 30 to 70 ft; and 4) provide data for evaluation of layering, perching, and groundwater mounding. Future numerical modeling will evaluate the effects of layering, perching, and groundwater mounding.

Infiltration testing was conducted at four sites within the City of Tacoma. Two pits and three shallow test wells were tested at each site. The pits ranged from 4 to 8.5 ft deep and were typically 4 ft wide and 6-7 ft long. The wells were drilled using either a solid-stem auger mounted on a backhoe or a vactor truck typically used to clean sewers or excavate borings to clear sites for utilities. The test wells ranged in depth from 6.25 ft to 10.5 ft and were completed with 2.5 ft of screen with a sandpack interval that covered a slightly longer interval. The test facilities were installed in a range of soil types, including glacial till, fill, advance outwash, and recessional outwash.

Drilling boreholes with the solid-stem auger was difficult given the gravelly soils encountered at all four test sites. Cobbles were sometimes difficult to remove from the bottom of the hole and caving was a challenge in looser soils. Drilling shallow boreholes with the vactor truck was much faster and provided a clean and well-defined borehole.

The FHBP method provided reasonable estimates of K_b in the glacial till soils. However, the FHBP tests in more permeable soils significantly underestimated K_b, consistent with numerical simulations that demonstrated the difficulty of conducting FHBP tests in soils with $K_b > 1.6$ ft/d (0.5 m/d).

USSBP tests were conducted in each of the test pits. K_b values from the pit test at the four sites ranged from 0.024 m/d in the glacial till soils to 9.1 m/d in the recessional outwash, demonstrating that the sites covered a broad range of soil types.

USSBP and CSSBP tests were conducted in each of the test wells. K_b values from the four sites ranged from 0.08 in the fill soils to 61 ft/d in the recessional outwash. In most of the wells the CSSBP method provides higher estimates of K_b than the USSBP method, ranging from a difference factor of 1.07 to a difference factor of 4. (The difference factor is the larger K_b divided by the smaller K_b.) The reason for this difference will be evaluated later in the study using numerical simulations.

Comparison of test well results with test pit results at each site indicates that the well tests provide higher K_b estimates than the pit tests, generally by a difference factor of 1.1 to 3.4. This is likely because well tests are dominated by horizontal flow and test pit tests are dominated by vertical flow. Layered soils usually include lower-permeability layers that restrict vertical flow, resulting in a higher apparent K_b in well tests than pit tests. This will be evaluated later in the study using numerical simulations.

Although the test facilities at each site are within 70 ft of each other, the K_b estimates for comparable facilities (wells compared with wells and pits compared with pits) demonstrate significant variability over relatively short distances. For the glacial till soils at Point Defiance Elementary and the recessional outwash soils at Roosevelt Park the spatial variability difference factors ranged from 1.25 to 1.8. The advance outwash soils at Verlo Playfield included one test well with significantly different soils than the other test facilities and the spatial variability difference factors ranged from 1.2 for the test pits to 6.5 for the test wells. The fill soils at Tacoma Power were highly variable, although there was a trend from lower K_b at one end of the site to higher K_b at the other end of the site. The spatial variability difference factors for Tacoma Power ranged from 6.6 for the test pits to 7.2 for the test wells.

Most of the infiltration tests conducted in test wells appeared to be at or very close to steady state at the end of the 6-hr test, although there are some exceptions. Steady state conditions were not achieved in most of the pit tests, even those tests conducted in permeable sandy gravel. Although it's expected that tests in lower permeable soils such as

TP-TP-1 would not achieve steady state in 6 hr, the non-steady test results in relatively permeable soils at Roosevelt Park and Verlo Playfield are not consistent with numerical simulations. One potential explanation for this difference between field results and numerical results is that the test facility may be underlain by a less permeable layer that is causing groundwater mounding. This potential explanation will be evaluated later in the study using numerical simulations.

6 References

Kindred JS, Reynolds WD (2020) Using the borehole permeameter to estimate saturated hydraulic conductivity for glacially over-consolidated soils, Hydrogeology Journal 28:1909–1924, DOI:10.1007/s10040-020-02149-3

Reynolds, WD (2011). Measuring soil hydraulic properties using a cased borehole permeameter: falling-head analysis. Vadose Zone Journal. 10: 999-1015.

WSDOE (Washington State Department of Ecology) (2019) Stormwater Management Manual for Western Washington, July 2019, Publication Number 19-10-021

Appendix A: Soil Testing Results

Table A-1: Summary of Moisture Content and Grainsize Analyses

Sample Name	Lab	Location	Depth (ft)	% Gravel	% Sand	% Silt	USCS Class	% Moisture
PD-MA-1-7	HMA	PD-MA-1	7	53	42	4.4	GP	4.3%
PD-TP-1-4	HMA	PD-TP-1	4	27	56	18	SM	9.0%
PD-Q1-1-4	*HMA*	*PD-TP-1*	*4*	*23*	*59*	*18*	*SM*	*9.2%*
PD-Q2-1-4	*ETA*	*PD-TP-1*	*4*	*12*	*73*	*15*	*SM*	*9.0%*
PD-MA-2-6.5	HMA	PD-MA-2	6.5	40	50	10	SP-SM	8.3%
PD-TP-2-4	HMA	PD-TP-2	4	32	53	15	SM	7.3%
PD-MA-3-6	HMA	PD-MA-3	6	3.9	80	16	SM	15.2%
TP-TP-1-7	HMA	TP-TP-1	7	27	54	19	SM	11.9%
TP-MA-1-9	HMA	TP-MA-1	8	24	51	25	SM	13.0%
TP-MA-1-9.5	HMA	TP-MA-1	9.5	36	59	4.8	SP	15.8%
TP-MA-2-8	HMA	TP-MA-2	8	40	53	6.5	SP-SM	4.3%
TP-TP-2-7.5	HMA	TP-TP-2	7.5	25	67	8.2	SP-SM	9.3%
TP-MA-3-8	HMA	TP-MA-3	8	23	77	1.1	SP	5.1%
TP-MA-Q2-8	*ETA*	*TP-MA-3*	*8*	*10*	*87*	*2.4*	*SP*	*5.0%*
TP-MA-Q1-8	*HMA*	*TP-MA-3*	*8*	*28*	*69*	*2.7*	*SP*	*4.4%*
RP-V-1-6	HMA	RP-V-1	6	33	66	1.4	SP	4.1%
RP-TP-1-4.25	HMA	RP-TP-1	4.25	51	48	0.8	GP	4.3%
RP-V-2-6	HMA	RP-V-2	6	41	58	1.4	SP	4.5%
RP-Q2-2	*ETA*	*RP-V-2*	*6*	*34*	*52*	*?*	*SP*	*4.1%*
RP-TP-2-4.5	HMA	RP-TP-2	4.5	50	48	1.6	GP	3.9%
RP-V-3-6	HMA	RP-V-3	6	54	40	5.9	GP-GM	7.0%
VP-V-1-9	HMA	VP-V-1	9	63	33	4.0	GW	9.9%
VP-TP-1-8	HMA	VP-TP-1	8	43	47	10	SP-SM	9.6%
VP-V-2-9	HMA	VP-V-2	9	64	27	8.7	GP-GM	9.2%
VP-TP-2-8	HMA	VP-TP-2	8	50	39	11	GP-GM	9.4%
VP-Q-1-2	*HMA*	*VP-TP-2*	*8*	*59*	*32*	*8.5*	*GW-GM*	*8.3%*
VP-V-3-9	HMA	VP-V-3	9	74	18	7.2	GP-GM	7.9%

HMA – Hayre McElroy & Associates, LLC; ETA – Eurofins TestAmerica Laboratories, Inc.
Red font identifies QA/QC samples.

Appendix B: Test Pit and Well Logs

June 7, 2021

PD-MA-1 boring excavated using 9-inch solid stem auger mounted on backhoe. Conditions are summarized below:
    0-3.5'- medium dense, slightly moist, gray, silty sand with gravel (fill, SM)
    3.5 - thin layer of black organics (topsoil?)
    3.5-7.0' - dense, slightly moist, reddish brown silty sand with gravel (glacial till, SM). Sample from 7.0 ft is very sandy gravel with trace silt (GP), not representative of soils in screened interval.
    BOH at 7.0 ft. 0.75 ft of sluff. No seepage

    Installed 2.5 ft of screen and 5 ft of solid 2-inch casing. Bottom of casing 75 inches below ground. 16 inches of casing stick-up above ground.
    3 bags of pea gravel, top of pea gravel 45 inches below ground.
    3 bags of Holeplug, top of Holeplug 21 inches below ground

PD-TP-1 testpit excavated using backhoe. Bottom area is 4 ft by 7.5 ft.
Conditions are summarized below:
    0-4'- medium dense, slightly moist, gray, silty fine sand with gravel (SM)
    4'- dense, slightly moist, gray, gravelly silty fine sand (glacial till, SM). Thin layer of black organics (topsoil?)
    BOH at 4.0 ft. No seepage

PD-TP-2 testpit excavated using backhoe. Bottom area is 4 ft by 7 ft. Conditions are summarized below:
    0-4'- medium dense, slightly moist, gray, silty sand with gravel (SM)
    4'- dense, slightly moist, gray, very gravelly, silty fine-medium SAND (glacial till, SM). Thin layer of black organics (topsoil?)
    BOH at 4.0 ft. No seepage

PD-MA-2 boring excavated using 9-inch solid stem auger mounted on backhoe. Conditions are summarized below:
    0-4.0'- medium dense, slightly moist, gray, silty sand with gravel (SM)
    4.0'- thin layer of black organics (topsoil?)
    4.0-7'- dense, slightly moist, reddish brown, gravelly, slightly silty, fine-medium sand (glacial till, SP-SM)
    BOH at 7 ft. No seepage.

    Installed 2.5 ft of screen and 5 ft of solid 2-inch casing. Bottom of casing 77 inches below ground (some caving in bottom of hole). 14 inches of casing stick-up above ground.
    3 bags of pea gravel, top of pea gravel 43 inches below ground.
    2.25 bags of Holeplug, top of Holeplug 19 inches below ground

PD-MA-3 boring excavated using 9-inch solid stem auger mounted on backhoe. Conditions are summarized below:
    0-4.0'- medium dense, slightly moist, gray, silty sand with gravel (SM)
    4.0'- thin layer of black organics (topsoil?)
    4.0-7'- dense, slightly moist, reddish brown silty fine SAND, trace gravel (glacial till, SM)
    BOH at 7 ft. No seepage.

    Installed 2.5 ft of screen and 5 ft of solid 2-inch casing. Bottom of casing 78 inches below ground (some caving in bottom of hole). 13 inches of casing stick-up above ground.
    2.5 bags of pea gravel, top of pea gravel 40 inches below ground.
    1.75 bags of Holeplug, top of Holeplug 14 inches below ground

June 8, 2021

TP-TP-1 testpit excavated using backhoe. Bottom area is 4 ft by 6 ft.
Conditions are summarized below:

      0-5'- loose, slightly moist, gray, silty sand with gravel and garbage (concrete, wire, plastic, wood, etc.)
      Some caving (SM)
      5-7.5'- medium dense, moist, gray, gravelly, silty fine-medium sand (clean fill, SM)
      BOH at 7.5 ft. No seepage

TP-TP-2 testpit excavated using backhoe. Bottom area is 4 ft by 6.5 ft. Conditions are summarized below:

      0-6'- loose, slightly moist, gray, silty sand with gravel and garbage (concrete, wire, plastic, wood etc.)
      Some caving. (SM)
      5-7.5'- medium dense, slightly moist, brown, gravelly, slightly silty fine-coarse sand (clean fill, SP-SM)
      BOH at 7.5 ft. No seepage

TP-MA-1 boring excavated using 9-inch solid stem auger mounted on backhoe. Conditions are summarized below:

      0-6.5'- loose, slightly moist, gray, silty sand with gravel and wood debris. Some caving. (SM)
      6.5-7.5'- loose, slightly moist, black, silty sand, caving (clean fill, SM)
      7.5-9' – loose, slightly moist, gray silty gravelly fine-medium sand (clean fill, SM)
      9-9.5' – loose, slightly moist, brown, very gravelly fine-coarse sand, trace silt (clean fill, SP)
      9.5-10' – changes to very silty sand (clean fill, SM)
      BOH at 10 ft. No seepage

      Installed 2.5 ft of screen and 5 ft of solid 2-inch casing. Not enough solid casing so installed temporary
      black casing to provide access to top of well. Additional 5 ft of casing added later before testing.
      Bottom of casing 10 ft (120 inches) below ground. 31 inches of casing stick-up above ground.
      3 bags of pea gravel, top of pea gravel 84 inches below ground.
      3 bags of Holeplug, top of Holeplug 48 inches below ground

TP-MA-2 boring excavated using 9-inch solid stem auger mounted on backhoe. Conditions are summarized below:

      0-2 ft – loose, dry, gray, slightly silty sand
      2.5-6.5'- loose, slightly moist, black/gray, silty sand with debris (fill, SM)
      6.5-10' –loose, slightly moist, brown, very gravelly, slightly silty fine-medium sand (fill, SP-SM)
      BOH at 10 ft. No seepage

      Installed 2.5 ft of screen and 10 ft of solid 2-inch casing.
      Bottom of casing 10 ft (120 inches) below ground. 31 inches of casing stick-up above ground.
      3 bags of pea gravel, top of pea gravel 84 inches below ground.
      3 bags of Holeplug, top of Holeplug 42 inches below ground

TP-MA-3 boring excavated using 9-inch solid stem auger mounted on backhoe. Conditions are summarized below:

      0-7' ft – loose, slightly moist, gray, silty sand with gravel (fill, SM), more silt from 4-7 ft
      7-10' –loose, slightly moist, brown, gravelly fine-medium sand, trace silt (fill, SP)
      BOH at 10 ft. No seepage

      Installed 2.5 ft of screen and 10 ft of solid 2-inch casing.
      Bottom of casing 9.25 ft (111 inches) below ground. Some caving in bottom. 40 inches of casing stick-up
      above ground.
      3 bags of pea gravel, top of pea gravel 72 inches below ground.
      3 bags of Holeplug, top of Holeplug 48 inches below ground

November 1, 2021

RP-V-1 boring excavated using vactor truck with 12-inch tube. Collect soil samples using hand auger approximately every foot. Conditions are summarized below:

> 0-1.5'- sod over loose, moist, gray slightly silty f-m SAND with gravel, organics (SP-SM)
> 1.5-2.5'- medium dense, moist, brown, weathered, slightly silty f-c SAND with gravel (fill, SP-SM)
> 2.5-7.5' – medium dense, slightly moist, gray, very gravelly medium-coarse SAND, trace silt (recessional outwash, SP)
>
> Collect sample from 6-7.5 ft
> Installed 2.5 ft of screen and 5 ft of solid 2-inch casing.
> 3 ft of pea gravel (2 cf) from bottom of hole and bentonite chips up to 6 inches below ground surface

RP-V-2 boring excavated using vactor truck with 12-inch tube. Collect soil samples using hand auger approximately every foot. Conditions are summarized below:

> 0-1.5'- sod over loose, moist, gray slightly silty f SAND with gravel, organics (SP-SM)
> 1.5-2.5'- medium dense, very moist, black and brown, silty gravelly SAND with organics (fill, SM)
> 2.5-3.5' – medium dense, moist, brown, weathered slightly silty f-c SAND with gravel (fill, SP-SM)
> 3.5-7.5' – medium dense, slightly moist, gray, very gravelly medium-coarse SAND, trace silt (recessional outwash, SP)
>
> Collect sample from 6-7.5 ft
> Installed 2.5 ft of screen and 5 ft of solid 2-inch casing.
> 3 ft of pea gravel (2 cf) from bottom of hole and bentonite chips up to 6 inches below ground surface

RP-V-3 boring excavated using vactor truck with 12-inch tube. Collect soil samples using hand auger approximately every foot. Conditions are summarized below:

> 0-1.5'- sod over loose, moist, gray slightly silty f SAND with gravel, organics (SP-SM)
> 1.5-3.5' – medium dense, moist, brown, weathered slightly silty f-c SAND with gravel (fill, SP-SM)
> 3.5-7.5' – medium dense, slightly moist, gray, very sandy, slightly silty, fine-coarse gravel (recessional outwash, GP-GM)
>
> Collect sample from 6-7.5 ft
> Installed 2.5 ft of screen and 5 ft of solid 2-inch casing.
> 4 ft of pea gravel (2.5 cf) from bottom of hole and bentonite chips up to 3 inches below ground surface

VP-V-1 boring excavated using vactor truck with 12-inch tube. Collect soil samples using hand auger approximately every foot. Conditions are summarized below:

> 0-1.5'- sod over loose, moist, brown, very silty f-m SAND with gravel, organics (SM)
> 1.5-3.5'- medium dense, moist to very moist, brown, very silty f-c SAND with gravel, mottling from 3-3.5 ft (fill, SM)
> 3.5-6' – dense, moist, olive gray, silty, gravelly f-c SAND, more gravel below 5.5 ft (ice contact deposits? SM)
> 6-10' – dense, moist, olive gray, very sandy, trace to slightly silty, fine GRAVEL with cobbles (GW-GM). Less silt below 8 ft. (GW) (advance outwash?)
>
> Collect sample from 9-10 ft
> Installed 2.5 ft of screen and 10 ft of solid 2-inch casing.
> 4 ft of pea gravel (4.5 cf) from bottom of hole and bentonite chips up to 3 ft below ground surface

VP-V-2 boring excavated using vactor truck with 12-inch tube. Collect soil samples using hand auger approximately every foot. Conditions are summarized below:

> 0-1.5' - sod over loose, moist, brown, very silty f-m SAND with gravel, organics (SM)
>
> 1.5-3.5' - medium dense, moist to very moist, brown, very silty f-c SAND with gravel, mottling from 3-3.5 ft (fill, SM)
>
> 3.5-6' – dense, moist, olive gray, silty, gravelly f-c SAND, more gravel below 5.5 ft (ice contact deposits?, SM)
>
> 6-10.5' – dense, moist, olive gray, sandy, slightly silty, fine GRAVEL with cobbles. Less silt between 7-8.5 ft. (advance outwash?, GP-GM)
>
> Collect sample from 9-10 ft
>
> Installed 2.5 ft of screen and 10 ft of solid 2-inch casing.
>
> 4.5 ft of pea gravel (6.5 cf) from bottom of hole and bentonite chips up to 3 ft below ground surface

VP-V-3 boring excavated using vactor truck with 12-inch tube. Collect soil samples using hand auger approximately every foot. Conditions are summarized below:

> 0-1.5' - sod over loose, moist, brown, very silty f-m SAND with gravel, organics
>
> 1.5-3.5' - medium dense, moist to very moist, brown, very silty f-c SAND with gravel, mottling from 3-3.5 ft (fill)
>
> 3.5-6' – dense, moist, olive gray, silty, gravelly f-c SAND, more gravel below 5.5 ft (ice contact deposits?, SM)
>
> 6-10' – dense, moist, olive gray, sandy, slightly silty fine-coarse GRAVEL with cobbles. Less silt below 8 ft. (advance outwash?, GP-GM) VP-V-3 doesn't have the cleaner gravel zone observed in the other two borings.
>
> Collect sample from 9-10 ft.
>
> Installed 2.5 ft of screen and 10 ft of solid 2-inch casing.
>
> 4 ft of pea gravel (4.5 cf) from bottom of hole and bentonite chips up to 3 ft below ground surface.

November 2, 2021

VP-TP-1 testpit excavated using track-mounted excavator with 4-ft wide bucket. Conditions are summarized below:

> 0-1.5' - sod over loose, moist, dk brown, very silty f-m SAND with trace gravel, organics (SM)
>
> 1.5-4.5' - medium dense, moist, brown, very silty f-c SAND with gravel, mottling from 3-3.5 ft (fill, SM) Slow seepage at 4.0 ft.
>
> 4.5-7' – dense, moist, olive gray, silty, gravelly f-c SAND, more gravel below 5.5 ft (ice contact deposits?, SM)
>
> 7-8.5' – dense, moist, olive gray, very gravelly, slightly silty fine-coarse SAND with cobbles (advance outwash?, SP-SM)
>
> Collected sample from 8-8.5 ft.

VP-TP-2 testpit excavated using track-mounted excavator with 4-ft wide bucket. Conditions are summarized below:

> 0-1.5' - sod over loose, moist, dk brown, very silty f-m SAND with trace gravel, organics (SM)
>
> 1.5-4.5' - medium dense, moist, brown, very silty f-c SAND with gravel, mottling from 3-3.5 ft (fill, SM) No seepage.
>
> 4.5-7' – dense, moist, olive gray, silty, gravelly f-c SAND, more gravel below 5.5 ft (ice contact deposits?, SM)
>
> 7-8.5' – dense, moist, olive gray, very sandy, slightly silty, fine-coarse GRAVEL with cobbles (advance outwash?, GW-GM)
>
> Collected sample from 8-8.5 ft.

November 4, 2021

RP-TP-1 testpit excavated using track-mounted excavator with 4-ft wide bucket. Conditions are summarized below:

 0-1.5'- sod over loose, moist, gray slightly silty fine SAND with gravel, organics (SP-SM)

 1.5-2.5'- medium dense, very moist, brown, silty gravelly SAND with organics, organic rich zones (fill, SM)

 2.5-3.5' – medium dense, moist, brown, weathered slightly silty f-c SAND with gravel (fill, SP-SM)

 3.5-4.25' – medium dense, slightly moist, gray, very sandy, fine gravel, trace silt (recessional outwash, GP)

 Collected sample from 4.25 ft.

RP-TP-2 testpit excavated using track-mounted excavator with 4-ft wide bucket. Conditions are summarized below:

 0-1.5'- sod over loose, moist, gray slightly silty f SAND with gravel, organics (SP-SM)

 1.5-3.5' – medium dense, moist, brown, weathered slightly silty f-c SAND with gravel (fill, SP-SM))

 3.5-4.5' – medium dense, slightly moist, gray, very sandy, fine Gravel, trace silt (recessional outwash, GP)

 Collected sample from 4.5 ft.

VOLUME V: DEEP INFILTRATION TESTING TO ESTIMATE SATURATED HYDRAULIC CONDUCTIVITY

Near-Term Action (NTA) 2018-0827: Flexible Infiltration Test Methods for Evaluating Infiltration Feasibility

Project No. TAC-20-1 • October 10, 2022

Volume V - Contents

Volume 5 - List of Tables

Volume V - List of Figures

Volume V - Abstract

Volume V provides the results of infiltration testing in deep drilled wells to both demonstrate the use of these three methods under field conditions and determine if they provide similar estimates of bulk hydraulic conductivity (K_b). This testing will also provide data for evaluation of layering, perching, and groundwater mounding.

Infiltration testing was conducted in eight test wells, previously installed for either Seattle Public Utilities projects or the King County Wastewater Treatment Division (WTD) University Basin project. The wells were completed in boreholes that ranged from 6 to 8 in. in diameter and were completed with either 2-in. or 4-in. diameter polyvinyl chloride (PVC) screen and casing. They ranged in depth from 21 to 87 ft and were completed with either 15 ft or 20 ft of screen with a sandpack interval that covered a slightly longer interval. The wells were all screened across glacially over-consolidated sandy deposits, identified as either Vashon-age advance outwash (Qva), Pre-Vashon non-glacial coarse-grained deposits (Qpfnc), or Pre-Vashon glacial undifferentiated (Qpgu). All these deposits are dense fluvial sandy deposits and were evaluated as Qva. Seven of the wells were drilled using a sonic drilling rig and one well was drilled using a hollow-stem auger drilling rig.

Well development was attempted in three wells using a surge block and a hand-actuated pump. Although we were able to surge water through the sandpack in the wells drilled using the sonic rig, we were not able to remove any water from these wells. We did not see any appreciable change in performance in these wells after development. We were able to pump water from the well drilled using the hollow-stem auger rig (U-B-102), which started with 3.7 ft of sediment in the bottom of the screen. Although we were able to remove the sediment and pump water from the screen, the well development efforts did not appear to be successful. The K_b estimates from the tests in this well were at least two orders of magnitude less than expected based on the soil texture (trace to slightly silty fine sand) and the results are not considered valid due to clogging of the sandpack. We have observed clogging issues with other test wells constructed using hollow-stem auger drilling methods. In addition, STP sampling used during hollow-step auger drilling is often infeasible in dense gravelly soils and sample recovery is often limited to a less than a foot for every five feet of drilling. In contrast, sonic drilling generally provides continuous core and better stratigraphic detail, important when a thin layer of silt can result in perched groundwater. For these reasons, we recommend drilling test wells using sonic methods.

The seven sonic wells had K_b values between 3.7 and 16.9 ft/d based on both USSBP and CSSBP results. FHBP tests were not feasible in these seven wells because the hydraulic conductivity exceeded 1.6 ft/d (0.5 m/d) and the test facilities were relatively large (see conclusions in Volume III). In general, the CSSBP estimates of K_b were the same or higher (up to 84% higher) than the USSBP K_b estimates. The higher values are likely due to more permeable sediments higher in the sandpack interval. This explanation will be evaluated with numerical modeling simulations in a later study.

The test durations ranged from 5.5 to 8.3 hr and most of the wells were close to steady state at the end of the tests. The combined decrease in flow rate and/or rise in head was generally less than 2% in the last 30-60 minutes of both the USSBP and CSSBP tests, which is higher than was predicted by numerical simulations (Volume I). This is likely due to perching on low-permeability layers and perhaps groundwater mounding.

Four of the wells had been previously tested. All four wells saw a decrease in the K_b estimate from the previous test to the most recent test, ranging from 2% less in NG-B-201, 11% less in NG-B-204, and more than 60% less in U-TW-6 and U-TW-9. These wells had not received any runoff in between the tests and the reasons why the wells had decreased capacity is uncertain.

This study documented significant head loss across the screened interval in four wells due to air entrainment caused by water falling through air in the casing. The head loss across the screen interval ranged from 7 to 22.5 ft and the head loss per foot of casing ranged from 0.37 to 0.68. The head loss was significantly less per foot of

casing for the 4-in. diameter wells (0.37-0.41) compared with the 2-in. diameter wells (0.63-0.68). Extending the bottom of the drop pipe below the head in the bottom of the screen eliminated the head loss across the screen in all cases.

This study also documented that the water level above the bottom of the drop pipe (used to convey water deeper in the well) was often much lower than the head elevation below the bottom of the drop pipe. This difference in head was surmised to be due to the pressure exerted by the force of water moving though the casing and it referred to as velocity head. Velocity head only occurs below the bottom of the drop pipe and does not extend above the bottom of the drop pipe. The amount of velocity head appears to be related to the water velocity when it exits the drop pipe and expands to fill the well casing. The velocity head was 7-8 ft when the exit velocity was greater than 9.8 ft/s (96 gpm in a 2-in. diameter casing). When the exit velocity was between 4.9 and 8.0 ft/s (48 to 78 gpm in a 2-in. diameter casing) the velocity head ranged from 1-2 ft. Below an exit velocity of 2 ft/s (20 gpm in a 2-in. diameter casing) the velocity head was zero. For a given flow rate, the velocity head decreases as the casing diameter increases. For this reason, velocity head can be significant in 2-in. diameter wells but insignificant in larger wells.

This study also demonstrated that once the bottom of the drop pipe was below the head in the bottom of the well the velocity head did not change over the sandpack interval. This means that velocity head does not affect the validity and accuracy of the test as long as the drop pipe is below the head in the bottom of the well and above the screened interval.

Most of the wells were tested on two consecutive days to assess the potential that higher moisture content could reduce the infiltration capacity of infiltration wells. This was not observed during this study. In general, the second day of testing provided K_b estimates that were the same or higher than the K_b estimates from the first day of testing. Since USSBP tests were conducted during the first day and CSSBP tests were conducted the second day, the higher K_b results may reflect more permeable soils in the upper portion of the sandpack interval.

Wells with both 4-in. and 2-in. diameter well casing were tested in this study. Although slightly more expensive to install, the 4-in. diameter well casing facilitates higher flow rates and provides easier access for transducers and water level tapes.

1 Introduction

Stormwater infiltration is now required where feasible for new development in Washington State and the 2019 Stormwater Management Manual for Western Washington (WSDOE 2019) provides a variety of methods for sizing infiltration facilities. The preferred method is either the small or large pilot infiltration test (PIT). Volume I provides a brief summary of the PIT method.

A more accurate and reliable approach is to determine infiltration rate and capacity using measurements of soil saturated hydraulic conductivity (K_s) obtained from test methods that formally account for both flow directions (vertical, horizontal), and all three components of soil water flow (pressure, gravity, capillary). This study evaluates three different infiltration methods that do account for these flow dynamics, including the uncased steady-state borehole permeameter (USSBP), the cased steady-state borehole permeameter (CSSBP) and the cased falling-head borehole permeameter (FHBP). Numerical simulations have been conducted to calibrate and evaluate these methods for relatively permeable soils typically considered for stormwater infiltration (Volumes I, II, and III).

Numerical simulations facilitate calibration and validation for a broad range of soil types using prescribed soil parameters intended to generally represent the range of soils suitable for infiltration. The numerical validation efforts conducted for this study simulated homogenous and isotropic conditions, in accordance with the assumptions of the borehole permeameter methodology. In the real world, soils are generally layered (anisotropic) and can be highly variable over short distances. In order to illustrate that the isotropic and homogeneous assumptions are violated in the real world, the term "bulk hydraulic conductivity" (K_b) is used rather than K_s for reporting field test results.

The purpose of this field study is to conduct testing in actual test wells using readily available equipment and water sources to: 1) demonstrate and refine the field procedures; 2) illustrate the analytical methods used to estimate bulk hydraulic conductivity (K_b); 3) determine if the three methods provide similar estimates of hydraulic conductivity; and 4) provide data for evaluation of layering, perching, and groundwater mounding. Future numerical modeling will evaluate the effects of layering, perching, and groundwater mounding.

1.1 Scope of Work

The scope of work for this task included field infiltration testing in eight previously installed test wells in the City of Seattle. The goal was to select wells with a range of permeabilities and drilling methods (hollow-stem auger versus sonic). The original plan was to conduct all three test methods in each well and experiment with well development techniques. Other considerations for well selection included proximity to a fire hydrant and approval by public outreach staff. During discussions with Seattle Public Utilities (SPU) it was discovered that they needed testing for two new project-related test wells that also met the needs of this project.

FHBP tests were attempted in seven of the eight wells. A FHBP test was not attempted in U-TW-6 because the top of the sandpack was 3.5 ft below the ground surface and there was not enough solid casing above the sandpack to conduct a valid FHBP test. Following the FHBP test, a short USSBP test was conducted in some of the wells to determine the pre-development capacity of the test well. Well development was attempted in these wells using a surge block and a down-hole foot valve to pump water from the well. With or without well development, a longer USSBP test was conducted for approximately 6 hr. On the second day, a CSSBP test was conducted in the well. The test results were analyzed using the previously developed analytical methods described in Volumes I, II, and III. The results using different testing methods within the same facility were compared to determine the degree of agreement or divergence between the methods. A summary of the results, lessons learned, and recommendations are provided in this volume.

2   Materials and Methods

2.1   Test Well Characteristics

The deep infiltration test wells were selected from previously installed test wells located within the City of Seattle based on the following criteria:

- Permission from Seattle Public Utilities (SPU) or the King County Wastewater Treatment Division (WTD) to test the wells.
- Test sites should include soils types that are typically used for stormwater infiltration, such as advance outwash (Qva) or other sandy soils with K_b above 0.25 in./hr (0.5 ft/d).
- A fire hydrant within 600 ft of the test wells that did not require running hose across a busy street.
- No shallow groundwater within 10 ft of the base of the test well sand pack (to avoid groundwater mounding effects).
- The majority of the wells allow comparison of CSSBP and USSBP testing with at least 20 ft of cased and sealed well above the sandpack.
- Test wells installed using both sonic and hollow-stem auger (HSA) drilling rigs.
- Test wells constructed using both 2-in. diameter and 4-in. diameter screen and casing.

Eighteen potential test sites owned by WTD were evaluated and the most favorable four wells were selected for testing. A similar number of SPU wells were evaluated and the most favorable four wells were selected for testing. Four of the selected wells had been previously tested and four were tested for the first time.

Borehole logs and well completion details for the eight test wells are provided in Appendix A and summarized in Table 1. All the wells were constructed between June 2016 and August 2021. Four of the wells (CH-B-102, CH-B-104, NG-B-201, NG-B-204) were constructed for SPU projects and four of the wells (U-B-102, U-B-118, U-TW-6, and U-TW-9) were completed for the WTD to support the University Basin green stormwater infrastructure project.

Table 1: Deep Infiltration Test Wells.

Test Name	Borehole Depth (ft)	Drilling Method	Install Month -Year	Borehole Dia. (in)	Casing Dia. (in)	Depth to Groundwater (ft)	Sandpack Interval (depth-ft)	Geologic Unit Tested
CH-B-102	80	Sonic	Aug-21	8.0	4.0	>85	17 – 42	Qva
CH-B-104	110	Sonic	Aug 21	8.0	4.0	94	63 – 87	Qpfnc
NG-B-201	95	Sonic	Feb-20	6.0	2.0	79	38 - 61	Qva
NG-B-204	55	Sonic	Feb-20	6.0	2.0	50	14 - 36	Qva
U-B-102	61.5	HSA	Jun-18	8.0	2.0	59	23 - 47	Qva
U-B-118	65	Sonic	Jun-18	6.0	2.0	55	22 – 47	Qpgu
U-TW-6	40	Sonic	Jun-16	6.0	2.0	31	3.5 - 21	Qva
U-TW-9	107	Sonic	Jun-16	6.0	2.0	>109	47- 74	Qva

Notes: Sonic – Sonic drilling rig; HSA – Hollow stem auger drilling rig; Qva - Vashon-age advance outwash; Qpfnc - Pre-Vashon non-glacial coarse-grained deposits; Qpgu – Pre-Vashon glacial undifferentiated

U-B-102 was drilled using a hollow-stem auger drilling rig and the remaining wells were drilled using a sonic drilling rig. The borehole diameters ranged from 6 in. to 8 in. and the wells were constructed as standard groundwater monitoring wells, although they were screened above the water table. In general, the wells were constructed of either 2-in. or 4-in. slotted polyvinyl chloride (PVC) well screen and solid casing. With the exception of U-TW-6, which was completed with 15 ft of screen, all the wells were completed with 20 ft of screen. The

annular space within the screened interval was filled with clean sand to provide a filter pack between the screen and the native soils. The sandpack generally extended a few feet above and below the screen. The annular space above the sandpack was sealed with bentonite chips and the top of the wellhead was protected by a flush-mounted steel monument. Wells CH-B-104 and NG-B-201 were completed with solid casing and bentonite chips below the screen interval to facilitate installation of a vibrating-wire piezometer below the groundwater table.

All the wells were screened across glacially over-consolidated sandy deposits, identified as either Vashon-age advance outwash (Qva), Pre-Vashon non-glacial coarse-grained deposits (Qpfnc), or Pre-Vashon glacial undifferentiated (Qpgu). All these deposits are glacially-consolidated sandy deposits and were evaluated as Qva.

2.2 Test Procedures

All the infiltration tests for this study were conducted in September 2021. In addition, infiltration test data from previous studies in 2016 and 2020 were evaluated and compared with the recent testing. A variety of infiltration tests were conducted in each of the test wells. Although FHBP tests were attempted in most of the wells, only the test in U-B-102 was considered valid given the relatively high K_b values in the remaining wells (see conclusions of Volume III). USSBP tests were conducted in all the wells by maintaining the water level near the top of the sandpack interval. CSSBP tests were conducted in all the wells except U-TW-6, which was a shallow well and it was not feasible to raise the water level significantly higher than the top of the sandpack. Details of the test methodology are provided below.

2.2.1 Falling-Head Borehole Permeameter Tests

The FHBP tests were conducted using the following procedures:

1) A pressure transducer was placed in the bottom of the well and was set to record the water depth every second. The pressure transducer was connected to a data cable that allowed real-time monitoring of the depth of water during the test.

2) All head elevations used in the analysis are referenced from the bottom of sandpack, based on the assumption that water flows freely through the sandpack with minimal head loss. Therefore, the depth of sandpack beneath the screen was added to the transducer reading for graphing and analysis.

3) Water from a fire hydrant was discharged into the well as quickly as possible with the intention of filling the well to the top of casing. If the water level did not reach the top of the casing within one-two minutes the water was turned off.

4) The amount of water discharged into the test well was recorded.

5) The water level in the well was allowed to fall until it reached the top of the screened interval.

6) The results were evaluate using the FHBP method provided in Volume III.

2.2.2 Uncased Steady-State Borehole Permeameter Tests

The USSBP tests were conducted using the following procedures:

1) A pressure transducer was placed in the bottom of the well and was set to record the water depth once per minute. The pressure transducer was connected to a data cable that allowed real-time monitoring of the depth of water during the test.

2) All head elevations used in the analysis are referenced from the bottom of sandpack, based on the

assumption that water flows freely through the sandpack with minimal head loss. Therefore, the depth of sandpack beneath the screen was added to the transducer reading in the bottom of the well for graphing and analysis.

3) In some cases, a second pressure transducer was placed near or above the top of the screen and was set to record the water depth once per minute. The pressure transducer was connected to a data cable that allowed real-time monitoring of the depth of water during the test. The target depth of the transducer below the top of casing was measured and marked on the data cable before the transducer was lowered into the well. All head readings account for the depth of the top-of-screen transducer and are referenced to the bottom of the sandpack to allow comparison with the bottom-of-screen transducer.

4) Water from a fire hydrant was discharged into the well at a rate that maintained the water level (based on the pressure transducer in the bottom of the well) near the top of the sandpack.

5) A drop pipe was attached to the flowmeter assembly to convey the water into the well casing.

6) Initial short-term tests (2 hr or less) were conducted in some of the wells to estimate K_b before well development.

7) Well development was attempted in some of the wells (CH-B-102, NG-B-204, and U-B-102) using a surge block and a down-hole foot valve attached to 1-in. diameter PVC casing to pump water from the well. Water was introduced into the well in an attempt to maintain the water level near the top of casing. Water was lifted from the well by manually lifting the assembly up and down. Well development was not conducted in the remaining wells because the attempts in wells with higher K_b were not able to remove any water and did not appear to significantly change the well capacity.

8) Longer USSBP tests of approximately 6 - 8 hr were conducted in all the wells.

9) Flow rates were measured using flowmeters and recorded at regular intervals during the tests.

10) The flow rate in U-B-102 was less than 0.12 gpm, significantly less than the calibration range of the smallest flowmeter. For this test, short bursts of water were added at regular intervals to maintain the water depth between 20 and 22 ft of head. The flow rate was calculated by dividing the volume of water added by the duration between bursts of water.

11) Water levels were recorded at regular intervals during the tests to determine when it was necessary to change the flow rate to maintain the water level near the top of the sandpack.

12) The transducer was left in the well after the water was turned off to record the water levels during the falling head portion of the test. This information is useful for identifying perching layers or groundwater mounding using numerical simulations.

13) The results were evaluated using the USSBP method provided in Volume I.

2.2.3 Cased Steady-State Borehole Permeameter Tests

The CSSBP tests were conducted using the following procedures:

1) A pressure transducer was placed in the bottom of the well and was set to record the water depth once per minute. The pressure transducer was connected to a data cable that allowed real-time monitoring of the depth of water during the test.

2) All head elevations used in the analysis are referenced from the bottom of sandpack, based on the assumption that water flows freely through the sandpack with minimal head loss. Therefore, the depth of sandpack beneath the screen was added to the transducer reading in the bottom of the well for graphing and analysis.

3) In some cases, a second pressure transducer was placed near or above the top of the screen and was set to record the water depth once per minute. The pressure transducer was connected to a data cable that allowed real-time monitoring of the depth of water during the test. The target depth of the transducer below the top of casing was measured and marked on the data cable before the transducer was lowered into the well. All head readings reported account for the depth of the top-of-screen transducer and are referenced to the bottom of the sandpack to allow comparison with the bottom-of-screen transducer.

4) Water from a fire hydrant was discharged into the well at a rate that maintained the water level (based on the pressure transducer in the bottom of the well) near the top of the well, or as high as possible given the maximum capacity of the fire hydrant.

5) A drop pipe was attached to the flowmeter assembly to convey the water into the well casing.

6) The maximum capacity of the fire hydrants ranged from 80 to 135 gpm depending on the pressure in the hydrant, the length of fire hose, and the diameter and length of the drop pipe. The 2-in. drop pipe could be used in the 4-in. diameter well casings, but the 2-in. diameter well casings were limited to 1-in. diameter drop pipe.

7) When feasible given the hydrant capacity, the flow rate was adjusted to maintain the water level near the top of the well. If the water level was significantly below the top of the well at the maximum hydrant capacity, the flow rate was set at the maximum rate and the water level was allowed to rise during the duration of the tests.

8) The CSSBP tests were all approximately 6 hr long.

9) Flow rates were measured using flowmeters and recorded at regular intervals during the tests.

10) Water levels were recorded at regular intervals during the tests to determine when it was necessary to change the flow rate to maintain the water level near the top of the sandpack.

11) The transducer was left in the well after the water was turned off to record the water levels during the falling head portion of the test. This information is useful for identifying perching layers or groundwater mounding using numerical simulations.

12) The results were evaluated using the CSSBP method provided in Volume II.

2.3 Analysis of Test Results

The test results were analyzed to determine hydraulic conductivity using the methods for FHBP tests (Volume III), USSBP tests (Volume I), and CSSBP tests (Volume II). All three methodologies assume a flat-bottom cylindrical test facility, isotropic and homogeneous soil, and no water-table effects.

2.3.1 FHBP Test Analysis Method

The FHBP test analysis method is only valid while the water level is above the screen or sandpack interval. As described in Volume III, the single-point FHBP method used for this study is based on the following equation:

$$K_{\mathrm{b}} = \frac{r_{\mathrm{c}}^2}{4\,r_0\,t}\,\tau_{\mathrm{E}} \quad (\mathrm{Eq.\,1})$$

where r_c is the radius of the casing, r_0 is the radius of the equivalent sphere discharge surface (elaborated below), and t is the time when K_b is estimated. τ_E is dimensionless time, based on the following equation:

$$\tau_E = \left(1 + \frac{1}{2A_E}\right) ln \left(\frac{A_E^3 - 1}{A_E^3 - \rho_E^3}\right) - \frac{3}{2A_E} ln \left(\frac{A_E - 1}{A_E - \rho_E}\right) + \frac{\sqrt{3}}{A_E} \left[\tan^{-1}\left(\frac{A_E + 2\rho_E}{\sqrt{3} A_E}\right) - \tan^{-1}\left(\frac{A_E + 2}{\sqrt{3} A_E}\right)\right] \text{ (Eq. 2)}$$

where:

$$A_E^3 = \frac{3r_c^2\left(H_0 + \alpha^{*-1}\right)}{4r_0^3 \, \Delta\theta} + 1 \text{ (Eq. 3)}$$

$$\rho_E^3 = \frac{3r_c^2(H_0 - H_t)}{4r_0^3 \, \Delta\theta} + 1 \text{ (Eq. 4)}$$

$$\Delta\theta = \theta_{fs} - \theta_i \text{ (Eq. 5)}$$

H_0 is the effective pressure head in the borehole screen at $t = 0$, H_t is the effective pressure head in the borehole screen at time t (elaborated below), α^* is the soil sorptive number, θ_s is the porosity (aka field-saturated volumetric soil-water content), and θ_i is the background volumetric soil-water content. As described in Kindred and Reynolds (2020) α^* represents the capillarity of the soil. The single-point FHBP method used for this study assumed a value for α^* based on soil characteristics, as calculated in Volume I and summarized in Table 2.

The equivalent sphere radius (r_0) is calculated the following expression:

$$r_0 = \left(\frac{r_b^2}{4} + \frac{r_b L}{2}\right)^{1/2} \text{ (Eq. 6)}$$

where r_b = radius of the borehole and L is the length of the sandpack interval. As discussed in Reynolds (2011), the effective pressure head H_t is calculated using:

$$H_t = D_t - E \text{ (Eq. 7)}$$

where E is the screen factor:

$$E = \frac{L^2}{r_b + 2L} \text{ (Eq. 8)}$$

for combined vertical and radial discharge. D_t is actual water depth at time t. H_0, the initial effective pressure head, is calculated using Eq. 7 by replacing H_t with H_0 and D_t with D_0, the initial or target fill depth.

Table 2: *Sorptive Number (α^*) for different soil types typically considered for stormwater infiltration.*

Soil Type	α^* (ft^{-1})
Silty fine sand (SM)	0.5
Silty fine-coarse sand (SM)	1.7
Qvt (SM)	0.36
Silty Qva (SM)	0.41
Fine sand (SP-SM)	1.1
Medium sand (SP)	3.4
Sandy gravel (GW)	17.4
Fine Qva (SP-SM)	0.76
Fine-Medium Qva (SP)	1.2
Fine-Coarse Qva (SW)	7.6

2.3.2 USSBP Test Analysis Method

As discussed in Volume I and Kindred and Reynolds (2020), the USSBP method is based on the following equation:

$$K_S = \frac{C_u Q}{2\pi H^2 + \pi r_b^2 C_u + \frac{2\pi H}{\alpha^*}} \quad (Eq.\,9)$$

where

$$C_u = \left[\frac{(H/r_b)}{Z_1 + Z_2(H/r_b)} \right]^{Z_3} \quad (Eq.\,10)$$

H is the ponding head at the end of the steady state test and Q is the flow rate at the end of the steady state test. Eq. 9 assumes that H is less than the uncased or screened portion of the test facility. α^* is the soil sorptive number (ft^{-1}), C_u is the uncased shape function (dimensionless), and Z_1, Z_2, and Z_3 are the shape function fitting parameters (dimensionless). Values for Z_1, Z_2, Z_3 for the USSBP method are provided in Table 3.

Table 3: Uncased *shape function* (C_u) parameters for USSBP tests based on different soil classifications using the Unified Soil Classification System. Different shape function parameters are developed for test configurations where ponded head (H) to borehole radius (r_b) ratio was $H/r \leq 20$ or $H/r \geq 20$, and for soils with > 12% silt or < 12% silt.

Soil Type	Low Ponded Head ($H/r \leq 20$)			High Ponded Head ($H/r \geq 20$)		
	Z_1 (-)	Z_2 (-)	Z_3 (-)	Z_1 (-)	Z_2 (-)	Z_3 (-)
Sand and gravel with > 12% Silt (SM, GM)	2.11	0.192	0.91	2.04	0.0224	0.547
Sand and gravel with < 12% Silt (SP-SM, SP, SW, GW, GP)	2.03	0.207	0.98	2.11	0.0273	0.605

2.3.3 CSSBP Test Analysis Method

As discussed in Volume II, the CSSBP method uses the same form of the equation used in the USSBP method with minor adjustments:

$$K_S = \frac{C_c Q}{2\pi L H + \pi r_b^2 C_c + \frac{2\pi L}{\alpha^*}} \quad (Eq.\,11)$$

and

$$C_c = \left[\frac{(L/r_b)}{Z_1 + Z_2(L/r_b)} \right]^{Z_3} \quad (Eq.\,12)$$

where L, the length of the sandpack or screen, replaces one of the H values in the first term of the denominator and the H in the third term of the denominator. C_c is the cased shape function and used different Z_1, Z_2, and Z_3 fitting parameters than the C_u shape function, as provided in Table 4.

The USSBP method is calibrated for uncased scenarios where $H = L$ and the CSSBP method is calibrated for cased scenarios when $H > L$. However, there is a transition interval as the water level begins to rise above the sandpack into the solid casing extending above the sandpack. Based on simulations provided in Volume II, the USSBP

method is recommended when H/L is less than 1.2 and the CSSBP method is recommended when H/L is greater than 1.2

Table 4: Uncased s*hape function* (C_c) parameters for CSSBP tests based on different soil classifications using the Unified Soil Classification System. Different shape function parameters are developed for test configurations where screen/sandpack length (L) to borehole radius (r_b) ratio was $L/r_b < 20$ or $L/r_b \geq 20$, and for soils with > 12% silt or < 12% silt.

Soil Type	Short Sandpack ($L/r_b < 20$)			Long Sandpack ($L/r_b \geq 20$)		
	Z_1 (-)	Z_2 (-)	Z_3 (-)	Z_1 (-)	Z_2 (-)	Z_3 (-)
Sand and gravel with > 12% Silt (SM, GM)	3.06	0.12	0.674	2.32	0.0286	0.463
Sand and gravel with < 12% Silt (SP-SM, SP, SW, GW, GP)	2.45	0.214	0.93	1.87	0.0354	0.501

3 Results

This section presents the test results for the 8 test wells included in this study. Unless otherwise indicated, all testing was conducted in September 2021. All the head elevations referenced in this section are measured from the base of the sandpack, not the base of the screen. In other words, if the transducer was set in the bottom of the well casing and the sandpack extended 2 ft below the bottom of the wells casing, the transducer reading was increased by 2 ft. In addition, the sandpack length used in the analyses includes sandpack above and below the screen. This correction is based on the assumption that flow is relatively unhindered within the sandpack below the bottom of the screen and above the top of the screen.

3.1 FHBP Results

As discussed in Volume III, the FHBP method assumes instantaneous filling of the well casing to a depth that is higher than the top of the sandpack and slight deviations from this assumption can significantly impact the results when $K_b \geq 1.6$ ft/d and for larger test wells (e.g., $L \geq 3.3$ ft, $D_0 \geq 6.6$ ft, $r_b \geq 4$ in.). None of the test facilities included in this scope of work were within these dimensions and only one test well (U-B-102) had $K_b \leq 1.6$ ft/d.

Despite these limitations, FHBP tests were attempted in CH-B-102, CH-B-104, NG-B-201, NG-B-204, U-B-102, and U-B-118. The original intention was to fill the well to the top of casing and then shut the water off. This was not achieved within 60 seconds in any wells other than U-B-102, which was filled within 18 seconds. The only other well that was filled above the top of the sandpack within 30 seconds was NG-B-201, which achieved a ponding depth of 50 ft at 78 seconds. Results for these two wells are provided below for illustration purposes, although the K_b estimates are unlikely to be valid given the relatively long fill times.

3.1.1 FHBP Results for Test Well U-B-102

U-B-102 was the only well in this study that was drilled with a hollow-stem auger drilling rig. Initial sounding of the well determined that there was 3.7 ft of sediment in the bottom of the well casing. It was not feasible to remove the sediment without adding water and the addition of water before testing would have complicated interpretation of the FHBP test results. Therefore, FHBP testing was conducted before well development.

Fig. 1 illustrates the FHBP test results for U-B-102. As shown on the figure, the water rose to the top of casing ($D_0 = 53.8$ ft) within 18 seconds at a rate of 130 gpm. When the water was turned off the water dropped quickly and bounced up and down around a ponding depth of 40 ft before slowly dropping below the top of the sandpack at 120 seconds. The test results were analyzed using Eq. 1 and the assumptions and results are summarized in Table 5.

The calculation time was selected to be when the water level was just above the top of the sandpack (118 sec) minus the fill time of 18 seconds. The values for θ_s and θ_i were based on the soil properties for fine-medium Qva assumed in the numerical validation work (Volume I) and α^* is the value for fine-medium Qva provided in Table 1. The estimated K_b is 0.024 ft/d, which is several orders of magnitude less than expected based on the soil texture across the sandpack interval (trace to slightly silty fine sand). The sandpack is likely clogged with silt and is controlling the flow rate more than the native soils.

As shown on Fig. 1, the well was only 47 ft deep (top of casing line on Fig. 1), so the observed head of 54 ft in the bottom of the well was higher than the water level above the drop pipe due to the force of the water flowing down the casing. At 130 gpm through a 2-in. diameter casing, the water velocity entering the screen is 13 ft/sec. This velocity slows as water flows out of the screen and is zero at the bottom of the casing but the pressure from the velocity of the water at the top of the screen is still enough to add approximately 7 ft of head at the bottom of the screen compared with the water level at the top of the casing. This velocity head is also observed in some of the steady-state tests described in later sections. The fluctuating water level for a few second after the water turned off reflects the rapid decrease in the velocity head when the water was turned off.

Fig. 1: FHBP test results for U-B-102.
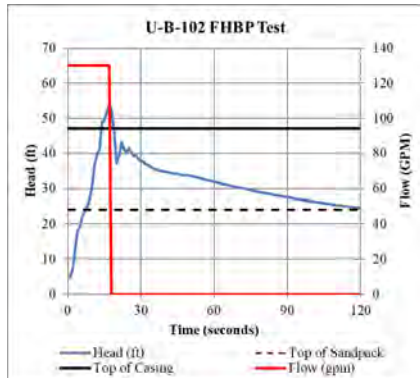
Table 5: Results of FHBP method for test well U-B-102.

Parameter	Units	Value
Initial water depth (D_0)	ft	52.3
Water depth at time t (D_t)	ft	24.7
Calculation time (t)	sec	100
Casing radius (r_c)	in.	0.083
Borehole radius (r_b)	in.	0.25
Sandpack length (L)	ft	24.00
Saturated volumetric soil-water content (θ_s)	-	0.3
Background volumetric soil-water content (θ_i)	-	0.1
Assumed Sorptive Number for F-M Qva (α^*)	1/ft	1.2
Calculated K_b	**ft/d**	**0.024**

3.1.2 FHBP Results for Test Well NG-B-201

Fig. 2 illustrates the FHBP test results for NG-B-201. The casing was filled with water to a depth of 50 ft after 79 seconds at a rate of 134 gpm. When the water was turned off the water level dropped quickly and smoothly. No velocity head was observed in this test because the water depth never rose above the bottom of the drop pipe (at a head elevation of 56 ft). The test results were analyzed using Eq. 1 and the assumptions and results are summarized in Table 6.

The calculation time was selected to be when the water level was just above the top of the sandpack (86 sec) minus the fill time of 79 seconds. The values for θ_s and θ_i are based on the soil properties for fine-medium Qva assumed in the numerical validation work (Volume I) and α^* is the value for fine-medium Qva provided in Table 1. As discussed in Section 4.1, the FHBP K_b estimate of 0.41 ft/d is more than an order of magnitude less than the USSBP test results. This significant difference reflects the long fill time. In retrospect, this test would have provided more accurate results if the water had been turned off at 20 seconds when the rate of water-level rise began to slow. However, the original intention was to fill the casing to the ground surface and making split-second modifications to the test plan during these very quick tests is difficult.

Fig. 2: FHBP test results for NG-B-201.
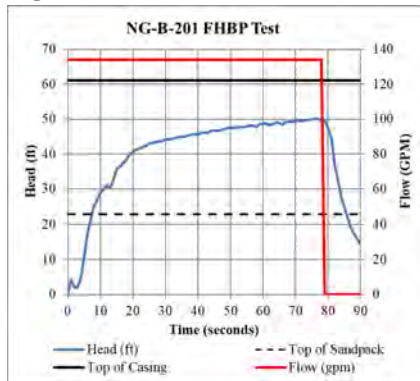
Table 6: Results of FHBP method for test well NG-B-201.

Parameter	Units	Value
Initial water depth (D_0)	ft	49.6
Water depth at time t (D_t)	ft	22.1
Calculation time (t)	sec	7
Casing radius (r_c)	in.	0.083
Borehole radius (r_b)	in.	0.25
Sandpack length (L)	ft	23.00
Saturated volumetric soil-water content (θ_s)	-	0.3
Background volumetric soil-water content (θ_i)	-	0.1
Assumed Sorptive Number for F-M Qva (α^*)	1/ft	1.2
Calculated K_b	**ft/d**	**0.41**

3.2 USSBP and CSSBP Results

This section provides the USSBP and CSSBP results for the eight test wells. For the four wells that were previously tested, these older results are also provided for comparison. All the tests were conducted in glacially over-consolidated soils categorized as either fine Qva (SP-SM) or fine-medium Qva (SP) depending on the dominate soil texture reported in the soil logs.

3.2.1 *Steady State Test Results for Test Well CH-B-102*

Fig. 3 illustrates the USSBP and CSSBP test results for CH-B-102. The initial USSBP test ran for 98 minutes with a final flow rate of 42 gpm. The test was paused to conduct approximately 1.5 hr of well development. Water was discharged into the well during development to maintain head within the screened interval. The weight of the water was significant in this 4-in. diameter wells and it was difficult to maintain the surging action by hand for an extended period of time. Although the entire screened interval was treated with the surge block, it was not possible to remove any water during development, likely because the water level could not be maintained high enough and sediment or other material was preventing the ball valve from closing entirely. Following development, no sediment was detected within the well screen using a sounding probe to measure the depth to the bottom of the well screen.

After development, the second USSBP test began with a flow rate of 42 gpm to see if any improvement in well capacity had occurred. After 55 minutes at this flow rate the head elevation was approximately the same as before development, indicating that well development had not changed the capacity of the test well.

The second USSBP test continued for a total of 375 minutes with a constant head of approximately 22.5 ft. By the end of the test, the flow rate had dropped to 33 gpm. As shown on Fig. 3, the drop pipe was only 5 ft below the top of casing, well above the water level in the well during the test. The test results were analyzed using Eq. 9. As summarized in Table 7, the estimated K_b value for the uncorrected USSBP test is 10.3 ft/d. The air entrapment phenomenon had not been recognized when this test was conducted and the average ponding depth across the screened interval was likely higher than measured in the bottom of the well. Therefore, the K_b value is likely overestimated for the USSBP test.

The CSSBP test was conducted the day after the USSBP test. As shown on Fig. 3, the ponding head was maintained at approximately 22.3 ft for the first 107 minutes to allow comparison with the USSBP test the previous day. The flow rate of 36 gpm at 100 minutes was less than the flow rate for the first 330 minutes of the USSBP test and slightly more than the final flow rate for the USSBP test. These results suggest that the water content was still elevated from the previous day's test, allowing the CSSBP test to reach steady state sooner.

The flow rate was increased at 107 minutes and the water level was observed near the top of the casing at 120 minutes with a flow rate of 53 gpm in a 4-in. diameter casing. However, the head at the bottom of the well was still 10 to 12 ft below the top of the well. This difference indicates significant head loss between the bottom of the drop pipe and the bottom of the well. At 140 minutes a second transducer was set in the well 23 ft above the bottom of the sandpack, just below the top of the sandpack. As shown on Fig. 3 (CSSBP test) this transducer confirmed significant head loss between the top of the screen and the bottom of the screen. The head difference across the 23 ft of sandpack is approximately 7 ft with a flow rate of 53 gpm. This head loss was attributed to air entrainment.

At 228 minutes the drop pipe was extended from 5 ft below the top of casing to 20 ft below top of casing. Once this occurred the flow rate could be increased to 79 gpm while maintaining the water level just below the top of casing. As shown on Fig. 3 (CSSBP test) the water level in both transducers was also at top of casing, indicating no measurable head loss either above or within the screen. In addition, these results indicate that there was no significant velocity head in the 4-in. well casing at this flow rate.

The CSSBP test was run for a total of 500 minutes and was at steady state after 280 minutes. The results were analyzed using Eq. 11. As indicated in Table 7, the flow rate of 79 gpm and the ponding head of 42.1 ft provides an estimated K_b value of 9.4 ft/d, 9% less than the uncorrected USSBP test.

A corrected USSBP test analysis was conducted assuming that the average head across the screen was higher than the head measured in the bottom of the well. Assuming the head losses are linear, the 7 ft difference between the top of screen transducer and the bottom of screen transducer observed 200 minutes into the CSSBP test suggests that the average head across the screen is 3.5 ft higher than the head in the bottom transducer. As indicated in Table 7, increasing the ponding head by 3.5 ft provides a corrected USSBP estimate of 8.2 ft/d for K_b. This corrected USSBP value is 19% less than the uncorrected USSBP analysis, and 13% less than the CSSBP test. The 7 ft of head difference during the CSSBP test was at a higher flow rate (53 gpm versus 33 gpm in the USSBP test) so the head losses across the screen during the USSBP test might be less than 7 ft, which would increase the corrected K_b estimate.

Fig. 3: USSBP and CSSBP test results for CH-B-102.
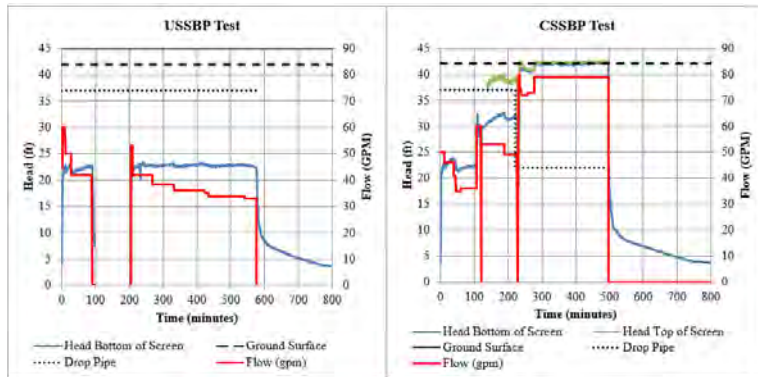
Table 7: Results of USSBP and CSSBP tests in well CH-B-102.

Parameter	Units	USSBP Test	Corrected[2] USSBP Test	CSSBP Test
Ponding Head (H)	ft	22.7[1]	26.2	42.1
Flow Rate (Q)	gpm	33	33	79
Borehole radius (r_b)	in.	4.0		
Well casing radius (r_c)	in.	2.0		
Saturated Sandpack length (L)	ft	22.7	24.0	24.0
Assumed Sorptive Number for F Qva (α^*)	1/ft	0.76		
Soil Classification		SP-SM		
Calculated K_b	**ft/d**	**10.3[1]**	**8.2**	**9.4**

[1]Ponding head does not account for air entrainment. K_b value is likely overestimated.

[2]"Uncorrected" means the bottom of well ponding head was used to calculate K_b. "Corrected" means the average ponding head across the screen was used to calculate K_b

3.2.2 Steady State Test Results for Test Well CH-B-104

Fig. 4 illustrates the USSBP and CSSBP test results for CH-B-104. Based on the experience in CH-B-102, well development was not attempted in CH-B-104. The first 260 minutes of the USSBP test was conducted with the drop pipe 5 ft below the top of casing and the head loss between the top of screen and the bottom of screen decreased from about 10.5 ft at 70 gpm to 8.5 ft at 60 gpm. At 260 minutes the drop pipe was extended to 65 ft below the top of casing and the head loss across the screen essentially disappeared. By the end of the USSBP test, the flow rate had dropped to 65 gpm and the ponding head was 28.7 ft. The test results were analyzed using Eq. 9. As summarized in Table 8, the estimated K_b value for the USSBP test is 13.9 ft/d.

The USSBP testing had demonstrated that the maximum flow rate from this hydrant with 600 ft of fire hose and 65 ft of 1-in. diameter drop pipe was 76 gpm. Therefore, the CSSBP test was delayed for 10 days when we could return with 10 ft of 2-in. drop pipe that would facilitate a higher flow rate.

For the CSSBP test, the upper transducer was set 30 ft below the ground surface and 57 ft above the bottom of the sandpack. As shown on Fig. 4 (CSSBP), 30 minutes into the CSSBP test the flow rate was 80 gpm and the ponding head was at 24.7 ft. At this point the flow rate was increased to 135 gpm, the maximum discharge from this hydrant using 10 ft of 2-in. diameter drop pipe. At the end of the test, the head at the bottom of the screen was 43.7 ft and the head for the upper transducer (57 ft above the bottom of the sandpack) was 66.2. The water level was at least 10 ft

below the bottom of the drop pipe; the head loss due to air entrainment between the upper and lower transducer was approximately 22.5 ft. Assuming the head loss occurs over a distance of 55 ft, this is 0.41 ft of head loss per foot of well casing, or 8.2 ft of head loss across 20 ft of sandpack. Based on this analysis, the average head across the screen is 47.8 ft.

The CSSBP results were analyzed using Eq. 11 and are provided in Table 8. The head in the bottom transducer (43.7 ft) provides an estimated K_b value of 15.5 ft/d, 12% more than the USSBP test. The average head across the sandpack (47.8 ft) provides an estimated K_b value of 14.2 ft/d, 2% more than the USSBP test.

Fig. 4: USSBP and CSSBP test results for CH-B-104.
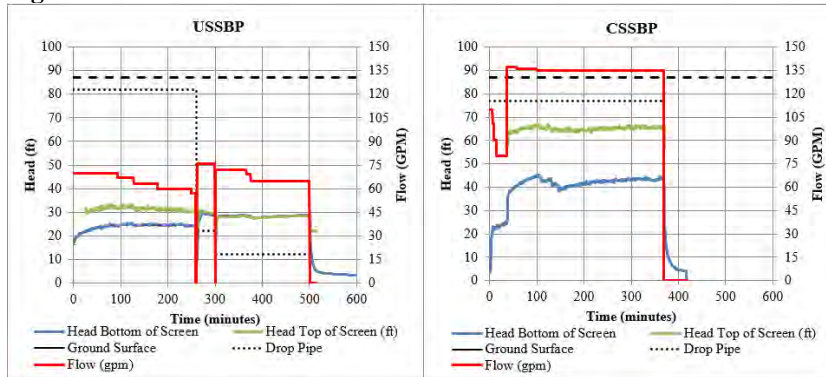
Table 8: Results of USSBP and CSSBP tests in well CH-B-104.

Parameter	Units	USSBP Test	Uncorrected[2] CSSBP Test	Corrected[2] CSSBP Test
Ponding Head (*H*)	ft	28.7	43.7[1]	47.8
Flow Rate (*Q*)	gpm	65	135	135
Borehole radius (*r*$_b$)	in.	4.0		
Well casing radius (*r*$_c$)	in.	2.0		
Saturated Sandpack length (*L*)	ft	24.0	24.0	24.0
Assumed Sorptive Number for F Qva (*α**)	1/ft	0.76		
Soil Classification		SP-SM		
Calculated K_b	**ft/d**	**13.9**	**15.5[1]**	**14.2**

[1] Ponding head does not account for air entrainment. K_b value is likely overestimated.
[2] "Uncorrected" means the bottom-of-well ponding head was used to calculate K_b. "Corrected" means the average ponding head across the screen was used to calculate K_b

3.2.3 Steady State Test Results for Test Well NG-B-201

Fig. 5 illustrates the USSBP and CSSBP test results for NG-B-201, including a test that was conducted in March 2020. The March 2020 USSBP test was conducted for 264 minutes with an ending flow rate of 7.5 gpm and a head of 15.0 ft. As summarized in Table 9, these results provide an estimated K_b value of 4.6 ft/d. This test was conducted with a short section of drop pipe, and it was uncertain if air entrainment and head loss were significant at this low flow rate.

The recent USSBP test was conducted with the drop pipe 45 ft below the top of casing and below the water level during the test. As summarized in Table 9, the ending flow rate of 9.9 gpm and a ponding head of 18.2 ft provided an estimated K_b value of 4.5 ft/d. This result is within 2% of the March 2020 USSBP test, suggesting that air entrainment was not a significant factor for the March 2020 USSBP test, given a flow rate of 7.5 gpm.

As shown in Fig. 5, the CSSBP test was run for 434 minutes with an ending flow rate of 78 gpm and a ponding head of 59 ft. As summarized in Table 9, these ending values provide an estimated K_b value of 6.7 ft/d, 49% higher than the USSBP test. One potential reason for this higher estimate is that the more permeable soils are present in the upper portion of the sandpack interval (see NG-B-201 boring log in Appendix A).

The CSSBP test shown in Fig. 5 illustrates that the drop pipe was 10 ft below the top of casing for the last 350 minutes of the test. During this time, the head in the bottom of the screen was very close to the ground surface. At the same time, the observed water level in the top of the well was usually within 1.5 ft of the top of casing. This indicates that there was approximately 1 ft of velocity head during this portion of the test.

Fig. 5: USSBP and CSSBP test results for NG-B-201.
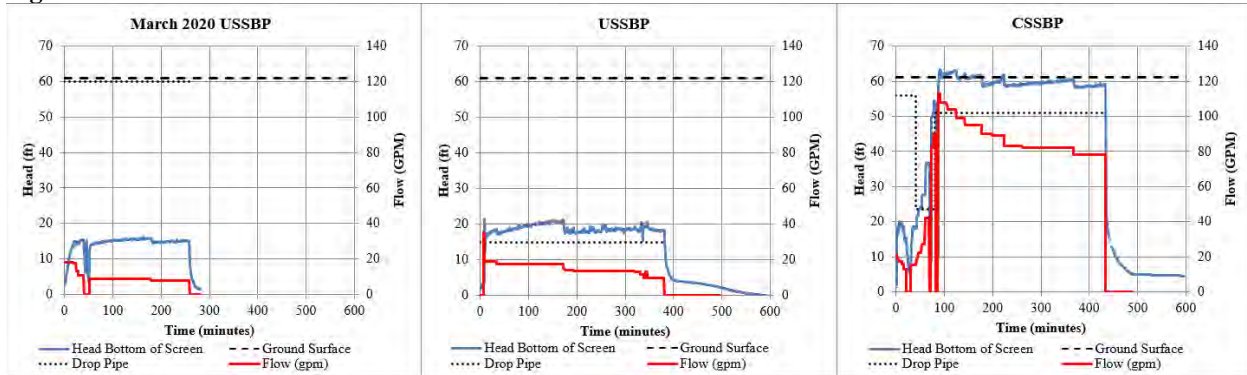
Table 9: Results of USSBP and CSSBP tests in well NG-B-201.

Parameter	Units	Mar. 2020 USSBP Test	USSBP Test	CSSBP Test
Ponding Head (H)	ft	15.0[1]	18.2	59.0
Flow Rate (Q)	gpm	7.5	9.9	78
Borehole radius (r_b)	in.	3.0		
Well casing radius (r_c)	in.	1.0		
Saturated Sandpack length (L)	ft	15.0	18.2	23.0
Assumed Sorptive Number for F-M Qva (α^*)	1/ft	1.19		
Soil Classification		SM		
Calculated K_b	**ft/d**	**4.5[1]**	**4.4**	**6.7**

[1] Ponding head does not account for air entrainment. K_b value may be slightly overestimated.

3.2.4 Steady State Test Results for Test Well NG-B-204

Fig. 6 illustrates the USSBP and CSSBP test results for NG-B-204, including a test that was conducted in May 2020. The May 2020 USSBP test was conducted for 299 minutes with an ending flow rate of 48 gpm and a ponding head of 18.3 ft. The test results were analyzed using Eq. 9. As summarized in Table 10, these results provide an estimated K_b value of 23.8 ft/d. This test was conducted with a short section of drop pipe and it is likely that air entrainment and head loss were significant at this relatively high flow rate.

As shown in Fig. 6, the recent USSBP test was run for 454 minutes with the drop pipe 10 ft below the top of casing and likely above the water level during the test. Well development was conducted between 111 and 136 minutes into the test but no water could be lifted from the well. There was no improvement in well performance after development. As summarized in Table 10, the ending flow rate of 55 gpm and a ponding head of 21.4 provided an estimated K_b value of 21.2 ft/d. This result is 11% less than the May 2020 USSBP test. Corrected results were not possible since there was no transducer at the top of the screen.

As shown in Fig, 6, the initial portion of the CSSBP test was designed to replicate the USSBP test conducted the previous day. At a flow rate of 55 gpm, the ponding head was 20 ft after 86 minutes, similar to the results for the previous USSBP test.

The CSSBP test ended at 460 minutes with an ending flow rate of 128 gpm and a ponding head of 43.7 ft in the bottom of the screen. The drop pipe was 5 ft below the top of casing and well below the water level. The test results were analyzed using Eq. 11. As summarized in Table 10, these ending values provide an estimated K_b value of 16.9 ft/d, 20% less than the USSBP test conducted the previous day. The likely reason for this difference is that the USSBP test did not account for air entrainment and head losses over the sandpack interval. If the average head in the USSBP test was 3.1 ft higher (similar to previous tests with similar flow rates) the estimated K_b value would be the same for both tests.

Fig. 6 illustrates that the ponding head at the bottom of the screen during the CSSBP test was approximately 8 ft higher than the ground surface. This indicates approximately 8 ft of velocity head in a 2-in. diameter well at a flow rate of 128 gpm.

Fig. 6: USSBP and CSSBP test results for NG-B-204.
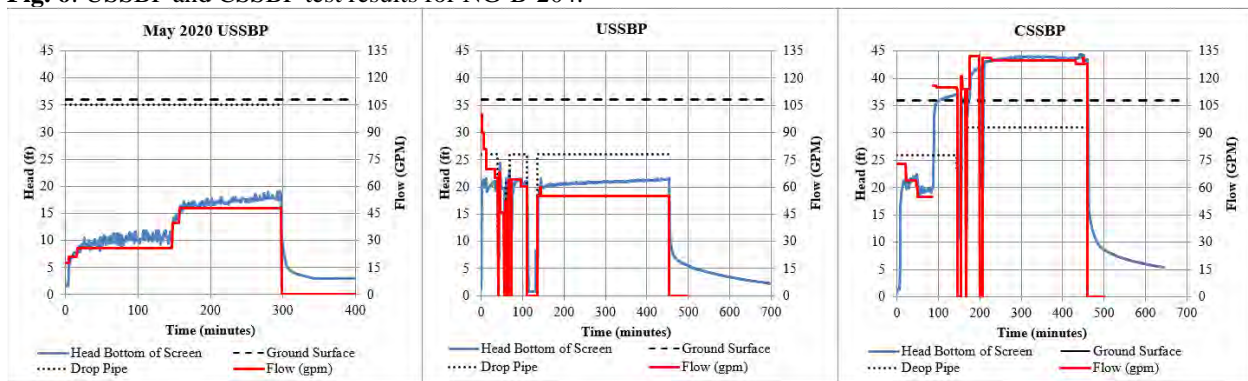
Table 10: Results of USSBP and CSSBP tests in well NG-B-204.

Parameter	Units	Mar. 2020 USSBP Test	Uncorrected[2] USSBP Test	CSSBP Test
Ponding Head (H)	ft	18.3[1]	21.4[1]	43.7
Flow Rate (Q)	gpm	48	55	128
Borehole radius (r_b)	in.	3.0		
Well casing radius (r_c)	in.	1.0		
Saturated Sandpack length (L)	ft	18.3	21.4	22.0
Assumed Sorptive Number for F-M Qva (α^*)	1/ft	1.19		
Soil Classification		SP-SM		
Calculated K_b	**ft/d**	**23.8[1]**	**21.2[1]**	**16.9**

[1] Ponding head does not account for air entrainment. K_b value may be overestimated.
[2] "Uncorrected" means the bottom of well ponding head was used to calculate K_b. "Corrected" means the average ponding head across the screen was used to calculate K_b

3.2.5 *Steady State Test Results for Test Well U-B-102*

Fig. 7 illustrates the USSBP and CSSBP test results for U-B-102. As discussed previously, this well was drilled with a hollow-stem auger drilling rig and there was 3.7 ft of sediment in the bottom of the well casing when we first sounded the well. We were able to remove the sediment and reduce the turbidity of the water after 1.5 hr of well development before the USSBP test.

As shown in Fig. 7, the USSBP test was run for 330 minutes with the drop pipe 0.5 ft below the top of casing. The flow rate was below the range of the flowmeter and the effective range of the valve. Therefore, the water level was maintained near an average head of 21 ft by refilling the well to 22 ft whenever the water level dropped to approximately 20 ft. The flow rate was calculated by dividing the volume of water added over a discrete time period, generally between 10 and 30 minutes. As summarized in Table 11, the ending flow rate of 0.08 gpm and a ponding head of 20.8 provided an estimated K_b value of 0.032 ft/d. This result is at least two orders of magnitude less than we would expect based on the soil texture observed in the boring (trace to slightly silty fine sand). It is likely that the well is clogged. Air entrainment is not expected to occur at these low flow rates.

As shown on Fig. 7, the flow rate during the CSSBP test was above 0.5 gpm and feasible to measure using a flowmeter. The test ended at 390 minutes with an ending flow rate of 0.71 gpm and a ponding head of 47.6 ft in the bottom of the screen. The test results were analyzed using Eq. 11. As summarized in Table 11, these ending values provide an estimated K_b value of 0.80 ft/d, more than twice the USSBP estimate. Furthermore, the flow rate increased from 0.5 gpm to 0.8 gpm during the test with no change in head, suggesting that some development did occur during the test.

Fig. 7: USSBP and CSSBP test results for U-B-102.
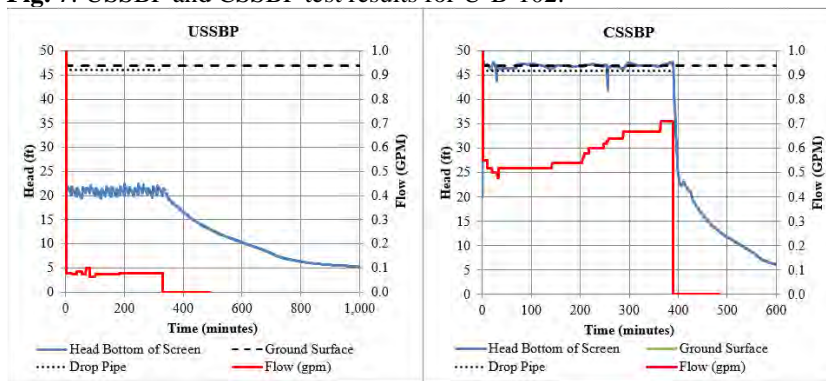
Table 11: Results of USSBP and CSSBP tests in well U-B-102.

Parameter	Units	USSBP Test	CSSBP Test
Ponding Head (H)	ft	20.8	47.6
Flow Rate (Q)	gpm	0.08	0.71
Borehole radius (r_b)	in.	3.0	
Well casing radius (r_c)	in.	1.0	
Saturated Sandpack length (L)	ft	20.8	24
Assumed Sorptive Number for F-M Qva (α^*)	1/ft	1.19	
Soil Classification		SP-SM	
Calculated K_b	**ft/d**	**0.032**	**0.080**

3.2.6 Steady State Test Results for Test Well U-B-118

Fig. 8 illustrates the USSBP and CSSBP test results for U-B-118. The first 130 minutes of the USSBP test was conducted with the drop pipe 5 ft below the top of casing. This resulted in approximately 17 ft of head loss across the sandpack and remained relatively unchanged as the flow rate dropped from 85 gpm to 45 gpm. When the drop pipe was extended to a depth of 17.5 ft below the top of casing (2 ft above the top of screen transducer) the head value for the the top of screen transducer dropped to the bottom of the drop pipe and decreased the head loss across the sandpack to 11.7 ft. This behavior suggests that the drop pipe needs to extend below the bottom of screen head to eliminate the air entrainment head loss.

By the end of the USSBP test, the flow rate had dropped to 40.5 gpm and the bottom of screen ponding head was 22.3 ft. The average head across the screen at the end of the test was 25.8 ft. The test results were analyzed using Eq. 9. As summarized in Table 12, the estimated K_b value using the bottom of screen head (uncorrected) was 14.2 ft/d and the estimated K_b value using the average head across the screen (corrected) was 11.2 ft/d.

For the CSSBP test, the upper transducer was set 5 ft below the ground surface for the first 23 minutes of the test and lowered to 10 ft below the ground surface for the remainder of the test. As shown on Fig. 8, the head loss across the screen decreased as the head in the bottom of screen approached the bottom of the drop pipe and was eliminated when the head was approximately 3 ft above the bottom of the drop pipe. These observations suggest that the drop pipe should extend several feet below the head in the bottom of the screen to eliminate the head loss associated with air entrainment under these conditions (2-in. diameter well, flow rate of 95-100 gpm).

As summarized in Table 12, at the end of the CSSBP test the flow rate was 95 gpm (the maximum flow rate from this hydrant with 10 ft of 1-in. drop pipe) and the ponding head was 43 ft, which provided a K_b value of 11.2 ft/d, the same as the corrected USSBP test.

Fig. 8: USSBP and CSSBP test results for U-B-118.
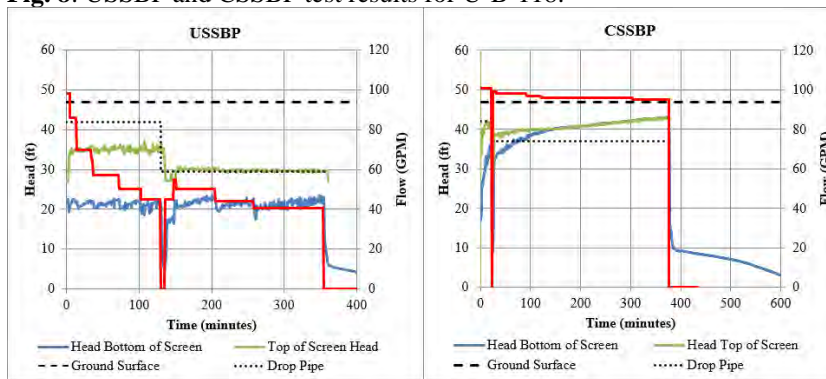
Table 12: Results of USSBP and CSSBP tests in well U-B-118.

Parameter	Units	Uncorrected[2] USSBP Test	Corrected[2] USSBP Test	CSSBP Test
Ponding Head (H)	ft	22.3[1]	25.8	43.0
Flow Rate (Q)	gpm	40.5	40.5	95
Borehole radius (r_b)	in.	3.0		
Well casing radius (r_c)	in.	1.0		
Saturated Sandpack length (L)	ft	22.3	25.5	25.5
Assumed Sorptive Number for F Qva (α^*)	1/ft	0.76		
Soil Classification		SP-SM		
Calculated K_b	**ft/d**	**14.2[1]**	**11.2**	**11.2**

[1] Ponding head does not account for air entrainment. K_b value may be overestimated.
[2] "Uncorrected" means the bottom of well ponding head was used to calculate K_b. "Corrected" means the average ponding head across the screen was used to calculate K_b

3.2.7 Steady State Test Results for Test Well U-TW-6

Fig. 9 illustrates the results for a USSBP test conducted in July 2016 and the recent CSSBP for U-TW-6. The July 2016 USSBP test was conducted for 172 minutes with 27-minute break in the middle to refill the water truck. As summarized in Table 13, the ponding head in the bottom of the screen was 17.4 ft and the flow rate was 80 gpm (the

maximum flow rate out of the water truck), which provided an estimated K_b value of 43.2 ft/d. This test was conducted with a short section of drop pipe and it is likely that air entrainment and head loss were significant at this relatively high flow rate.

As shown in Fig. 9, the USSBP test was run for 389 minutes with the drop pipe 10 ft below the top of casing. The drop pipe was well below the water level and head loss due to air entrainment did not occur. The water level at the top of the well was near the top of casing after 60 minutes and the velocity head ranged from approximately 7 ft at a flow rate of 96 gpm to 2 ft at a flow rate of 48 gpm. As summarized in Table 13, the ending flow rate of 48 gpm and a ponding head of 22.4 provided an estimated K_b value of 14.6 ft/d, 66% less than the July 2016 USSBP test. Potential explanations for this dramatic reduction over five years are provided in later sections.

Fig. 9: USSBP and CSSBP test results for U-TW-6.
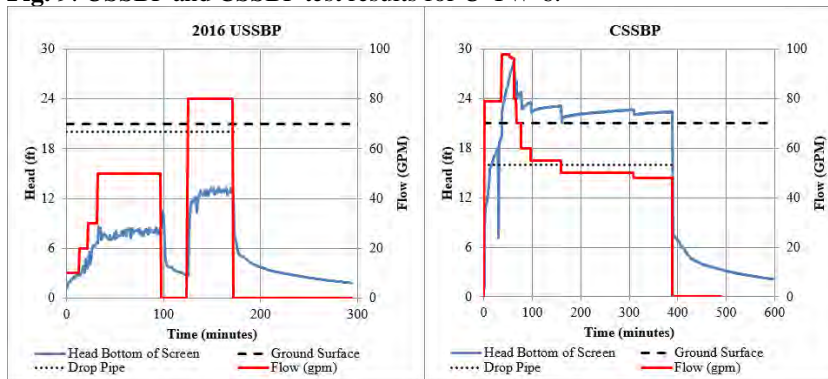
Table 13: Results of USSBP and CSSBP tests in well U-TW-6.

Parameter	Units	July 2016 USSBP Test	CSSBP Test
Ponding Head (H)	ft	12.9[1]	22.4
Flow Rate (Q)	gpm	80	48
Borehole radius (r_b)	in.	3.0	
Well casing radius (r_c)	in.	1.0	
Saturated Sandpack length (L)	ft	12.9	21.4
Assumed Sorptive Number for F-M Qva (α*)	1/ft	1.19	
Soil Classification		SP	
Calculated K_b	**ft/d**	**69[1]**	**14.6**

[1] Ponding head does not account for air entrainment. K_b value may be overestimated.

3.2.8 *Steady State Test Results for Test Well U-TW-9*

Fig. 10 illustrates the results for the USSBP and CSSBP tests for U-TW-9, including a USSBP test conducted in July 2016. The July 2016 USSBP test was conducted for 143 minutes with 39-minute break in the middle to refill the water truck. As summarized in Table 14, the ponding head in the bottom of the screen was 14.6 ft and the flow rate was 80 gpm (the maximum flow rate out of the water truck), which provided an estimated K_b value of 57 ft/d. This test was conducted with a short section of drop pipe and it is likely that air entrainment and head loss were significant at this relatively high flow rate, which means the actual K_b value is significantly lower.

As shown in Fig. 10, the recent USSBP test was run for 354 minutes with the drop pipe 5 ft below the top of casing. The upper transducer was set at a depth of 47.5 ft below the top of casing. The head loss over the screened interval due to air entrainment was approximately 12.5 ft. As summarized in Table 14, the uncorrected analysis using the bottom of screen head value of 24.1 ft and a flow rate of 18.5 gpm provided an estimated K_b value of 5.8 ft/d. The

corrected analysis using the average head value across the screen of 31.8 ft and a flow rate of 18.5 gpm provided an estimated K_b value of 3.7 ft/d.

As shown in Fig. 10, the CSSBP test was run for 368 minutes with the drop pipe 5 ft below the top of casing for the first 98 minutes and 10 ft below the top of casing for the rest of the test. The head loss over the screened interval shrank from approximately 2 ft to approximately zero ft as the head at the bottom of screen approached the bottom of the drop pipe. As summarized in Table 14, the final head value of 62.6 ft and a flow rate of 87 gpm (the maximum flow rate from this hydrant with 10 ft of drop pipe) provided an estimated K_b value of 6.8 ft/d, 85% higher than the corrected USSBP estimate. The reason for the significant differences between the USSBP and CSSBP estimates may be due to less silty and more permeable soils in the upper 4 ft of the sandpack.

Similar to U-TW-6, the recent testing provided estimated K_b value significantly less than the 2016 test (5.8 ft/d versus 57 ft/d for uncorrected test results). Because the flow rate in the 2016 test was so much higher (80 gpm versus 18.5 gpm) the air entrainment and head losses in the 2016 test were likely considerably higher, but these head losses cannot fully account for the dramatic decline in capacity. Even with 12 ft of additional head loss, this would only lower the 2016 estimate of K_b to 33 ft/d. Potential explanations for this dramatic reduction over five years are provided in later sections.

Fig. 10: USSBP and CSSBP test results for U-TW-9.
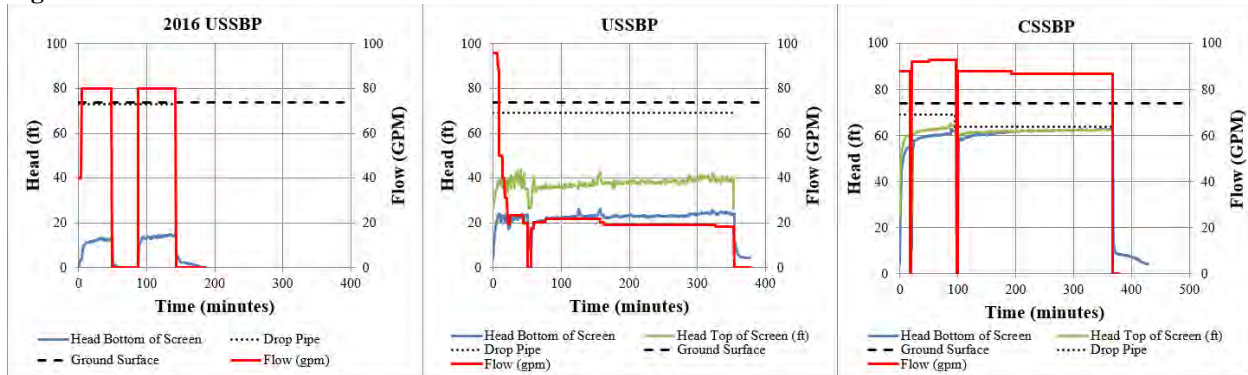
Table 14: Results of USSBP and CSSBP tests in well U-TW-9.

Parameter	Units	July 2016 USSBP Test	Uncorrected[2] USSBP Test	Corrected[2] USSBP Test	CSSBP Test
Ponding Head (H)	ft	20.6[1]	24.1[1]	31.8	62.6
Flow Rate (Q)	gpm	80	18.5	18.5	87
Borehole radius (r_b)	in.	3.0			
Well casing radius (r_c)	in.	1.0			
Saturated Sandpack length (L)	ft	20.6	24.1	26.8	26.8
Assumed Sorptive Number for F-M Qva (α^*)	1/ft	1.19			
Soil Classification		SP			
Calculated K_b	**ft/d**	**57[1]**	**5.8[1]**	**3.7**	**6.8**

[1] Ponding head does not account for air entrainment. K_b value may be overestimated.

[2] "Uncorrected" means the bottom of well ponding head was used to calculate K_b. "Corrected" means the average ponding head across the screen was used to calculate K_b

4 Discussion

4.1 Comparison of Different Methods in Same Test Well

Table 15 summarizes the K_b estimates from all the infiltration tests for each of the eight test wells, including tests that were conducted in previous studies.

FHBP test results are only provided for NG-B-201 and U-B-102. Although FHBP tests were conducted in most of the other wells, the results could not be analyzed because the water level never rose above the top of the sandpack or the fill time was too long. The FHBP test in NG-B-201 is not valid because $K_b \geq 1.6$ ft/d (based on USSBP and CSSBP test results) and the long fill time (80 seconds) saturated the soils around the borehole before the falling head portion of the test began. The FHBP test in U-B-102 was conducted before well development and provided a K_b of 0.024 ft/d, lower than the USSBP K_b estimate of 0.032 ft/d. The FHBP results are suspect because the sandpack is likely clogged with silt and is controlling the flow rate more than the native soils. In addition, the FHBP test results are likely biased low due the non-instantaneous fill time of 18 seconds.

Some of the USSBP and CSSBP tests were subject to air entrainment and head loss across the screen and there was no transducer near the top of the sandpack to estimate the average head value across the screen. Under these conditions, the head value at the bottom of the screen is less than the average value and overestimates the K_b value. These estimates are identified as uncorrected K_b estimates in Table 15.

As discussed in Section 3.2.5, the K_b estimates for U-B-102 are several orders of magnitude lower than expected based on the soil texture. This well was drilled using a hollow-stem auger rig and it is likely that the sandpack is clogged with silt. Furthermore, the rising flow rate during the CSSBP test suggests that some well development did occur during the test.

Valid comparison of USSBP and CSSBP results are not available for NG-B-204 (due to no corrected K_b value for the USSBP test), U-B-102 (due to well development during the CSSBP test) and U-TW-6 (not enough casing above the sandpack to conduct a USSBP test). Based on comparison of corrected K_b estimates for the remaining five wells, the USSBP and CSSBP results were within 15% in three wells (CH-B-102, CH-B-104, U-B-118). The CSSBP results in NG-B-201 and T-TW-9 were significantly higher than the USSBP results (49% and 85% respectively). The reason for these significant increases may be due to the presence of more permeable soils near the top of the sandpack interval.

Table 15: Summary of Infiltration Test Results conducted for this study (2021) and from previous years (2016 and 2020) in the same wells.

Well	Casing Diameter (in.)	Soil Type	K_b Estimates (ft/d)			
			FHBP (2021)	Previous USSBP (year)	USSBP (2021)	CSSBP (2021)
CH-B-102	4	F Qva (SP-SM)			$10.3^1/8.2^2$	9.4
CH-B-104	4	F Qva (SP-SM)			13.9	$15.5^1/14.2^2$
NG-B-201	2	F-M Qva (SM)	0.41^3	4.5^1 (2020)	4.4	6.7
NG-B-204	2	F-M Qva (SP-SM)		23.8^1 (2020)	21.2^1	16.9
U-B-102	2	F-M Qva (SP-SM)	0.024		0.032	0.080
U-B-118	2	F Qva (SP-SM)			$14.2^1/11.2^2$	11.2
U-TW-6	2	F-M Qva (SP)		69^1 (2016)		14.6
U-TW-9	2	F-M Qva (SP-SM)		57^1 (2016)	$5.8^1/3.7^2$	6.8

Notes:

[1] Likely overestimated due to air entrainment. Uncorrected K_b estimate based on head value at bottom of screen.

[2] Subject to air entrainment. Corrected K_b estimate based on average of head values at top and bottom of screen.

[3] FHBP K_b estimate is not valid due to long fill time.

4.2 Challenges with FHBP Tests in Deep Test Wells

The FHBP method assumes instantaneous filling of the well casing before the falling head test begins and slight deviations from this assumption can significantly impact the results. As determined using numerical simulations (Volume III, Table 6), FHBP tests using realistic flow rates to fill the well casing and sandpack tend to underpredict K_b. These simulations suggest that FHBP test results are not valid when $K_b \geq 1.6$ ft/d and for larger test wells (e.g., $L \geq 3.3$ ft, $D_0 \geq 6.6$ ft, $r_b \geq 4$ in.). None of the test facilities included in this scope of work were within these dimensions and only one test well (U-B-102) had $K_b \leq 1.6$ ft/d.

The field FHBP tests in this study confirm the conclusions of the numerical study. The only wells that could be filled above the sandpack using maximum flows from the fire hydrants (approximately 130 gpm) were NG-B-201 and U-B-201. The NG-B-201 test, which had an 80 second fill time, provided an estimated K_b value of 0.41 ft/d that was more than an order of magnitude less than the USSBP test. Although the casing was filled within 18 seconds during the U-B-102 test, the estimated K_b value of 0.024 ft/d is still 25% less than the USSBP test.

One of the challenges of the FHBP method is that filling the casing occurs very quickly and both air entrapment and velocity head can significantly affect the results. Furthermore, as illustrated during the NG-B-201 test, making split-second modifications to the filling plan during these very quick tests is difficult and any errors are difficult to fix. For example, during one attempted FHBP test the transducer reading interval was accidentally left at 1 minute rather than 1 second. The test began and ended with only two readings and interpretation of the results was not feasible.

If the test has issues, immediate retesting is not feasible because the moisture content around the borehole is now much higher than background and the assumption of a uniform moisture content within the test domain is no longer valid. It is necessary to wait hours or days for the moisture content near the borehole to equilibrate before performing another FHBP test. The inability to conduct multiple tests in a short period of time is a significant disadvantage of the FHBP method.

4.3 Well Development

Well development was attempted in three wells (CH-B-102, NG-B-204, and U-B-102). U-B-102 was drilled with a hollow-stem auger drilling rig and had 3.7 ft of sediment in the bottom of the well casing. Significant sediment and

water were removed from U-B-102 during development. However, it does not appear that well development was able to remove enough silt from the sandpack to restore the expected capacity of the test well based on the observed soil texture across the sandpack interval (trace to slightly silty fine sand).

Well development was not able to remove any water from NG-B-204 and U-B-102. Furthermore, well development did not appear to significantly improve well capacity based on the USSBP tests conducted before and after well development.

Based on these results, and confirmed by previous experience, sonic drilling appears to provide a relatively clean test well and sandpack and well development does not appear necessary. In comparison, significant sediment was observed in U-B-102 and is often observed in wells completed using a hollow-stem auger. Well development did not appear to restore the capacity of U-B-102.

4.4 Air Entrainment Effects

This study documented significant head loss across the screened interval in four wells due to air entrainment caused by water falling through air in the casing. The head loss was determined by subtracting the head in the upper transducer (usually near the top of the sandpack) with the transducer in the bottom of the well. It is presumed that air entrainment reduced the effective density of water within the well casing. As illustrated in Table 16, the head loss ranged from 7 to 22.5 ft and the head loss per foot of casing ranged from 0.37 to 0.68. The head loss was significantly less per foot of casing for the 4-in. diameter wells (0.37-0.41) compared with the 2-in. diameter wells (0.63-0.68). The flow rate appears to be a second order factor, with a slightly higher head loss per foot of casing at higher flow rates. Extending the bottom of drop pipe below the head in the bottom of the screen eliminated the head loss across the screen in all cases.

Table 16: Summary of head losses associated with air entrainment as a function of casing diameter and flow rate.

Well	Casing Diameter (in.)	Flow Rate (gpm)	Distance Between Transducers (ft)	Head Loss (ft)	Head Loss/Foot of Casing
CH-B-102	4	53	19	7	0.37
CH-B-104	4	135	55	22.5	0.41
U-B-118	2	45-85	25	17	0.68
U-TW-9	2	20	20	12.5	0.63

4.5 Velocity Head

The goal of the CSSBP tests was to maintain the head in the well at the top of the casing unless the maximum capacity of the fire hydrant was not sufficient to raise the head to that elevation. As hydrogeologists, we are accustomed to assuming that the head in the bottom of the well is the same as the head in the top of the well and we can measure the pressure head in the bottom of the well simply by observing the water level in the top of the well. Early in the testing program it was observed that the head in the bottom of the well was above the top of casing even when the water level at the top of the well was at or below the top of casing. Because the drop pipe extended below the top of casing this excess head was surmised to be due to the pressure exerted by the force of water moving though the casing and it referred to as velocity head. Velocity head only occurs below the bottom of the drop pipe and does not extend above the bottom of the drop pipe.

The water level needed to rise up near the top of casing to observe the velocity head and Table 17 summarizes the velocity head when it was observed. The exit velocity is calculated by dividing the flow rate by the cross-sectional area of the well casing and represents the water velocity when it exits the drop pipe and expands to fill the well casing. The velocity decreases as it enters the screened interval and begins to exit the well.

As shown in Table 17, the velocity head was 7-8 ft when the exit velocity was greater than 9.8 ft/s. When the exit velocity was between 4.9 and 8.0 ft/s the velocity head ranged from 1-2 ft. Below an exit velocity of 2 ft/second the velocity head was zero. For a given flow rate, the velocity head decreases as the casing diameter increases. For this reason, velocity head can be significant in 2-in. diameter wells but insignificant in larger wells.

As illustrated by the CSSBP tests shown in Figs. 3, 8, and10, once the bottom of the drop pipe was below the head in the bottom of the well the velocity head did not change over the sandpack interval. This means that velocity head does not affect the validity and accuracy of the test as long as the drop pipe is below the head in the bottom of the well and above the screened interval.

Table 17: Summary of velocity head as a function of casing diameter, flow rate, and the exit velocity at the bottom of drop pipe. The exit velocity is the flow rate divided by the cross-sectional area of the well casing.

Well	Casing Diameter (in.)	Flow Rate (gpm)	Exit Velocity (ft/s)	Velocity Head (ft)
CH-B-102	4	79	2.0	0
NG-B-201	2	78	8.0	1
NG-B-204	2	128	13.1	8
U-B-102 (CSSBP)	2	0.71	0.07	0
U-B-102 (FHBP)	2	130	13.3	7
U-TW-6	2	96	9.8	7
U-TW-6	2	48	4.9	2

4.6 Well Capacity Following Back-to-Back Runoff Events

Infiltration capacity can be affected by the background moisture content in the soils and for fine-grained soils the infiltration capacity can be significantly less at higher moisture content (Volume I). Volume I conducted numerical simulations of back-to-back runoff events in a deep borehole that lasted for 6 hr with a 24-hr recovery period between tests. These simulations predicted that infiltration capacity for fine-grained soils (classified as SM) would be reduced by 5-9%. Less than 2% reduction was predicted for coarser-grained soils (including SM-SP, SP, SW, and GW).

One of the questions explored by this study was to determine if field experiments would confirm these numerical simulation results. This was addressed by running the CSSBP tests the day after the USSBP test were conducted for the majority of the wells (CH-B-104 and U-TW-6 were the exceptions). As summarized in Table 15, the estimated K_b on the second day of testing was the same or greater than the K_b on the first day of testing (when comparing estimates based on the average head across the screened interval). NB-B-201 was the only well with soils classified as predominately SM. All the remaining wells included in this comparison were dominated by soils classified as predominately SP-SM.

In some cases, shorter USSBP tests were conducted at the beginning of the second day to eliminate the differences between the USSBP and CSSBP tests. This was conducted in CH-B-102 (Fig. 3) and NG-B-204 (Fig. 6). For CH-B-102, the estimated K_b was 10.3 on the first day and 11.6 ft/d on the second day (uncorrected values). For NG-B-204, the estimated K_b was 21.2 on the first day and 24.3 ft/d on the second day (uncorrected values). The estimated K_b was higher than on the second day than the first day in both cases, most likely due to the shorter duration of the USSBP tests on the second day.

Comparison of second day results with first day results indicated that well capacity is not significantly reduced the day after a significant runoff event for the soil types included in this study (predominately SP-SM). These results are consistent with the numerical modeling results in Volume I.

4.7 Time to Achieve Steady-State Conditions

Volume I included numerical simulations to compare results after 6 hrs with results after 24 hrs to determine if steady state conditions had been achieved at the end of a 6-hr test. The ratio of flow capacity after 6 hr (Q_6) divided by flow capacity after 24 hr (Q_{24}) in a deep borehole (head between 13 and 33 ft) ranged from 1.13 for silty Qva to 1.0 for fine-medium Qva and was generally higher for soils with more silt.

Most of the infiltration tests conducted for this study appeared to be at or very close to steady state at the end of the test. The combined decrease in flow rate and/or rise in head was generally less than 2% in the last 30-60 minutes of both the USSBP and CSSBP tests in CH-B-102, Ch-B-104, NG-B-201, NG-B-204, U-TW-6, and U-TW-9. The head rose about 6% during the last hour of the USSBP test in U-B-118 but rose less than 2% during the last hour of the CSSBP test in the same well. The capacity of U-B-102 actually rose during the two tests, likely due to well development during the tests.

4.8 Loss of Well Capacity over Time

Table 15 summarizes the results for the four wells tested in previous studies. All four wells saw a decrease in the K_b estimate from the previous test to the most recent test, ranging from 2% less in NG-B-201, 11% less in NG-B-204, and more than 60% less in U-TW-6 and U-TW-9. The reason for this decrease over time is uncertain. Test data for several dry wells installed in California actually showed an increase in capacity over 8-9 years (email from Bill De Jong, Torrent Resources). It seems unlikely that biofouling would be clogging the well since there has not been any water injected into the well since it was first tested. There is speculation that perched water may form on silt layers during the wet season and are draining into the test wells, transporting silt from the formation into the sandpack in the process.

4.9 4-in. Well Casing Versus 2-in. Well Casing

Two of the wells (CH-B-102 and CH-B-104) were constructed with 4-in. diameter well casing and the remaining wells were constructed with 2-in. diameter well casing. Although 2-in. well casing is less expensive to install, the 4-in. well casing has significant advantages, including: 1) the ability to use 2-in. diameter drop pipe rather than 1-in. drop pipe, facilitating significantly higher flow rates, and 2) there is not enough space in a 2-in. diameter well casing with a 1-in. drop pipe to run transducers and water level tapes up and down the well without removing the drop pipe.

5   Conclusions

Infiltration testing was conducted in eight test wells to evaluate three different infiltration test methods, including the uncased steady-state borehole permeameter (USSBP), the cased steady-state borehole permeameter (CSSBP) and the cased falling-head borehole permeameter (FHBP). The wells were completed in boreholes that ranged from 6 to 8 in. in diameter and ranged in depth from 21 to 87 ft with either 15 ft or 20 ft of screen and a sandpack interval that covered a slightly longer interval. The wells were all screened across glacially over-consolidated sandy deposits and were evaluated as advance outwash (Qva). Seven of the wells were drilled using a sonic drilling rig and one well was drilled using a hollow-stem auger drilling rig.

Well development was attempted in three wells using a surge block and a hand-actuated pump while adding water at the top of the well casing. Although we were able to surge the well screens we were not able to pump any water from the wells installed using the sonic drilling rig and it did not appear to significantly improve the infiltration capacity of any of the test wells. Well development was successful in removing 3.7 ft of sediment from the well drilled using the hollow-stem auger rig. However, the K_b estimates from the tests in the hollow-stem auger well after development were at least two orders of magnitude less than expected based on the soil texture (trace to slightly silty fine sand) and the results are not considered valid due to clogging of the sandpack. We have observed clogging issues with other test wells constructed using hollow-stem auger drilling methods. In addition, STP sampling used during hollow-step auger drilling is often infeasible in dense gravelly soils and sample recovery is often limited to a less than a foot for every five feet of drilling. In contrast, sonic drilling generally provides continuous core and better stratigraphic detail, important when a thin layer of silt can result in perched groundwater. For these reasons, we recommend drilling test wells using sonic methods.

FHBP tests were not feasible in seven of the wells because the hydraulic conductivity exceeded 1.6 ft/d (0.5 m/d) and the test facilities were relatively large (see conclusions in Volume I). The seven sonic wells had K_b values between 3.7 and 16.9 ft/d based on both USSBP and CSSBP results. In general, the CSSBP estimates of K_b were the same or higher (up to 84% higher) than the USSBP K_b estimates. The higher values are likely due to more permeable sediments higher in the sandpack interval. This explanation will be evaluated with numerical modeling simulations in a later study.

Most of the wells were close to steady state at the end of the tests, and the combined decrease in flow rate and/or rise in head was generally less than 2% in the last 30-60 minutes of both the USSBP and CSSBP tests. However, numerical simulations of tests in similar soils (see Volume I) predicted that the wells would be closer to steady state after 6 hr of testing. The difference between numerical simulations and actual test results is likely due to perching on low-permeability layers and perhaps groundwater mounding.

Four of the wells had been previously tested. All four wells saw a decrease in the K_b estimate from the previous test to the most recent test, ranging from 2% less in NG-B-201, 11% less in NG-B-204, and more than 60% less in U-TW-6 and U-TW-9. These wells had not received any runoff in between the tests and the reasons why the wells had decreased capacity is unknown.

This study documented significant head loss across the screened interval in four wells due to air entrainment caused by water falling through air in the casing. The head loss across the screen interval ranged from 7 to 22.5 ft and the head loss per foot of casing ranged from 0.37 to 0.68. The head loss was significantly less per foot of casing for the 4-in. diameter wells (0.37-0.41) compared with the 2-in. diameter wells (0.63-0.68). Extending the bottom of drop pipe below the head in the bottom of the screen eliminated the head loss across the screen in all cases.

This study also documented that the water level above the bottom of the drop pipe (used to convey water deeper in the well) was often much lower than the head elevation below the bottom of the drop pipe. This difference in head was surmised to be due to the pressure exerted by the force of water moving though the casing and it referred to as velocity head. Velocity head only occurs below the bottom of the drop pipe and does not extend above the bottom of the drop pipe. The amount of velocity head appears to be related to the water velocity when it exits the drop pipe and

expands to fill the well casing. The velocity head was 7-8 ft when the exit velocity was greater than 9.8 ft/s (96 gpm in a 2-in. diameter casing). When the exit velocity was between 4.9 and 8.0 ft/s (48 to 78 gpm in a 2-in. diameter casing) the velocity head ranged from 1-2 ft. Below an exit velocity of 2 ft/s (20 gpm in a 2-in. diameter casing) the velocity head was zero. For a given flow rate, the velocity head decreases as the casing diameter increases. For this reason, velocity head can be significant in 2-in. diameter wells but insignificant in larger wells.

This study also demonstrated that once the bottom of the drop pipe was below the head in the bottom of the well the velocity head did not change over the sandpack interval. This means that velocity head does not affect the validity and accuracy of the test as long as the drop pipe is below the head in the bottom of the well and above the screened interval.

Most of the wells were tested on two consecutive days to assess the potential that higher moisture content could reduce the infiltration capacity of infiltration wells. This was not observed during this study. In general, the second day of testing provided K_b estimates that were the same or higher than the K_b estimates from the first day of testing. Since USSBP tests were conducted during the first day and CSSBP tests were conducted the second day, the higher K_b results may reflect more permeable soils in the upper portion of the sandpack interval.

Wells with both 4-in. and 2-in. diameter well casing were tested in this study. Although slightly more expensive to install, the 4-in. diameter well casing facilitates higher flow rates and provides easier access for transducers and water level tapes.

6 References

Kindred JS, Reynolds WD (2020) Using the borehole permeameter to estimate saturated hydraulic conductivity for glacially over-consolidated soils, Hydrogeology Journal 28:1909–1924, DOI:10.1007/s10040-020-02149-3

Reynolds, WD (2011). Measuring soil hydraulic properties using a cased borehole permeameter: falling-head analysis. Vadose Zone Journal. 10: 999-1015.

WSDOE (Washington State Department of Ecology) (2019) Stormwater Management Manual for Western Washington, July 2019, Publication Number 19-10-021

Appendix A: Well Logs

SOIL DESCRIPTION

Surface Elevation: NAVD88

Depth, ft	Symbol	USCS	Samples	Blows/6"	Recovery, %	Lab tests	Ground Water

FILL

Brown, SILTY fine SAND, few coarse sand and gravel; moist. — SM

ADVANCE OUTWASH

Medium dense, yellow brown, SILTY fine SAND, trace medium sand; moist; occasional rootlets (weathered Qva). — SM

Medium dense, gray, fine to medium SAND WITH GRAVEL, few coarse sand; dry to moist. — SP / SP-SM

Very dense, gray, fine to medium SAND WITH SILT, trace coarse sand and gravel; moist; interbedded seams and layers (1/8" to 1 1/2" thick) of light brown silty fine sand.

Becomes dense, no interbedded silty fine sand, 1 inch layer of silt at 15.8 feet.

Gray, SILT; moist; occasional yellow brown laminations, scattered dilatant layers. — ML

Very dense, gray, fine SAND WITH SILT, few medium sand; moist; scattered pockets of silty fine sand. — SP-SM

No pockets of silty fine sand.

Sample	Blows/6"	Recovery, %
S-1	10,12,13	100
S-2	25,28,50/6	100
S-3	20,23,26	100
S-4		100
S-5	28,26,42	100
S-6		100
S-7		100
S-8		100

(Continued)

Penetration Resistance

▲ Blows per foot (SPT)
▼ Blows per foot (non-standard)

PL   Water Content %   LL

Penetration values plotted: 5 ft ~35; 10 ft 50/6; 15 ft ~48; 20 ft 68

Date Completed: 8/25/2021
Driller: Cascade Drilling
Equipment: DB320 Track Sonic
Drilling Method: 8-in OD casing, 7-in OD core barrel.
Hammer System: Automatic

Approximate Location: 50.5 feet west of sewer MH at intersection of 17th Ave NW and NW 89th Street. 6.5 feet S of NW 89th Street.

Crown Hill NDS
Seattle, WA

Seattle Public Utilities
Geotechnical Engineering

C600443

LOG OF BORING CH-B-102

FIGURE A-3

LOG OF BORING (2/1/11) CROWN HILL NDS.GPJ DATA_TEMPLATE_(7-21-11).GDT 8/30/21

SOIL DESCRIPTION

Surface Elevation: NAVD88

Depth, ft	USCS	Samples	Recovery, %	Soil Description

Trace medium sand, scattered pockets of silty fine sand.

Trace coarse gravel, numerous pockets of silt and silty fine sand.

PRE-FRASER NON-GLACIAL DEPOSITS

Gray, SILTY fine SAND, trace fine gravel; moist; scattered dark brown organic matter, occasional mica flecks.

Gray, fine SAND WITH SILT, trace medium sand and gravel, scattered pockets of silt and silty fine sand.

Gray, SILTY fine SAND, trace fine gravel; moist; scattered dark brown organic matter, few mica flecks.

Brown, fine to medium SAND WITH SILT, trace gravel; moist.
56.5 to 56.8 feet bgs: Few gravel.

59 to 60 feet bgs: Scattered organic matter and gray clay (CH), scattered pockets and layers of dark brown to orange brown, wet, silty sand.
Numerous pockets of brown and gray, silty fine sand.

No gravel, scattered pockets of silty fine sand.

(Continued)

Depth markers / Samples:
- S-9 at ~40 ft, Recovery 100
- S-10 at ~45 ft, Recovery 100
- SM at ~46 ft
- SP-SM
- S-11, SM, Recovery 100
- SP-SM at ~55 ft
- S-12 at ~60 ft, Recovery 100
- S-13 at ~70 ft, Recovery 100

Penetration Resistance
▲ Blows per foot (SPT)
▼ Blows per foot (non-standard)
PL Water Content % LL
0 10 20 30 40 50 60

Date Completed: 8/25/2021
Driller: Cascade Drilling
Equipment: DB320 Track Sonic
Drilling Method: 8-in OD casing, 7-in OD core barrel.
Hammer System: Automatic

Approximate Location: 50.5 feet west of sewer MH at intersection of 17th Ave NW and NW 89th Street. 6.5 feet S of NW 89th Street.

Crown Hill NDS
Seattle, WA

Seattle Public Utilities
Geotechnical Engineering

LOG OF BORING CH-B-102

C600443

FIGURE A-3

Logged by: AJC   Reviewed by: Sheet 2 of 3

LOG OF BORING (2/1/11) CROWN HILL NDS.GPJ DATA_TEMPLATE_(7-21-11).GDT 8/30/21

SOIL DESCRIPTION

Surface Elevation: NAVD88

Occasional pockets of silty fine sand.

Trace medium sand.

Occasional pockets of dark gray, silty fine sand.

Boring completed at 85 feet below ground surface (bgs).
Groundwater not encountered at time of drilling. 4-inch
piezometer installed and screened between 19 and 39 feet
bgs. Well tag No. BNW-136.

Depth, ft	Symbol	USCS	Samples	Blows/6"	Recovery, %	Lab tests	Ground Water	Depth, ft
70								70
75			S-14		100			75
80								80
85			S-15		100			85
90								90
95								95
100								100
105								105

Penetration Resistance

▲ Blows per foot (SPT)
▼ Blows per foot (non-standard)

PL   Water Content %   LL

0   10   20   30   40   50   60

DRAFT

Date Completed: 8/25/2021
Driller: Cascade Drilling
Equipment: DB320 Track Sonic
Drilling Method: 8-in OD casing, 7-in OD core barrel.
Hammer System: Automatic

Approximate Location: 50.5 feet west of sewer MH at intersection of 17th
Ave NW and NW 89th Street. 6.5 feet S of NW 89th Street.

Crown Hill NDS
Seattle, WA

**Seattle Public Utilities
Geotechnical Engineering**

LOG OF BORING CH-B-102

C600443

FIGURE A-3

Logged by: AJC   Reviewed by: Sheet 3 of 3

LOG OF BORING (2/1/11) CROWN HILL NDS.GPJ DATA_TEMPLATE_(7-21-11).GDT 8/30/21

SOIL DESCRIPTION

Surface Elevation: NAVD88

Depth, ft	Symbol	USCS	Samples	Blows/6"	Recovery, %	Lab tests	PID (ppm)	Ground Water

Surface is asphalt over crushed rock.

FILL
Loose, yellow brown, SILTY fine to medium SAND, few gravel, trace coarse sand; moist; occasional black organic matter, rust mottled.

Increase silt, trace gravel, no organics or rust staining.

ADVANCE OUTWASH
Brown, SILTY fine to medium SAND, trace coarse sand and gravel; moist.
Becomes very dense, gray, decrease silt, scattered pockets of fine to medium sand with silt, moist to wet.

Dense, gray, fine to medium SAND WITH SILT, trace coarse sand and gravel, trace cobbles; moist.

Becomes very dense, occasional pockets fine to medium sand.

Increase silt, few gravel between 25 and 27 feet, scattered wet pockets.

No wet pockets, no pockets of fine to medium sand, trace gravel.

Decrease silt, increase medium to coarse sand.

(Continued)

USCS	Sample	Blows/6"	Recovery, %	PID (ppm)
SM				
SM	S-1	2,2,3	80	0
SM	S-2	19,23,27	87	0
SP-SM	S-3	14,20,26	100	0
	S-4	26,29,34	100	0
	S-5		100	
	S-6		100	
	S-7		100	

Penetration Resistance
▲ Blows per foot (SPT)
▼ Blows per foot (non-standard)
PL Water Content % LL
0 10 20 30 40 50 60

63

Date Completed: 8/24/2021
Driller: Cascade Drilling
Equipment: DB320 Track Sonic
Drilling Method: 8-in OD casing, 7-in OD core barrel.
Hammer System: Automatic

Approximate Location: In front of 5506 17th Ave NW. 5 feet W of sidewalk and 15 feet S of storm drain MH.

**Crown Hill NDS
Seattle, WA**

**Seattle Public Utilities
Geotechnical Engineering**

C600443

LOG OF BORING CH-B-104

FIGURE A-5

LOG OF BORING (2/1/11) CROWN HILL NDS.GPJ DATA_TEMPLATE_(7-21-11).GDT 8/30/21

SOIL DESCRIPTION

Surface Elevation: NAVD88

Depth, ft	Symbol	USCS	Samples	Blows/6"	Recovery, %	Lab tests	PID (ppm)	Ground Water

Penetration Resistance
▲ Blows per foot (SPT)
▼ Blows per foot (non-standard)
PL — Water Content % — LL
0 10 20 30 40 50 60

Increase silt, scattered pockets of silty fine to medium sand; moist to wet.

Decrease silt, moist. — S-8 — 100

Few coarse sand. — S-9 — 100

Gray, SILTY fine SAND, trace medium coarse sand; moist. — SM

Gray, fine to medium SAND WITH SILT, trace coarse sand and gravel; moist. — SP-SM
No coarse sand and gravel, scattered pockets silty fine sand. — S-10 — 100

Trace coarse sand. — S-11 — 100

Few coarse sand, trace gravel; numerous pockets of silty fine sand. — S-12 — 100

PRE-FRASER NON-GLACIAL DEPOSITS — SM
Brown mottled dark brown, SILTY fine to medium SAND; wet; scattered pockets of black organic matter, numerous mica flecks. — S-13 — 100 ; S-14 — 100 — ML — SP-SM — S-15 — 100

Gray, SILT; moist; numerous rust stain seams.

Brown, fine SAND WITH SILT; moist.

(Continued)

Date Completed: 8/24/2021
Driller: Cascade Drilling
Equipment: DB320 Track Sonic
Drilling Method: 8-in OD casing, 7-in OD core barrel.
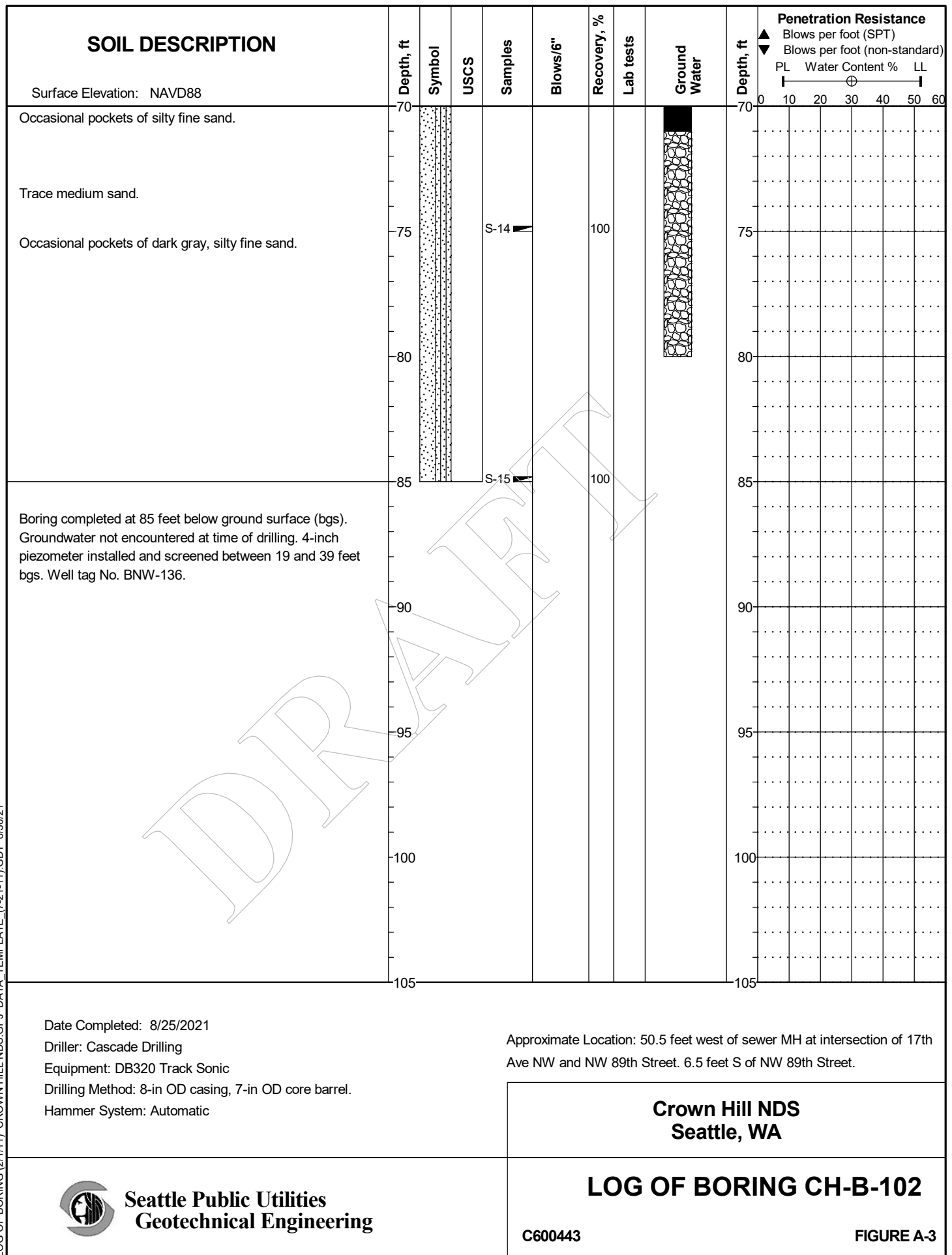Hammer System: Automatic

Approximate Location: In front of 5506 17th Ave NW. 5 feet W of sidewalk and 15 feet S of storm drain MH.

Crown Hill NDS
Seattle, WA
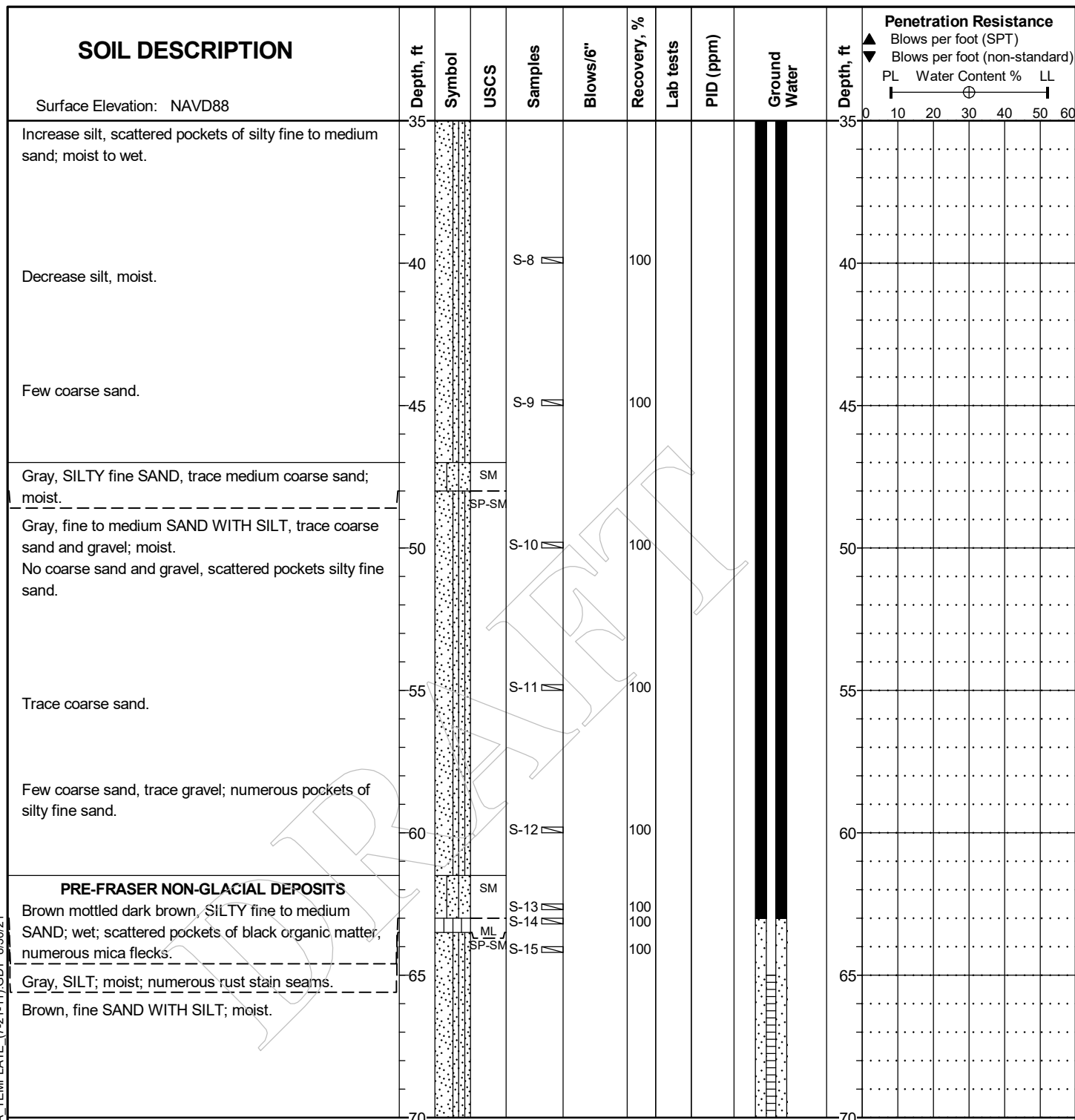
Seattle Public Utilities
Geotechnical Engineering

LOG OF BORING CH-B-104

C600443

FIGURE A-5

LOG OF BORING (2/1/11) CROWN HILL NDS.GPJ DATA_TEMPLATE_(7-21-11).GDT 8/30/21

SOIL DESCRIPTION

Surface Elevation: NAVD88

Depth, ft	Symbol	USCS	Samples	Blows/6"	Recovery, %	Lab tests	PID (ppm)	Ground Water
75			S-16		100			
85		SP	S-17		100			
			S-18		100			
90		SM						
95		SP-SM	S-19		100			ATD
100			S-20		100			

Brown, fine to medium SAND, trace silt; moist to wet.

Brown, SILTY fine SAND; moist to wet; scattered organic matter, numerous mica flecks.

Brown, fine to medium SAND WITH SILT, few coarse sand, trace gravel; wet.

(Continued)

Penetration Resistance

▲ Blows per foot (SPT)
▼ Blows per foot (non-standard)

PL ⊕ Water Content % LL

0 10 20 30 40 50 60

Depth, ft: 70, 75, 80, 85, 90, 95, 100, 105

Date Completed: 8/24/2021
Driller: Cascade Drilling
Equipment: DB320 Track Sonic
Drilling Method: 8-in OD casing, 7-in OD core barrel.
Hammer System: Automatic

Approximate Location: In front of 5506 17th Ave NW. 5 feet W of sidewalk and 15 feet S of storm drain MH.
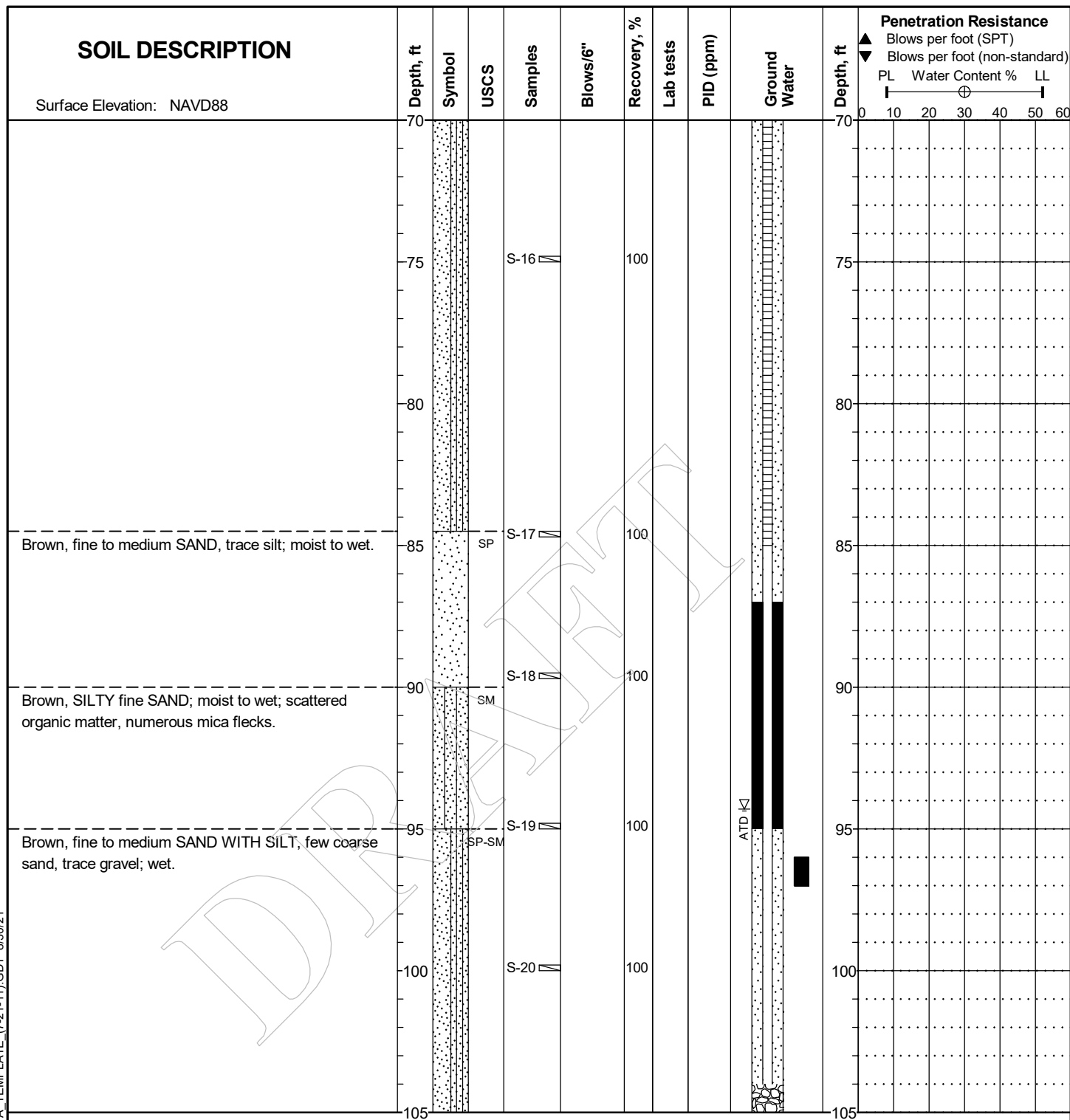
Crown Hill NDS
Seattle, WA

Seattle Public Utilities
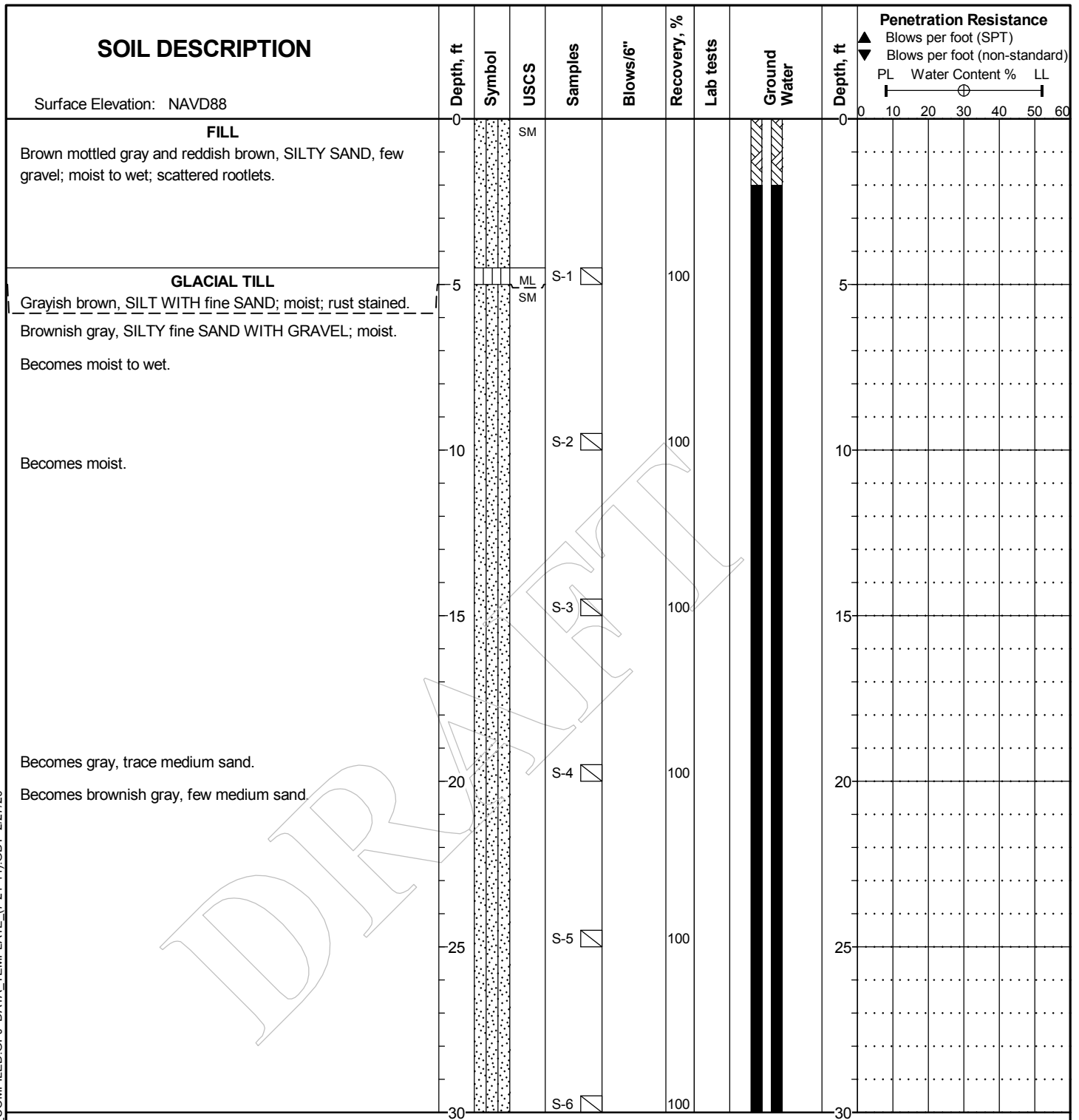**Geotechnical Engineering**

LOG OF BORING CH-B-104

C600443

FIGURE A-5

Logged by: AJC   Reviewed by: Sheet 3 of 4

LOG OF BORING (2/1/11) CROWN HILL NDS.GPJ DATA_TEMPLATE_(7-21-11).GDT 8/30/21

SOIL DESCRIPTION

Surface Elevation: NAVD88

Depth, ft	Symbol	USCS	Samples	Blows/6"	Recovery, %	Lab tests	PID (ppm)	Ground Water
110			S-21		100			

Boring completed at 110 feet below ground surface (bgs). Groundwater encountered at 94.3 feet bgs at time of drilling. 4-inch piezometer installed and screened between 65 and 85 feet bgs. Vibrating wire pressure transducer installed at 97 feet bgs. Well tag No. BNW-134.

Penetration Resistance
▲ Blows per foot (SPT)
▼ Blows per foot (non-standard)

PL   Water Content %   LL
0 10 20 30 40 50 60

Depth, ft: 105, 110, 115, 120, 125, 130, 135, 140

Date Completed: 8/24/2021
Driller: Cascade Drilling
Equipment: DB320 Track Sonic
Drilling Method: 8-in OD casing, 7-in OD core barrel.
Hammer System: Automatic

Approximate Location: In front of 5506 17th Ave NW. 5 feet W of sidewalk and 15 feet S of storm drain MH.

**Crown Hill NDS
Seattle, WA**

**Seattle Public Utilities
Geotechnical Engineering**

LOG OF BORING CH-B-104

C600443

FIGURE A-5

LOG OF BORING (2/1/11) CROWN HILL NDS.GPJ DATA_TEMPLATE_(7-21-11).GDT 8/30/21

DRAFT

SOIL DESCRIPTION

Surface Elevation: NAVD88

FILL
Brown mottled gray and reddish brown, SILTY SAND, few gravel; moist to wet; scattered rootlets.

GLACIAL TILL
Grayish brown, SILT WITH fine SAND; moist; rust stained.

Brownish gray, SILTY fine SAND WITH GRAVEL; moist.

Becomes moist to wet.

Becomes moist.

Becomes gray, trace medium sand.

Becomes brownish gray, few medium sand.

(Continued)

Depth, ft	USCS	Samples	Recovery, %
0	SM		
5	ML / SM	S-1	100
10		S-2	100
15		S-3	100
20		S-4	100
25		S-5	100
30		S-6	100

Penetration Resistance
▲ Blows per foot (SPT)
▼ Blows per foot (non-standard)
PL   Water Content %   LL

Date Completed: 2/18/2020
Driller: Cascade Drilling
Equipment: TSI 150CC
Drilling Method: 6-in OD casing, 4-in core barrel, Sonic
Hammer System: N/A

Approximate Location: 12 feet S of curb, 21 feet W of tree.

**Thornton Natural Drainage Systems
Seattle, WA**

**Seattle Public Utilities
Geotechnical Engineering**

LOG OF BORING NG-B-201

C316083

FIGURE A-1

Logged by: AJC   Reviewed by: Sheet 1 of 4

LOG OF BORING (2/1/11) THORNTON_NDS_C316083_COMPILED.GPJ DATA_TEMPLATE_(7-21-11).GDT 2/27/20

SOIL DESCRIPTION

Surface Elevation: NAVD88

Depth, ft	Symbol	USCS	Samples	Blows/6"	Recovery, %	Lab tests	Ground Water
35			S-7		100		
ADVANCE OUTWASH Brown, SILTY fine to medium SAND, trace fine gravel; moist to wet.		SM	S-8 (40)		100		
Brown, fine to medium SAND WITH SILT, trace fine gravel; moist.		SP-SM					
Brown, SILTY fine to medium SAND WITH GRAVEL; moist to wet.		SM					
Becomes moist.			S-9 (45)		100		
Brown, fine to medium SAND WITH SILT, trace fine gravel; moist.		SP-SM					
Brown, SILTY fine to medium SAND WITH GRAVEL, trace coarse sand; moist.		SM	S-10 (50)		100		
Brown, SILTY fine to medium SAND, trace gravel; moist; numerous cemented fragments.		SM					
			S-11 (55)		100		
			S-12 (60)		100		

(Continued)

Penetration Resistance
▲ Blows per foot (SPT)
▼ Blows per foot (non-standard)
PL ⊕——— Water Content % ———LL
0 10 20 30 40 50 60

Date Completed: 2/18/2020
Driller: Cascade Drilling
Equipment: TSI 150CC
Drilling Method: 6-in OD casing, 4-in core barrel, Sonic
Hammer System: N/A

Approximate Location: 12 feet S of curb, 21 feet W of tree.
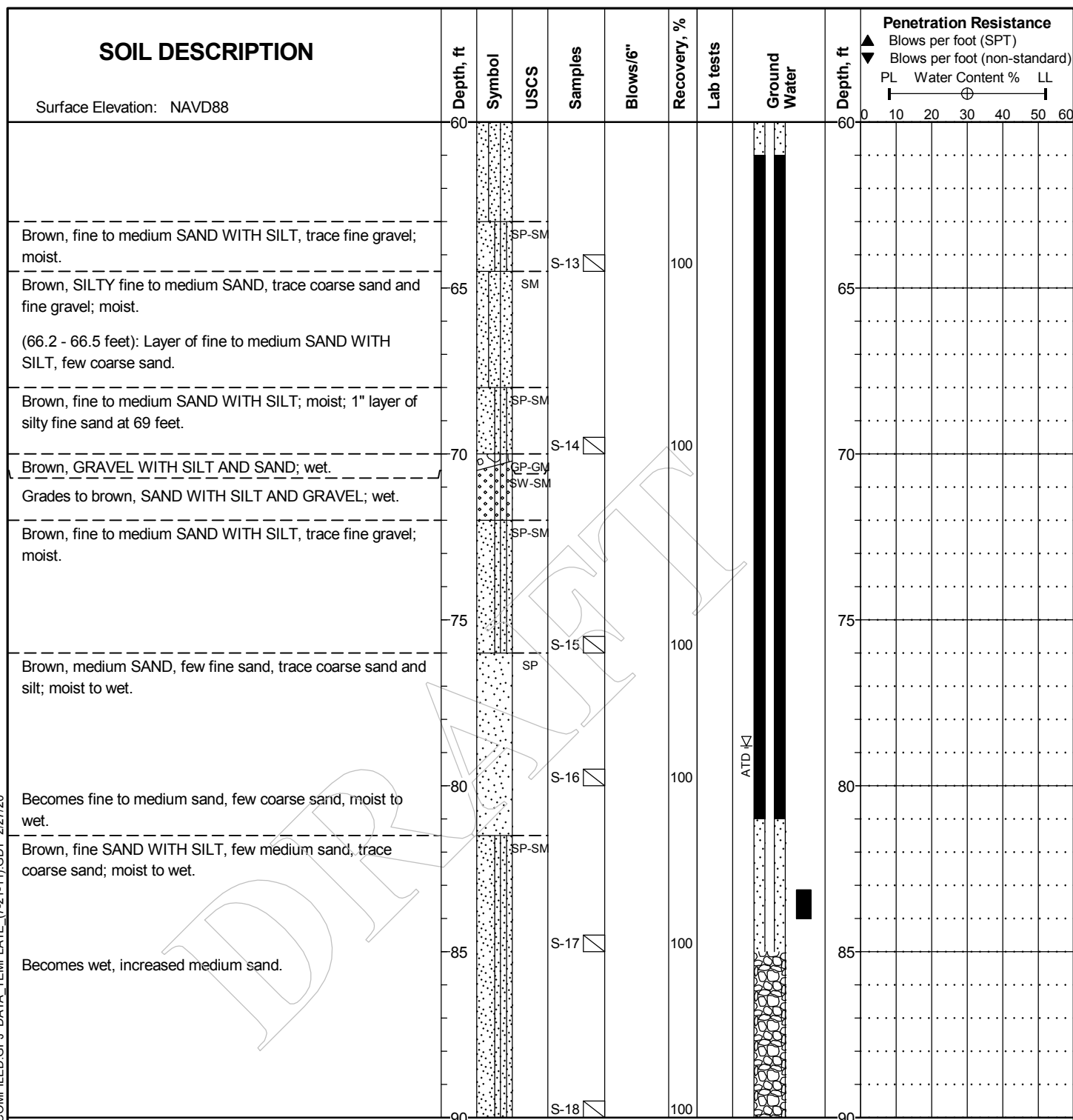
**Thornton Natural Drainage Systems
Seattle, WA**

**Seattle Public Utilities
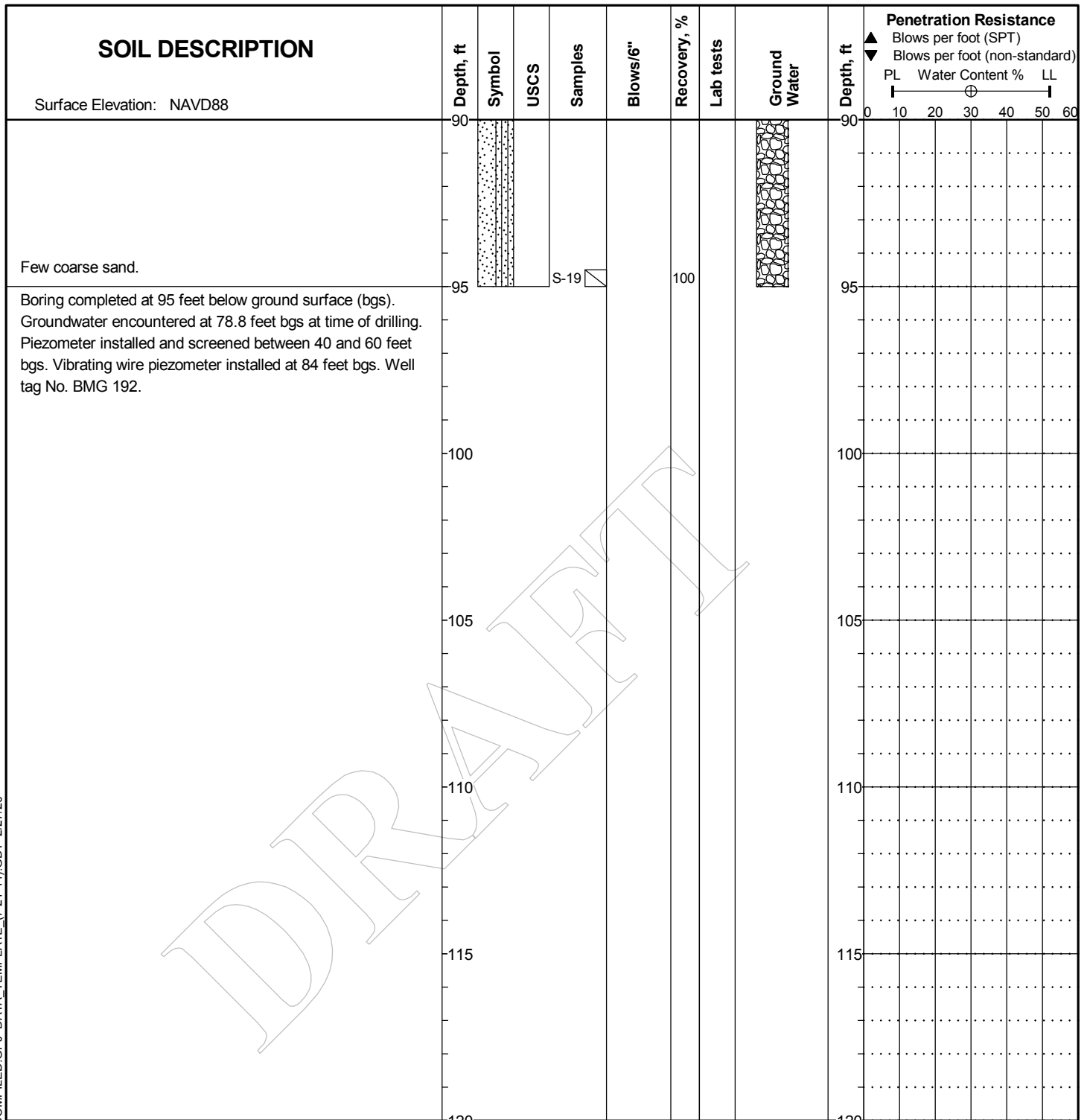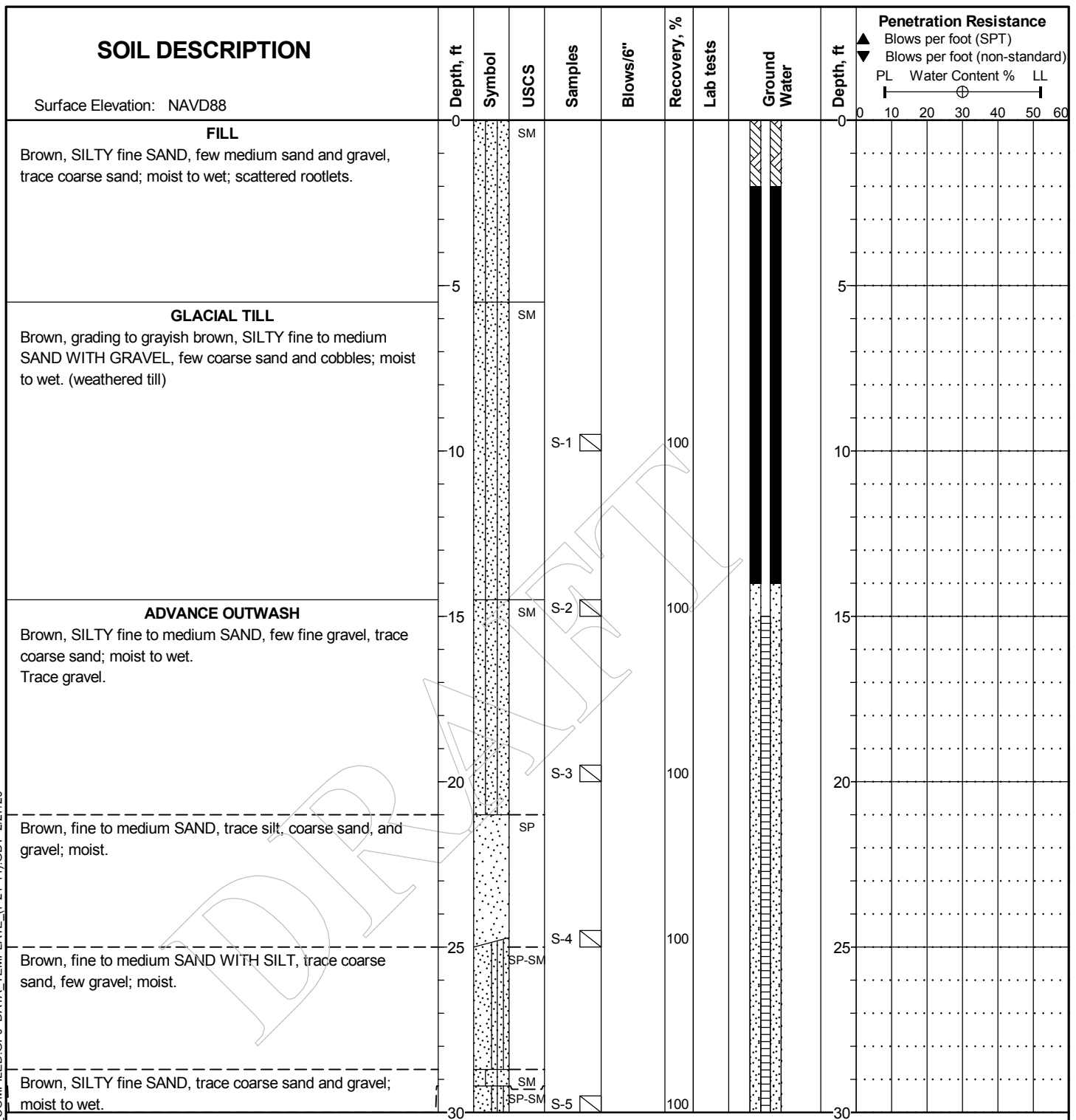Geotechnical Engineering**

LOG OF BORING NG-B-201

C316083
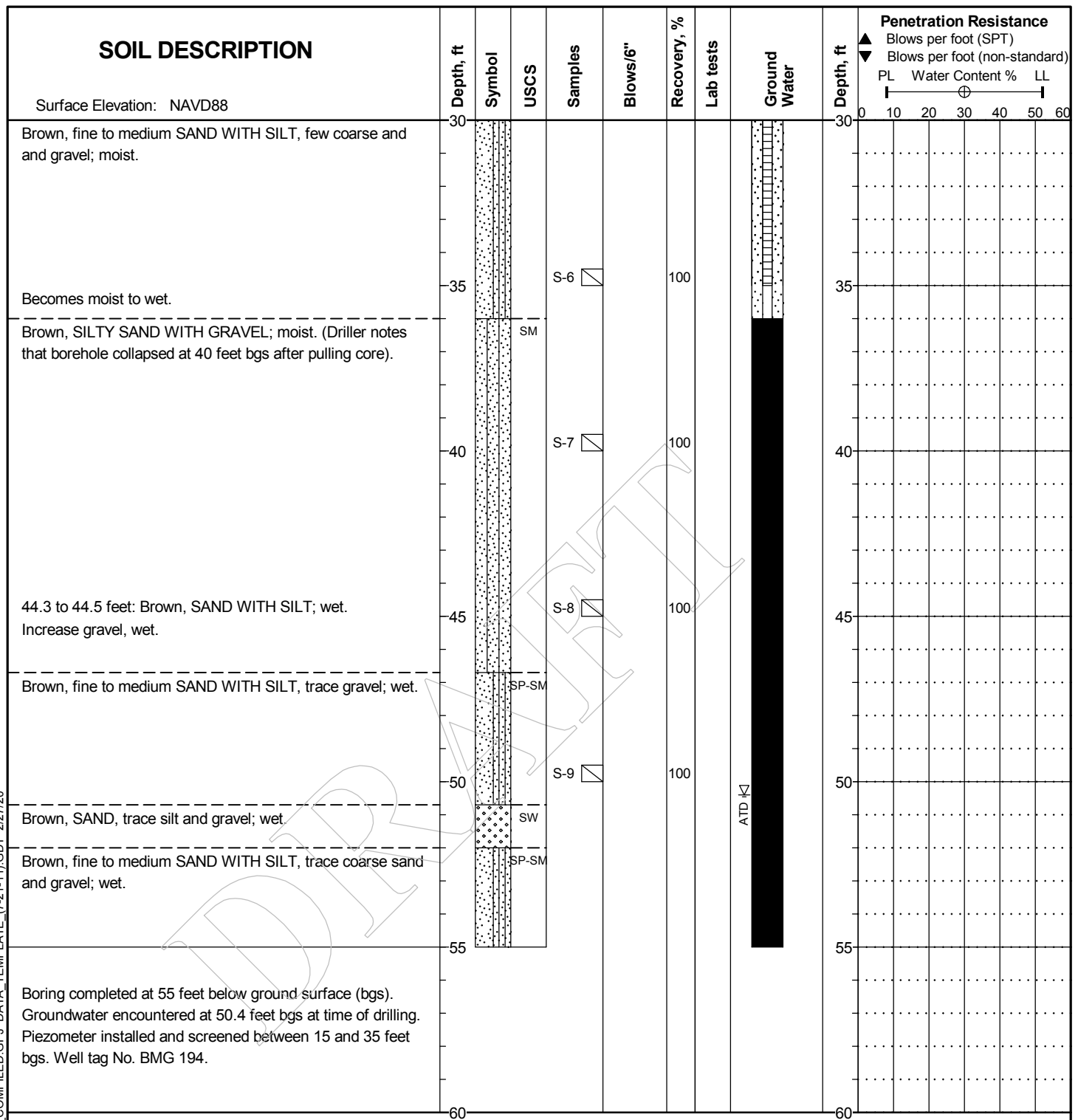
FIGURE A-1

LOG OF BORING (2/1/11) THORNTON_NDS_C316083_COMPILED.GPJ DATA_TEMPLATE_(7-21-11).GDT 2/27/20

SOIL DESCRIPTION

Surface Elevation: NAVD88

Depth, ft	Soil Description	USCS	Samples	Recovery, %
	Brown, fine to medium SAND WITH SILT, trace fine gravel; moist.	SP-SM	S-13	100
65	Brown, SILTY fine to medium SAND, trace coarse sand and fine gravel; moist.	SM		
	(66.2 - 66.5 feet): Layer of fine to medium SAND WITH SILT, few coarse sand.			
	Brown, fine to medium SAND WITH SILT; moist; 1" layer of silty fine sand at 69 feet.	SP-SM	S-14	100
70	Brown, GRAVEL WITH SILT AND SAND; wet.	GP-GM SW-SM		
	Grades to brown, SAND WITH SILT AND GRAVEL; wet.			
	Brown, fine to medium SAND WITH SILT, trace fine gravel; moist.	SP-SM		
75			S-15	100
	Brown, medium SAND, few fine sand, trace coarse sand and silt; moist to wet.	SP		
80			S-16	100
	Becomes fine to medium sand, few coarse sand, moist to wet.			
	Brown, fine SAND WITH SILT, few medium sand, trace coarse sand; moist to wet.	SP-SM		
85	Becomes wet, increased medium sand.		S-17	100
90			S-18	100

(Continued)

ATD ⋈

Penetration Resistance
▲ Blows per foot (SPT)
▼ Blows per foot (non-standard)
PL Water Content % LL
0 10 20 30 40 50 60

Date Completed: 2/18/2020
Driller: Cascade Drilling
Equipment: TSI 150CC
Drilling Method: 6-in OD casing, 4-in core barrel, Sonic
Hammer System: N/A

Approximate Location: 12 feet S of curb, 21 feet W of tree.

Thornton Natural Drainage Systems
Seattle, WA

Seattle Public Utilities
Geotechnical Engineering

LOG OF BORING NG-B-201

C316083

FIGURE A-1

Logged by: AJC   Reviewed by:

Sheet 3 of 4

LOG OF BORING (2/1/11) THORNTON_NDS_C316083_COMPILED.GPJ DATA_TEMPLATE_(7-21-11).GDT 2/27/20

SOIL DESCRIPTION

Surface Elevation: NAVD88

Few coarse sand.

Boring completed at 95 feet below ground surface (bgs). Groundwater encountered at 78.8 feet bgs at time of drilling. Piezometer installed and screened between 40 and 60 feet bgs. Vibrating wire piezometer installed at 84 feet bgs. Well tag No. BMG 192.

Depth, ft	Samples	Recovery, %
95	S-19	100

Penetration Resistance

▲ Blows per foot (SPT)
▼ Blows per foot (non-standard)

PL   Water Content %   LL

Date Completed: 2/18/2020
Driller: Cascade Drilling
Equipment: TSI 150CC
Drilling Method: 6-in OD casing, 4-in core barrel, Sonic
Hammer System: N/A

Approximate Location: 12 feet S of curb, 21 feet W of tree.

Thornton Natural Drainage Systems
Seattle, WA

Seattle Public Utilities
Geotechnical Engineering

LOG OF BORING NG-B-201

C316083

FIGURE A-1

LOG OF BORING (2/1/11) THORNTON_NDS_C316083_COMPILED.GPJ DATA_TEMPLATE_(7-21-11).GDT 2/27/20

SOIL DESCRIPTION

Surface Elevation: NAVD88

FILL
Brown, SILTY fine SAND, few medium sand and gravel, trace coarse sand; moist to wet; scattered rootlets.

GLACIAL TILL
Brown, grading to grayish brown, SILTY fine to medium SAND WITH GRAVEL, few coarse sand and cobbles; moist to wet. (weathered till)

ADVANCE OUTWASH
Brown, SILTY fine to medium SAND, few fine gravel, trace coarse sand; moist to wet.
Trace gravel.

Brown, fine to medium SAND, trace silt, coarse sand, and gravel; moist.

Brown, fine to medium SAND WITH SILT, trace coarse sand, few gravel; moist.

Brown, SILTY fine SAND, trace coarse sand and gravel; moist to wet.

(Continued)

Depth, ft	USCS	Samples	Recovery, %
0	SM		
5	SM		
10		S-1	100
15	SM	S-2	100
20		S-3	100
	SP		
25	SP-SM	S-4	100
30	SM / SP-SM	S-5	100

Penetration Resistance
▲ Blows per foot (SPT)
▼ Blows per foot (non-standard)
PL — Water Content % — LL
0 10 20 30 40 50 60

Date Completed: 2/19/2020
Driller: Cascade Drilling
Equipment: TSI 150CC
Drilling Method: 6-in OD casing, 4-in core barrel, Sonic
Hammer System: N/A

Approximate Location: 12 feet N of edge of pavement, 19 feet E of paved school entrance.

**Thornton Natural Drainage Systems
Seattle, WA**

**Seattle Public Utilities
Geotechnical Engineering**

LOG OF BORING NG-B-204

C316083

FIGURE A-

LOG OF BORING (2/1/11) THORNTON_NDS_C316083_COMPILED.GPJ DATA_TEMPLATE_(7-21-11).GDT 2/27/20

SOIL DESCRIPTION

Surface Elevation: NAVD88

Depth, ft	Symbol	USCS	Samples	Blows/6"	Recovery, %	Lab tests	Ground Water	Depth, ft

Penetration Resistance
▲ Blows per foot (SPT)
▼ Blows per foot (non-standard)
PL Water Content % LL
0 10 20 30 40 50 60

Brown, fine to medium SAND WITH SILT, few coarse and and gravel; moist.

Becomes moist to wet.

S-6 — 100 — at 35 ft

Brown, SILTY SAND WITH GRAVEL; moist. (Driller notes that borehole collapsed at 40 feet bgs after pulling core). — SM

S-7 — 100 — at ~40 ft

44.3 to 44.5 feet: Brown, SAND WITH SILT; wet.
Increase gravel, wet.

S-8 — 100 — at 45 ft

Brown, fine to medium SAND WITH SILT, trace gravel; wet. — SP-SM

S-9 — 100 — at ~50 ft

Brown, SAND, trace silt and gravel; wet. — SW

ATD ⊽

Brown, fine to medium SAND WITH SILT, trace coarse sand and gravel; wet. — SP-SM

Boring completed at 55 feet below ground surface (bgs).
Groundwater encountered at 50.4 feet bgs at time of drilling.
Piezometer installed and screened between 15 and 35 feet bgs. Well tag No. BMG 194.

Date Completed: 2/19/2020
Driller: Cascade Drilling
Equipment: TSI 150CC
Drilling Method: 6-in OD casing, 4-in core barrel, Sonic
Hammer System: N/A

Approximate Location: 12 feet N of edge of pavement, 19 feet E of paved school entrance.

**Thornton Natural Drainage Systems
Seattle, WA**

**Seattle Public Utilities
Geotechnical Engineering**

LOG OF BORING NG-B-204

C316083

FIGURE A-

LOG OF BORING (2/1/11) THORNTON_NDS_C316083_COMPILED.GPJ DATA_TEMPLATE_(7-21-11).GDT 2/27/20

Location: 118 North 82nd Street	**Boring U-B-102**
Ground Elevation: Approximately 310 feet **Logged by**: RJM	

Driller: Cascade   **Drilling Method**: Hollow Stem Auger

Date Started/Ended: 3-1-2018/3-1-2018   **Sampler**: Split-Spoon 140 Pound Hammer   **Depth**: 61.5 feet

Depth (feet)	Blow Counts/ Percent Recovery	Sample Interval	Graphic Log	USCS	Soil Description	Well Completion	Depth to GW	Comments/ Remarks
0					Brown, organic, silty SAND; moist. (Fill)			Vactored to 6.5 feet prior to drilling. Soil samples collected with hand auger.
					Vashon Advance Outwash (Qva)			
				SP-SM	Brown, slightly silty, fine to medium SAND; moist - trace gravel at 5.5 feet			
5								- sieve, moisture content
	4,12,14 100			SP-SM /SM	Medium dense, brown, slightly silty to silty fine SAND; moist			
10	3,13,15 100				- silty			- sieve, moisture content
	7,12,14 100			SP-SM	Medium dense to very dense, brown, trace to slightly silty fine SAND; moist			
15	13,23,30 100							
	9,22,22 100							
20	12,20,21 100			SP-SM /SM	Dense, brown, slightly silty to silty fine SAND; moist			
	10,23,26 100							
25	6,14,31 100			SP-SM	Dense, brown, trace to slightly silty fine SAND; moist			
	10,19,19 100				- scattered iron oxide staining			
30								

* See key for graphic log explanation

5,20,30 — Blow counts and sample depth interval	▼ Measured depth to groundwater (date and time)	Well monument	Well screen and filter pack
	▽ Estimated groundwater level at time of drilling (ATD)	Well riser pipe and concrete surface seal	Well riser pipe and sand filter pack
		Well riser pipe and bentonite chip seal	Bentonite chips

BORING AND MONITORING WELL LOG FOR B-102

Richard Martin Groundwater LLC	CH2M Hill Engineers, Inc. King County University GSI Seattle, Washington	June 26, 2018
		FIG. B-3 (Sheet 1 of 2)

Depth (feet)	Blow Counts/ Percent Recovery	Sample Interval	Graphic Log	USCS	Soil Description	Well Completion	Depth to GW	Comments/ Remarks
30	12,23,32 100			SP-SM	Dense to very dense, brown, trace to slighty silty, fine SAND; moist			
	18,27,37 100							
35	15,23,22 100			SP-SM	Very dense, brown, trace to slightly silty, fine SAND; moist			
	14,27,42 100							
40	17,23,34 100							
	17,29,36 100				- slightly silty			- sieve, moisture content
45	16,25,32 100							
	12,23,49 100				- slighty gravelly from 48.5 to 48.7 feet			
50	18,37,50/6" 100							
	24,40,50/6" 100							
55	22,41,50/6" 100							
	23,50/6" 100						ATD ▽	
60	27,50/5" 100							
					Bottom of boring @ 61.5 feet			
65								
70								

Richard Martin Groundwater LLC

CH2M Hill Engineers, Inc.
King County University GSI
Seattle, Washington

June 26, 2018

FIG. B-3 (Sheet 2 of 2)

GRAIN SIZE IN MILLIMETERS

COBBLES	COARSE	FINE	COARSE	MEDIUM	FINE	FINES: SILT OR CLAY
	GRAVEL			SAND		

Symbol	Boring Number	Depth (feet)	Sample Description	Percent Fines	USCS	Percent Water Content
●	B-102	42 to 44	Slightly silty, fine SAND	10.2	SP-SM	3.7
■	B-105	7.5 to 9	Silty, gravelly, SAND	22.7	SW	6.2
▲	B-106	7 to 7.5	Slightly gravelly, silty, fine SAND	29.2	SM	9.4
✚	B-106	14 to 15	Silty, fine SAND	16.4	SM	6.2
★	B-107	19 to 20	Slightly silty, fine SAND; trace gravel	7.4	SP-SM	6.7
◆	B-107	29 to 30	Slightly silty, fine SAND	9.1	SP-SM	7.5

NOTE: The sieve analyses were performed by Am Test Inc.
in general accordance with ASTM Method D422.

Grain Size Distribution

Location: Southwest corner of 9th Ave SW and Henderson Place SW

Boring U-B-118

Ground Elevation: Approximately 246 feet   **Logged by**: RJM

Driller: Holt Services   **Drilling Method**: Sonic - Track Mounted

Date Started/Ended: 2-5-2018/2-6-2018   **Core Diameter**: 4 inches   **Depth**: 65 feet

Depth (feet)	Run/Percent Recovery	Sample Interval	Graphic Log *	USCS	Soil Description	Well Completion	Depth to GW	Comments/Remarks
0					Brown, organic, silty SAND; moist; (Fill)			Vactored to 5 feet prior to drilling. Soil samples collected with hand auger.
					Vashon Advance Outwash (Qva)			
				SM	Brown, silty fine SAND; moist; trace gravel; mottled above 2 feet; weathered			- sieve, moisture content
5	Run 1 / 100 percent			SP-SM	Brown, slightly silty, fine to medium SAND; moist; trace gravel			- sieve, moisture content
10								
15	Run 2 / 100 percent			SP-SM /SM	Brown, slightly silty to silty fine SAND; moist			
				SP-SM	Brown, slightly silty, slightly gravelly, fine SAND; moist			
20				SM	Brown, silty fine SAND; moist; scattered iron oxide staining and organic material; finely laminated; (Paleo-soil?)			
				ML	**Pre-Vashon Glacial Undifferentiated (Qpgu)**			
	Run 3 / 100 percent				Tan, slightly sandy SILT; moist; trace clay; till-like			
				SP	Tan, fine to medium SAND; moist; trace silt; scattered gravel; till-like; slightly silty from 23 to 25 feet			
25					- hard drilling at 25 feet			- sieve, moisture content
	Run 4 / 100 percent			ML	Tan, fine sandy SILT; moist; till-like			
				SP-SM	Tan, slightly silty, fine SAND; moist; scattered gravel; till-like			- sieve, moisture content
30								

* See key for graphic log explanation

44-45 Sonic core grab sample depth interval

▼ Measured depth to groundwater (date and time)

▽ Estimated groundwater level at time of drilling (ATD)

Well monument

Well riser pipe and concrete surface seal

Well riser pipe and bentonite chip seal

Well screen and filter pack

Well riser pipe and sand filter pack

Bentonite chips

BORING AND INFILTRATION TEST WELL LOG FOR B-118

Richard Martin Groundwater LLC

CH2M Hill Engineers, Inc.
King County University GSI
Seattle, Washington

June 26, 2018

FIG. B-15 (Sheet 1 of 2)

Depth (feet)	Run/Percent Recovery	Sample Interval	Graphic Log	USCS	Soil Description	Well Completion	Depth to GW	Comments/ Remarks
30				SP-SM	Tan, slightly silty fine SAND; moist; till-like			
	Run 5 / 100 percent			SM	Tan, silty, fine SAND; moist; scattered gravel; till-like			- sieve, moisture content
35				SP	Tan, fine SAND; moist; trace silt			
40				SP-SM	Tan, slightly silty fine SAND; moist			
	Run 6 / 100 percent			SM	Tan, silty, fine SAND; moist; scattered layers of fine sandy silt (1-2")			- sieve, moisture content
45								
				SP-SM	Tan, trace to slightly silty, fine SAND; moist			
50	Run 7 / 100 percent			SP-SM	Tan, slightly silty to silty, fine SAND; moist; till-like at 55 feet			
55	Run 8 / 50 percent						ATD ▽	
60					**Pre-Vashon Non-Glacial Coarse-Grained (Qpnc)**			
	Run 9 / 100 percent			SP	Brown to gray, fine SAND; wet; trace silt; scattered mica; scattered red and yellow sand grains			
65					Bottom of boring @ 65 feet			
70								

Richard Martin Groundwater LLC

CH2M Hill Engineers, Inc.
King County University GSI
Seattle, Washington

June 26, 2018

FIG. B-15 (Sheet 2 of 2)

GRAIN SIZE IN MILLIMETERS

COBBLES	COARSE	FINE	COARSE	MEDIUM	FINE	FINES: SILT OR CLAY
	GRAVEL			SAND		

Symbol	Boring Number	Depth (feet)	Sample Description	Percent Fines	USCS	Percent Water Content
●	B-107	39 to 40	Silty, fine SAND	13.3	SP-SM	3.8
■	B-110	44 to 45	Slightly gravelly, slightly silty, fine to medium SAND	7.7	SP-SM	4.4
▲	B-110	56 to 57	Silty, fine SAND	12.8	SP-SM	7.8
✚	B-113	24 to 25	Slightly silty, fine SAND	10.2	SP-SM	7.7
★	B-113	49 to 50	Slightly silty, fine to medium SAND	11.4	SP-SM	3.1
◆	B-118	23 to 25	Fine to medium SAND; trace silt	3.8	SP	2.2

NOTE: The sieve analyses were performed by Am Test Inc.
in general accordance with ASTM Method D422.

Grain Size Distribution

Richard Martin Groundwater LLC	King County University GSI - CH2M Seattle, Washington	June 26, 2018
		Figure C-1, page 8 of 9
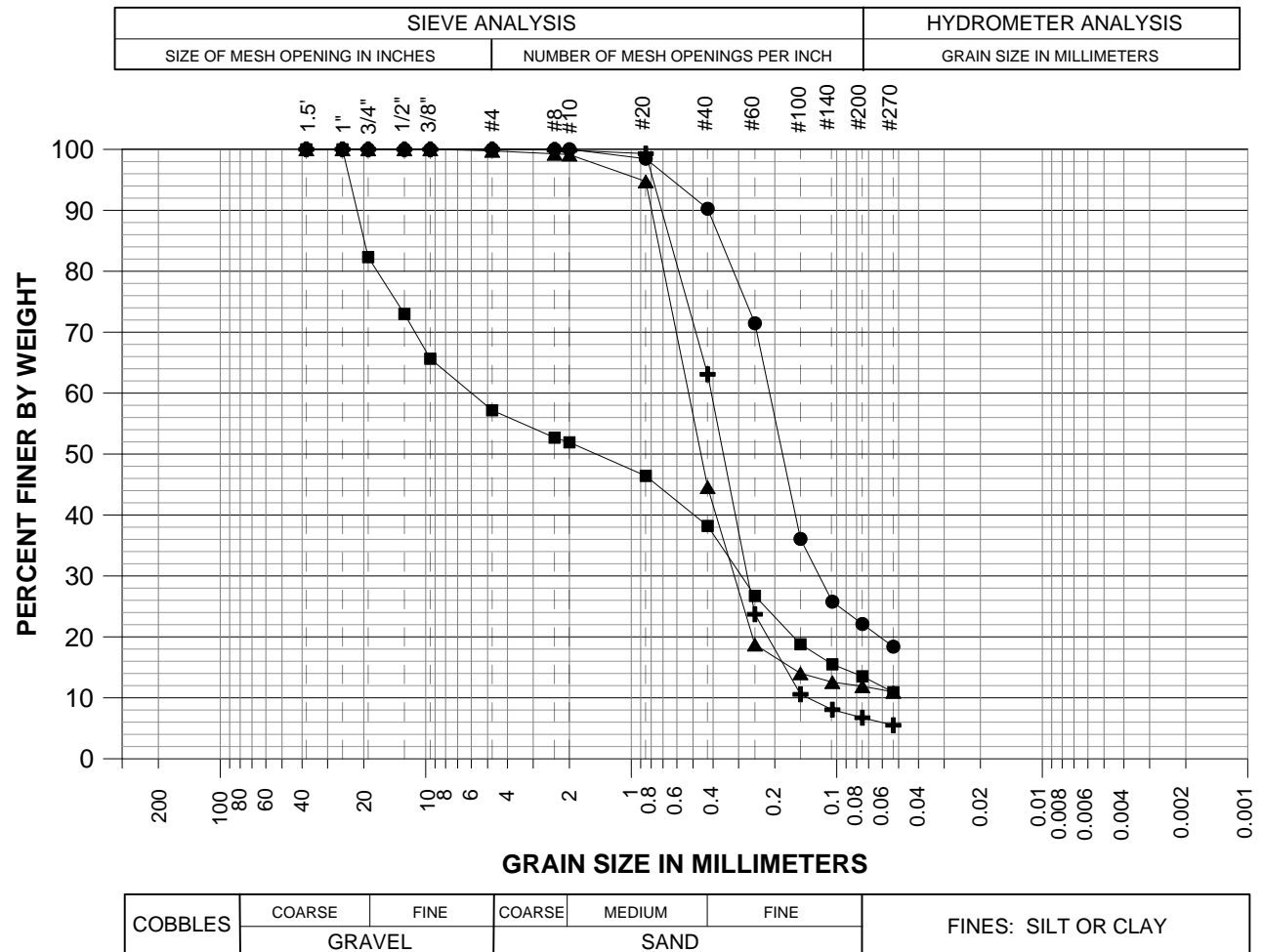
SIEVE ANALYSIS		HYDROMETER ANALYSIS
SIZE OF MESH OPENING IN INCHES	NUMBER OF MESH OPENINGS PER INCH	GRAIN SIZE IN MILLIMETERS

GRAIN SIZE IN MILLIMETERS

PERCENT FINER BY WEIGHT

COBBLES	COARSE	FINE	COARSE	MEDIUM	FINE	FINES: SILT OR CLAY
	GRAVEL			SAND		

Symbol	Boring Number	Depth (feet)	Sample Description	Percent Fines	USCS	Percent Water Content
●	B-118	44 to 46	Silty, fine SAND	22.1	SM	4.9
■	B-121	5	Silty, gravelly, SAND; well graded	13.5	SW-SM	5.3
▲	B-121	14 to 15	Slightly silty, fine to medium SAND	11.9	SP-SM	6.9
+	B-121	49 to 50	Slightly silty, fine to medium SAND	6.7	SP-SM	2.8

NOTE: The sieve analyses were performed by Am Test Inc. in general accordance with ASTM Method D422.

Grain Size Distribution

Richard Martin Groundwater LLC	King County University GSI - CH2M Seattle, Washington	June 26, 2018
		Figure C-1, page 9 of 9

Kindred Hydro

Well Log: U-TW-6						Project Name: University/Montlake Wells	
Project #: CAR-16-1						Ground Surface Elevation: 275 (est. from topo)	
Location: Seattle, WA						Depth to Water (ft BGS): 31 (open hole after drilling)	
Contractor: Holt Services, Inc.						Start/Finish Date: June 15, 2016	
Exploration Method: Sonic Drilling						Logged by: Richard Martin	
Sampling Method: Sonic Core							

Depth (ft)	Elev (ft)	Sample Type/I.D.	Water	USCS Class	Well Const.	Description
				SM	Flush Monument	**Sod (0-0.5 ft)**
						loose, slightly moist, brown, silty SAND with organics
				SP-SM/SM		**Vashon Advance Outwash (0.5 ft to BOH)**
1	274					Vacuum extraction to 8 ft. Moist, olive brown, slightly silty to silty, fine to medium SAND, few gravel
2	273					
3	272					
4	271					
5	270					
6	269					
7	268			SP		Moist, brown, fine to medium SAND, trace silt, few gravel, occational iron-oxide staining, lenses (< 1 inch thick) of silty sand to sandy silt between 10 and 14 feet.
8	267					
9	266	Core: 9 ft				
10	265					
11	264					
12	263					
13	262					

Well construction labels (Well Const. column):
- 2-inch Dia. PVC Solid Casing from 0.5-6 ft
- Bentonite chips from 1-8
- 2-inch Dia. PVC Slotted Well Screen from 6 to 21 ft

Kindred Hydro

Well Log: U-TW-6

Project #: CAR-16-1

Project Name: University/Montlake Wells

Ground Surface Elevation: 275 (est. from topo)

Depth (ft)	Elev (ft)	Sample Type/I.D.	Water	USCS Class	Well Const.	Description
13						
14	261					
15	260					
				SP/SP-SM		trace to slightly silty fine SAND
16	259					
17	258	Core: 17 ft				
18	257					
19	256			SP-SM/SM		Brown, slightly silty to silty fine SAND, few gravel, interbeds (< 1 inch) of till-like sandy silt.
20	255					
21	254					
22	253					
23	252					
24	251					
25	250					
26	249					
27	248			SP/SP-SM		Moist to wet, brown, trace to slightly silty, fine SAND, few gravel, occasional interbeds (< 1 inch) of silty sand to sandy silt

Well Const. column annotations:
- 2-inch Dia. PVC Slotted Well Screen from 6 to 21 ft
- #10-20 Colorado Silica Sand from 3.5 to 21 ft
- Bentonite chips from 21 to 40 ft

Kindred Hydro

Well Log: U-TW-6

Project #: CAR-16-1

Project Name: University/Montlake Wells

Ground Surface Elevation: 275   (est. from topo)

Depth (ft)	Elev (ft)	Sample Type/I.D.	Water	USCS Class	Well Const.	Description
28	247					
29	246					
30	245	Core: 30 ft				
31	244		6/15/16		Bentonite chips from 21 to 40 ft	
32	243					
33	242					
34	241					
35	240					
36	239					
37	238					
38	237					
39	236					
40	235					BOH @ 40 ft. Water at 31 ft during drilling.

Kindred Hydro

Well Log: U-TW-9	**Project Name**: University/Montlake Wells
Project #: CAR-16-1	**Ground Surface Elevation**: 294 (est. from topo)
Location: Seattle, WA	**Depth to Water (ft BGS)**: >107 (dry)
Contractor: Holt Services, Inc.	**Start/Finish Date:** June 21, 2016
Exploration Method: Sonic Drilling	**Logged by**: Richard Martin
Sampling Method: Sonic Core	

Depth (ft)	Elev (ft)	Sample Type/I.D.	Water	USCS Class	Well Const.	Description
				SM	Flush Monument	**Sod (0-0.5 ft)**
						loose, slightly moist, brown, silty SAND with organics
				SM		**Vashon Glacial Till (0.5 to 10 ft)**
1	293					Vacuum extraction to 2.5 ft. Moist, gray, silty SAND, few gravel
2	292					
3	291			SP-SM/SM		Brown, slightly silty to silty, gravelly SAND, moist, scattered cobbles
4	290					
5	289					
6	288					
7	287					
8	286					
9	285					
10	284			SM		**Vashon Advance Outwash (10 ft-BOH)**
						Brown, silty fine SAND, moist, few gravel
11	283					
12	282					
13	281					

Well Const. column notes: 2-inch Dia. PVC Solid Casing from 0.5 - 50 ft; Bentonite chips from 1 to 47 ft

Well Log: U-TW-9

Project #: CAR-16-1

Project Name: University/Montlake Wells

Ground Surface Elevation: 294　(est. from topo)

Depth (ft)	Elev (ft)	Sample Type/I.D.	Water	USCS Class	Well Const.	Description
13						
14	280					
15	279					
16	278					
17	277					
18	276			SP-SM/SM		Brown, slightly silty to silty, fine to medium SAND, moist, interbeds (< 2 inches) sandy silt.
19	275					
20	274					
21	273					
22	272					
23	271			SP-SM/SM		Brown, slightly silty to silty, fine to medium SAND, moist.
24	270					
25	269					
26	268					
27	267					

Well Const. column annotations: **2-inch Dia. PVC Solid Casing from 0.5 - 50 ft**, **Bentonite chips from 1 to 47 ft**

Kindred Hydro

Well Log: U-TW-9

Project #: CAR-16-1

Project Name: University/Montlake Wells

Ground Surface Elevation: 294 (est. from topo)

Depth (ft)	Elev (ft)	Sample Type/I.D.	Water	USCS Class	Well Const.	Description
28	266					
29	265					
30	264					
31	263					
32	262					
33	261					
34	260					
35	259					
36	258					
37	257					
38	256					
39	255					
40	254					
41	253					
42	252					

Well Const. column: 2-inch Dia. PVC Solid Casing from 0.5 - 50 ft; Bentonite chips from 1 to 47 ft

Well Log: U-TW-9

Project #: CAR-16-1

Project Name: University/Montlake Wells

Ground Surface Elevation: 294   (est. from topo)

Depth (ft)	Elev (ft)	Sample Type/I.D.	Water	USCS Class	Well Const.	Description
43	251					
44	250			ML		Brown, fine sandy SILT, moist.
45	249	Core: 45 ft				
46	248			SM/ML		Brown, slightly silty to silty, SAND, moist, interbeds of fine sandy silt, occational organics from 46.5 to 47 feet.
47	247			SP/SP-SM		Brown, trace to slightly silty SAND, moist.
48	246					
49	245					
50	244					
51	243			SM/ML		Brown, silty fine SAND to fine sandy SILT, moist.
52	242					
53	241					
54	240					
55	239			SP-SM/SM		Brown, slightly silty to silty, fine to medium SAND, moist
56	238					
57	237	Core: 57 ft				

Well Const. annotations:
- Bentonite chips from 3 to 47.5 ft
- 2-inch Dia. PVC Slotted Well Screen from 50 to 70 ft
- #10-20 Colorado Silica Sand from 47 to 74

Kindred Hydro

Well Log: U-TW-9

Project #: CAR-16-1

Project Name: University/Montlake Wells

Ground Surface Elevation: 294 (est. from topo)

Depth (ft)	Elev (ft)	Sample Type/I.D.	Water	USCS Class	Well Const.	Description
58	236					
59	235					
60	234					
61	233					
62	232					
63	231					
64	230					
65	229					
66	228					
67	227					
68	226	Core: 68 ft				
69	225					
70	224					
71	223					

Well Const. column: 2-inch Dia. PVC Slotted Well Screen from 50 to 70 ft; #10-20 Colorado Silica Sand from 47 to 74 ft

Kindred Hydro

Well Log: U-TW-9

Project #: CAR-16-1

Project Name: University/Montlake Wells

Ground Surface Elevation: 294 (est. from topo)

Depth (ft)	Elev (ft)	Sample Type/I.D.	Water	USCS Class	Well Const.	Description
72	222					
73	221					
74	220					
75	219					
76	218					
77	217					
78	216	Core: 78 ft			Bentonite chips from 74 to 107 ft	
79	215					interbeds of sandy silt from 78.5 to 79.5
80	214					
81	213					
82	212					
83	211					
84	210					
85	209					

Kindred Hydro

Well Log: U-TW-9

Project #: CAR-16-1

Project Name: University/Montlake Wells

Ground Surface Elevation: 294 (est. from topo)

Depth (ft)	Elev (ft)	Sample Type/I.D.	Water	USCS Class	Well Const.	Description				
86	208									
87	207									
88	206									
89	205									
90	204									
91	203					Bentonite chips from 74 to 107 ft				
92	202									
93	201									
94	200									
95	199									
96	198									
97	197									
98	196									
99	195									

Kindred Hydro

Well Log: U-TW-9

Project Name: University/Montlake Wells

Project #: CAR-16-1

Ground Surface Elevation: 294   (est. from topo)

Depth (ft)	Elev (ft)	Sample Type/I.D.	Water	USCS Class	Well Const.	Description
100	194					interbeds of sandy silt from 100 to 103 feet
101	193					
102	192				Bentonite chips from 74 to 107 ft	
103	191					
104	190					
105	189					
106	188					
107	187					
						BOH @ 107 ft. Dry.

VOLUME VI: EFFECTS OF STRATIGRAPHIC LAYERING AND GROUNDWATER MOUNDING ON INFILTRATION TESTING AND DESIGN

Near-Term Action (NTA) 2018-0827: Flexible Infiltration Test Methods for Evaluating Infiltration Feasibility

Project No. TAC-20-1 • October 10, 2022

Volume VI - Contents

Volume VI - List of Tables

Volume VI - List of Figures

Volume VI - Abstract

The purpose of Volume VI is to evaluate the effects of stratigraphic layering and groundwater mounding on infiltration testing and provide strategies and correction factors for addressing these effects in the design of infiltration facilities. The bulk hydraulic conductivity (K_b) provided by infiltration testing can be multiplied by appropriate correction factors to provide design hydraulic conductivity (K_d) used to size infiltration facilities.

Shallow field testing demonstrates significant variability in K_b over distances of 5 to 25 m. Some of this variability, but not all, can be explained by horizontal differences in soil texture. However, numerical simulations demonstrate that stratigraphic layering can have a significant impact on K_b, even for the same type of test facility. Small changes in the elevation of the perching/permeable layer relative to the test interval can change K_b by a factor of 2-4, depending on the permeability contrast. Based on field testing and the numerical simulations provided in this assessment, this variability and uncertainty can be addressed using the uncertainty correction factor (CF_u). A CF_u in the range of 0.2 to 0.5 may be appropriate for higher-risk infiltration facilities with limited infiltration test data. A higher CF_u (not to exceed 1) may be appropriate if numerous infiltration tests in the vicinity of the proposed infiltration facility are relatively consistent or if the consequences of under-predicting facility performance are insignificant (e.g., a small residential project with an offsite point of discharge).

As observed in field testing and confirmed with numerical simulations, shallow test wells tend to provide higher estimates of K_b than pit tests. Since well tests are dominated by horizontal flow and pit tests are dominated by vertical flow, pit test results are likely to be more representative of full-scale horizontal infiltration facilities, such as infiltration ponds and bioretention facilities. Well tests may be used for sizing horizontal infiltration facilities if an appropriate CF_w is applied. A CF_w of 0.5 is recommended for using well tests to size horizontal infiltration facilities and a CF_w of 1 is recommended for drywells.

Steady-state infiltration tests lasting 6 hr can generally detect the impacts of groundwater mounding within 1-3 m of the bottom of the test facility. However, these effects are more significant for larger full-scale facilities than typical test facilities. Groundwater mounding analysis should be conducted for larger facilities and it may be appropriate to apply a CF_m between 0.2 and 1 for smaller facilities, depending on the size of the full-scale facility, the permeability of the soil, and the depth to groundwater.

1 Introduction

This study evaluated three new analytical approaches for infiltration testing, including the uncased steady-state borehole permeameter (USSBP), the cased steady-state borehole permeameter (CSSBP) and the cased falling-head borehole permeameter (FHBP). Numerical simulations have been conducted to calibrate and evaluate these methods for relatively permeable soils typically considered for stormwater infiltration (Volumes I, II, and III). The numerical simulations provided calibrated fitting parameters for the USSBP and CSSBP methods with maximum errors of 11-13% and average errors of 3-5% for a broad range of test configurations across 10 soil types.

Shallow infiltration testing was conducted at four sites to compare these methods for both dug test pits and shallow test wells (Volume IV). Deep infiltration was conducted in eight wells to illustrate and compare these methods for deep test wells (Volume V). This field testing provided valuable information regarding which field methods are most effective, and real-world data regarding spatial variability and differences between the test methods. This real-world data was critical to guide the assessment of stratigraphic layering provided in this portion of the study.

The calibration and numerical assessments in Volumes I, II, and III used the term saturated hydraulic conductivity (K_s) to characterize the permeability of the soil and report the test results. As stated in these numerical assessments, using this term assumes a homogeneous, isotropic soil horizon throughout the test domain, consistent with the assumptions of the borehole permeameter methods. K_s will continue to be used to characterize soil layers that are homogeneous, and isotropic. Real soils, however, are anisotropic and heterogeneous and most infiltration testing will be impacted by stratigraphic layering, and sometimes by horizontal variability and groundwater mounding. Therefore, any test results that are impacted by these conditions will use the term "bulk hydraulic conductivity" (K_b). Using the term acknowledges that the test interval is anisotropic and heterogeneous. Furthermore, the test results may be impacted by the specific geometry, size, and location of the test facility in relation to stratigraphic layers and the groundwater table.

It is important to acknowledge that using K_b to design infiltration facilities with a different shape, size or location than the test facility is subject to significant uncertainty and error. To the extent feasible, uncertainty and potential error will be addressed with appropriate correction factors. The analysis provided in this this numerical assessment, combined with the results of the field testing, can provide a technical basis for these correction factors.

1.1 Scope of Work and Purpose

The numerical validation efforts conducted for this study have so far assumed homogenous and isotropic conditions. In the real world, as demonstrated in the field testing, soils are generally layered (anisotropic) and can be highly variable over short distances. This work will address the effects of stratigraphic layering and groundwater mounding and provide recommendations for addressing these effects. This includes simulation of selected portions of the field testing to illustrate why different testing approaches can provide different estimates of K_b.

The primary objectives of this task include the following:

- Demonstrate how K_b varies due to stratigraphic layering and groundwater mounding.

- Illustrate how correction factors can be used to address uncertainty associated with spatial variability.

- Based on field testing and numerical simulation, evaluate the feasibility of using well tests for sizing horizontal infiltration facilities and provide recommended correction factors.

- Demonstrate how USSBP and CSSBP tests in the same test well can provide different estimates of K_b.

- Evaluate how well 6-hr infiltration tests can account for layering and mounding and demonstrate how mounding effects vary as a function of soil type, depth to groundwater or the perching layer, and the size of the infiltration facility. Based on these results, illustrate how correction factors can be used to address groundwater mounding effects.

For consistency with previously published work, metric units are used throughout this volume.

2 Materials and Methods

The stratigraphic layering and groundwater mounding assessment was conducted using a number of typical test scenarios for dug pits, shallow wells, and deep wells across a range of soil types. In addition, a limited number of field tests were simulated to illustrate stratigraphic arrangements that provided reasonably close matches to the field tests.

2.1 Numerical Modeling Approach

A variety of scenarios were simulated to evaluate the impacts of stratigraphic layering and mounding on K_b. All the simulations were conducted using SEEP/W, a finite element numerical model that can simulate multidimensional and axisymmetric flow in saturated and unsaturated porous media (GEOSLOPE International Ltd., Calgary, Alberta, Canada). Unsaturated flow simulation requires specifying soil hydraulic properties in the form of the unsaturated volumetric soil water content function $\theta(\psi)$ (soil water content as a function of soil matric suction) and the unsaturated hydraulic conductivity function $K(\psi)$ (hydraulic conductivity as a function of soil matric suction). These hydraulic property functions are described in Volume I. All the simulations assumed axisymmetric flow, with no-flow boundaries along the top of the flow domain, a unit hydraulic head gradient boundary at the bottom of the flow domain, and a seepage face boundary on the outside of the axisymmetric domain.

The soil types used in this assessment were the same 10 "representative" soils defined in Volume I, including five glacially over-consolidated soils and five normally consolidated soils. The glacially over-consolidated soils included four advance outwash soils: silty Qva, fine Qva, fine-medium Qva, and fine-coarse Qva; and one glacial till: Qvt. The normally consolidated soils included well-sorted and poorly-sorted soils typical of recessional outwash or alluvium. These representative soils cover the range of soils usually considered for stormwater infiltration within the Puget Sound basin. A full discussion of the soil parameters is provided in Volume I). Volume I also provides a description of the unsaturated volumetric soil water content functions $\theta(\psi)$, the unsaturated hydraulic conductivity function $K(\psi)$, and the sorptive number (α^*) for each of the 10 soils. A summary of characteristics for the 10 soils is provided in Tables 1 and 2.

All the steady-state simulations were conducted by applying a constant head boundary at the inside of the test facility exposed to native soils (the bottom and sides of the pit test and the sandpack interval of the test wells). The bentonite seal was simulated as a material with $K_s = 1 \times 10^{-4}$ m/d and 50% porosity. The sandpack and well casing were not simulated in the steady-state numerical simulations.

Transient simulations of field tests in test wells were conducted using a numerical representation of the constructed well (including well casing, sandpack, and bentonite seal) and injecting water into the well at the rates recorded during the field tests. The well casing was simulated as a material with $K_s = 1,000,000$ m/d and 100% porosity. The sandpack was simulated as a material with $K_s = 100,000$ m/d and 40% porosity. The bentonite seal was simulated as a material with $K_s = 1 \times 10^{-4}$ m/d and 50% porosity. The water was injected at a node in the bottom of the well casing.

Table 1: Properties of representative glacially over-consolidated soil types and baseline SEEP/W soil parameters used in the soil water content and hydraulic conductivity functions. *Qva* is advance outwash, *Qvt* is glacial till, D_{60} and D_{10} are grain diameters corresponding, respectively, to 60% passing and 10% passing on the grain-size distribution curve, and *USCS* is Unified Soil Classification System.

Parameter	Soil Type				
	Qvt	Silty Qva	Fine Qva	Fine-Medium Qva	Fine-Coarse Qva
D_{60} (mm)	0.5	0.25	0.3	0.5	5
D_{10} (mm)	0.02	0.04	0.1	0.13	0.25
Silt Content (wt. %)	20	17	8	5	3
USCS Soil Type	SM	SM	SM-SP	SP	SW
Porosity, θ_S (vol. %)	17	25	30	30	30
Liquid Limit (%)	0	0	0	0	0
Saturated Hydraulic Conductivity, K_S (m/d)	0.1	0.5	2	10	5
Residual Soil Water Content, θ_r (vol. %)	5.5	4.8	3.0	2.6	1.5
Background Soil Water Content θ_b (%)	10	10	10	10	10
Background Soil Matric Suction, ψ_i (m)	3.1	1.8	0.8	0.5	0.09
van Genuchten Fitting Parameter α' (m^{-1})	0.06	0.09	0.18	0.28	1.6
van Genuchten Fitting Parameter n (-)	2.40	3.64	4.10	4.18	3.68
Sorptive Number α* (m^{-1})	1.17	1.33	2.5	3.9	25

Table 2: Properties of representative normally-consolidated soil types and baseline SEEP/W soil parameters used in the soil water content and hydraulic conductivity functions. D_{60} and D_{10} are grain diameters corresponding, respectively, to 60% passing and 10% passing on the grain-size distribution curve, and *USCS* is Unified Soil Classification System.

| Parameter	Soil Type				
	Silty Fine Sand	Silty Fine-Coarse Sand	Fine Sand	Medium Sand	Sandy Gravel
D_{60} (mm)	0.15	1.4	0.28	1.0	8.0
D_{10} (mm)	0.04	0.02	0.079	0.18	0.4
Silt Content (wt. %)	25%	15%	9%	5%	3%
USCS Soil Type	SM	SM	SM-SP	SP	GW
Porosity, θ_S (vol. %)	40	35	40	40	40
Liquid Limit (%)	10	5	0	0	0
Saturated Hydraulic Conductivity, K_S (m/d)	0.25	0.5	3	10	30
Residual Soil Water Content, θ_r (vol. %)	4.8	5.4	2.9	2.2	1.3
Background Soil Water Content θ_b (%)	9.8	10.4	7.9	7.2	6.3
Background Soil Matric Suction, ψ_i (m)	1.39	0.64	0.75	0.24	0.05
van Genuchten Fitting Parameter α' (m^{-1})	1.28	3.44	2.44	7.69	40
van Genuchten Fitting Parameter n (-)	4.3	3.2	4.2	4.3	3.9
Sorptive Number α* (m^{-1})	1.8	5.5	3.5	11	57

2.2 Layering Effects on USSBP Well and Pit Tests

One purpose of this study was to determine how test results are impacted by the presence of perching and/or permeable layers and determine if shallow well test results can be used to design and size horizontal infiltration facilities. The shallow field testing in pits and wells (Volume IV) provided K_b estimates that varied significantly over very short distances (5-10 m) even with the same type of test facility. Furthermore, comparison of well tests with pit tests indicates that well tests generally provide higher estimates of K_b than pit tests, ranging by a factor of 1.1 to 3.4 at the four sites. This was expected since well tests are dominated by horizontal flow and pit tests are dominated by vertical flow and stratigraphic layering tends to restrict vertical flow in comparison with horizontal flow.

The effects of layering on USSBP well and pit test was evaluated by simulating shallow well tests and pit tests in the same stratigraphic conditions by moving either a low permeability perching layer or a permeable layer up and down through the tested interval. Figure 1 shows three simulation domains with the perching layer at the bottom of the test pit (elevation 3.75 to 4.0 m). Two different test wells were simulated, one completed from 0.25 m above the pit bottom to 0.75 m below the pit bottom and the other completed from 1.0 m above the pit bottom to the pit bottom. The perching or permeable layer was 0.25 m thick and simulations were performed with the top of the perching layer at elevations of 5.0, 4.75, 4.5, 4.25, 4.0, 3.75, 3.5, 3.25, 3.0, 2.0, and 1.0 m above the bottom of the simulation domain. The ponding depth was 0.25 m for the pit tests and 1.0 m for the shallow well simulations.

Four combinations of soils were simulated: fine-coarse Qva ($K_s = 5.0$ m/d) with a perching layer of fine Qva ($K_s = 2.0$ m/d); fine-coarse Qva with a perching layer of silty Qva ($K_s = 0.5$ m/d); fine sand ($K_s = 3.0$ m/d) with a permeable layer of medium sand ($K_s = 10$ m/d); and fine sand with a permeable layer of sandy gravel ($K_s = 30$ m/d). The results are provided in Section 3.1.

Figure 1: Simulation domains for comparing results from a test pit with results from two test wells completed above and below the bottom of the test pit.
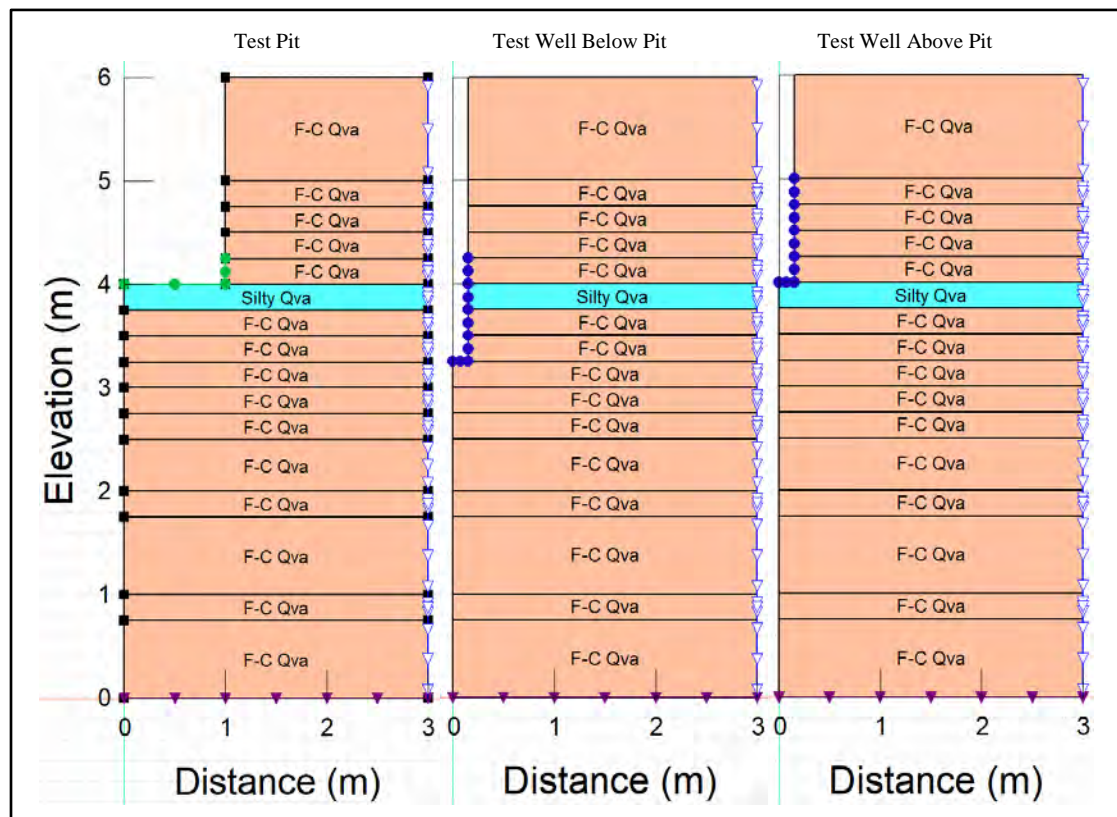
2.3 Layering Effects on USSBP and CSSBP Well Tests

Another purpose of this study was to determine how USSBP and CSSBP tests in the same well are impacted by the presence of perching and/or permeable layers. The USSBP and CSSBP field testing in shallow and deep wells suggested that CSSBP tests tended to provide higher estimates of K_b than the USSBP tests, ranging by a factor of 1.1 to 4 times higher in the shallow test wells (Volume IV) and by a factor of 1 to 1.85 in the deep test wells (Volume V).

The effects of layering on USSBP and CSSBP tests was evaluated by simulating both tests in the same test well configurations by moving either a thin perching or permeable layer up and down through the tested interval. Additional comparisons were conducted by moving a transition from one soil type to another soil type up and down through the test domain. Figure 2a shows an example of the thin layer simulations with a permeable layer at an elevation of 4.75 – 5.0 m and Figure 2b shows an example of a transition from sandy gravel to silty fine and at an elevation of 5.0 m. The thin perching or permeable layer was 0.25 m thick and layer simulations were performed with the top of the perching/permeable layer at elevations of 9.25, 8.25, 7.0, 5.0, 3.0, 2.75, 2.0, and 1.0 m above the bottom of the simulation domain. The transition simulations were conducted with the transition at elevations of 8.25, 8.0, 7.0, 5.0, 2.75 m, 2.0, and 1.0 m above the bottom of the simulation domain. The sandpack interval was between 3.0 and 8.0 m above the bottom of the simulation domain (5.0 m thick) and the ponding depth was 5.0 m for the USSBP simulations and 15 m for the CSSBP simulation.

Four combinations of soils were simulated: fine-coarse Qva ($K_s = 5.0$ m/d) with a perching layer of fine Qva ($K_s = 2.0$ m/d); fine-coarse Qva with a perching layer of silty Qva ($K_s = 0.5$ m/d); fine sand ($K_s = 3.0$ m/d) with a permeable layer of medium sand ($K_s = 10$ m/d); fine sand with a permeable layer of sandy gravel ($K_s = 30$ m/d); and a transition from sandy gravel to silty fine sand. The results are provided in Section 3.2.

Figure 2: Simulation domains for comparing USSBP results with CSSBP results in the same test facility with: (a) a permeable layer at 4.75 – 5.0 m, and (b) a soil transition from sandy gravel to silty fine sand at 5.0 m.
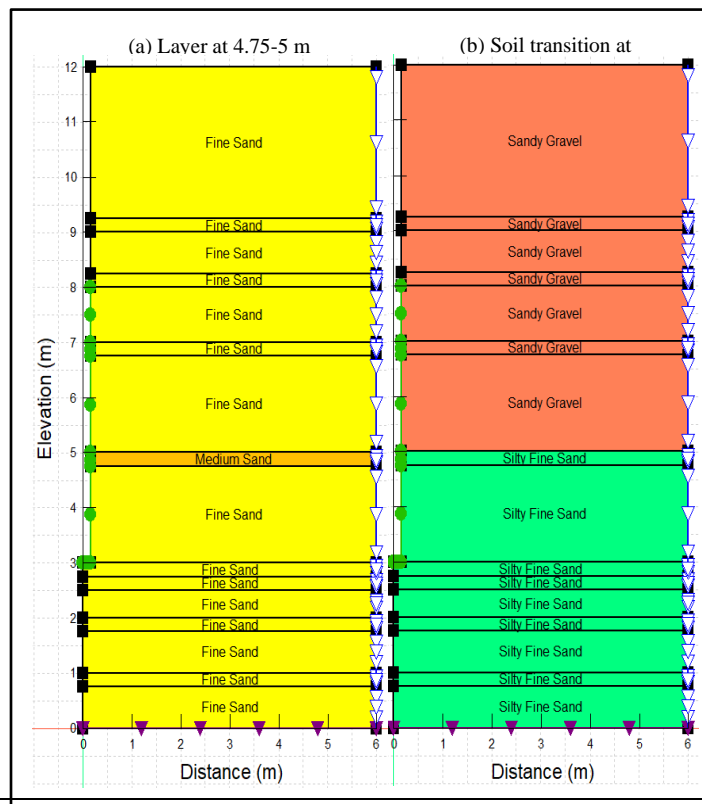
2.4 Groundwater Mounding Effects

Another purpose of this study was to determine how test results are impacted by the presence of shallow groundwater. Shallow groundwater is analogous to a perching layer because vertical migration of infiltrating water is impeded and a mound forms beneath the infiltration facility. If the mound rises high enough to intersect the infiltration facility, then the infiltration capacity of that facility is limited by the horizontal flow capacity of the saturated zone. The horizontal flow capacity is a function of K_s and the thickness of the saturated zone.

Stormwater regulations typically specify a minimum separation between the bottom of the infiltration facility and the seasonal high groundwater table. In Washington State, this separation ranges from 0.3 to 4.6 m (1 to 15 ft) depending on the size and type of infiltration facility. If some cases, groundwater mounding analysis is required to determine the size of the infiltration facility. Groundwater mounding analysis can be conducted using a numerical groundwater model that incorporates the time series of stormwater runoff flows (usually output from a hydrologic runoff model of the site), the dimensions of the proposed infiltration facility, and the hydrogeologic characteristics of the stratigraphy beneath the facility. The accuracy of groundwater mounding analysis is determined by the ability to accurately represent the subsurface conditions, which requires subsurface exploration and testing. Characterizing the subsurface can be expensive and groundwater mounding analysis is generally not warranted for small sites. For smaller sites, the potential effects of groundwater mounding can be approximated using correction factors.

The groundwater mounding analysis included comparison of simulated pit test results (assuming a radius of 1 m) with simulated results for larger infiltration facilities with radii of 2 and 4 m. The infiltration facility with a radius of 2 m was intended to represent a small single-family residential project and the infiltration facility with a radius of 4 m was intended to represent a commercial or roadway project. The three facilities were simulated for different initial depths to groundwater, including 0.25, 0.5, 0.75, 1, 2, 3, and 4 m, and an aquifer thickness of 1 m. Simulations were also conducted for different aquifer thicknesses with the depth to groundwater remaining fixed at 0.25 m. All the infiltration simulations assumed a fixed-head boundary condition of 0.25 m within the infiltration facility and a 6-hr test.

Figure 3 shows the axisymmetric numerical domains for the three facilities with three different depths to groundwater. Three aquifer materials were simulated: silty Qva with $K_s = 0.5$ m/d, fine sand with $K_s = 3.0$ m/d, and sandy gravel with $K_s = 30$ m/d. Qvt was assumed to underlie the aquifer material and the bottom of the domain was defined as a no-flow boundary condition. The outer boundary of the axisymmetric domain (the right-hand side) was defined as a fixed-head boundary condition.

For most of the simulations, the initial conditions were established by conducting a steady-state simulation with no flow from the infiltration facility. The challenge with steady-state simulations is that they allow the soil above the capillary fringe to completely drain to the residual moisture content. As shown in Figures 3(a) and 3(b), the capillary fringe rises at least 1 m above the water table using the steady-state approach. The water content above the capillary fringe is less than 5%. For fine sand and sandy gravel simulations with a deep-water table the capillary fringe is well below the bottom of the infiltration facility and the numerical model had difficulty simulating the flow of water into such dry soils. This challenge was overcome by conducting a transient simulation that allowed water to flow in from the outer boundary (the right-hand side) until a relatively flat-water table was established. The results of this approach are illustrated on Figure 3(c) for a water table that is 4 m below the bottom of the infiltration facility. As shown in the figure, the moisture content near the bottom of the infiltration facility is still in the range of 5-10%, wet enough to eliminate the numerical challenges. The results are provided in Section 3.3.

Figure 3: Numerical domains and initial conditions for conducting groundwater mounding simulations in facilities with: (a) $r = 1$ m and depth to groundwater = 0.25 m, (b) $r = 2$ m and depth to groundwater = 1.0 m, and (c) $r = 3$ m and depth to groundwater = 4.0 m.
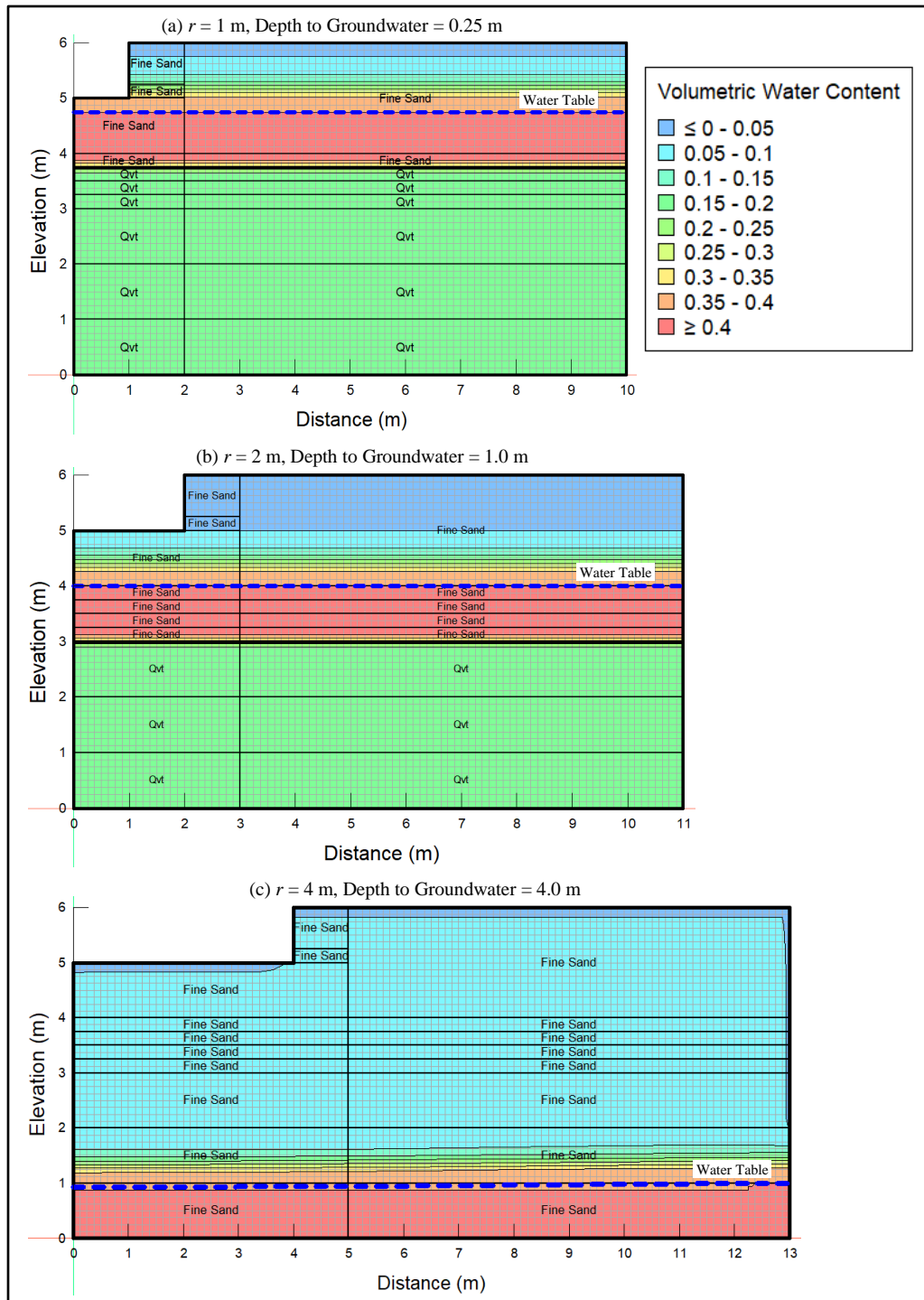
2.5 Numerical Simulations of USSBP and CSSBP Field Tests

If the soils in the test intervals are uniform and isotropic, USSBP and CSSBP tests in the same test well would provide similar estimates of K_b, although some differences would occur due to analytical error. In practice, however, these methods often provided significantly different estimates of K_b in the same test well. In general, the CSSBP estimates of K_b were higher than the USSBP estimates, up to 250% higher in the shallow test wells (Volume IV) and up to 84% higher in the deep test wells (Volume V). One purpose of the layering and mounding analysis was to explain these differences. In addition to the general layering and groundwater mounding simulations described above, numerical simulations of the field tests in VP-V-3, NG-B-201, and U-TW-9 were conducted to identify stratigraphic conditions that could explain the difference between the USSBP and CSSBP results in these wells. These test wells were selected because the USSBP and CSSBP tests provided significantly different estimates of K_b (the CSSBP estimate was 126% higher in VP-V-3, 49% higher in NG-B-201, and 84% higher in U-TW-9).

The numerical simulations were conducted using a numerical representation of the constructed well (including well casing, sandpack, and bentonite seal) and injecting water into the well at the rates recorded during the field tests. The initial stratigraphy in the numerical simulations was designed to generally match the stratigraphy observed during drilling of the wells. The stratigraphy was then modified during numerous simulations until an acceptable match was achieved between the observed head elevations and the simulated head elevations.

3   Results

3.1   Layering Effects on USSBP Well and Pit Tests

As discussed in Section 2.2, the effects of layering on USSBP well and pit tests were evaluated by simulating two different shallow test well configurations and a pit test in four combinations of a primary soil and a contrasting perching or permeable layer. The effects of the layer were evaluated in successive simulations by locating the perching/permeable layer at different elevations within the test domain.

Figures 4 and 5 show example results when the test facilities are completed in fine-coarse Qva ($K_s = 5.0$ m/d) with a perching layer of fine Qva ($K_s = 2.0$ m/d) and silty Qva ($K_s = 0.5$ m/d), respectively. For these examples, the perching layer is at the bottom of the test pit and result in K_b estimates ranging from 1.2 m/d to 4.7 m/d, lower than the 5.0 m/d of the primary soil type. In both stratigraphic scenarios, the well tests provide a higher estimate of K_b than the pit test.

Figures 6 and 7 show example results when the test facilities are completed in fine sand ($K_s = 3.0$ m/d) with a permeable layer of medium sand ($K_s = 10$ m/d) and sandy gravel ($K_s = 30$ m/d), respectively. For these examples, the permeable layer is located at the bottom of the test pit and result in K_b estimates ranging from 3.6 m/d to 7.0 m/d, higher than the 3.0 m/d of the primary soil type. The test well completed below the pit bottom provides a lower estimate of K_b than the pit test while the test well completed above the pit bottom provides a higher estimate of K_b than the pit test.

Figures 8 through 11 show how K_b varies for the three test facilities with the perching or permeable layer located at different elevations relative to the test interval for the four stratigraphic scenarios. The location of the test pit bottom and the test well intervals are shown on the figures. K_b varies significantly depending on the location of the perching or permeable layer. In particular, there is a very abrupt change in K_b when the perching layer is positioned near the bottom of the test pit (Figure 9) and the permeable layer is positioned near the bottom of the test well (Figure 11).

Figures 8 through 11 also allow comparison of the test well and test pit results for the same stratigraphic scenarios, i.e., when the elevation of the perching/permeable layer is the same. The difference between the test well results and the test pit results is expressed using the test well to test pit correction factor (CF_w), defined as follows:

$$CF_w = \frac{K_b^p}{K_b^{uw}}$$

K_b^p = Test pit bulk hydraulic conductivity

K_b^{uw} = Uncased test well bulk hydraulic conductivity

Figure 8 shows the simulation results for fine-coarse Qva ($K_s = 5.0$ m/d) with a perching layer of fine Qva ($K_s = 2.0$ m/d) (a permeability contrast of 2.5). When the test well is completed at and below the bottom of the test pit (Figure 8a) CF_w ranges from a low of 0.67 when the perching layer is near the bottom of the test pit to a high of 1.15 when the perching layer is near the bottom of the test well. When the test well is completed above the bottom of the test pit (Figure 8b) CF_w ranges from a low of 0.80 when the perching layer is just below the bottom of the test pit to a high of 1.16 when the perching layer is above the bottom of the test pit.

Figure 9 shows the same simulation results for fine-coarse Qva ($K_s = 5.0$ m/d) with a perching layer of silty Qva ($K_s = 0.5$ m/d) (a permeability contrast of 10). Comparison of Figures 4 and 5 indicates more horizontal spreading with the lower permeability perching layer and comparison of Figures 8 and 9 indicates a significantly greater range in CF_w with the greater permeability contrast. When the test well is completed at and below the bottom of the test pit (Figure 9a) CF_w ranges from a low of 0.26 when the perching layer is near the bottom of the test pit to a high of 1.18 when the perching layer is near the bottom of the test well. When the test well is completed above the bottom of the

test pit (Figure 9b) CF_w ranges from a low of 0.42 when the perching layer is just below the bottom of the test pit to a high of 1.36 when the perching layer is above the bottom of the test pit.

Figure 10 shows the simulation results for fine sand (K_s = 3.0 m/d) with a permeable layer of medium sand (K_s = 10 m/d) (a permeability contrast of 3.3). When the test well is completed at and below the bottom of the test pit (Figure 10a) CF_w ranges from a low of 0.65 when the permeable layer is at the bottom of the test well to a high of 1.07 when the permeable layer is just below the bottom of the test pit. When the test well is completed above the bottom of the test pit (Figure 10b) CF_w ranges from a low of 0.69 when the permeable layer is above the bottom of the test pit to a high of 0.97 when the permeable layer is below the bottom of the test pit.

Figure 11 shows the simulation results for fine sand (K_s = 3.0 m/d) with a permeable layer of sandy gravel (K_s = 30 m/d) (a permeability contrast of 10). When the test well is completed at and below the bottom of the test pit (Figure 11a) CF_w ranges from a low of 0.37 when the permeable layer is at the bottom of the test well to a high of 1.11 when the permeable layer is just below the bottom of the test pit. When the test well is completed above the bottom of the test pit (Figure 11b) CF_w ranges from a low of 0.44 when the permeable layer is above the bottom of the test pit to a high of 0.99 when the permeable layer is below the bottom of the test pit.

Although the discussion thus far has focused on comparison of test pit results with test well results, it's important to recognize that minor changes in the elevation of the test facility relative to a perching or permeable layer can result in major changes in K_b, even for the same type of facility. The example shown in Figure 12 demonstrates that a 0.25 m change in the elevation of the perching layer can change the test pit K_b results from 4.5 m/d to 1.2 m/d. Table 3 summarized the K_b range for the three test facilities and the four stratigraphic combinations with the perching/permeable layer at different elevations within the test domain. The largest K_b range (1.2 to 5.1 m/d) is for the test pit with a primary soil of F-C Qva and a perching layer of silty Qva. In general, test pits are more affected by perching layers and test wells are more affected by permeable layers.

Table 3: K_b range for a test pit and two different shallow test wells with the perching or permeable layer at different elevations within the test domain.

Primary Stratigraphy with K_s (m/d)	Perching/ Permeable Layer with K_s (m/d)	K_b Range (m/d)		
		Test Pit	**Test well completed below test pit bottom**	**Test well completed above test pit bottom**
Fine-Coarse Qva (5)	Fine Qva (2)	3.2 - 5.2	3.9 – 5.0	3.9 – 4.9
Fine-coarse Qva (5)	Silty Qva (0.5)	1.2 – 5.1	2.8 – 5.0	2.8 – 4.9
Fine Sand (3)	Medium sand (10)	2.7 – 3.9	3.1 – 4.4	3.1 – 4.4
Fine Sand (3)	Sandy gravel (30)	2.7 – 5.4	3.1 – 7.4	3.1 – 7.4

Figure 4: Simulation results for fine-coarse Qva ($K_s = 5.0$ m/d) with a layer of fine Qva ($K_s = 2.0$ m/d) at an elevation of 3.75 – 4.0 m for three test facilities: (a) a test pit, (b) a test well completed primarily below the pit elevation, and (c) a test well completed above the pit. Results shown for the end of the USSBP test at 6 hr.
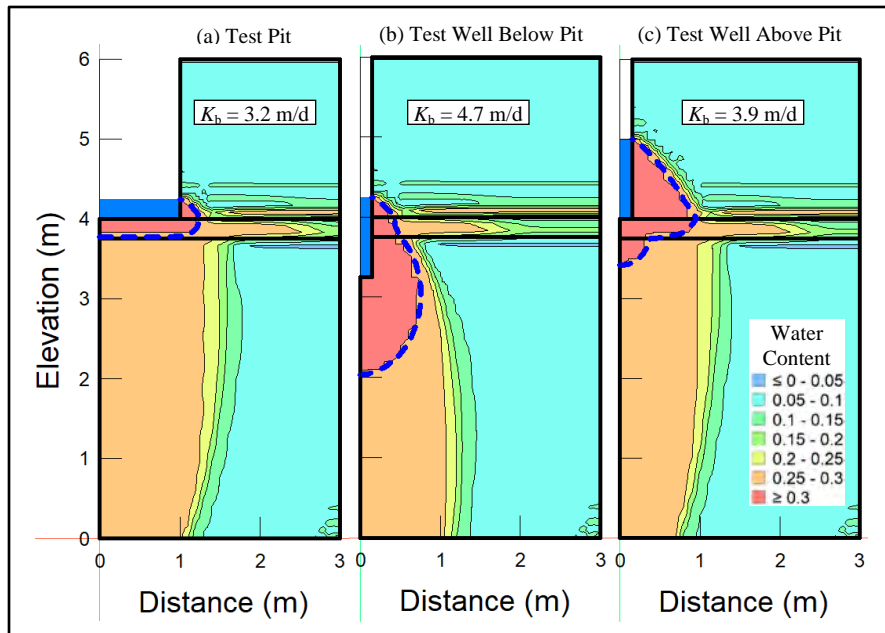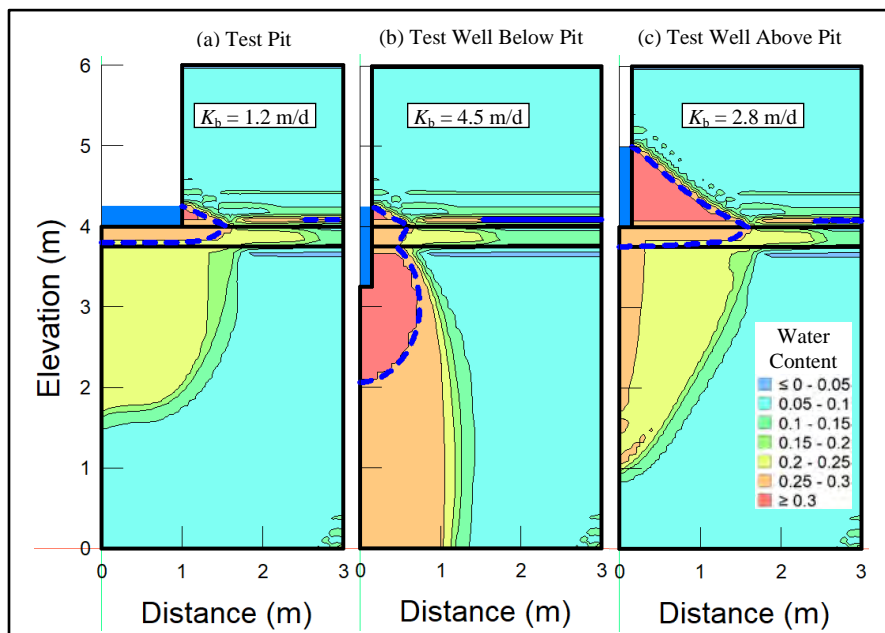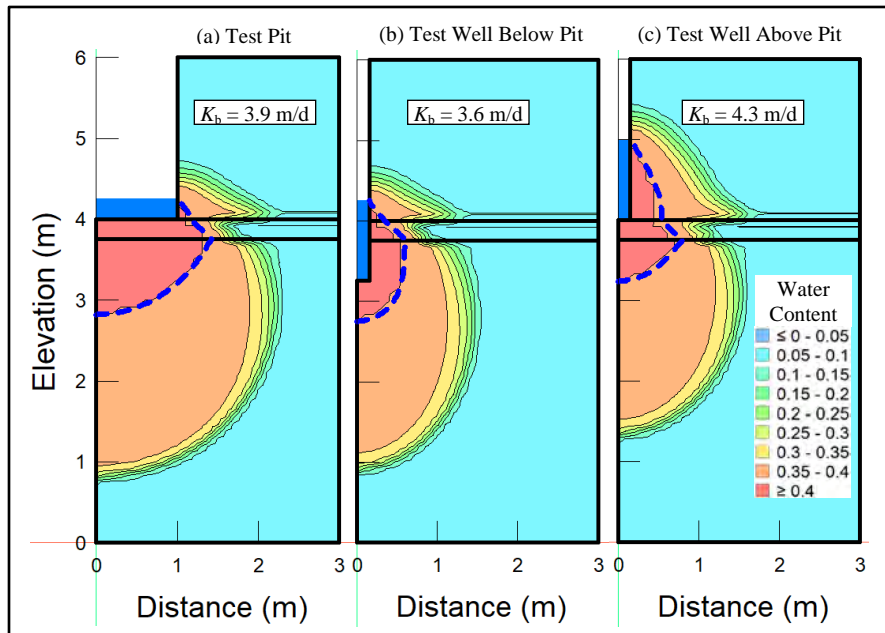

Figure 5: Simulation results for fine-coarse Qva ($K_s = 5.0$ m/d) with a layer of silty Qva ($K_s = 0.5$ m/d) at an elevation of 3.75 – 4.0 m for three test facilities: (a) a test pit, (b) a test well completed primarily below the pit elevation, and (c) a test well completed above the pit. Results shown for the end of the USSBP test at 6 hr.

Figure 6: Simulation results for fine sand (K_s = 3.0 m/d) with a layer of medium sand (K_s = 10 m/d) at an elevation of 3.75 – 4.0 m for three test facilities: (a) a test pit, (b) a test well completed primarily below the pit elevation, and (c) a test well completed above the pit. Results shown for the end of the USSBP test at 6hr.

Figure 7: Simulation results for fine sand (K_s = 3.0 m/d) with a layer of sandy gravel (K_s = 30 m/d) at an elevation of 3.75 – 4.0 m for three test facilities: (a) a test pit, (b) a test well completed primarily below the pit elevation, and (c) a test well completed above the pit. Results shown for the end of the USSBP test at 6 hr.
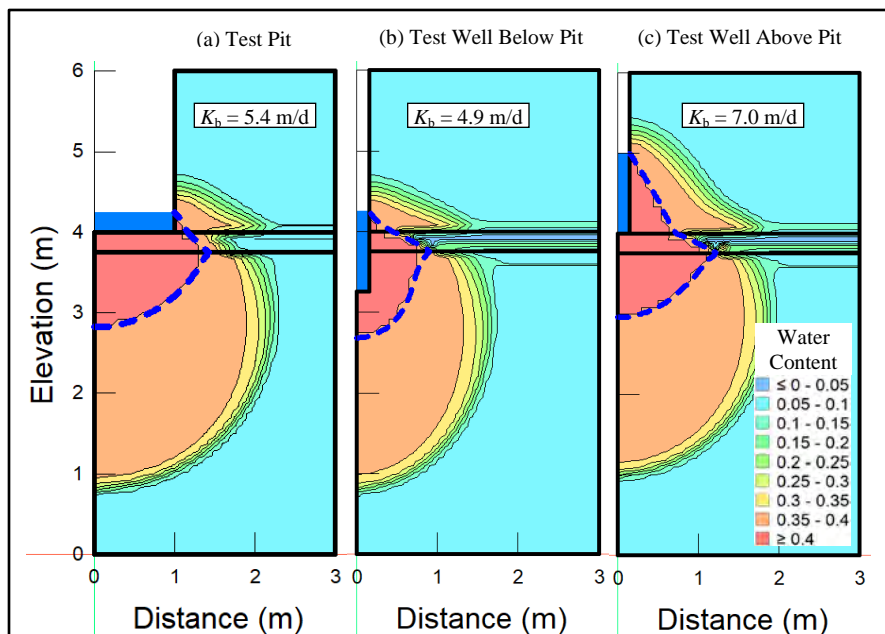
Figure 8: Comparison of perching layer effects on USSBP results for a fine-coarse Qva (K_s = 5.0 m/d) with a layer of fine Qva (K_s = 2.0 m/d) that is positioned at elevations between 1.0 m and 5.0 m above the bottom of the domain. Test pit results compared with two test wells completed over different intervals: (a) below the test pit bottom, and (b) above the test pit bottom.
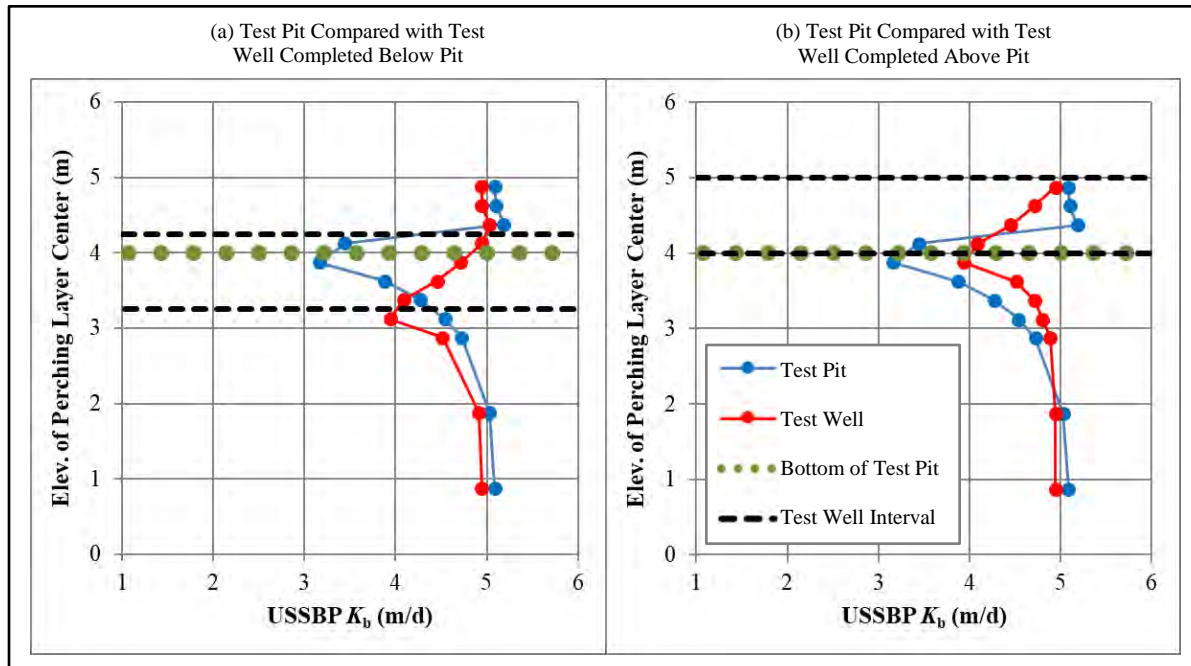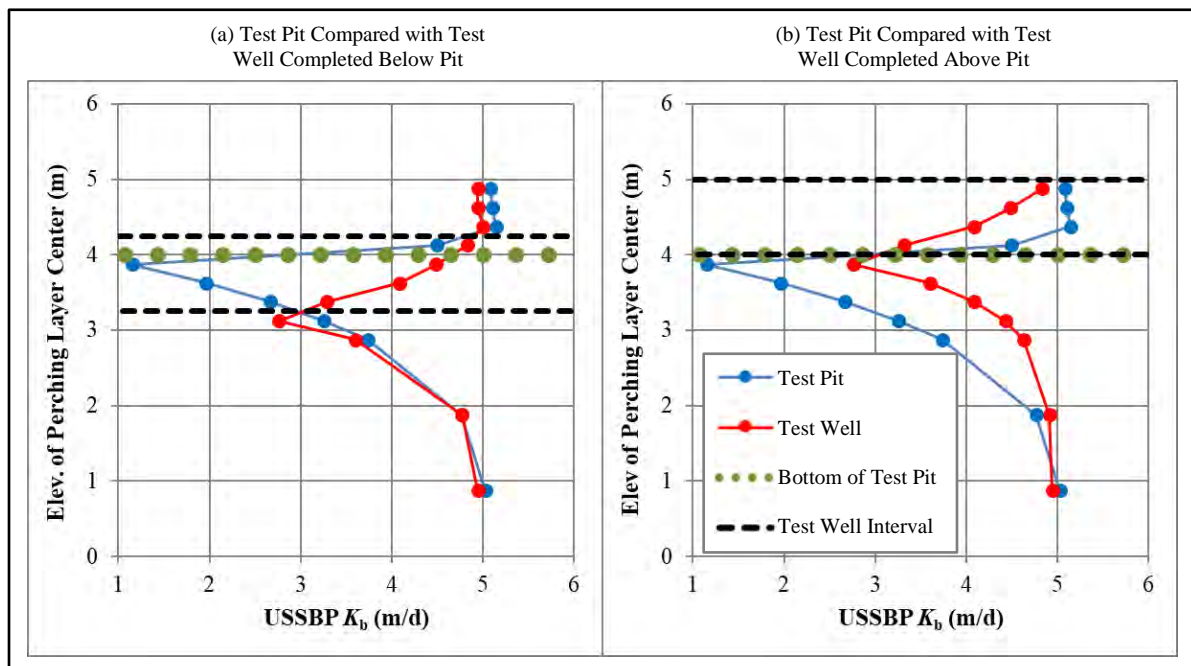

Figure 9: Comparison of perching layer effects on USSBP results for a fine-coarse Qva (K_s = 5.0 m/d) with a layer of silty Qva (K_s = 0.5 m/d) that is positioned at elevations between 1.0 m and 5.0 m above the bottom of the domain. Test pit results compared with two test wells completed over different intervals: (a) below the test pit bottom, and (b) above the test pit bottom.
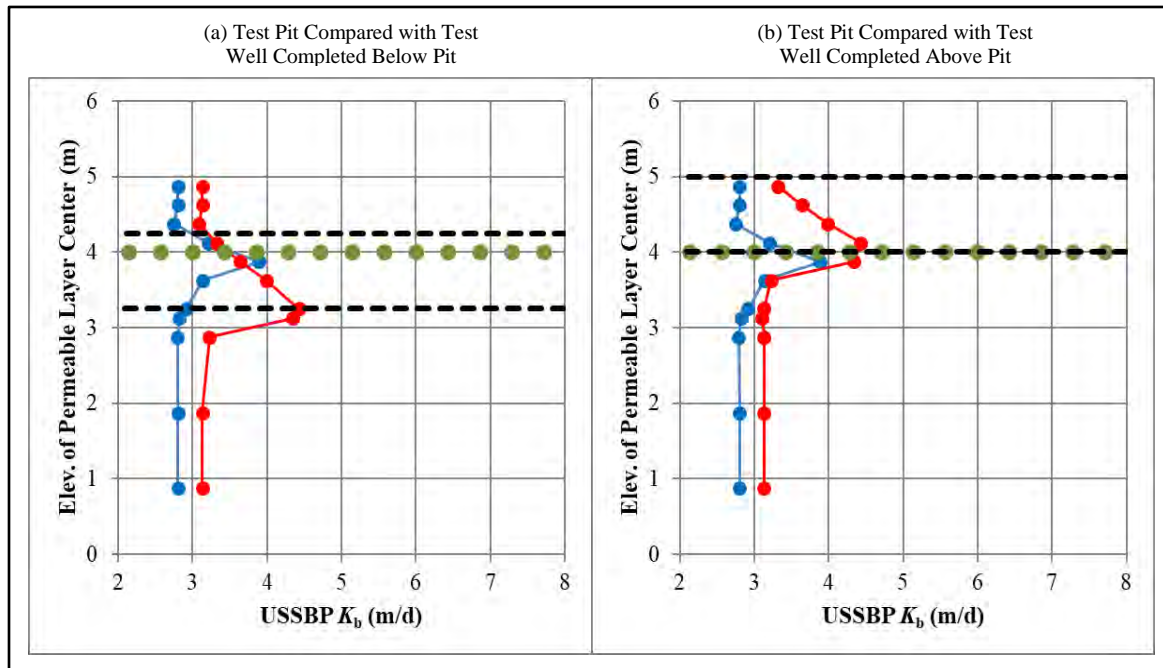
Figure 10: Comparison of permeable layer effects on USSBP results for a fine sand (K_s = 3.0 m/d) with a layer of medium sand (K_s = 10 m/d) that is positioned at elevations between 1.0 m and 5.0 m above the bottom of the domain. Test pit results compared with two test wells completed over different intervals: (a) below the test pit bottom, and (b) above the test pit bottom.
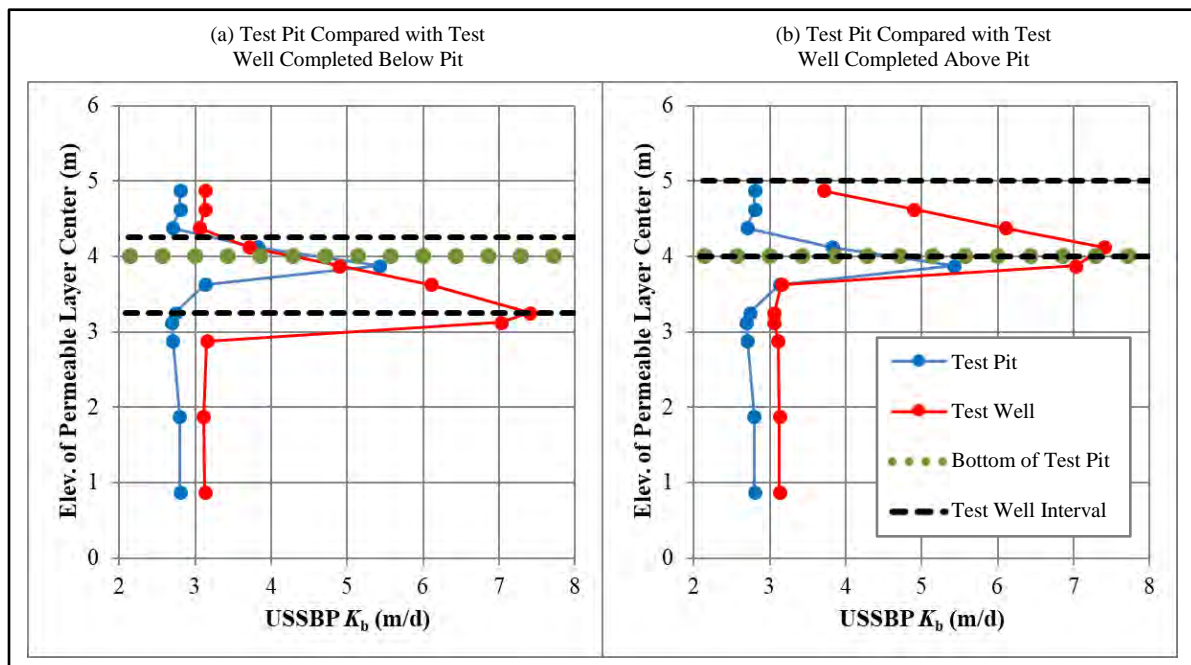

Figure 11: Comparison of permeable layer effects on USSBP results for a fine sand (K_s = 3.0 m/d) with a layer of sandy gravel (K_s = 30 m/d) that is positioned at elevations between 1.0 m and 5.0 m above the bottom of the domain. Test pit results compared with two test wells completed over different intervals: (a) below the test pit bottom, and (b) above the test pit bottom.
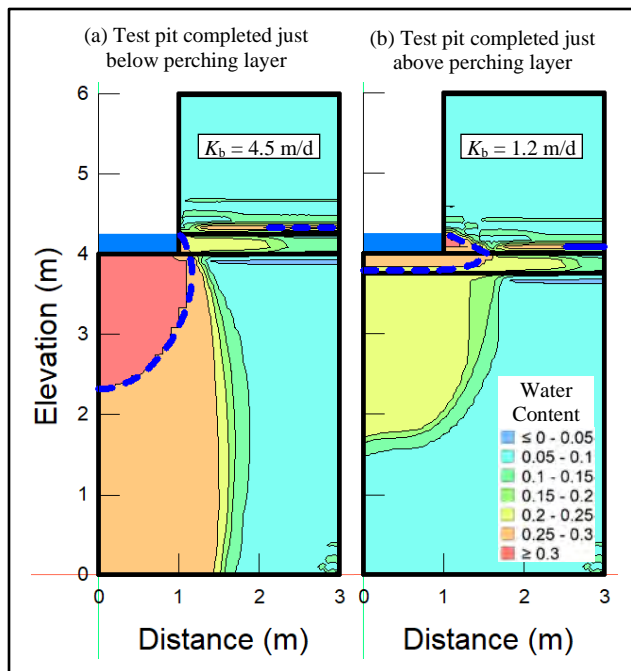
Figure 12: Comparison of USSBP results for a fine-coarse Qva ($K_s = 5.0$ m/d) with a layer of silty Qva ($K_s = 0.5$ m/d) with the bottom of the test pit: (a) just below the perching layer, and (b) just above the perching layer.

3.2 Layering Effects on USSBP and CSSBP Tests

As discussed in Section 2.3, the effects of layering on USSBP and CSSBP tests was evaluated by simulating both tests in the same test well configurations by locating either a thin perching or permeable layer at different elevations within the test domain. Additional comparisons were conducted by locating a transition from one soil type to another soil type at different elevations within the test domain.

Figure 13 shows example results when the test facilities are completed in fine-coarse Qva (K_s = 5.0 m/d) with a perching layer of fine Qva (K_s = 2.0 m/d) at the bottom of the sandpack. The perching layer at this elevation provides K_b estimates of 4.5 m/d for the USSBP test and 5.1 m/d for the CSSBP test. Figure 14 shows example results when the test facilities are completed in fine-coarse Qva with a perching layer of silty Qva (K_s = 0.5 m/d). Decreasing the permeability of the perching layer provides K_b estimates of 4.0 m/d for the USSBP test and 4.7 m/d for the CSSBP test.

Figure 15 show results when the test facilities are completed in fine sand (K_s = 3.0 m/d) with a permeable layer of medium sand (K_s = 10 m/d) near the top of the sandpack. The permeable layer at this elevation provides K_b estimates of 3.2 m/d for the USSBP test and 3.6 m/d for the CSSBP test. Figure 16 show results when the test facilities are completed in fine sand with a permeable layer of sandy gravel (K_s = 30 m/d) near the top of the sandpack. Increasing the permeability of the permeable layer provides K_b estimates of 3.5 m/d for the USSBP test and 4.3 m/d for the CSSBP test.

Figures 17 and 18 show how K_b varies for the USSBP and CSSBP tests with the perching or permeable layer at different elevations relative to the test interval for the four stratigraphic scenarios. The elevation of the test well interval is shown on the figures. K_b varies depending on the elevation of the perching or permeable layer, although the variability is significantly less than for the shorter test wells (shown on Figures 8-11). For a perching layer (Figure 17), the largest difference between the USSBP and CSSBP results occurs when the layer is at the bottom of the test well. For a permeable layer (Figure 18), the largest difference between the USSBP and CSSBP results occurs when the permeable layer is near the top of the test well. Table 4 compares the K_b range for the two different test methods and the four stratigraphic scenarios. The largest K_b range (3.1 – 4.7 m/d) is for the USSBP test well with a primary soil of fine sand and a permeable layer of sandy gravel. In general, USSBP tests are more affected by both perching and permeable layers than CSSBP tests.

Figure 19 show example results for a permeability transition scenario with sandy gravel (K_s = 30 m/d) above and silty fine sand (K_s = 0.25 m/d) below, and the transition occurring at an elevation of 7.0 m. As shown on the figure, the large difference in permeability for these soils results in a 5-fold difference in K_b results for the USSBP and CSSBP tests at this transition elevation. Figure 20a shows the USSBP and CSSBP K_b results for the same combination of soils as the transition elevations varies from 1.0 m to 8.0 m and Figure 20b shows the ratio USSBP K_b / CSSBP K_b for the same range of transition elevations. As shown in Figure 20b, the USSBP K_b / CSSBP K_b ratio reaches a minimum when the transition occurs near the top of the sandpack interval.

Table 4: K_b range for the USSBP and CSSBP tests in a deep test well with the perching or permeable layer at different elevations within the test domain.

Primary Stratigraphy with K_s (m/d)	Perching/ Permeable Layer with K_s (m/d)	K_b Range (m/d)	
		USSBP Test Well	**CSSBP Test Well**
Fine-Coarse Qva (5)	Fine Qva (2)	4.5 – 4.9	5.1 – 5.3
Fine-coarse Qva (5)	Silty Qva (0.5)	4.0 – 4.9	4.7 – 5.3
Fine Sand (3)	Medium sand (10)	3.1 – 3.6	3.3 – 3.7
Fine Sand (3)	Sandy gravel (30)	3.1 – 4.7	3.3 – 4.5

Figure 13: Simulation results for fine-coarse Qva (K_s = 5.0 m/d) with a perching layer of fine Qva (K_s = 2.0 m/d) at an elevation of 2.75 – 3.0 m for: (a) the USSBP test with H = 5.0 m, and (b) the CSSBP test with H = 15 m. Results shown for the end of the tests at 6 hr.
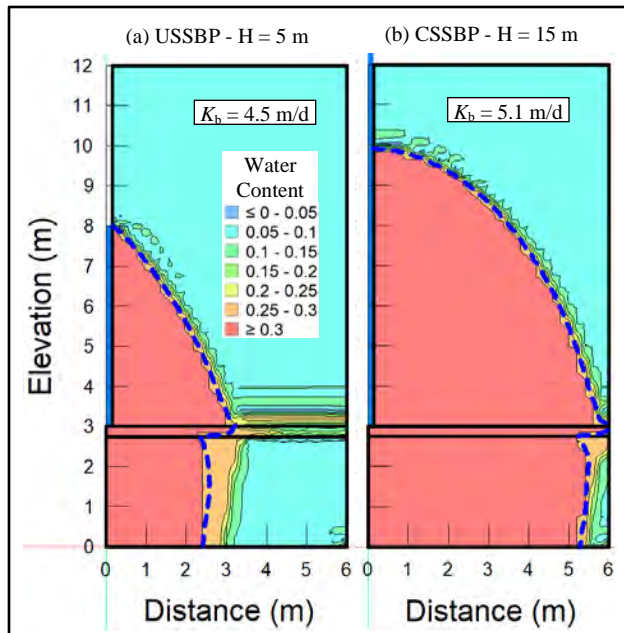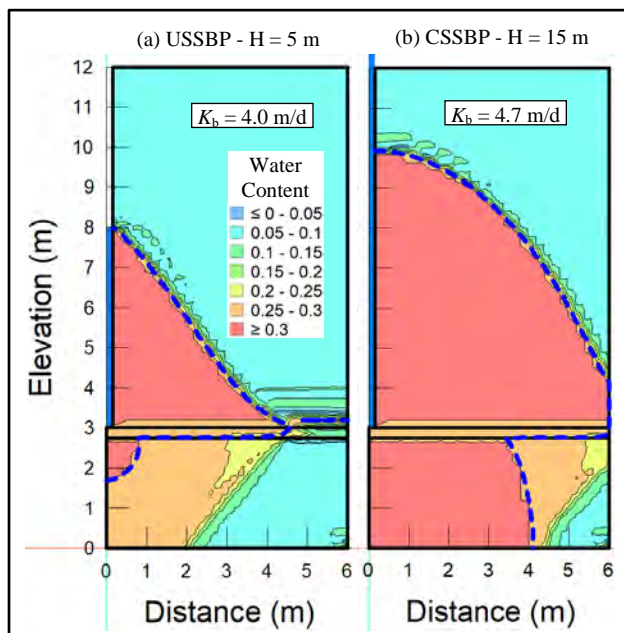

Figure 14: Simulation results for fine-coarse Qva (K_s = 5.0 m/d) with a perching layer of silty Qva (K_s = 0.5 m/d) at an elevation of 2.75 – 3.0 m for: (a) the USSBP test with H = 5.0 m, and (b) the CSSBP test with H = 15 m. Results shown for the end of the tests at 6 hr.

Figure 15: Simulation results for fine sand (K_s = 3.0 m/d) with a permeable layer of medium sand (K_s = 10 m/d) at an elevation of 6.75 – 7.0 m for: (a) the USSBP test with H = 5.0 m, and (b) the CSSBP test with H = 15 m. Results shown for the end of the tests at 6 hr.
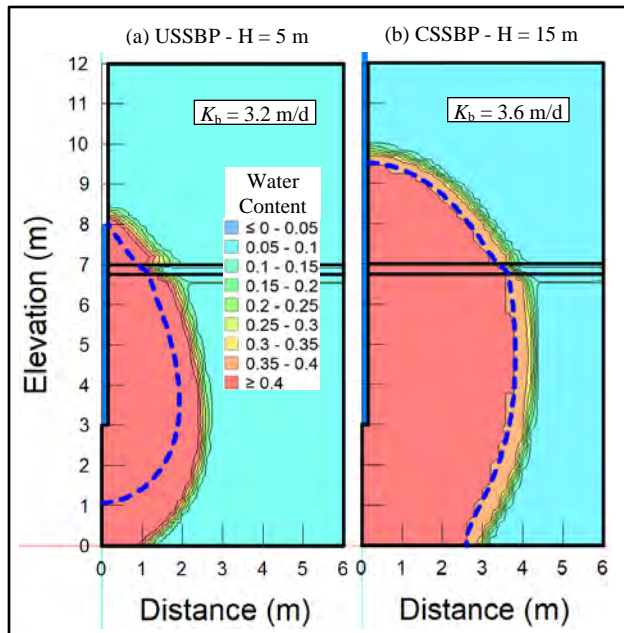

Figure 16: Simulation results for fine sand (K_s = 3.0 m/d) with a permeable layer of sandy gravel (K_s = 30 m/d) at an elevation of 6.75 – 7.0 m for: (a) the USSBP test with H = 5.0 m, and (b) the CSSBP test with H = 15 m. Results shown for the end of the tests at 6 hr.
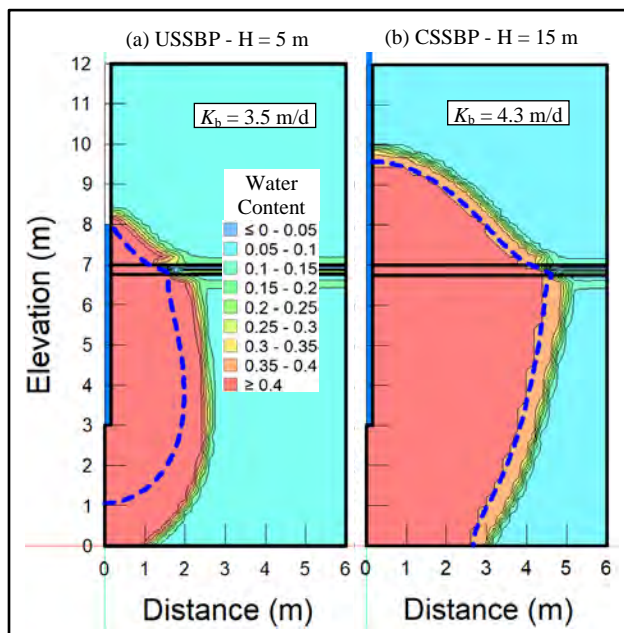
Figure 17: Comparison of perching layer effects on USSBP and CSSBP results for fine-coarse Qva ($K_s = 5.0$ m/d) with: (a) a layer of fine Qva ($K_s = 2.0$ m/d), and (b) a layer of silty Qva ($K_s = 0.5$ m/d), with the layer positioned at elevations between 1.0 m and 9.0 m above the bottom of the domain.
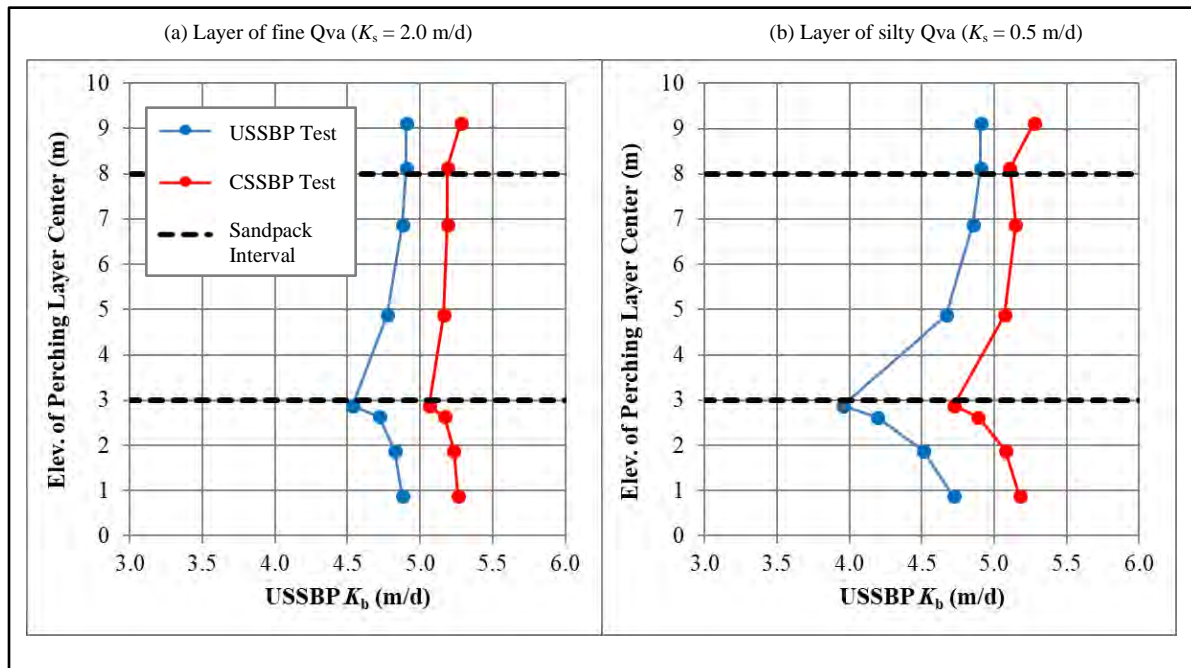

Figure 18: Comparison of permeable layer effects on USSBP and CSSBP results for fine sand ($K_s = 3.0$ m/d) with: (a) a layer of medium sand ($K_s = 10$ m/d), and (b) a layer of sandy gravel ($K_s = 30$ m/d), with the layer positioned at elevations between 1.0 m and 9.0 m above the bottom of the domain.
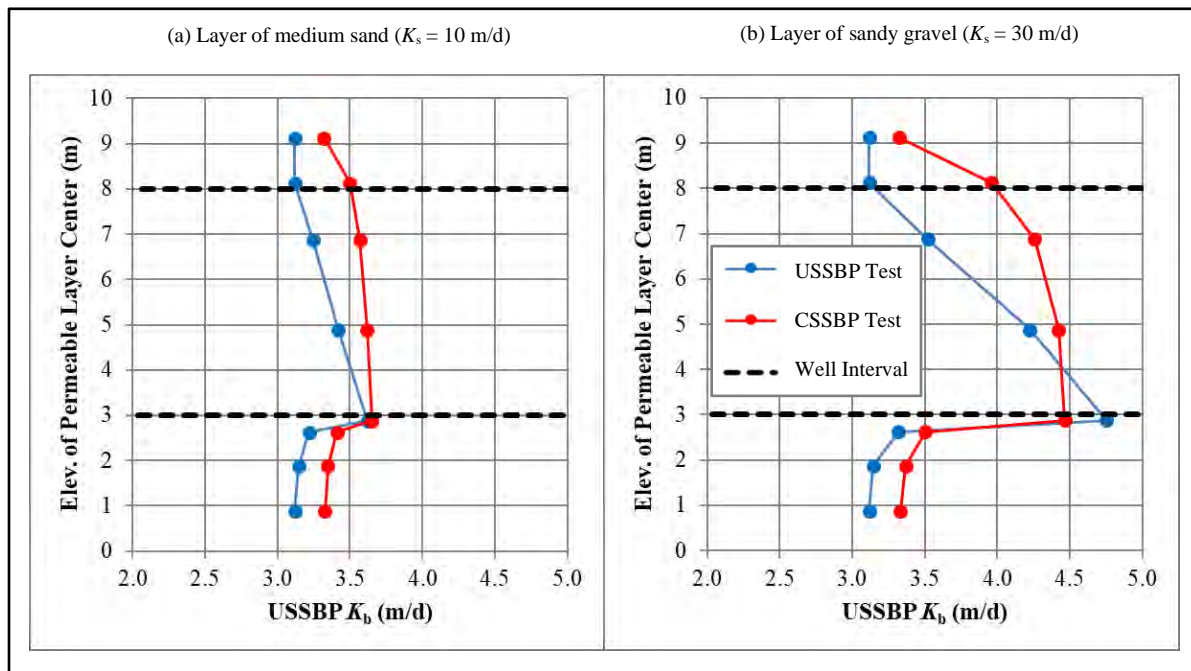
Figure 19: Simulation results for a transitional scenario with sandy gravel (K_s = 30 m/d) above and silty fine sand (K_s = 0.25 m/d) below, and the transition located at an elevation of 7.0 m. Results shown for the end of the tests at 6 hr.
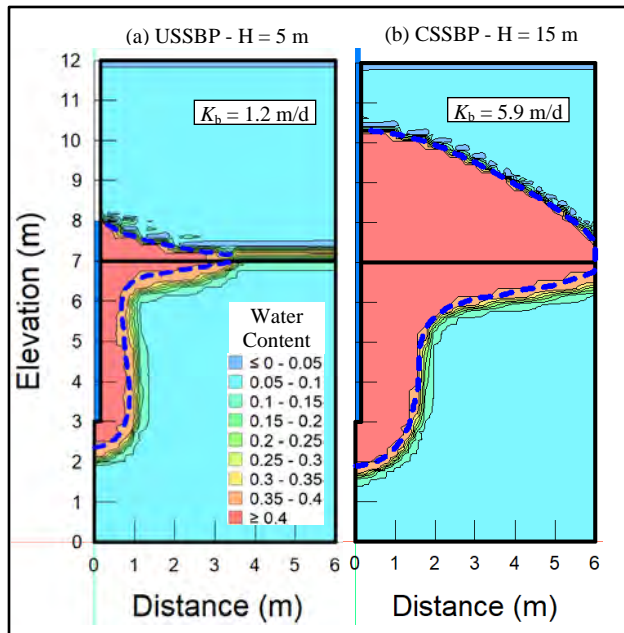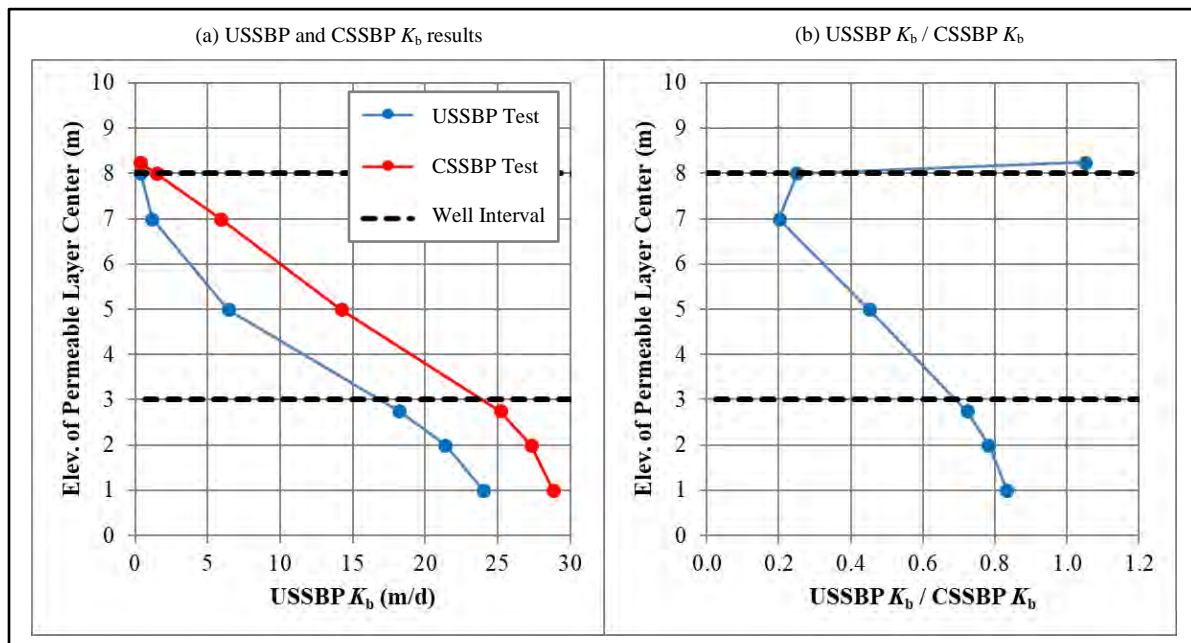

Figure 20: Comparison of USSBP and CSSBP results for a transition scenario with sandy gravel (K_s = 30 m/d) above and silty fine sand (K_s = 0.25 m/d) below, with the transition ranging from an elevation of 1.0 m to 8.0 m within the domain. Figure (a) shows USSBP and CSSBP K_b, and Figure (b) shows the ratio USSBP K_b / CSSBP K_b.

3.3 Groundwater Mounding Effects

As discussed in Section 2.4, the effects of groundwater mounding were evaluated by comparing simulated pit test results (assuming $r = 1$ m) with simulated results for hypothetical full-scale infiltration facilities with $r = 2$ and 4 m. Simulations were conducted for depth to groundwater ranging from 0.25 m to 4 m and three different soil types: silty Qva with $K_s = 0.5$ m/d, fine sand with $K_s = 3.0$ m/d, and sandy gravel with $K_s = 30$ m/d. Although groundwater mounding simulations are not provided for test wells, groundwater mounding would have similar impacts to the performance of operational drywells.

Figure 21 shows example results for fine sand with $r = 2$ m and three different depths to groundwater at the end of a 6-hr test. As indicated on the figure, K_b increases from 0.5 m/d when groundwater is 0.25 m below the bottom of the facility to 3.0 m/d when groundwater is 4 m below the bottom of the facility. As shown in Figure 21c, the infiltration zone of saturation does not extend to the groundwater table when groundwater is 4.0 m below the bottom of the facility. Since no mounding occurs in this scenario, groundwater has no effect on facility performance.

Figure 22 shows how K_b varies for three different sized infiltration facilities as a function of depth to groundwater for: (a) silty Qva ($K_s = 0.5$ m), (b) fine sand ($K_s = 3$ m), and (c) sandy gravel ($K_s = 30$ m). These results are based on 6-hr tests. These figures show that groundwater mounding has a significant impact on K_b and the reduction in K_b is greater as the size of the infiltration facility increases. In addition, comparison of the results for the three different soils shows that the reduction is greater for more permeable soils.

The reduction in K_b for larger infiltration facilities can be expressed using the mounding correction factor (CF_m), defined as follows:

$$CF_m = \frac{K_b^t}{K_b^o}$$

$K_b^t = $ Test bulk hydraulic conductivity

$K_b^o = $ Operational bulk hydraulic conductivity

Figure 23 shows how CF_m varies as a function of depth to groundwater for two operational facilities ($r = 2$ and 4 m) and the three soil types. Comparison of CF_m for the two different sized facilities shows that it decreases as the size of the facility increases. CF_m also decreases as the permeability of the soil increases and increases as the depth to groundwater increases. For these example scenarios, CF_m varies from 0.2 to 1 depending on the soil type, the size of the facility, and the depth to groundwater.

Although these mounding scenarios described above assumed an initial saturated aquifer thickness of 1 m, simulations with different saturated aquifer thicknesses demonstrated that the results were relatively insensitive to saturated aquifer thickness.

Figure 21: Groundwater mounding results for fine sand ($K_s = 3$ m/d) with $r = 2$ m and three different depths to groundwater: (a) 0.25 m, (b) 2.0 m, and (c) 4.0 m. Results shown for the end of the test at 6 hr.
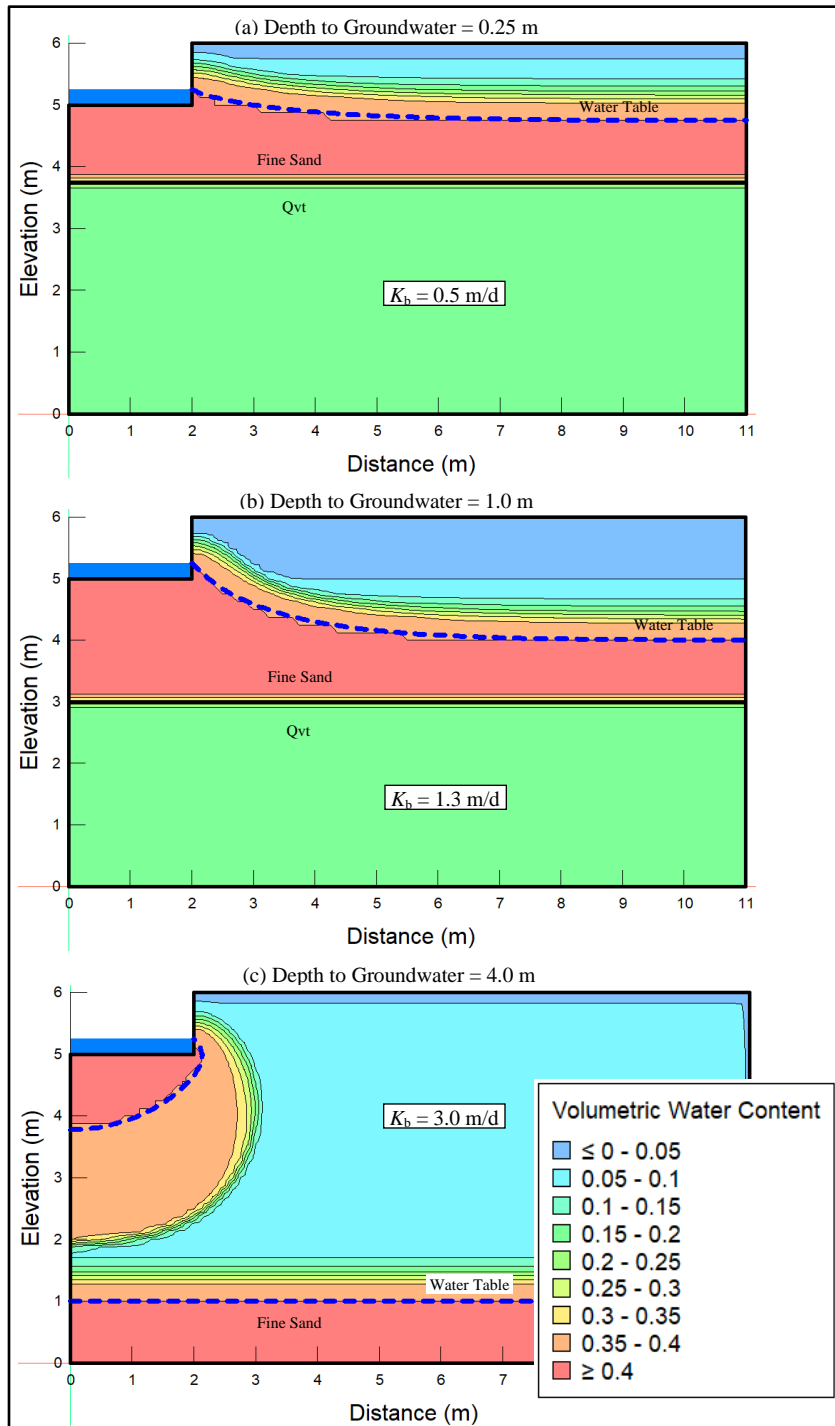
Figure 22: K_b for three different sized infiltration facilities as a function of depth to groundwater for: (a) silty Qva ($K_s = 0.5$ m/d), (b) fine sand ($K_s = 3$ m/d), and (c) sandy gravel ($K_s = 30$ m/d). Results shown for the end of the tests at 6 hr.

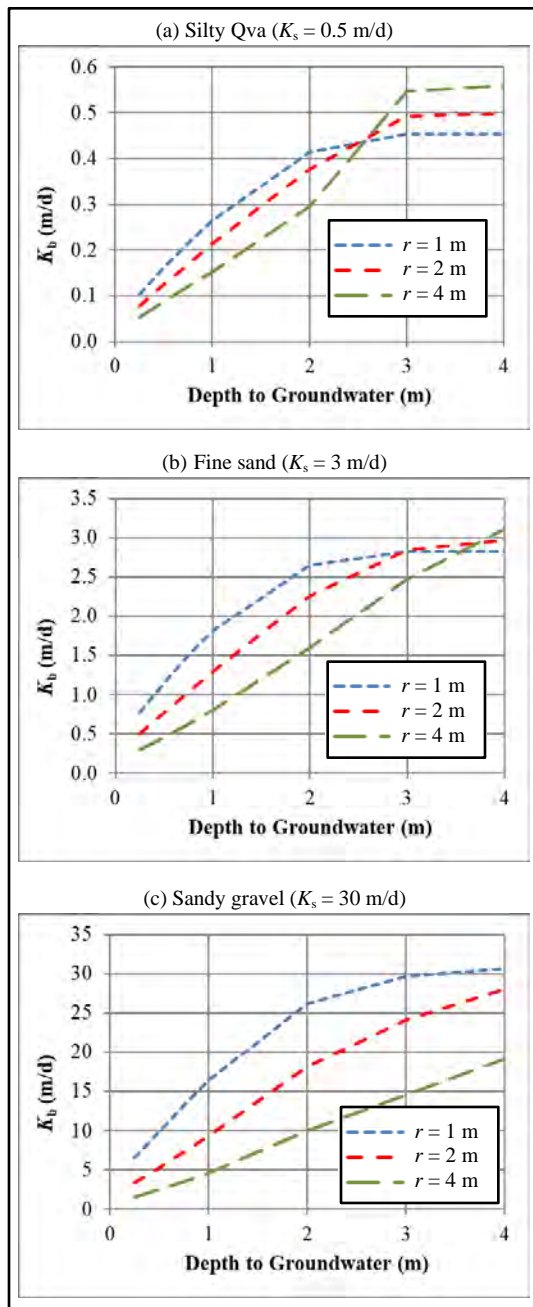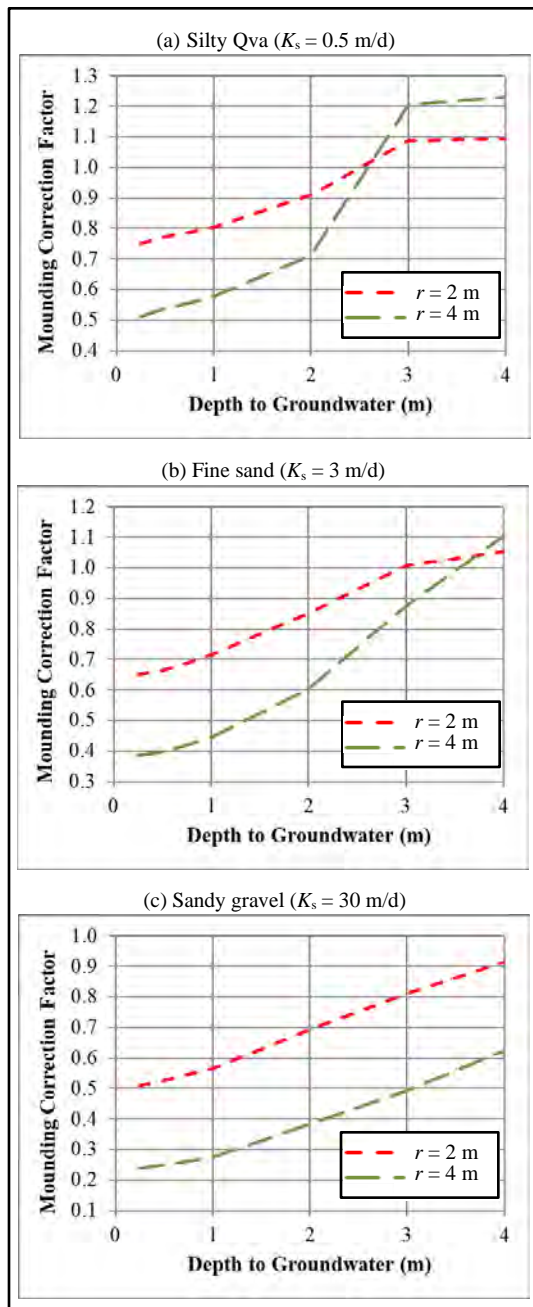**Figure 23**: Groundwater mounding correction factor for two different sized infiltration facilities as a function of depth to groundwater for: (a) silty Qva ($K_s = 0.5$ m/d), (b) fine sand ($K_s = 3$ m/d), and (c) sandy gravel ($K_s = 30$ m/d).

3.4 Numerical Simulation of USSBP and CSSBP Field Tests

As shown in previous sections, the K_b estimates based on USSBP and CSSBP field tests can be greatly influenced by layering and mounding. Unfortunately, a single steady-state test provides no information regarding the stratigraphy or groundwater mounding. If multiple steady-state tests with different head elevations are conducted, however, the results of these tests along with the falling head observations after the water is turned off can be used to calibrate a numerical simulation of the test facility. The examples provided below demonstrate how subsurface conditions observed during drilling can be modified within the numerical simulation until the calibrated model provides a reasonable match with the observed head conditions. Three field tests were calibrated: shallow well VP-V-3, deep well NG-B-201, and deep well U-TW-9.

The well log, test procedures, and test results for VP-V-3 are provided in Volume IV. This well was completed in advance outwash and was 3.1 m deep with 1.2 m of sandpack. The USSBP test provided a K_b estimate of 0.70 m/d and the CSSBP test provided a K_b estimate of 1.6 m/d. The simulated water content results at the end of the steady-state portion of the two tests are shown on Figures 24b and 24c and Figure 24a shows the calibrated stratigraphy for the test well. As shown on Figure 25, the match between the observed head and simulated head was very close for both tests. Based on this calibration (Figure 24a) the lower portion of the well is completed in a lower permeability material with $K_s = 0.22$ m/d and the upper portion of the well is completed in higher permeability materials with K_s of 5.0 and 7.0 m/d. The calibrated stratigraphy does not correlate particularly well with the well log as the advance outwash below 2.4 m was observed to contain less silt than the soil layers above 2.4 m. Generally, less silt would be associated with higher permeability.

The well log, test procedures, and test results for NG-B-201 are provided in Volume V. This well was completed in advance outwash and was 18.6 m deep with 7.0 m of sandpack. The USSBP test provided a K_b estimate of 4.5 m/d and the CSSBP test provided a K_b estimate of 6.7 m/d. The simulated water content results at the end of the steady-state portion of the two tests are shown on Figures 26b and 26c and Figure 26a shows the calibrated stratigraphy for the test well. As shown on Figure 27, the match between the observed head and simulated head was fairly close for both tests, although there was some deviation during the falling head portion of the CSSBP test after 450 min. Based on this calibration (Figure 26a), most of the lower portion of the well is completed in a lower permeability material with $K_s = 0.8$ m/d and the upper portion of the well is completed in higher permeability materials with K_s of 3.0 and 5.0 m/d. In addition, there was a relatively permeable layer ($K_s = 8.0$ m/d) at the base of the well. The calibrated stratigraphy does not correlate particularly well with the well log as the advance outwash was described as fairly uniform over the sandpack interval.

The well log, test procedures, and test results for U-TW-9 are provided in Volume V. This well was completed in advance outwash and was 22.6 m deep with 8.3 m of sandpack. The USSBP test provided a K_b estimate of 1.1 m/d and the CSSBP test provided a K_b estimate of 2.1 m/d. The simulated water content results at the end of the steady-state portion of the two tests are shown on Figures 28b and 28c and Figure 28a shows the calibrated stratigraphy for the test well. As shown on Figure 29, the match between the observed head and simulated head was fairly close during the steady-state portion of the test, although there was some deviation during the falling head portion of the tests. Based on this calibration (Figure 28a), most of the lower portion of the well is completed in a lower permeability material with $K_s = 0.5$ m/d and 0.8 m/d and the upper portion of the well is completed in higher permeability materials with K_s of 24 m/d. The calibrated stratigraphy does correlate particularly well with the well log as the advance outwash contained less silt in the upper 1.2 m of the sandpack interval.

Figure 24: Numerical simulation of VP-V-3 infiltration well test. (a) stratigraphy and Ks for each layer, (b) water content results at end of USSBP test, and (c) water content results at end of CSSBP test. Sandpack interval between -1.83 m and -3.05 m.

Figure 25: Comparison of observed and simulated head conditions for the VP-V-3 well tests: (a) USSBP test, and (b) CSSBP test.

Figure 26: Numerical simulation of NG-B-201 deep infiltration test. (a) stratigraphy and Ks for each layer, (b) water content results at end of USSBP test, and (c) water content results at end of CSSBP test. Sandpack interval between -11.6 m and -18.6 m.
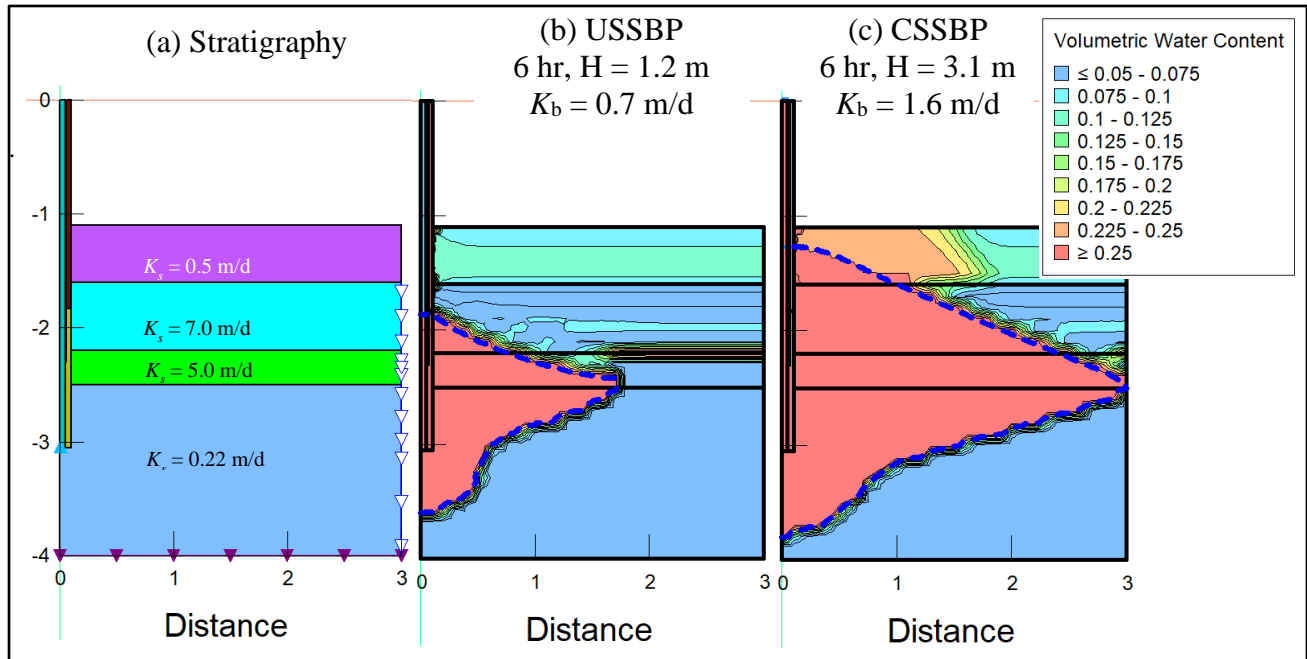
Figure 27: Comparison of observed and simulated head conditions for the NG-B-201 deep infiltration tests: (a) USSBP test, and (b) CSSBP test.
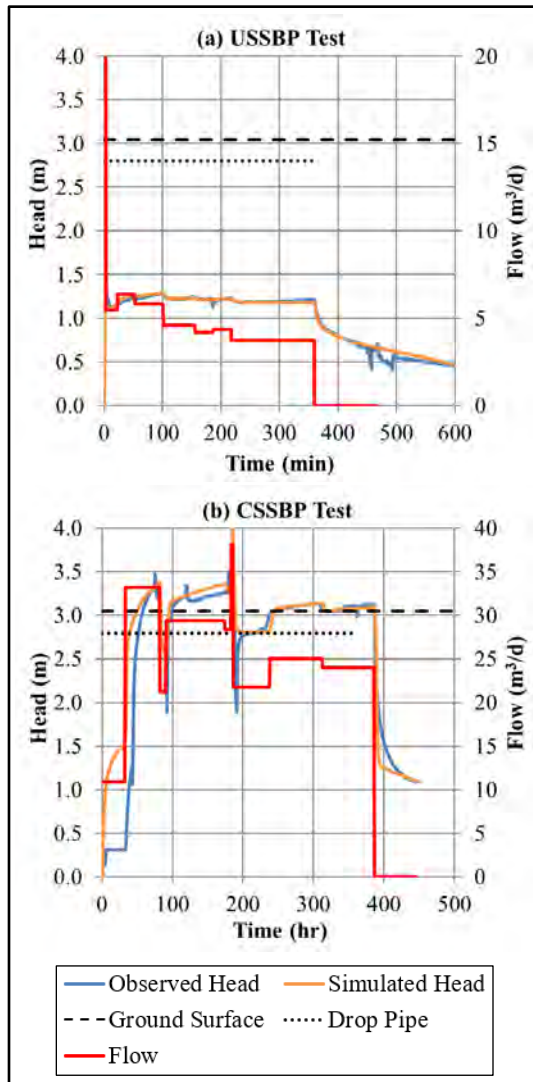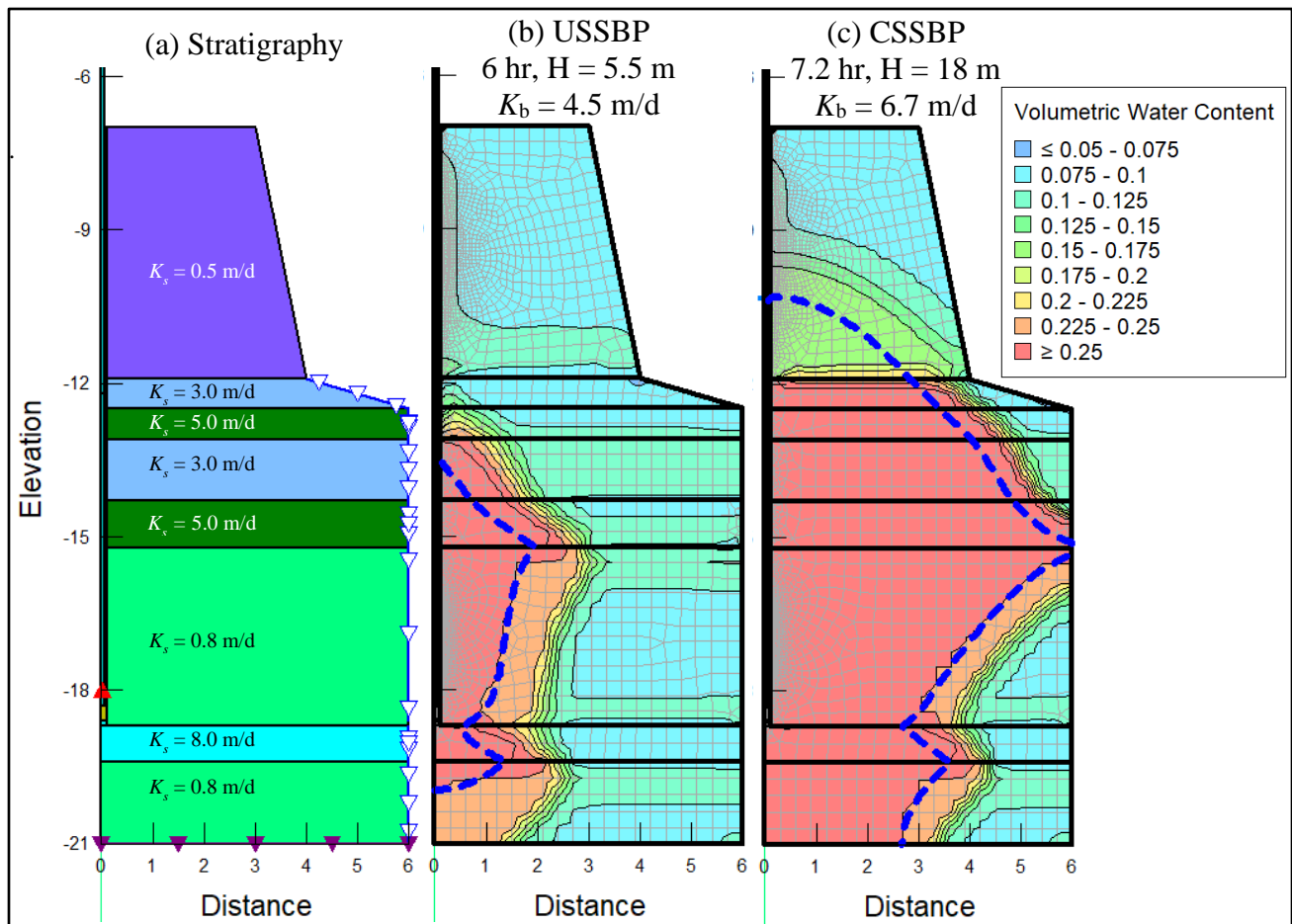
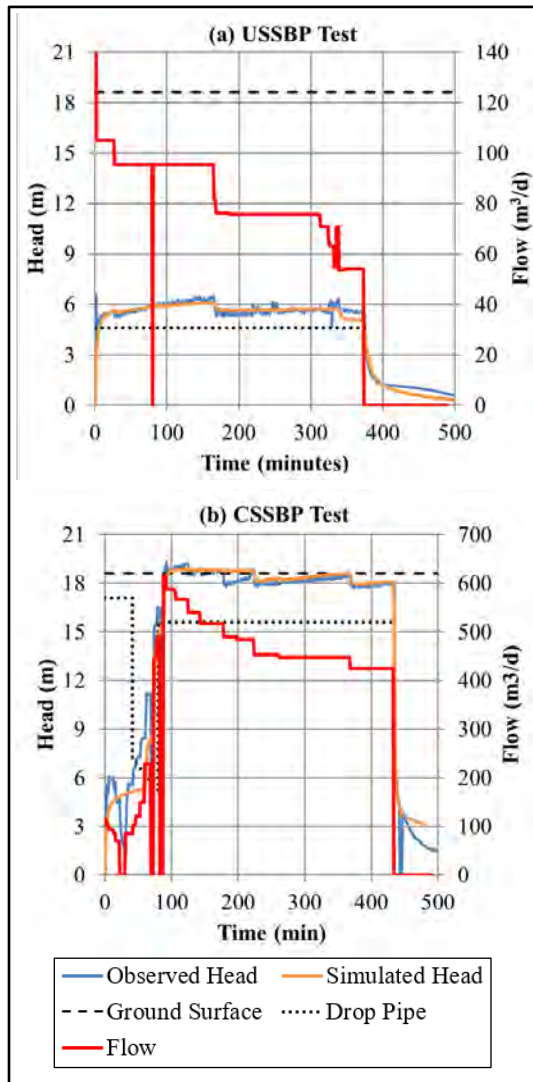**Figure 28**: Numerical simulation of U-TW-9 deep infiltration test. (a) stratigraphy and Ks for each layer, (b) water content results at end of USSBP test, and (c) water content results at end of CSSBP test. Sandpack interval between -14.3 m and -22.6 m.
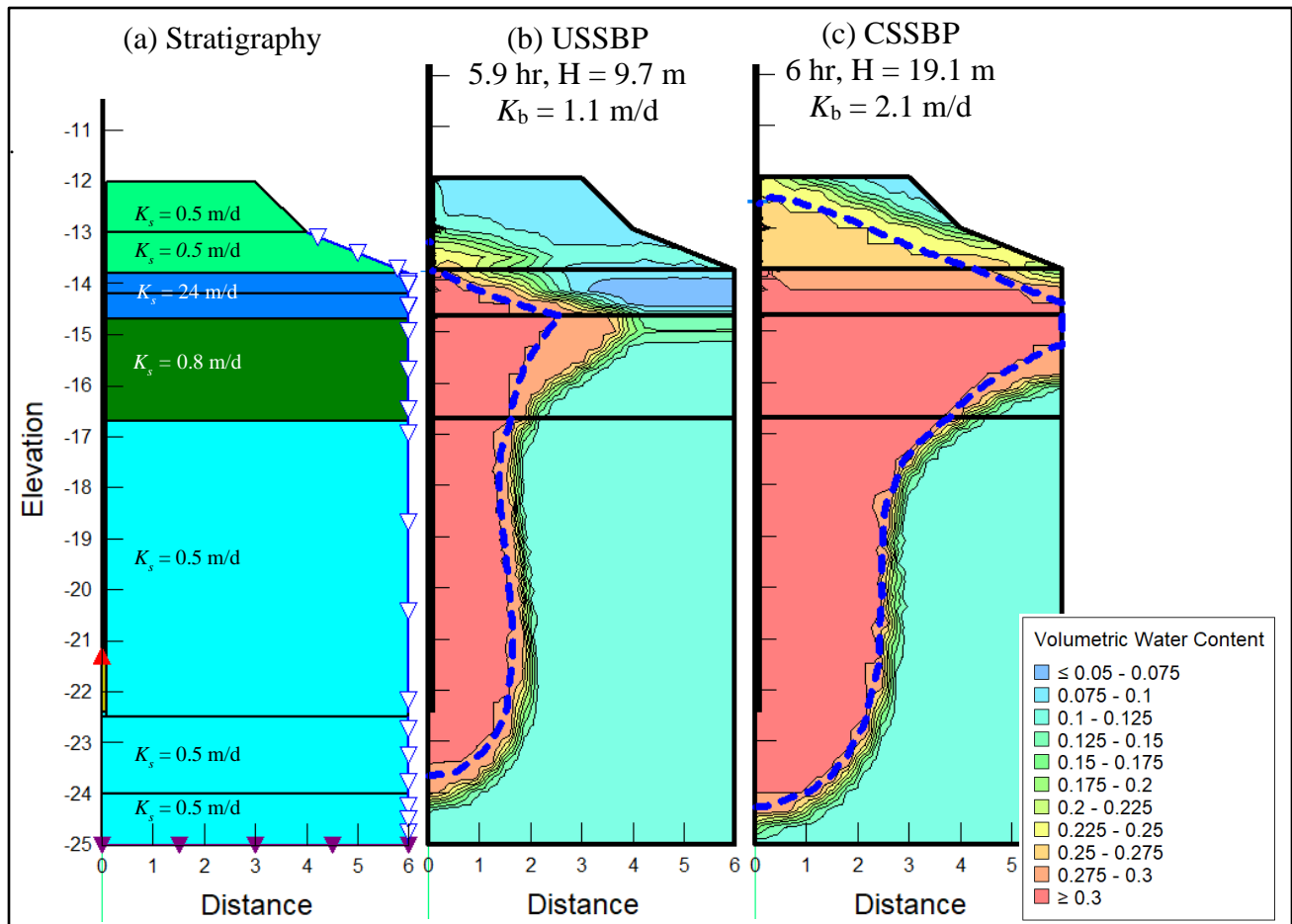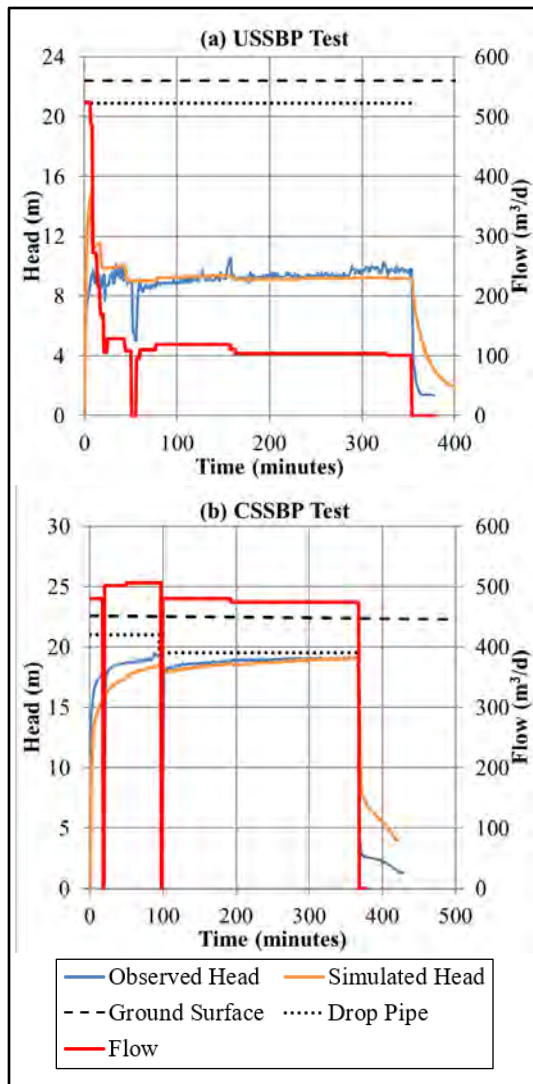
Figure 29: Comparison of observed and simulated head conditions for the U-TW-9 deep infiltration tests: (a) USSBP test, and (b) CSSBP test.

4 Discussion

4.1 Explaining Variability in Field Testing

The shallow field testing (Volume IV) identified significant variability in estimated K_b over horizontal distances of 5 to 25 m in shallow infiltration test facilities. Some of this variability could be explained by differences is soil texture between test facilities. However, some of the variability could not be readily explained by differences in soil texture. In addition, USSBP and CSSBP tests in the same deep infiltration test well provided significantly different K_b estimates in some cases, which should not be the case if the soils are uniform and isotropic. Numerical simulations were conducted in an effort to determine the effects of stratigraphic layering and determine if these factors could explain the variability observed in the field testing.

Numerical simulations of pit tests and shallow well tests in the same stratigraphic sequence indicate that the elevation of a perching or permeable layer compared with the elevation of the test facility could reduce or increase K_b by a factor of 2-4 depending on the contrast in K_s and the elevation of the perching/permeable layer. K_b was particularly affected if the layer was located just below the bottom of the test facility.

Simulations of USSBP and CSSBP tests in deep test wells with the same stratigraphic sequence indicate that the presence of a perching or permeable layer can cause the CSSBP test to provide a higher estimate of K_b than the USSBP test, up to 50% higher in some scenarios. For a perching layer, the largest difference between the USSBP and CSSBP results occurs when the perching layer is at the bottom of the test well. For a permeable layer, the largest difference between the USSBP and CSSBP results occurs when the permeable layer is near the top of the test well.

Numerical simulations were also conducted to evaluate the effect of a permeability transition within the sandpack interval of a deep test well. When more permeable soils are present over less permeable soils, the CSSBP test provided a higher estimate of K_b than the USSBP test. This is particularly true when the transition occurs in the upper portion of the sandpack interval. In an extreme example, with a 120-fold contrast in permeability, the CSSBP test provided a K_b that was up to 5 times higher than the USSBP test.

4.2 Uncertainty Correction Factor (CF_u)

As illustrated in Section 3.1, steady state infiltration tests can be significantly affected by perching and permeable layers. Numerical simulations indicate that K_b can vary by a factor of up to 4 depending on the location of the layering relative to the elevation of the test facility. This means that infiltration testing should be conducted as close as possible to the elevation of the planned infiltration test facility to minimize the effects of layering. Furthermore, given the variability of typical glacial and alluvial deposits, an infiltration test that is located some distance from the planned infiltration facility may not provide an accurate estimate of K_b even if the elevation of the test facility is close to the elevation of the planned infiltration facility. The variability predicted by the numerical simulations of layered systems is consistent with the variability observed in the shallow field testing summarized in Volume IV.

The uncertainty in K_b due to layering and spatial variability means that test results may either under-predict or over-predict the performance of full-scale facilities. If the project includes numerous small facilities, it is likely that the over-estimates of performance will tend to balance the under-estimates of performance and the overall project is likely to achieve the overall flow-control objectives. However, if the consequences of under-predicting facility performance are significant (e.g., will result in flooding or erosion) then it may be appropriate to apply an uncertainty correction factor (CF_u) that will reduce the likelihood of under-predicting facility performance.

The numerical modeling results provided in Volume VI suggest a CF_u of 0.25 to 0.5 for high-risk facilities, which is calculated by dividing the lower K_b by the higher K_b from the three simulations of field tests presented in Section 3.4. Defining CF_u in this manner only considered the potential for over-predicting the performance of the full-scale facility. It excludes all the comparisons where the test results under-predict the performance of a full-scale facility. The shallow field testing (Volume IV) provided a median CF_u of 0.56 and a 20th percentile of 0.19. Because all the

test comparisons that under-predict the performance of the full-scale facility are excluded, a CF_u of less than 0.19 only occurred in 10% of the field test comparisons.

A CF_u in the range of 0.2 to 0.5 may be appropriate for higher-risk infiltration facilities with limited infiltration test data. A higher CF_u (not to exceed 1) may be appropriate if numerous infiltration tests in the vicinity of the proposed infiltration facility are relatively consistent or if the consequences of under-predicting facility performance are insignificant (e.g., a small residential project with an offsite point of discharge).

4.3 Estimates of the Test Well Correction Factor (CF_w) for Sizing Horizontal Infiltration Facilities

As illustrated in Section 3.1, infiltration test results from wells may provide different estimates of K_b than tests conducted in test pits due to stratigraphic layering. In most cases, test well results tend to provide higher K_b estimates than test pit results. If the results will be used to size a horizontal infiltration facility (e.g., a pond or bioretention facility) it may be appropriate to apply a test well to test pit correction factor (CF_w), as defined in Section 3.1. The numerical simulations suggest a CF_w of between 0.25 and 1.0, depending on the location of the perching or permeable layer relative to the test facility. The field testing conducted by Kindred (2011d) provided a median CF_w of 0.53 and a 20th percentile of 0.32.

4.4 Groundwater Mounding Correction Factor (CF_m)

The groundwater mounding correction factor is not applicable if a groundwater mounding analysis is conducted. As discussed in Section 2.4, since a groundwater mounding analysis is not warranted for smaller sites, the effects of groundwater mounding can be addressed using the groundwater mounding correction factor (CF_m) defined in Section 3.3.

Section 3.3 evaluates the potential groundwater mounding effects associated with horizontal infiltration facilities of different sizes. Although 6-hr steady state infiltration tests can reflect the impact of groundwater mounding within 1 to 3 meters of the bottom of the test facility, these effects are greater for larger full-scale facilities than the relatively small test facilities (both pits and shallow wells). This difference can be expressed using (CF_m).

For the example scenarios simulated in this study, CF_m varies from 0.2 to 1 depending on the soil type, the size of the facility, and the depth to groundwater. As shown in Figure 23, CF_m decreases as the permeability of the soil increases, as the depth to groundwater decreases, and as the size of the facility increases. In general, groundwater mounding effects are minor ($CF_m > 0.9$) when $K_s < 3.0$ m/d, the depth to groundwater is greater than 3 m, and the area of the infiltration facility is less than 50 m^2.

The mounding examples provided above should be considered illustrative of how shallow groundwater may affect interpretation of the infiltration test results, and do not reflect actual groundwater mounding scenarios for operational facilities. The test scenarios were based on maximum infiltration rates applied continuously for a period of 6 hr. Runoff rates are generally highly variable during a storm event and groundwater mounding will vary depending on the antecedent runoff history during the previous hours, days and weeks. This topic is deserving of a more detailed assessment that would include hydrologic runoff modeling, a broad range of infiltration facility sizes and shapes, and a broad range of subsurface conditions.

5 Conclusions

Shallow field testing demonstrates significant variability in K_b over distances of 5 to 25 m. Some of this variability, but not all, can be explained by horizontal variability in soil texture. However, soil layering and groundwater mounding can also explain variability in K_b. The purpose of this task was to use numerical modeling to evaluate how stratigraphic layering and groundwater mounding can affect K_b and provide strategies for addressing these factors.

Numerical simulations demonstrate that stratigraphic layering can have a significant impact on K_b, even for the same type of test facility. Small changes in the elevation of a perching/permeable layer relative to the test interval can change K_b by a factor of 2-4, depending on the permeability contrast. Based on these results, a CF_u in the range of 0.2 to 0.5 may be appropriate for higher-risk infiltration facilities with limited infiltration test data. A higher CF_u (not to exceed 1) may be appropriate if numerous infiltration tests in the vicinity of the proposed infiltration facility are relatively consistent or if the consequences of under-predicting facility performance are insignificant (e.g., a small residential project with an offsite point of discharge).

As observed in field testing, shallow test wells tend to provide higher estimates of K_b than pit tests, with a median CF_w of 0.53 and a 20th percentile of 0.32. Numerical simulations demonstrate that these differences can be explained by stratigraphic layering. Since well tests are dominated by horizontal flow and pit tests are dominated by vertical flow, pit test results are likely to be more representative of full-scale horizontal infiltration facilities, such as infiltration ponds and bioretention facilities. Well tests may be used for sizing horizontal infiltration facilities if an appropriate CF_w is applied. A CF_w of 0.5 is recommended for using well tests to size horizontal infiltration facilities and a CF_w of 1 is recommended for drywells.

Steady-state infiltration tests lasting 6 hr can generally detect the impacts of groundwater mounding within 1-3 m of the bottom of the test facility. However, these effects are more significant for larger full-scale facilities than typical test facilities. Groundwater mounding analysis should be conducted for larger facilities and it may be appropriate to apply a CF_m between 0.2 and 1 for smaller facilities, depending on the size of the full-scale facility, the permeability of the soil, and the depth to groundwater.